STUDIES OF PHYSICAL PROPERTIES OF NOVEL LITHIUM POLYMER ELECTROLYTES

by

Razali Idris

Thesis submitted in partial fulfilment for the degree of Doctor of Philosophy
De Montfort University, Leicester

De Montfort University
January 2001

ACKNOWLEDGEMENTS

I would like to thank my supervisors Prof. Roger Latham, Malcolm Glasse and Walkiria Schlindwein for their on going advice and guidance. With the help and encouragement from them has published some of the results from this thesis in Journal of power sources and presentation at Symposium-Electrochem in Dublin City University, September, 2000.

I would like to express my gratitude to Prof. Roger Linford, Dean Faculty of Applied Sciences to highlight preliminary result of this work at oral presentation in an International Conference on Interfacial Phenomena in Batteries, Rome, December 1999.

I also appreciate all the advice and supplying of ENR polymer being used for the research work in this thesis by Dr. Andy Chapman from Tun Abdul Razak Research centre in London. In addition, I also appreciate, Mr. Ong Kian Huat from Green (M) Sdn Bhd, Malaysia to supply polymethyl methacrylate grafted natural rubber latex (abbreviated MEGATEX 49) partly used for this work.

In particular, I would like to thank Mr. Ian Fletcher for his assistance and help to produce SEM images. Also I would like to thank the research staff and students who provide the valuable entertaining distractions, that encourage spirit motivation to succeed.

I am also very grateful to Norma Garrington for her help and advice in collecting data from delicate IR and thermal analysis equipments. I would like to express thanks to the laboratory staff and store officer for supplying the appropriate chemicals.

I am indebted to my wife and children for their strong support, patience and painstaking throughout the entire three years duration until completion of this thesis.

Finally, I would like to thank the government of Malaysia for the financial support of this work during the period of this study.

STUDIES OF PHYSICAL PROPERTIES OF NOVEL LITHIUM POLYMER ELECTROLYTES

by

RAZALI IDRIS

Abstract

Polymer electrolyte systems using thermoplastic polyester polyurethane (TPU), modified natural rubbers and modified natural rubbers/polyethylene oxide polymer hosts have been investigated. Three types of modified natural rubber, namely 25 percent epoxidised natural rubber (ENR25), 50 percent epoxidised natural rubber (ENR50) and polymethyl methacrylate grafted natural rubber were employed as polymer hosts.

In this study the ionic conductivity, thermal, FTIR spectroscopy and morphology have been determined for both unplasticised and plasticised polymer electrolyte systems understudied. The following characterization results explain the effect of the polymer electrolyte films made by systematic compositional ratio of lithium triflate and EC/PC plasticisers introduced into the polymer aided by volatile solvent.

Without any plasticiser, the TPU/$LiCF_3SO_3$, modified natural rubber and modified natural rubber/PEO blend based polymer electrolyte systems have ionic conductivity in the range 10^{-6} to 10^{-5} S cm^{-1} at ambient temperature. Incorporating 50-100% of EC/PC by weight to the understudied polymer electrolyte systems yielded mechanically stable films and ionic conductivities in the range of 10^{-4} to 10^{-3} S cm^{-1} at ambient temperature.

Thermal analyses have shown the detection of single glass transition temperatures for the TPU and modified natural rubber based polymer electrolyte system. FTIR spectroscopy indicates that the interaction of lithium salt with polymer hosts occurred by the increasing band intensities within polymer electrolyte system. The mechanical properties of the systems showed that at low plasticiser content the stiffness of the polymer electrolytes is less affected but has a low ionic conductivity.

In summary, results from SEM spectroscopic data in conjunction with thermal analysis show that the degree of crystallinity, melting temperature, crystallisation rate and microstructure of PEO in PEO/ENR blends have been perturbed weakly by the presence of ENR. In addition SEM images showed a rather complicated blend morphology, which is composition dependent, arising from phase separation.

CONTENTS

LIST OF TABLES

LIST OF SYMBOLS

A	Area of electrode, cm^2
DSC	Diffrential Scanning Calorimeter
EC	Ethylene carbonate
ENR	Epoxidized natural rubber
FTIR	Fourier Transform Infrared
$LiCF_3SO_3$	Lithium trifluoromethanesulphonate
MG-49	Polymethylmethacrylate grafted natural rubber
MPa	Megapascal
NBR	Poly(acrylonitrile-co-butadiene) rubber
PAN	Polyacrylonitrile
PC	Propylene carbonate
PEO	Poly(ethylene oxide)
PMMA	Polymethyl methacrylate
PVC	Polyvinylchloride
PVDF	Poly(vinylidene fluoride)
R_b	Bulk resistance
S	Siemen
SBR	Poly(styrene-co-butadiene) rubber
T_g	Transition glass temperature
THF	Tetrahydrofuran
T_m	Melting temperature
TPU	Thermoplastic polyurethane
Z'	Real part of impedance
Z''	Imaginary part of impedance

Chapter1. INTRODUCTION TO POLYMER ELECTROLYTES

1.1 General Introduction

In today's digital technology many sophisticated instrumental, electronic devices have been designed by engineers to cater for consumer aspiration in daily life. There are countless consumer products in the market, from clocks and digital watches, personal CD players, laptop and mobile phones etc. Astronauts and the team in space mission need wide varieties of space applications such as launch vehicles, earth-orbiting spacecraft. Many of these devices and applications demand new and better durable batteries to power them. A battery system for space application must be able to sustain a severe condition and can provide maximum electrical energy in minimum weight and volume (Halpert, Frank and Surampurdi, 1999). It was cited in the article that the evolution of flight batteries started with Ag-Zn battery in the early days of space mission. It was then used Ni-Cd batteries followed by Ni-H_2 battery began to play a role in the 80s. Recently, advanced batteries have been developed such as Li-ion rechargeable batteries, which are compact, lightweight are available in the consumer market. These are attractive but have not yet been used in the space.

NASA has developed research programme and plan to use it for future space mission. From the surveyed internet-based information a recent completed project funded by the Defence Advanced Research Projects Agency (DARPA) under the Technology Reinvestment Program has resulted in the development and scale up of new lithium-ion polymer battery technology for military and aerospace applications. The contractors for this cost-shared project were undertaken by Lockheed Martin Missile & Space and Ultralife Batteries, Incorporation whereas contract for management and technical oversight was provided by NASA Research Centre. The final products of the project were a portable15 volt (V),10 ampere-hour (A-hr) military radio battery and a 30 V, 50 A-hr marine/aerospace battery (Hagedorn, 1999). The new lithium-ion polymer battery technology has shown a threefold or fourfold reduction in mass and volume, relative to current's commonly used nickel-cadmium, nickel-hydrogen and nickel-metal hydride batteries.

A battery basically is a simple electrochemical power source to store electrical energy as chemicals. Battery can be classified into two types namely primary and rechargeable battery. The former one apply to cell that is disposable after discharged once whereas the latter one refers to battery that can be recharged and use again. Between the two options, rechargeable battery or cell is preferred one. The overall discharge process involves the flow of electrons from the negative electrode to the positive via the external circuit doing electrical work (Figure1.1). The overall charge process is the opposite. The two electrodes are separated by an electrolyte that conducts ions. The majority of conventional batteries utilize an aqueous solution electrolyte whereas more advanced battery systems use polymer electrolyte films. Each of these systems has a limitations and related deficiencies, which make them unsuitable for various applications.

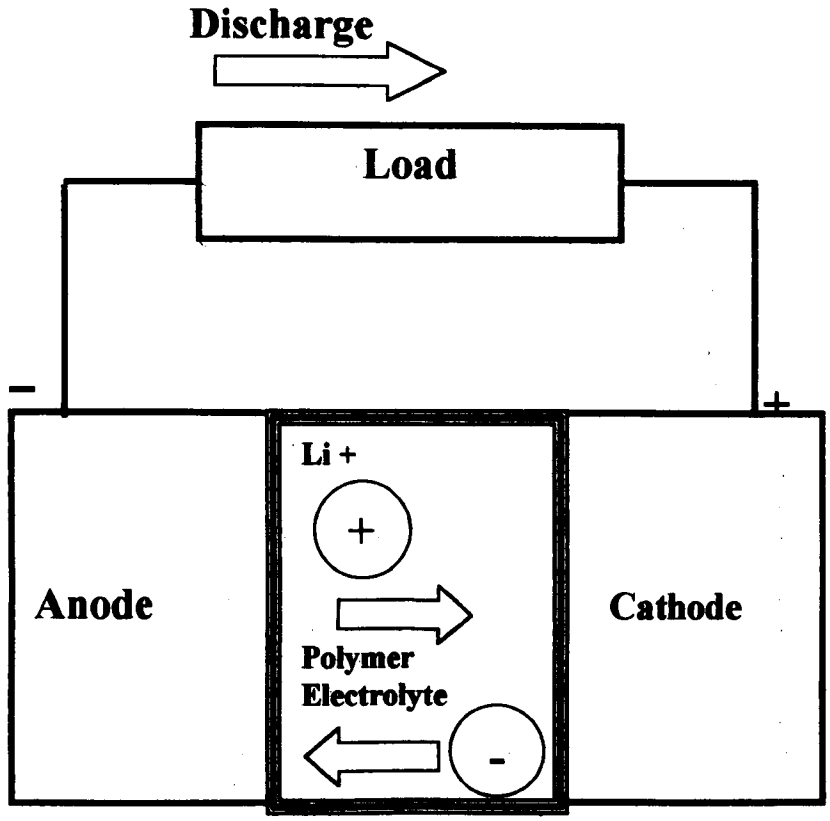

Figure 1.1 A cell under discharge.

Liquid electrolytes, e.g. non-aqueous propylene carbonate (PC) and ethylene carbonate (EC) containing salt possess acceptable ionic conductivity, tend to leak out of the cell into which they are encapsulated. The effect is reduced efficiency in cell service of life. Although better manufacturing techniques have decrease the occurrence of leakage, cells still do leak potentially hazardous liquid electrolytes from time to time.

This is particularly true for current lithium ion battery. In addition the resulting of leakage will reduce the composition of electrolyte species in the cell, thus reducing the effectiveness of the cell. Cells utilizing liquid electrolytes are not available in different specified shapes and sizes of batteries.

The alternative approach to the above-mentioned problems was to engage solid electrolytes for use in solid-state battery. A great effort of research work on new materials with high ionic mobility intensified in the late 1960s and early 1970s. Most of solid electrolytes are highly crystalline and ceramic types with high ambient temperature conductivity. These included compounds such as MAg_4I_5 (M = Rb, K, etc.) (Gray, 1997; Bruce, 1995) which are silver ion conductors, and sodium β-alumina, which is a solid sodium ion conductor. The major drawback for alkali metal electrolytes is the maintenance of a high operating temperature and the use of highly aggressive agents, leading to technical difficulties. Another accounted problem with solid electrolytes is the difficulty of producing a good interface between the electrolyte and the electrode. Disadvantages also prevailed with mechanical properties. These materials are hard and brittle and are therefore very difficult to use in larger batteries.

The preferred option is polymer electrolyte, which is relatively a latecomer in the broader field of solid-state ionics. The consequence for this is that these materials have to compete with other established solid-state materials that already proved excellent transport properties. The development of intercalation electrodes, which is one of the major advances of early solid-state ionic research, has provided suitable material to partner with polymer electrolyte for polymer-electrolyte-based cell.

The intercalation materials are far less suited to glass or ceramic-electrolyte-based cells. The flexible polymeric material has capacity to accommodate volume changes on intercalation and deintercalation process compared to rigid electrolyte. It can be manufactured as a thin, large area of film, offers a reliable candidate for use in electrochemical devices. Taking into account the above matters has provided the interest of this thesis topic. In response to this high energy density utilizing polymer electrolyte system is an option in place with high capacity electrodes for new breed of batteries. The trend of battery development is illustrated as follows;

Higher capacity lightweight Slimness

Ni-Cd battery >>>> Ni-MH battery >>>> Li-ion battery >>>>Polymer battery

The concept of an all-solid state battery is very appealing in term of safety, lightweight and flexibility. Recently, intense research pursuit by universities, private laboratories and research institutions for an important development in lithium ion battery technology involves the replacement of the liquid electrolyte to produce what has been termed the plastic lithium ion battery (PLI). This is an interesting concept, since it provides the prospect of a favourable combination of the high energy and the long life typical of the lithium ion cell, with the reliability and process ability typical of a polymer-based all solid-state configuration. The practical exploitation of PLIs requires the availability of polymer electrolytes having a conductivity approaching that of the liquid solutions. A successful approach has been reported by the Belcore laboratory in the United States with the use of a membrane separator formed as a copolymer of vinylidene fluoride and hexafluoropropylene (PVDF-HFP), which is capable of absorbing large quantities of liquid electrolyte (Vincent and Scrosati, 1997). The role of the HFP component is to decrease the crystallinity of the PVDF copolymer and thus to enhance its ability to absorb liquid.

In respond to the research and development of lithium ion polymer batteries the trend of secondary batteries within Japan has changed recently. Many Japanese battery companies have announced the shipment of Li-ion polymer batteries. Matsushita battery

Table 1.1 Battery sizes and applications. Source : From Dell (2000)

Battery type	*Stored energy/Wh*	*Applications*
Miniature/button cells	0.1–5	Watches, calculators, heart pacemakers
Portable communications	2–100	Mobile phones, laptops.
Domestic uses	2–100	Portable radio and TV, flashlamps, toys, video cameras, powertools
Automotive	10^2–10^3	Starting batteries for cars, trucks, buses, boats *etc* Traction batteries for lawnmowers, golfcarts, invalid chairs *etc*
Remote area power supply	10^3–10^5	Lighting, water pumping, telecommunications *etc*
Traction	10^4–10^6	Electric vehicles, forklift trucks, tractors, torpedoes
Stationary	10^4–10^6	Standby batteries, un-interruptable power supply (UPS)
Submarine	10^6–10^7	Underwater propulsion
Load levelling	10^7–10^8	Electricity supply industry, load levelling, peak shaving, spinning reserve

Industry Co. has started marketing Li-ion batteries last year followed up by counterpart Sony Energy Tech. Co. The main question is what is so exciting about Li-ion polymer batteries at present time. It is mainly the reduced thickness and weight reduction of the cell. Table 1.1 is listed different types of batteries for various applications. Taking into account the all-state battery system described above has provided the interest of this thesis topic. Finally, polymeric electrolytes an important class of electrolytes suitable for lithium batteries that have compromise solid-to-liquid structure is chosen for this work.

1.2 Background of Polymer Electrolytes

It takes almost two centuries to revolutionize an advanced new lightweight batteries using polymer electrolyte system. To arrive at this stage many events have taken place in the field of electrochemistry.

The credits should attribute to individual scientists and research group's relentless effort has undertaken difficult years to materialize reliable batteries for commercial and domestic uses. Professor Alessandro Volta pioneered the first generation of electricity using electrochemical battery in 1800 (Vincent and Scrosati, 1997). From the small beginning the development of electrochemical cell has become a great interest by scientist in a number of countries. The progress of research in solid-state electrochemistry has developed steadily up to the late 60's and early 70's. During this period the desire to realise technological goals has motivated the discovery of many new solid electrolytes and intercalation electrodes. The oil crisis of the early 70's has change the research scenario to focus on development of energy storage devices.

In the late 1970's polymer electrolyte has received a great attention for potential application in electrochemical devices such as batteries and electrochromic windows. Polymer electrolyte is relatively new area to the broader field of solid state ionics compare with established ceramic-based solid electrolytes proven excellent in their transport property and stability. Unlike solid electrolytes, polymer electrolyte has capacity and property that make it possible to construct all solid-state batteries.

The polymer conforms to the volume changes of the electrode that typically occur during in service of discharging and charging, which far less apparent to glass or ceramic-electrolyte-based cells. The great interest of polymer electrolytes has driven several research groups to explore new polymer electrolyte system, physical studies of their structure and charge transport and theoretical modelling of the charge transport processes. The detailed finding and progress in this field has been reported in literature (Armand, 1986; MacCallum and Vincent, 1987, 1989; Ratner and Shriver, 1988; Vincent, 1989; Tonge and Shriver, 1989; Cowie and Cree, 1989; Bruce and Vincent, 1993; Linford, 1987, 1990).

It was described in literature (Bruce, 1995) that the structure and charge transport mechanism for polymer electrolytes entirely different from those of inorganic solid electrolytes as such the following will describe the general consideration of polymer electrolytes. Basically, polymer acts as solvating solvent for cation for the formation of polymer electrolytes. According to most research on new polymer electrolytes stated that ion transport is preferable on local motion of the polymer (segmental motion) in the vicinity of the ion. For the past two decades there are two general types of polymer electrolytes have been intensively investigated. They are bi-ion conductor polymer-salt complexes and polyelectrolytes. In the former one a typical example is dissolution of salt, e.g. $LiClO_4$ in coordinating polymer, usually polyether. Both anions and cations can be mobile in these types of electrolytes.

Polyelectrolytes, on the other hand, a positively or negatively charged ion covalently attached to the polymer backbone with only the counterion is significantly mobile. These type of electrolytes are also known as single-ion-conducting solid polymer electrolytes. Some examples of polyelectrolyte hosts are sodium poly (styrene sulfonate), lithium poly (2-sulfoethyl methacrylate) (Gray, 1997) and lithium polyphenolates (Mandal, Walsh, Sooksimuang and Behroozi, 2000). For this work most of the reviewed articles/journals focused on bi-ion-conducting polymer electrolyte systems, which are closely related to the thesis topic.

1.3 Polymer Electrolyte Development

It is reviewed from literature that the study of polymer electrolyte involves various scientific discipline and techniques. As it was mentioned in the previous section polymer electrolyte is new area in the broader field of solid-state ionics. As such many researchers in various scientific discipline have great interest to explore new polymer electrolyte system based on guided principle as reported by previous investigator.

For more than two decades since the early discovery of ionic conductive polymer by Wright *et al* (1973) to present time, there are many approaches have been attempted to fulfill criteria for electrochemical devices applications as far as polymer electrolyte research is concerned. The results previous investigations on polymer electrolytes are well-documented in books and conference proceedings. From the literature reviews, which focused on the polymer electrolyte systems, it can be roughly divided into main groups. They can be divided into conventional polymer electrolytes and non-conventional polymer electrolyte systems.

1.3.1 Conventional Polymer Electrolytes

Poly(ethylene oxide), PEO, is a linear polymer and the regularity of the –(CH_2-CH_2O)- unit contributes a high degree crystallinity (70-85 %)(Gray, 1997). Pure PEO adopts helical conformation as shown in Figure 1.2 below.

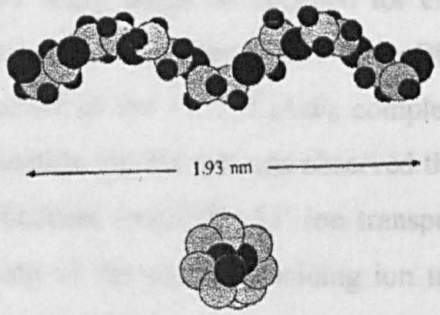

Figure 1.2 Structure of polyethylene oxide, PEO, viewed parallel and normal to the axis of the helix. The black circles represent oxygen atoms. Source : From Gray (1997).

PEO on heating displays melting point of the crystalline phase, T_m, at 65^{0}C and glass transition temperature, T_g, at – 60^{0}C. The dielectric constant of the polymer is low (~ 5-8) and this has an important influence on the properties of the electrolytes. The first solvent free polymer electrolytes were based on high molecular weight PEO, which remains the basis for all the solvent-free systems. It serves as a prototype for the structural features in most of the advanced polymer electrolyte hosts.

A number of alkali metal salts formed complexes with PEO at a range of concentration and to act as a binder for other phases (Best, Ferry, MacFarlane and Forsyth, 1999). In general a polymer, which is capable of strongly coordinating cations is necessary for the formation of electrolyte. Other typical examples of coordinating polymers, which can act, as solid solvents like PEO are polyethylene imine and polyethylene succinate.

PEO based Li salt complexes are generally exhibited conductivity in the range 10^{-7} to 10^{-8} S cm^{-1}at room temperature, which is not acceptable for practical application (Kim, Oh and Choi, 1999; Sun, Sohn, Yamamoto, Takeda and Imanishi, 1999). Reasonable conductivity in PEO-salt polymer electrolyte can be achieved (~ 10^{-5} S cm^{-1}) above 100^0C but at the expense of mechanical properties of the polymer. A high degree crystalline phase in PEO is a great obstacle to impede ionic conductivity at room temperature. Then, cross-linking between chains in polymer electrolytes restricts the local chain motion, as consequence decreases conductivity (Angell, 1983).

However, contrary result might be obtained for crystalline form of PEO-salt complex. Recently, a group work of researchers (MacGlashan, Andreev and Bruce, 1999) reported the structure of the PEO: $LiAsF_6$ complex with a 6:1 composition. From the structural determination carried out was observed that the 6:1 crystal structure possesses highly aligned cylindrical tunnel for Li^+ ion transport. In this case, cross-linking serves to introduce pairing of the chains providing ion transport along the tunnel. Thus, the mere presence of cross-linking does not necessarily impose a significant decrease in conductivity in every case. There are several other factors that contribute to affect and finally limit conductivity in PEO based electrolyte systems. There are three main factors could be mentioned here; first the strong dependence of ion mobility on the segmental motion of polymer backbone (Gray, 1991); second, a low volume fraction of the amorphous phase of the PEO complex below the melting point of the crystalline PEO phase (Berthier, Gorecki, Minier, Armand, Chabago, and Rigaud, 1983); and last, a relatively low number of charge carriers due to the low degree of charge separation as well as ion association (Reiche, Steurich, Sandner, Lobitz and Fleischer, 1995).

Various strategies have been applied for PEO to enhance ionic conductivity by controlling one of these factors. For example, research into modification of PEO based polymer electrolytes have been reported and reviewed (Gray, 1997). Then, an approach with incorporation fine particles of ceramic material into the polymer-salt complex was reported to increase the ionic conductivity (Scrosati, Crose and Persi, 2000). An improvement of conductivities was reported by addition of plastizers such as ethylene carbonate, propylene carbonate and the mixtures into PEO-salt complexes (Bandara, Dissalayake and Mellander, 1998) or plasticizing salts like Li $(CF_3SO_2)_2N$ to PEO as a result of facilitating segmental motion of polymer chains.

Alternatives to PEO polymer host have also been explored with the intention to achieve suitable candidate for electrochemical device applications. Different materials such as polyacrylonitrile, PAN (Starkey and Frech, 1997; Abraham and Alamgir, 1990), poly (methyl methacrylate), PMMA (Quartarone, Tomasi, Musrtarelli, Appetecchi and Croce, 1998; Bohnke, Frand, Rezrazi, Rousselot and Truche, 1993), polyvinylidene fluoride PVDF (Fuller, Breda and Carlin, 1997; Voice, Southall, Rogers, Matthews, Davies, McIntyre and Ward, 1994), polyvinyl chloride, PVC (Sung, Wang and Wan, 1998), and polyurethane, PU (Venugopal, Reichert and Zhang, 1996), nitrile-butyl-rubber and styrene-butadiene-rubber, NBR/SBR (Matsumoto, 1996) have been studied to this aim. In the following section discusses some of these different classes of the second-generation polymer electrolytes, which fall under categories non-conventional polymer electrolytes.

1.3.2 Non-Conventional Polymer Electrolytes.

The 90's era has produced new second-generation polymer electrolyte systems, which fall under category non-conventional polymer electrolyte system. With regards to the interest of second-generation polymer electrolyte systems, the related articles and journals parallel to this thesis topic are reviewed and described in this section. This present review will embrace three classes of solid-state electrolytes namely polymer gel electrolytes, blend based polymeric electrolytes and composite polymer electrolytes.

1.3.2.1 Polymer gel electrolyte.

Polymers have been used widely for automotive components, electronic kits, toy products, building panels etc. In addition to this growing list is the utilisation of plastics or elastomers as a solid medium to replace the liquid electrolyte counterparts as the components of electrochemical devices such as displays, sensors, electrochromic windows, supercapacitors and rechargeable batteries. Numerous papers and patents have been published regarding the use of polymeric materials for their application as polymer gel electrolytes in solid polymer batteries (Murai *et al* 1997; Nashiura, Kono, Namegaya and Matsuda, 1998; Hikmat, Peeters, Lub and Nijssen, 1999). These systems have shown improved ionic conductivities over previous conventional polymer electrolyte systems (Yavaroy, Wang and Wunder, 1999; Kim, Oh and Choi, 1999).

Dissolving a salt in a polar liquid and adding an inactive polymeric material to give material mechanical stability form a gel electrolyte by definition. Basically polymer gel consists of polymer, an ionic salt and a solvent. Organic plasticisers are employed to increase the flexibility of the polymer host main chain. Several polymer hosts that have been investigated as polymer gel electrolytes for lithium batteries include PEO (Appetecchi, Croce and Scrosati, 1997), PAN (Ostrovskii, Torell, Appetecchi and Scrosati, 1998), PVdF (Wang, Huang and Wunder, 2000) and PMMA (Yarovoy, Wang and Wunder, 1999). Whereas polar solvents such as ethylene carbonate (EC), propylene carbonate (PC), dimethyl carbonate (DMC), have been added into polymer matrix to form polymer gel-type electrolyte. Most of the polymer gel systems retain high amounts of electrolyte species (40-85 wt %) in their polymer matrix and registered ionic conductivity value 10^{-3} S cm^{-1} at ambient temperature (Wang, Huang and Wunder, 2000).

From the cited literature five methods of preparing polymer gel electrolytes have been studied by several research groups (Croce, Brown, Greenbaum, Slane and Solomon, 1993; Jiang, Carroll and Abraham, 1997; Matsumoto, Rutt and Nishi, 1995; Wang, Huang and Wunder, 2000; Kono, Hayashi, Nishiura and Watanabe, 2000). The preparation of the polymer gels are briefly described as follows; first one involved heating at elevated temperature the mixture of polymer, ionic salt and plasticiser until forming homogenous viscous melt solution. The viscous solution is cast and forms electrolyte film on cooling. The second method involves dissolving the polymer host in a lithium salt electrolytic solution and common low boiling point solvent. The mixture solution is cast and forms a polymer gel film after the solvent evaporated off. The third method involves an activation process, in which a polymer film is soaked in electrolytic solution. The fourth method polymer electrolyte film is prepared by thermal extrusion. The detailed preparative method is described elsewhere (Abraham and Alamgir, 1990). The fifth one the gel electrolyte is prepared by UV cross-linking technique illustrated below;

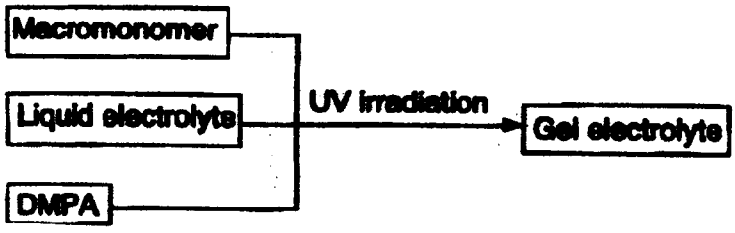

DMPA : Thermal initiator

Source: From Kono *et al* (2000)

To date polymer gel electrolytes technology has been successfully applied in lithium ion polymer battery being commercially produced. Some of the companies from Japan and U.S.A involved with Li-ion polymer battery are given in Table1.2 (Osaka, 1999).

Table 1.2 List of some battery companies using polymer gel electrolyte for lithium ion polymer batteries. Source: From Osaka (1999).

	Cathode	Electrolyte	Anode	Voltage	Size mm	Capacity mAh	Energy Wh/L	Density Wh/kg	Application	Production Start
Matsushita Battery	$LiCoO_2$	PVDF gel	Graphite	3.7	35x62x3.8	500	250	125	Cellular	January 1999
Sony	$LiCoO_2$	PVDF gel	Graphite	3.7	35x62x3.8	540	245	125	Cellular, PC	Spring 1999
Japan Storage Battery	$LiCoO_2$	PVDF gel	Graphite	3.6	32x62x3.4	510	210	125	Cellular, MiniDisc	Summer 1999
Hitachi Maxell	$LiCoO_2$	PEO gel	Graphite	3.6	54x86x3.0	500	130	90	Cellular, PC	April 1999
Sanyo	$LiCoO_2$	PEO gel?	Graphite	3.6	37x75x3.5	550	200	120	Cellular	Summer 1999
Toshiba Battery	$LiCoO_2$	PVDF gel	Graphite	3.6	36x74x3.6	650	245	115	Cellular, PC	Fall 1999
Yuasa Corp.	$LiCoO_2$	PEO gel	Coke	3.6	54x74x2.2	400	165	95	Cellular, MiniDisc	Fall 1999 August 1998, primary
Hirion/Mitsubishi Chem.	$LiCoO_2$	PEO gel	Graphite	3.7	34x48x4	500	280	130	Cellular, PC	Spring 1999
Ultralife (US)	$LiMn_2O_4$	PVDF gel	Graphite	3.7	51x103x6.5	1700	185	105	Cellular, PC	3Q 1997
Valence (US)	$LiMn_2O_4$	PVDF gel	Graphite	3.7	36x65x9.0 102x127x5	1200 3900	220	110	PC	3Q 1998
Thomas & Betts (HET) (US)	$LiCoO_2$	PVDF gel	Graphite	3.7	30x48x6.5	530	220	120	Cellular	4Q 1998
Lithium Tech. (US)	$LiCoO_2$	PVDF gel	Graphite	3.6	203x305x6.4	2400?	240	125	PC	4Q 1999
Shubilla (Malaysia)	$LiCoO_2$	PVDF gel	Graphite	3.65	58x30x4.4	450	215	120	Cellular	Fall 1998
Electrofuel (CA)	$LiCoO_2$	PVDF gel	Graphite	3.6	108x138x6	10800	435	175	PC	2Q 1999
Moltech (US)	Org. sulfur polymer	Org. solvent	Li metal	2.1	34x48x5.0	800	210	170	Cellular	3Q 1999

Physical and electrochemical properties are the crucial factors for any polymer electrolyte systems before taking into account for their commercial use in electrochemical devices applications. Various topics of investigations have been carried out and reported in the literature that discussed the changes in the properties of polymer gels, introduced by variation of components and their relative amounts. For example mentioned here some of the results from reviewed articles that produced by polymer gel electrolytes such as reduce its conductivity upon increasing the amount of polymer added and long storage in the series of investigation, the loss of mechanical strength upon high retention of plasticiser were reported in the literature.

It has been reported the gels consisting of polymer-rich and polymer-poor phases by polymerisation of apolar diacrylates in a mixture with a liquid electrolyte (Hikmet, Peeters, Lub and Nijssen, 1999). In this system was found that with increasing diacrylate concentration, the ion conductivity showed a decrease. The decrease in the ion conductivity was associated with the decrease in the free volume within the system.

A promising conductivity was reported by immobilisation in a poly (methyl methacrylate) PMMA matrix, $LiN(CF_3SO_2)_2$ salt solvated in an ethylene carbonate-dimethyl carbonate (EC-DMC) mixture (Quartarone, Tomasi, Mustarelli, Appectecchi and Croce, 1998). These system electrolytes have shown electrical conductivity at room temperature as high as 10^{-3} S cm^{-1}. However, one of the drawbacks of these gels is their lack of long-term structural stability, which causes a reduction of the contact area with the electrode and a resultant fall in conductance. PMMA-based gel electrolytes tend to crystallize and, possibly, to phase separate with aging, depending on the solvent utilized in gel preparation.

Several research workers have reported mechanical properties of polymer gels with high retention liquid electrolyte. It was found that tensile strength of the gel electrolytes, prepared from the tri-functional macro monomer polymer host decreased with increasing liquid electrolyte content up to 90-wt % (Kono, Hayashi and Watanabe, 1999).

PVDF gel electrolyte, containing 80-wt % liquid electrolyte attained 1.4 MPa tensile strength and 170 % elongation at break, while maintaining an ionic conductivity of 10^{-3} S cm^{-1} (Jiang, Carroll and Abraham, 1997). In the case of PAN-based gel electrolytes have shown good mechanical properties even when the liquid electrolyte content was added higher than 90-wt % (Tatsuma, Taguchi, Iwaku, Oyama and Sotomura, 1997). From the information described above suggests that different approaches of investigated polymer gel systems creating wide range of properties for the complete electrolyte.

1.3.2.2 Blend based polymeric electrolytes

In this section the review will discuss the blend based polymer electrolytes from the point of performance, structure and stability. Blending of polymer system is obtained from homogeneous solutions of two components in an appropriate common solvent. PEO has been widely used to blend with other polymers to gain significant advantages such as to improve structural, mechanical and electrochemical properties. For example PEO/PVDF blend based electrolytes have shown improved ionic conductivity than pristine conventional PEO base electrolyte and performed good mechanical property (Jacob, Prabaharan and Radhakrishna,1997). The ionic conductivity and mechanical integrity of PVDF: $LiClO_4$ polymer electrolyte complex were studied as a function of PEO concentration. The addition of PEO into PVDF:$LiClO_4$ complex enhances the room temperature conductivity and mechanical stability of the thin film electrolyte membrane. The maximum conductivity at 30^0C was found to be 2.0×10^{-5} S cm^{-1} for PVDF-$LiClO_4$: PEO (80:20) w/o.

Wiezorek et al reported solvent casting or thermal polymerisation preparation technique of the blends of PMMA and PEO doped with sodium and lithium salts. The two ways of synthesis were compared and revealed that the technique of preparation affecting the conductivity of blend system studied. During the reaction of thermal polymerisation of MMA monomers in the presence of high molecular weight PEO, a graft copolymerisation occurs. The increased conductivity was reported due to the formation of the grafted PEO-PMMA phase, which acts as an internal plasticiser and compatibiliser. This has resulted increases the flexibility and the free segmental motion of polyether amorphous phase. The outcome was an increase in the distances among the PEO chains and a reduction in the crosslinking effect of the cation is observed. The presence of a grafted-phase has attained the higher values of room temperature conductivities (10^{-4} – 10^{-5} S cm^{-1}) in the whole temperature range (Quartarone, Mustarelli and Magistris, 1998). It was also reported that DSC experiments also show T_g values lower than those of the cast films.

The intrinsic structure of the PEO-PMMA blends and PMMA stereoregularity have strongly influenced the conductivity of such electrolytes. The PMMA configuration is a key factor, which determines the reorganisation of the two polymers in the blends and their compatibility are quite different. This has been reported (Florjanczyk, Such and Wieczorek, 1992) that isotactic one (IPMMA) when blended with PEO, its conductivity is at least one magnitude higher than of systems containing the atactic and sindiotactic isomers. The use of 30% IPMMA in the blend with PEO can reach maximum room temperature conductivity value of 9×10^{-5} S cm^{-1}.

There are two other polymeric fillers such as polyacryloamides and polyacrylates have been studied to blend with PEO show lower T_gs than PMMA. The resulted polymer electrolytes show a remarkable chain flexibility, higher ionic transport and conductivity (Wieczorek, Such, Florjanczyk and Przyluski, 1992). In addition, polyacryloamides (PAAM) have side polar groups that contribute to the higher dielectric constant of the polymeric blends and the salt dissociation. These multiphase polymer electrolyte systems have two T_gs, corresponding to PEO-rich phase and PAAM-rich phase. DSC experiments revealed that the addition of stiff PAAM suppresses PEO crystallinity and improves the mechanical properties.

The remarkable effect of these polymers in blending with PEO is the competition between two Lewis base centres, O of ether and N of amide groups. Thus, the presence of these different ligands has caused the formation of more than one polymer-cation complex. As reported in FTIR characterisations (Wieczorek, Such and Steven, 1994) suggest that in the PEO-PAAM blend doped with $LiClO_4$, three types of complexes are identified: (i) the classical crown-ether PEO-Li-PEO; (ii) the system PEO-Li-PAAM, in which Li^+ is coordinated by the PEO heteroatom oxygen and N of amide groups. The compositions containing PAAM and $LiClO_4$ are optimised (20-30 PAAM vol % and 10 mol % $LiClO_4$). The system PEO-Li-PAAM is favoured, which has a decrease in T_g value, attributed to the amorphous region of PEO and then the maximum ionic conductivity (4×10^{-5} S cm^{-1}).

1.3.2.3 Composite polymer electrolytes

Several research workers and investigators in universities and research institutions have investigated PEO based composite electrolyte systems. Some of them in the list include Weston *et al* (1982), Stevens and Mellander (1986), Plocharski *et al* (1988), Chen Liquan (1988) and Wieczorek *et al* (1990). Conductivities at room temperature in excess of 10^{-5} S cm^{-1} were obtained and maximum amount of filler concentration in the range 10-20 wt % of the ceramic additive. The reason for the increase in conductivity with respect to the corresponding unfilled electrolytes was attributed both to the enlargement of the total amorphous phase in the polymer matrix and to some not well-understood interactions among polymer chains and the ceramic grains. The effect of the filler grain dimension on the conductivity was also ascertained (Wieczorek, Such, Wycisklik and Plocharski, 1989).

Other PEO based composite electrolyte systems were also studied by Scrosati and coworkers. The addition of β''-Al_2O_3 to the systems PEO: NaI and PEO: $LiClO_4$ was reported (Croce, Bonino, Panero, and Scrosati, 1989; Croce, Passerini, Selvaggi and Scrosati, 1990). In the system was found that the conductivity has reduced but it performed better mechanical resistance towards crystallisation. The systems were assembled in solid-state electrochemical devices and also being discussed (Scrosati, 1989).

In the most recent one reported by the same group (Scrosati, Croce and Persi, 2000) was PEO-based nanocomposite polymer electrolytes. In the investigation was reported an impedance spectroscopy of two different types of nanocomposites polymer electrolyte membranes. The systems were having a different salt-to-PEO composition ratio and based on different types of fillers, i.e., the $(PEO)_8LiClO_4$ + 10 wt % TiO_2 and the $(PEO)_{30}LiClO_4$ + 10 wt % SiO_2 membranes. It was found that ceramic filler can perform both as a sort of solid plasticiser for the polymer chains (by kinetically inhibiting their crystallisation and their reorganisation at ambient temperature) and act as solid solvent (by interacting with the lithium salt ionic species).

This has resulted in an enhancement, both at the macroscopic and microspoic level, of the electrolyte characteristics. Furthermore, the dispersion of the ceramic particles substantially improves the mechanical strength of the nanocomposite polymer electrolytes.

The recent work (Abraham, Koch and Blakely, 2000) was also presented a class of polymer-ceramic composite electrolytes in which the organic component is a gel electrolyte based on PVDF-HFP copolymer, and inorganic ceramic component is Li^+-conductive oxide solid electrolyte. The electrolyte films comprising PVDF (polymer host), PGDME-$LiN(SO_2C_2F_5)_2$ (plasticiser) and (LiAlTiP) as the ceramic filler have produced ionic conductivities of 2.6×10^{-4}, 3.7×10^{-4} and 6×10^{-4} S cm^{-1} at 20, 35 and 50^0C, respectively.

1.4 Project aims and rational

This research thesis was aimed to investigate a viability of modified natural rubber as polymer host to form polymer electrolyte systems for use in rechargeable lithium batteries at ambient temperature. Prior to the above interest the work devoted to the thesis title, Studies of Physical Properties of Novel Lithium Polymer Electrolytes. These can be outlined and identified as follows:

- To study fundamental concept underlying principle of polymer electrolyte system parallel to current polymer battery technology

- To improve deficiencies of conventional polymer electrolyte systems directed to its electrochemical device applications

- To extend the knowledge and develop the method of processes occurring in preparation of polymer electrolyte system

- To achieve reliable physical properties of polymeric electrolytic material compatible with rechargeable lithium battery system

- To seek alternative for a cheaper polymeric material in response to a critical price hike of commercial synthetic thermoplastic materials.

- To explore alternative approach for the future trend of polymer electrolyte system.

To achieve this, the following will describe the chapters of individual research tasks contributing for the thesis. In the Chapter 1 will describe a scope of research work undertaken with the thesis topic, Studies of physical properties of novel lithium polymer electrolyte. This will follow up by significance literature review of the beginning and recent polymer electrolyte related to thesis topic.

In Chapter 2 will present the theory part of lithium conducting polymer electrolyte and its applications. In Chapter 3, Experimental technique and instruments are discussed. In the following chapter of work conducted on Polymer electrolyte based on modified natural rubber will begin with a brief review of work reported in the literature, which is directly relevant to it. Then, will be followed by the presentation of the results of study. Next in Chapter 4 discusses plasticised and non-plasticised thermoplastic polyurethane based polymer electrolyte systems. Thus, in Chapter 5 modified natural rubber based systems containing doped and undoped lithium salt polymer electrolyte are discussed with emphasise on different level of salt concentration incorporated in the polymer host which leads to increase the conductivity and transition glass temperature. Properties of plasticised modified natural rubber based polymer electrolyte systems containing mixed composition EC/PC are also discussed.

The effect of concentration of the plasticiser, the methods of the preparation of the polymer film on the conductivity and thermal events of the system are discussed. In Chapter 6 the properties of the ENR/PEO blends both undoped and doped polymer electrolyte systems are discussed. The effect of the concentration of the PEO added into the ENR mixture on the conductivity and physical properties at ambient temperature is discussed.

Finally concluding remarks is drawn in Chapter 7 the physical properties of polymer electrolyte entire systems based on elastomeric TPU and modified natural rubber. The correlation between morphology, thermal analyses, infrared studies and ambient temperature conductivities is rationalised by introducing various amounts of electrolyte components in the investigated polymer hosts.

The structure of this thesis can be classified into two parts; First part involved studies on plasticised and non-plasticised TPU and modified natural rubber based polymer electrolytes; and the second part dealt with plasticised and non-plasticised polymer electrolytes based on modified natural rubber blend with PEO.

In the first part was investigated a series of polymer electrolytes employing thermoplastic polyurethane (TPU) and modified natural rubber polymer hosts. Soft solid rubbery electrolyte films were successfully produced using thermoplastic polyurethane and modified natural rubber with different level of lithium triflate salt introduced to the systems. Then, various compositions of TPU and modified natural rubber based containing salt with and without plasticisers were investigated. The properties of the polymer gel films such as ionic conductivity, thermal phase transition, infrared spectroscopy and mechanical strength were characterised.

The second part describes the entire experimental work dealt with preparation and characterisation of polymer electrolytes using epoxidised natural rubber (ENR) and its blends with polyethylene oxide (PEO) as polymer hosts.

The ENR/PEO blend based electrolytes were attempted for comparison purposes to the preceding work dealt with single polymer host electrolytes using thermoplastic polyurethane and modified natural rubbers. Basically, these samples were classified into two series as mentioned above with the compositional regimes of non-plasticised and plasticised polymer electrolytes at ambient temperature. In the first series neat masticated epoxidized natural rubber was chosen for this work, as principal host because of its interesting chemical structure and mechanical properties. Epoxidised natural rubber has an advantage as elastomeric amorphous is highly polar, which can easily dissolve in high dielectric solvent such as THF. The resulting dissolution of polymer in the solvent has produced viscous polymer solution, which can be easily cast to form film electrolyte. For the second series polymer electrolyte films of blends consisting of epoxidised natural rubber incorporated with PEO as disperse phase were prepared in similar manner.

The technique of sample preparation, percentage of ENR/PEO, its molecular weight and polarity seem to be crucial parameters in affecting the conductivity of ENR/PEO blend based polymer electrolyte systems studied. In this chapter the properties of blends consisting of epoxidised natural rubber (ENR) as polymer matrix component and various percentage of PEO as disperse phases are described.

The ENR/PEO blend based electrolytes obtained by the dissolution of the two high molecular weight polymers and other components in THF solvent followed by the evaporation of the solvent used. Despite the ease of preparation of the blend electrolyte systems they are even more difficult to evaluate than simple conventional polyether electrolytes as was pointed out in literature review.

The intent to obtain improved mechanical rigidity and ionic conductivity the blends of ENR/PEO compositions have been selected and optimised. To accomplish this, the salt, $LiCF_3SO_3$ concentration was fixed throughout this investigation while PEO content was varied to study the effect of addition of PEO into ENR- $LiCF_3SO_3$ polymer electrolytes by monitoring the morphology, thermal and ionic conductivity properties. As such the relation between phase structure, morphology and ionic conduction of the entire systems were discussed in detail.

From DSC data and SEM studies indicate that, the crystallinity of PEO can be inhibited by blending with epoxidised natural rubber (ENR). According to the results of SEM phase studies ENR/PEO blends polymeric electrolytes have been divided into inhomogeneous and partially miscible systems. The SEM images have shown that spherulite crystalline phase of polyethylene oxide predominate for the high weight percent containing PEO in the blend whereas addition of dopant salt and plasticiser into the blend revealed no traces of aggregates in the blends. It has been determined that a considerable increase in conductivity can be achieved by incorporation of mixed EC/PC into the system. This is consistent with tendencies observed by DSC (single transition glass at lower range temperature and no melting temperature in the upper range temperature) and impedance measurement.

The studies concerning the miscibility of ENR/PEO blends can also be observed from DSC and FTIR investigations. Thermal analysis has displayed a single glass transition temperature. FTIR spectra of pure ENR, pure PEO and their blend electrolytes (plasticised and non-plasticised) have been collected and analysed for comparison. Although the initial finding of ENR based electrolytes unable to achieve high ionic conductivity at 10^{-3} S cm^{-1} at room temperature, they partly contributed a novel material as host polymer. The oil crisis has triggered the rising cost of material to produce synthetic polymers. As such the manufacturers are looking for other option to explore natural polymer, which is cheaper and available.

Chapter 2. Lithium Conducting Polymer Electrolytes

2.1 Polymer Electrolyte Morphology

There are various structural states present in the polymer systems that can be considered in relation with the understanding of ion conduction in polymer electrolyte as far as polymer host is concerned. Generally, there are four stages that can exist in the polymer system to undergo phase transition behaviour upon heating or cooling. They are identified as crystalline, melting, glassy and elastomeric states. Crystalline state can be achieved by polymer, which can be arranged in highly-regular structures called crystallite. Each crystallite consists of rows of folded chains. This is often referred to a high degree homopolymers such as polyethylene and polyethylene oxide for which the structural repeat units are simple. For the crystallisation process to occur a sufficient thermal energy is needed to provide the necessary molecular mobility for the chain-folding process at temperature above transition glass temperature. There is no perfect crystalline polymer, even the most crystalline one contains unordered amorphous region. Crystalline polymers may exhibit both. Transition glass temperature corresponding to long-range segmental motions in the amorphous regions and a melting temperature, T_m, which disordered crystallites resulting an amorphous disordered melt is formed. For ionic conduction in polymer electrolyte system amorphous phase is preferable than crystalline phase.

In the melting state, a sufficient thermal energy is high enough for long segments of each polymer to move in random micro-Brownian motions. As the melt is cooled, the temperature below which all long-range segmental motions ceases. This temperature is known as the glass transition temperature, T_g. For example a fast cooling of a liquid homopolymer, a glassy state is formed. Below this temperature, physical properties such as density, viscosity, diffusion and conduction become less sensitive to temperature. The last state, which is unique to polymeric material and highly preferential to polymer electrolyte systems refer to elastomeric state.

This is generally a high temperature event, above T_g in which long-range segment mobility is prohibited by either chain entanglement, at very high molecular length or cross-link network. At macroscopic point of view, polymers at this state are rubbery or elastic, i.e. deformation occurs when applying a stress to it but revert to its original size by removal of the applied stress. At microscopic level they are liquid-like, mobile create a small amount of space or free volume, which promote vibrational motion can occur.
From the above account it presents that the distinction between the various states of polymer is significant to ionic conductivity approach. The selection of polymer host can be determined from its chemical structure whether it will be crystalline or amorphous in the solid state. Thus, based on reviewed article/journals the ionic conductivities become prominent in the liquid or elastomeric state, where there is sufficient molecular mobility persist.

2.2 Mechanism of ionic conductivity

The mode of ionic transport in polymer electrolyte systems differ from ceramic-based or glass solid electrolyte by quite a different mechanism. Ion transport in polymer occurs by reforming and breaking coordination with coordinating site atom aided by segmental motion of the polymer backbone. On the other hand in ceramic-based solid electrolyte ion is transported by means of hopping within interstitial sites in the rigid solid framework. These features can be illustrated in Figure 2.1 and 2.2. The idea of ionic conduction applied in plasticised polymer system is governed by the electrolyte species of low molecular weight, high dielectric constant solvent encapsulated in the polymer matrix.
In the early 1970's research into ion conducting polymers began in the solid electrolyte field indicate that conductive properties were initially assigned to the crystalline complexes according to the solid state vacancy mechanism.

Conductivity was suggested based on the hopping of cations between vacant sites in a regular helical polymer sheath, paralleling the hopping mechanism of the conventional solid-state ionic conductors. NMR studies carried out by Berthier and co-workers (1983) have changed the direction that polymer electrolyte research was to take. The idea of ions moving through crystalline material along helical tunnels was incorrect.

NMR experiments showed that the mobility of ions belonging to an amorphous phase is higher than those belonging to a crystalline polymer phase. The ionic conductivity in polymer electrolyte is generally fitted in terms of the Vogel-Tamman-Fulcher (VTF) equation (Armand *et al*, 1979). It can be expressed as

$$\sigma = \frac{A}{T^m} \exp\left(\frac{-E_0}{T - T_0}\right)$$

The polymer segmental motion promotes ion mobility by making and breaking the coor-dination bonds between cation and polymer and providing free volume into which ion can diffuse under the influence of an electric field. Figure 2.2 shows this type of motion schematically.

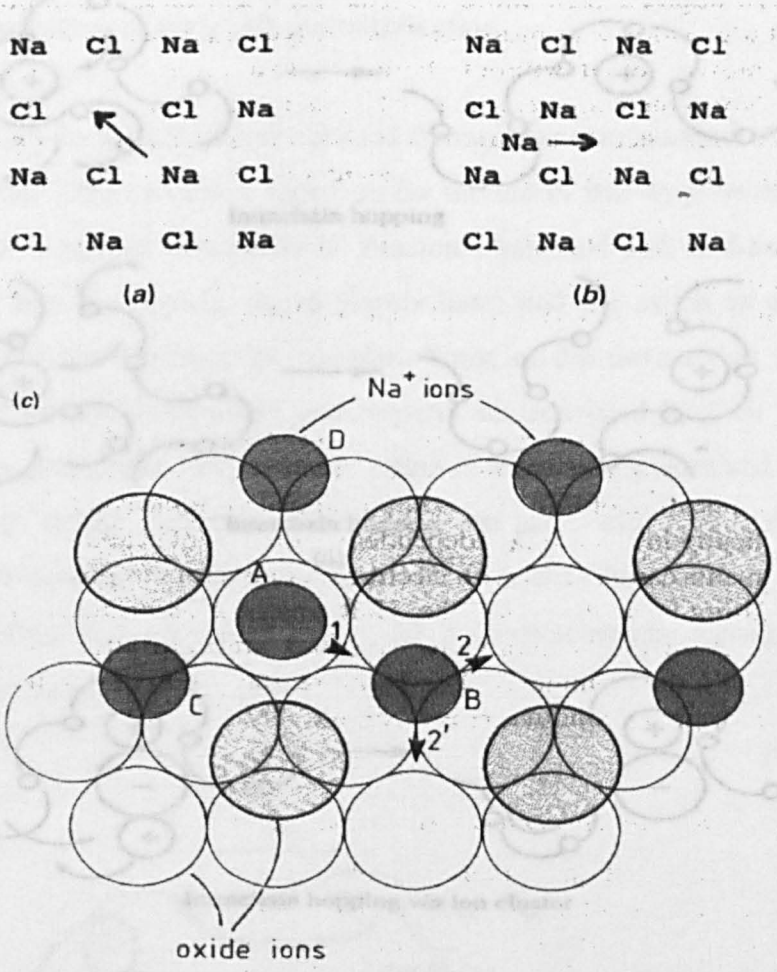

Figure 2.1 Illustration of ionic conduction mechanism in solid electrolytes. (a) Vacancy (b) interstitial and (c) interstitialcy conduction mechanism. In (c), Na^+ ion A can move only by first ejecting Na^+ from its site. Source: From Bruce (1995).

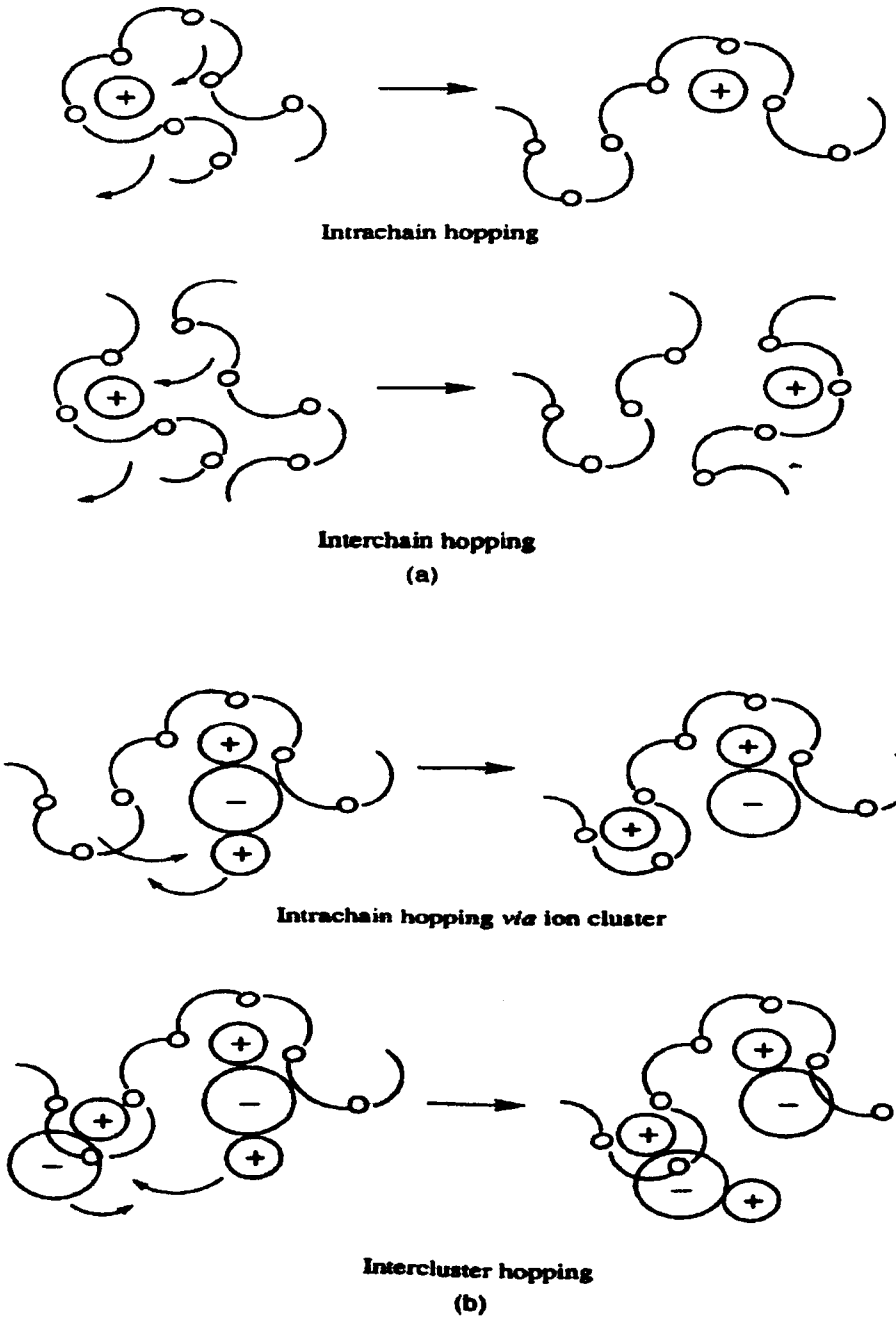

Figure 2.2 Representation of cation motion in a polymer electrolyte; (a) assisted by polymer chain motion only; (b) taking account of ionic cluster contributions. Source: From Bruce (1995).

2.3 Incorporation of ionic salt and implication

Polymer electrolytes are complexes obtained through direct interaction of alkali salt and a macromolecule. The concept is based on the motion of ions in polymeric matrices in the absence of a solvent. According to Pearson's hard and soft acid-base theory, the polymer acts as a nucleophilic ligand (Lewis base) and the cation as an electrophile (Lewis acid) for the formation of complex. Some of the factors that limit polymers compare to their liquid-electrolyte counterparts are restricted by their low dielectric constant, crystalline phase morphologies, range of molecular weight and dissolution of ionic salt leads to the formation of free ions, ion pairs, triplets and multiplets. The resulting ionic conductivity value produced is lower than liquid based electrolytes at room temperature. For example in Figure 2.3 is given schematic representation of the ionic species in polymer/salt complex.

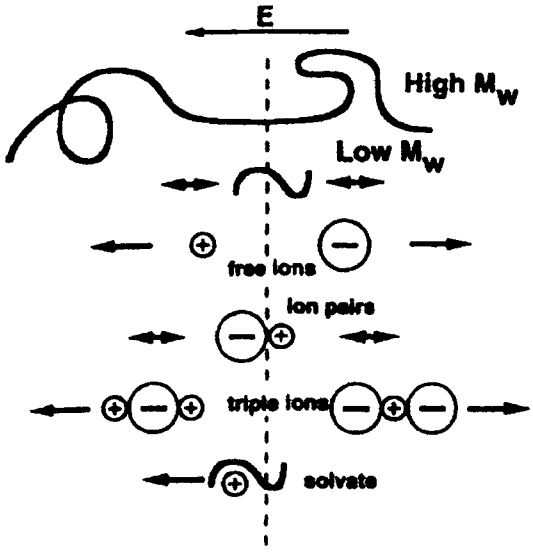

Figure 2.3 Schematic illustrations of the species presence in a polydisperse solvating polymer/salt complex. Source : From Baril *et al* (1997).

2.4 Addition of plasticiser or co-solvent

Polymers that have little or considered non ion-solvating properties can be transformed to become ionic conductors by incorporating a compatible plasticiser. The choice of using liquids with low vapour pressure and high dielectric constant introduce into the polymer system to lower its transition glass temperature is widely used. The plasticiser is absorbed into the polymer structure and the resultant sample appears as single-phase soft rubbery material. For instance, PMMA plasticised with EC/PC plasticisers has changed its hard tough resin to become soft elastomeric material. The plasticisers converts the parent, semicrystalline, polymer electrolyte into an amorphous material, lower the electrolyte viscosity and increase ionic mobility by reducing the potential barrier to ionic motion. Diffusion of plasticiser from the polymer matrix in the long-term storage has reduced the ionic conductivity properties of the polymer electrolyte system. However, addition of cosolvent into polymer matrix has increased the uptake of plasticiser and retaining the solvent effectively within polymer electrolyte system. PVC based electrolyte system using vinyl acetate as cosolvent has proven an increase of ionic conductivity.

2.5 Application in lithium polymer batteries

The ultimate system is targeted to operate in a suitable battery that generates a large amount of energy in a small package. The solid lithium polymer battery, which is both light and safe, actually uses polymer gel electrolytes. There is a huge demand in the current world market because this leading edge rechargeable polymer battery technology is ideal for cellular telephone, notebook computers, and other portable electronic applications. For almost 20 years since the early development of polymer electrolyte technology in 1978, only a few organisations have long-term expertise in lithium polymer electrolyte rechargeable battery technology.

Recently, Ultralife Batteries Incorporation, U.S.A (Osaka, 1999) has produced solid polymer electrolyte battery to generate 4.0 V. A U.K company, AEA (Daily Mail, 1999) has recently announced the production of lightweight batteries.

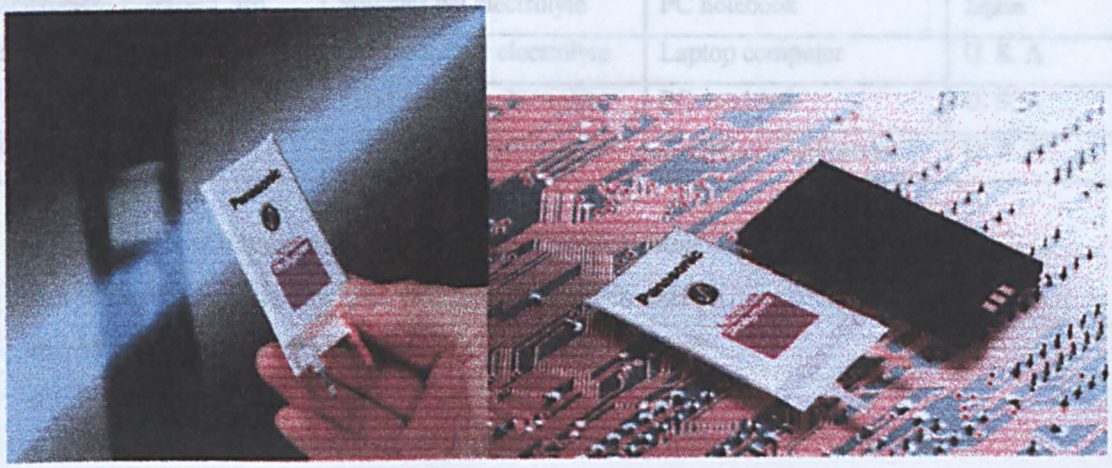

Figure 2.4 Lithium ion Polymer batteries. Source: From Osaka, (1999)

Presently, there are significant increases in the level of research and development activities in Asia related to polymer electrolytes. These activities are mainly focussed on the development of practical devices using gel-based polymer systems. In Japan, the Mitsubishi Electric Company has developed batteries using polymer gels. Figure 2.4 shows a photograph of Li-ion polymer battery the latest development by Panasonic.

Established research organisations and battery companies have made efforts relating to polymer gel systems using novel synthesised polymers for solid polymer batteries. Some of the most important activities are given in Table 2.1.

Table 2.1 Lithium Polymer Electrolyte Battery Technology Development Activity in some countries worldwide.

Developer	Technology	Application	Country
3M-Hydro-Quebec[a]	Solid polymer electrolyte	Electric vehicle	N. America
Belcore[b]	Polymer gel electrolyte	LCD display	N. America
Mitsubishi Electric Corp[c].	Polymer gel electrolyte	PC notebook	Japan
Battery Engineering, Inc[d].	Solid polymer electrolyte	Laptop computer	U. S. A
Ultralife Batteries[e]	Solid polymer electrolyte	PC notebook	U. S. A
Ultralife & Lockheed [f]	Solid polymer electrolyte	Aerospace Equipment	U. S. A

a- http://www.lithium polymerbattery.com/perform.html

b- http://www.edtn.com/news/oct12/101298tnews2.html.

c- http://www.edtn.com/news/dec04/120498tnews2.html

d- http://www.batteryeng.com/whats_new.html

e- http://www.polymerbattery.com/sss.html

f- http://www.grc.nasa.gov/WWW/RT1998/5000/5420hagedorn.html

Most recent research and development activities have been focused on ambient temperature applications, and consequently on the improvement of the ambient conductivity of polymer electrolyte systems. To date numerous reports and patents have reported that polymer gel electrolytes achieved considerable ionic conductivitity in the range 10^{-4} - 10^{-3} S cm^{-1}at ambient temperature. Some of the recent polymer electrolyte systems are listed in Table 2.2.

Table 2.2 Some polymer gel electrolyte systems using various types of polymer hosts

Polymer electrolyte system	Conductivity/Scm^{-1}	Temp/ ^{0}C	Ref
PAN/EC/PC/$LiClO_4$	$1.1x10^{-3}$	25	f
Diacrylate/PC/$LiPF_6$	$1.0x10^{-3}$	25	g
PVDF/DMF/$LiCF_3SO_3$	$1.6x10^{-3}$	25	h
i-PMMA- a-PMMA /PC/$LiCF_3SO_3$	$1.6x10^{-3}$	25	i
AMC/EC/DMC/ $LiClO_4$/fume silica	$5.3x10^{-4}$	25	j
TPU/EC/PC/ $LiCF_3SO_3$	$1.0x10^{-3}$	25	This work
ENR/EC/PC/ $LiCF_3SO_3$	$2.9x10^{-4}$	25	This work
MG-49/EC/PC/ $LiCF_3SO_3$	$3.2x10^{-4}$	25	This work

[f] Appetecchi, Croce, and Scrosati, (1997).

[g]Hikmet, Peeters, Lub and Nijssen, (1999).

[h]Heuman and Stevens, (1995).

[i]Yavaroy, Wang and Wunder, (1999).

[j]Kim, Oh and Choi, (1999).

Chapter 3. Experimental Techniques

This chapter will describe some of the most important parts of the experimental work in relation to the methodology of this thesis topic is concerned. By definition of polymer electrolyte system, it consists of a polymer matrix to act as a host for a guest of an alkali metal salt. The current work is pursued after taking into consideration the basic knowledge and understanding with guided references from journals the related aspect of work to the thesis topic. The materials were chosen and experimental works proceed for the preparation of the polymer electrolyte systems. Characterisation techniques utilising DSC, impedance spectroscopy, SEM, FTIR performed on the prepared samples were also discussed. The main components of polymer electrolyte systems are the polymer matrix to act as a host and a guest for an alkali metal salts. Additives such as plasticisers were used to enhance the ionic properties of the polymer electrolyte systems. To achieve this, the materials concerned to formulate the polymer electrolyte system for the investigation are detailed in Table 3.1 and 3.2.

Table 3.1 Some characteristics of polymer hosts used

Material	T_g/ °C	M_w	M_n
[a]Masticated ENR25	-43	271 000	139 600
[b]Masticated ENR50	-24	258 000	148 300
[c]Heveaplus MG-49	-61	970 000	203 000
[d]Desmopan 385	-42	367 000	143 000
[e]PEO	-60	600 000	

M_w : Weight average molecular weight

M_n : Number average molecular weight

Notation:

[a]Masticated ENR25 and [b]ENR50- The masticated samples were supplied by Tun Abdul Razak Research Centre London. The ENR rubbers are nominally of 25 and 50 mol % epoxidation level.

[c]Heveaplus MG-49- Methyl methacrylate grafting natural rubber latex was obtained from Green HPSP Company, Petaling Jaya, Malaysia.

[d]Desmopan 385-Thermoplastic poly (ester)-polyurethane was supplied by ALBIS Company, U.K. [e]PEO- Poly(ethylene oxide) was purchased from ALDRICH supplier.

Table 3.2 Details of the chemicals used.

Chemicals	Abbreviation	Source	Molecular mass	Purity
Lithium triflate	$LiCF_3SO_3$	Fluka	156.01	99.8
Ethylene carbonate	EC	Fluka	88.06	99.8
Propylene carbonate	PC	Fluka	102.09	99.7
Tetrahydrofuran	THF	Aldrich	72.12	99.9
Toluene	$C_6H_5CH_3$	Aldrich	92.14	99.8

A dopant salt with a large anion is chosen to maximise the solubility and dissociated ion concentration. Lithium triflate was selected from a number ionic salts being used because of their extensive charge delocalisation and low lattice energy. The chosen salt was easily soluble in the polymer electrolyte system at ambient temperature. The structure of the salt is depicted below.

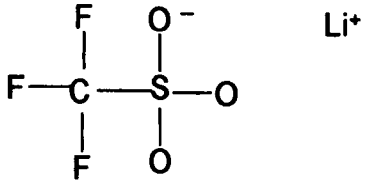

Figure 3.1 Structure of lithium trifluoromethane sulfonate

Plasticisers using ethylene carbonate (EC) and propylene carbonate (PC) mixtures have been chosen in this work as plasticising solvent systems. Comprehensive studies have been published on EC-PC mixtures (Klassen, Aroca and Nazri, 1998; Tao Li and Balbuena, 1999; Croce, Appetecchi, Mustarelli, Quartarone, Tomasi and Cazzanelli, 1998). Solutions of lithium salts in cyclic organic solvents such as EC/PC mixtures are used as electrolytes and have proven to be among the most efficient in term of battery cyclability. EC has been proposed as a better solvent than PC due to its higher dielectric constant and lower viscosity. These properties enhance ionic conductivity because they favour salt dissociation and high ionic diffusion rates.

The physical properties and molecular structures of the plasticizing solvents used in this work are given in Table 3.3 and Figure 3.2.

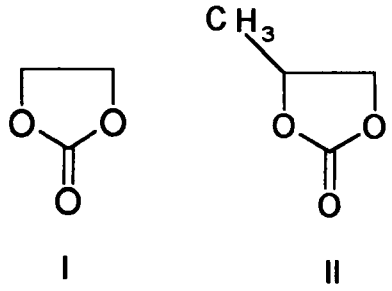

I II

Figure 3.2 Chemical structures of EC (I) and PC (II).

Table3.3 Physical properties of plasticisers used in this study

Solvents	Molar mass	m.p. (^{0}C)	b.p. (^{0}C)	Density (g/cm^3)	Dielectric constant	Viscosity (cP*)
EC	88.1	39.5	248	1.32	89.6	1.86
PC	102.1	- 49.2	241	1.20	64.4	2.53

* 1 cP = 0.001 kg m^{-1} s^{-1}

3.1 Polymer electrolyte composition

In the polymer electrolyte system formulation it is possible to calculate the lithium ion concentration relative to the other components in various ways that make different assumptions about the nature of the complex formation. Lithium ions may be regarded as complexing solely with the solvent or alternatively with the polymer and the solvent. In addition the nature of the complex in each case is not clearly identified. Lithium contents in polymer electrolytes are usually expressed in terms of an O/Li ratio based on the atomic concentration of each element, but only those atoms believed to complex with lithium are included in the calculation. Thus the O/Li ratios in this work are given by the following generic formula as shown below:

For example the calculation of O/Li is presented for $(ENR25/50)_x$($LiCF_3SO_3$) system,

$$O/Li = \frac{(m_p \times MW_s) \times n_p}{m_s \times MW_m}$$

where, MW_m : molar mass of monomer

MW_s : molar mass of salt

m_s : mass of salt

m_p: mass of polymer

n_p : no. of active oxygen atoms per repeat unit

e.g. ENR25/ $LiCF_3SO_3$ system

$$O/Li = \frac{2.0 \times 156}{0.1 \times 288}$$

$$= 11$$

The ratio of O/Li for plasticised system, ENR25/ $LiCF_3SO_3$/EC/PC was calculated by the following equation,

$$O/Li = \frac{(m_T \times MW_s)}{m_s \left[\frac{MW_m}{n_m} + \frac{MW_{EC}}{n_{EC}} + \frac{MW_{PC}}{n_{PC}} \right]}$$

Where, MW_s : molar mass of salt

MW_m : molar mass of monomer

MW_{EC} : molar mass of ethylene carbonate

MW_{PC} : molar mass of propylene carbonate

m_T : total mass of polymer + plasticisers

n_m : no. of active oxygen per monomer unit

n_{EC} : no. of active oxygen in ethylene carbonate

n_{PC} : no. of active oxygen in propylene carbonate

3.2 Preparation of polymer electrolyte films

Solvent casting technique was used to prepare most of the films for this work. The technique of film preparation adopted one of the methods described in the literature (Tsuchida *et al* 1983). First of all, it involved dissolution of ENR rubber and $LiCF_3SO_3$ salt in tetrahydrofuran solvent. It was stirred magnetically for about 24 h at room temperature until a homogeneous solution was obtained. For plasticised polymeric electrolytes, appropriate amounts of plasticisers were added into the viscous homogeneous solution, which was stirred further for another 12 hours. Thin films of the ENR polymer films, were obtained typically 0.2 –0.3mm thick, prepared by casting the viscous polymer solution inside a glass ring placed on a Teflon plate. Solvent evaporation was conducted in the fume chamber until pinhole-free films of uniform thickness visually observed. The samples were initially dried at room temperature and then transferred to a vacuum oven for final drying at about 45-50^{0}C.

3.2.1 $(MG\text{-}49)_n$ $LiCF_3SO_3$ system

The first step was casting of MG-49 latex to obtain a dry rubber film. Then the MG dried rubber film was sliced into grain size. About 4 weight percent MG-49 polymer concentration was prepared by dissolving 4.0 g of it in 250 cm^3 quickfit stoppered conical flask, containing 100 cm^3 of toluene with efficient magnetic stirring (Kohjiya *et al* (1990). It was left overnight with continuous stirring until there was complete dissolution of polymer into clear viscous solution. A lithium triflate salt solution of tetrahydrofuran (THF) was prepared separately. Then, these two solutions were mixed together to obtain a homogenous solution.

The solutions were cast onto glass ring moulds with Teflon sheet underneath and the solvent was allowed to evaporate in a fume cupboard at room temperature. A free-standing film was obtained when all the solvent had evaporated off. Residual solvent was further removed in a vacuum oven for 48 h at 50^{0}C.

The samples were reweighed to check whether any solvent loss had occurred, and stored in sealed containers in a desiccator. The compositions of prepared electrolytes are presented in Table 3.4 and 3.5.

3.2.2 ENR rubber based polymer electrolyte system

The masticated ENR rubber was cut into grain size and dissolved into tetrahydrofuran with efficient magnetic stirring. The viscous solution of ENR rubber was formed after it was left overnight with continuous stirring. Then lithium triflate salt was added to the solution. The THF solution of the ENR rubber mixed with lithium triflate was cast into glass ring formers on a Teflon surface. A free-standing polymer electrolyte film of ENR rubber was obtained after the THF solvent evaporated off. The final films were further dried under vacuum oven for 48 h to remove residual solvent. Then, the films were kept in desiccator until further use. The detailed compositions of the prepared electrolyte were listed in Tables 3.6, 3.7, 3.8 and 3.9.

Table 3.4: The compositions of MG 49 /$LiCF_3SO_3$ system

No.	1	2	3	4	5	6
NR-MG49 LS	4	4	4	4	4	4
$LiCF_3SO_3$	2	5	10	15	20	60

Table 3.5: Compositions of the MG 49/ $LiCF_3SO_3$ /EC/PC system

No	1	2	3	4
NR-MG49 LS	4	4	4	4
EC+PC	25	50	100	200
$LiCF_3SO_3$	5	5	5	5

Table 3.6: Compositions of ENR-25/ $LiCF_3SO_3$ systems

No	1	2	3	4	5	6
Masticated ENR-25[a]	4	4	4	4	4	4
$LiCF_3SO_3$[b]	2	5	10	15	20	60

[a]wt.% relating to polymer.

[b]wt.% relating to polymer

Table 3.7: Compositions of ENR-25/ EC/PC/ $LiCF_3SO_3$ systems

No	1	2	3	4
Masticated ENR-25	4	4	4	4
EC+PC	25	50	100	200
$LiCF_3SO_3$	5	5	5	5

Table 3.8: Compositions of ENR-50/ $LiCF_3SO_3$ systems

No	1	2	3	4	5	6
Masticated ENR-50	4	4	4	4	4	4
$LiCF_3SO_3$	2	5	10	15	20	60

Table 3.9: Compositions of ENR-50/ EC/PC/ $LiCF_3SO_3$ systems

No	1	2	3	4
Masticated ENR-50	4	4	4	4
$LiCF_3SO_3$	5	5	5	5
EC+PC	25	50	100	150

All electrolyte components are given as weight percent (wt. %) relative to polymer dry weight. ENR rubber is given in weight percent (wt. %) relative to solvent. The amount of plasticiser is expressed in wt. % relative to ENR polymer.

Example, $y\% = \left[\frac{wt(P)}{wt(ENR}\right] \times 100$

3.2.3 ENR/PEO blend based polymer electrolyte system

All the electrolytes were prepared by solvent cast technique. The solution of film cast were prepared by dissolving appropriate amounts of the ENR rubber, PEO and $LiCF_3SO_3$ together in THF solvent. The viscous solutions were poured into the same sized glass moulders and the THF was allowed to evaporate under atmosphere at room temperature. After evaporation of the THF, mechanically free-standing films of the same weight and similar thickness (250-300μm) were obtained and peeled from the moulder. The films were further dried in the vacuum oven at 45-50^{0}C to remove any traces of THF solvent.

3.2.4 Thermoplastic Polyurethane (TPU) based electrolyte systems.

All samples were obtained by the solvent casting technique. Appropriate amounts of PU resin and salt were mixed and dissolved in THF to form the 4 % by weight solution. The compositions of the prepared samples are presented in Table 3.10 and 3.11.

Table 3. 10: Compositions of TPU/ $LiCF_3SO_3$ system.

No	1	2	3	4	5	6	7
Desmopan 385	4	4	4	4	4	4	
$LiCF_3SO_3$	20	30	40	50	60	70	100

Table 3. 11: Compositions of TPU/EC/PC/ $LiCF_3SO_3$ system

No	1	2	3	4	5	6
Desmopan 385	4	4	4	4	4	4
$LiCF_3SO_3$	20	20	20	20	60	70
EC/PC	20/20	30/30	40/40	50/50	60/60	70/70

All electrolyte components are given as weight percent (wt. %) based on polymer dry weight.The amount of plasticiser is expressed as weight percent (wt. %) of the TPU present.

Example, $y\ \% = \left[\frac{wt(P)}{wt(TPU)}\right] \times 100$

3.3 Characterization Techniques

3.3.1 Impedance Spectroscopy

A Solartron model 1250 Frequency Response Analyser and 1286 Electrochemical interface was used to measure the impedance of electrolyte films of known thickness at constant pressure cell with blocking electrodes. The samples were scanned at frequency range 0.1 Hz to 65 kHz.

3.3.1.1 Conductivity cell for polymer electrolytes

A schematic diagram of the apparatus is given in Figure 3.3. A typical complex impedance spectrum at ambient temperature for gel electrolyte is depicted in Figure 3.12. It shows a flattened semicircle and a non-vertical spike (described section 3.3.1.1.1). The point at which the semicircle and spike meet on the real axis gives the value for R_b. The conductivity of the gel electrolyte was calculated from the expression:

$$\sigma = l/R_b A$$

Where; l is the thickness of the polymer electrolyte film;

R_b is the bulk resistance value; A is the surface area of the polymer electrolyte film.

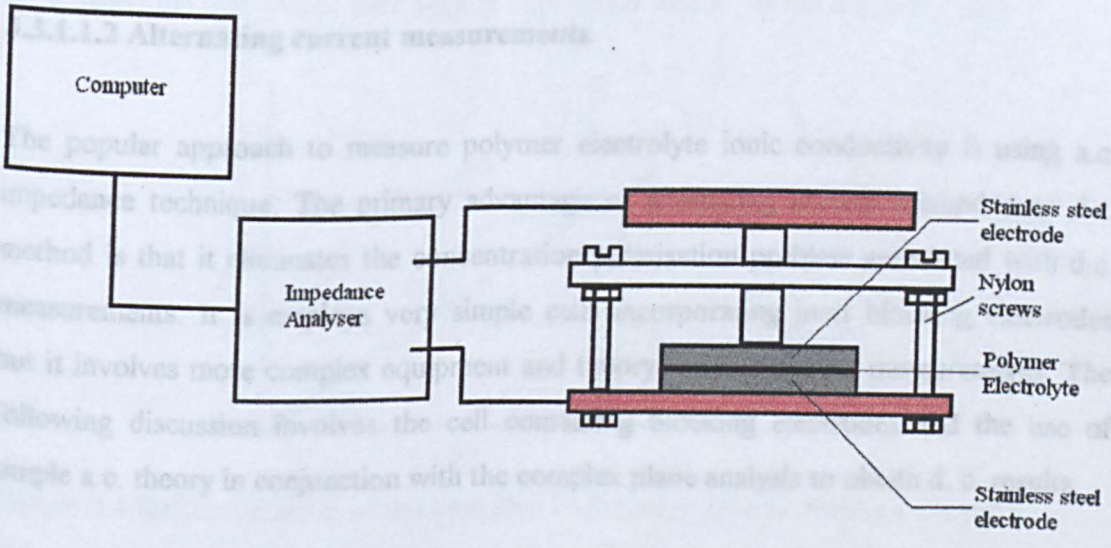

Figure 3.3: Schematic diagram of the conductivity apparatus for polymer electrolyte.

3.3.1.1.1 Conductivity measurements in polymer electrolytes

Polymer electrolytes are basically complexes between the polymers and ionic salts. The polymer acts as a solvent for a salt charge carrier, which becomes partially dissociated in the matrix leading to electrolyte behaviour. Ionic conductive polymers generally exhibit a modest ionic conductivity ~ 10^{-5} S cm^{-1} at room temperature. It is preferable for a polymeric electrolyte to have acceptable ionic conductivity for electrochemical device application with negligible electronic contribution. To achieve maximum ionic conductivity in a polymeric material it must possess a large number of ionic charge carriers as well as high ionic mobility. The ionic conductivity of an electrolyte can be expressed in the equation by the sum of the product of the concentration of ionic charge carriers and their mobility, written as;

$$\sigma = \sum n_i z_i \mu_i$$

In this equation, n_i is the number of charge carriers, z_i is the ionic charge and μ_i is ionic mobility. Ionic conduction measurements can be obtained by D.C (direct current) or a.c methods.

3.3.1.1.2 Alternating current measurements

The popular approach to measure polymer electrolyte ionic conductivity is using a.c. impedance technique. The primary advantage of alternating current method over d.c. method is that it eliminates the concentration polarisation problem associated with d.c. measurements. It is employs very simple cells incorporating inert blocking electrodes but it involves more complex equipment and theory to interpret the measurements. The following discussion involves the cell containing blocking electrodes and the use of simple a.c. theory in conjunction with the complex plane analysis to obtain d. c. results.

3.3.1.1.3 Simple a. c. theory

In an a. c experiment a sinusoidal voltage is applied to a cell and the sinusoidal current passing through the cell as a result of this perturbation is determined. Two parameters are required to relate the current flowing to the applied potential. One represents the opposition to the flow of charge and is equal to the ratio of the voltage and current maxima, V_{max}/I_{max} and is analogous to the resistance in direct current (d.c) measurements. The other parameter is the phase shift, ϕ, of the voltage and current. The combination of these parameters represents the impedance, Z, of the cell. For an electrochemical cell, both the magnitude of the impedance $|Z| = V_{max}/I_{max}$ and its phase angle θ are functions of the applied frequency. A typical a.c. experiment consists of determining the complex impedance of a cell as a function of the signal frequency and presenting the results in the form of a complex impedance plot. The impedance has both a magnitude and a direction and is therefore a vector quantitiy. Thus, it is represented in terms of (a) its magnitude and phase angle, $|Z|$ and θ, or by its real and imaginary parts within the complex impedance plane. Figure 3.4 shows a diagram generally known as complex plane plots.

Z' is called the real part of the complex impedance and Z'' is the imaginary part.

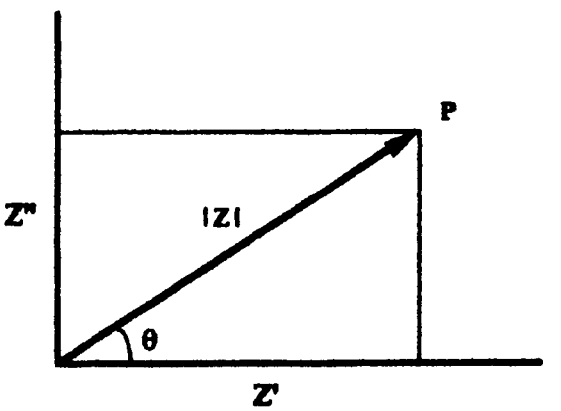

Figure 3.4 Representation of the complex impedance plot or Argand diagram.
Source: From, MacCallum and Vincent, (1987).

The simple equivalent circuit consists of individual components, principally resistors and capacitors to model the impedance data of the electrochemical cell.

a) **Resistor**

A sinusoidal voltage applied across a resistor is in phase with the current passing through it. The amplitude of the current waveform is reduced as shown in Figure 3.5. Figure 3.6 shows the result of the electrochemical cell containing a pure resistor, **R**, the phase angle, θ, is zero and the imaginary part of the impedance is also zero. Therefore the Argand diagram (Figure 3.6) has only a single point because there is no dependency on the a.c. frequency.

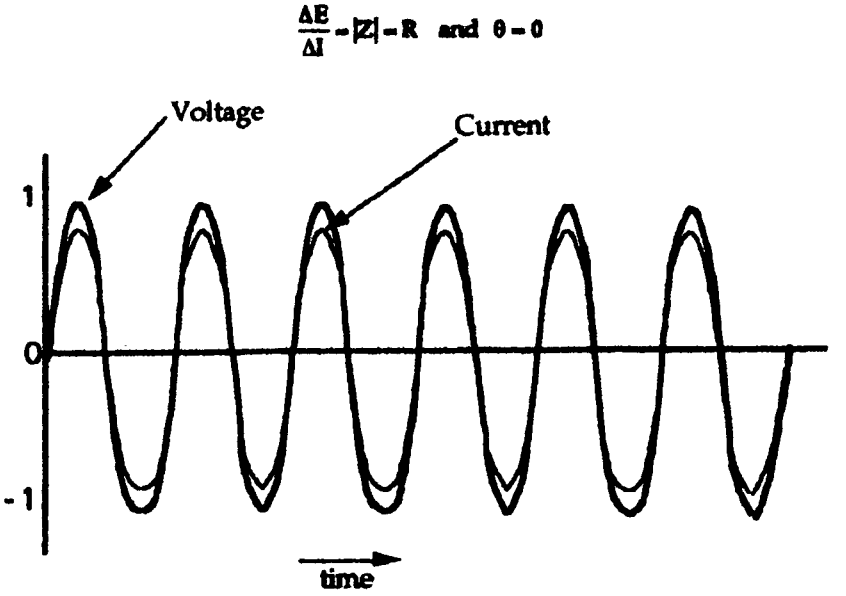

Figure 3.5 Relationship between a sinusoidal voltage and current response for pure resistor.

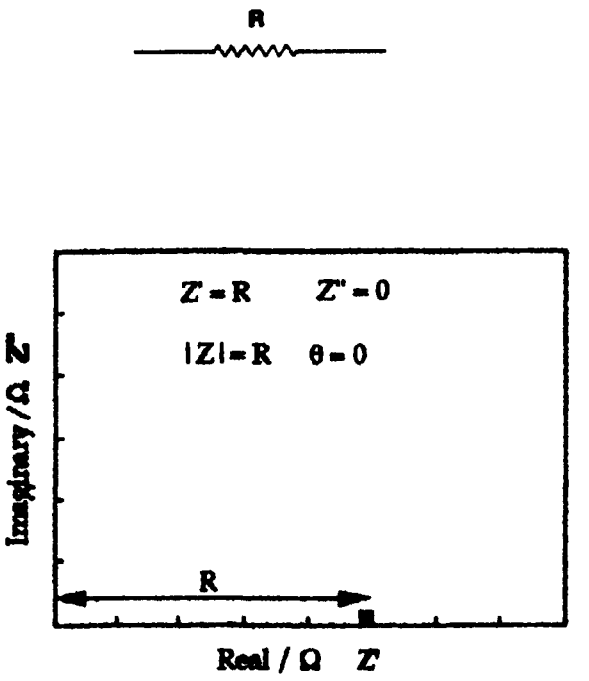

Figure 3.6 Representation of a resistor in the complex impedance plane.

b) Pure capacitor

For an electrochemical cell containing a pure capacitor the voltage lags behind the current by 90^0 or $\theta = -\frac{\pi}{2}$ as shown in Figure 3.7.

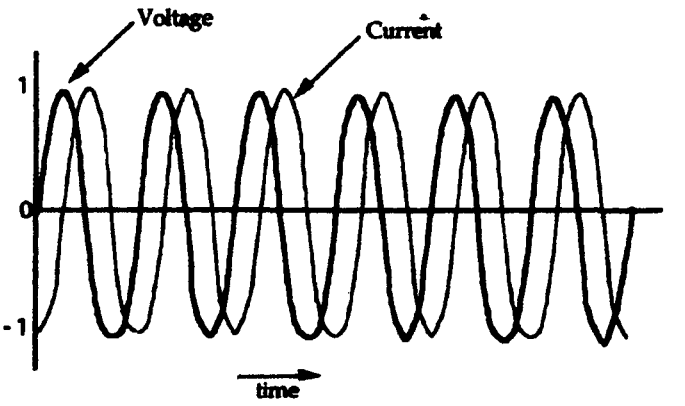

Figure 3.7 The relationship between a sinusoidal voltage and the current response for a pure capacitor.

The result of this is that the real part of impedance becomes zero, the imaginary part has a value of $\frac{j}{\omega C}$ and the impedance is frequency dependent. As a function of frequency, the impedance of a capacitor defines a vertical line in parallel with the imaginary axis (Figure 3.8). The impedance of the circuit can be described mathematically as

$$|Z| = \frac{1}{j\omega C}$$

where j = $\sqrt{-1}$ and $\omega = 2\pi f$.

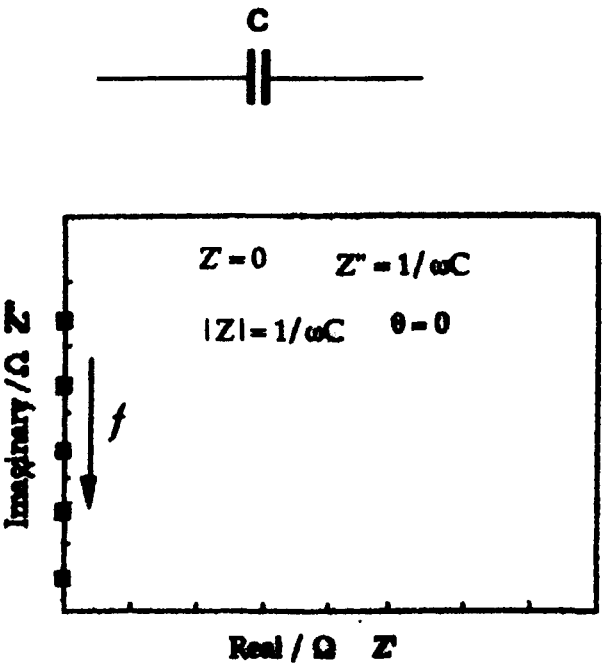

Figure3.8 Representation of a capacitor in the complex impedance plane.

In actual fact electrochemical cells do not contain single components but consist of the combination of components themselves. The equivalent circuit involves correct combination of capacitors and resistors for complex plane analysis to modelling the impedance data whose frequency response is the same as that of the test cell.

For this the two simplest networks of components or equivalent circuits are considered:

i) Resistor and capacitor in series

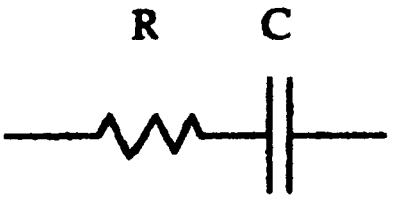

For series circuits it means that for a resistance and capacitance in series the individual impedances are directly additive. Complex impedance plots in Figure 3.9 illustrate this.

$$Z_{total} = Z_1 + Z_2 + Z_3 + ...$$

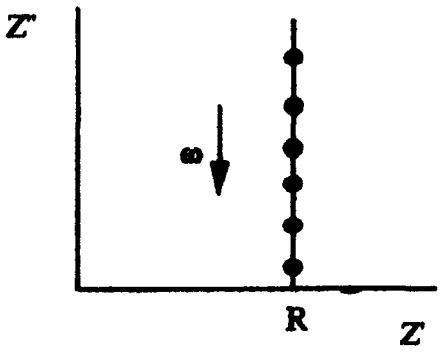

Figure 3.9 Complex impedance plots for a combination of a resistor, R, and capacitor in series.

$$\mathbf{Z} = \mathbf{R} - \mathrm{j}\,\frac{j}{\omega C}$$

The complex impedance plane therefore takes the form of single vertical line intercepting the axis for the real component at the value of R.

For parallel combinations:

When resistance and capacitor are connected in parallel, however, the impedances are not directly additive, but addition of the reciprocal impedance contributions for each of the components as below;

$$\frac{1}{Z_T} = \frac{1}{\sum Z_i}$$

Hence, the total impedance;

$$\frac{1}{Z_T} = R\left[\frac{1}{1+(\omega CR)^2}\right] - j\,R\left[\frac{\omega RC}{1+(\omega RC)^2}\right]$$

A resistor and capacitor in parallel gives a semi-circle on the real axis with diameter, **R** in Figure 3.10.

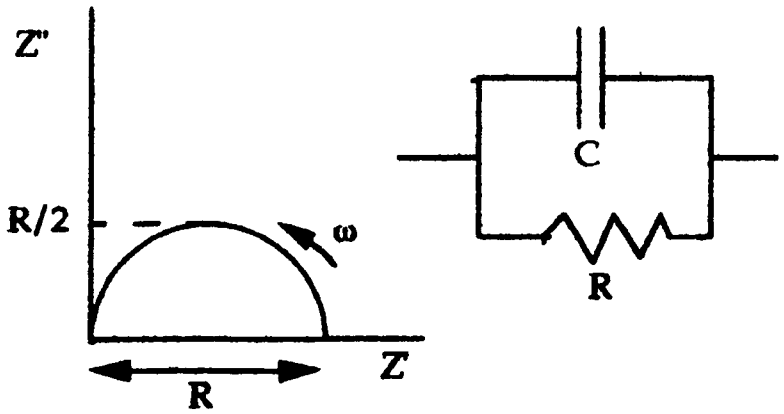

Figure 3.10 complex impedance plots for a combination of a resistor, R, and capacitor in parallel.

This work was used in the test cell, which had the following configuration;

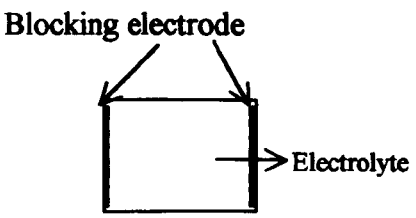

In the ideal equivalent circuit, it considers the following contributions

i) R_b and C_g denote the resistance of the bulk electrolyte resistance and geometric capacitance

ii) C_{dl} represents the double-layer capacitance at the electrode/electrolyte interface

The ideal equivalent circuit produces the impedance plot shown in Figure 3.11 Finally a resistance and capacitance in parallel, which are than combined in series with another resistance gives a semicircle and vertical spike.

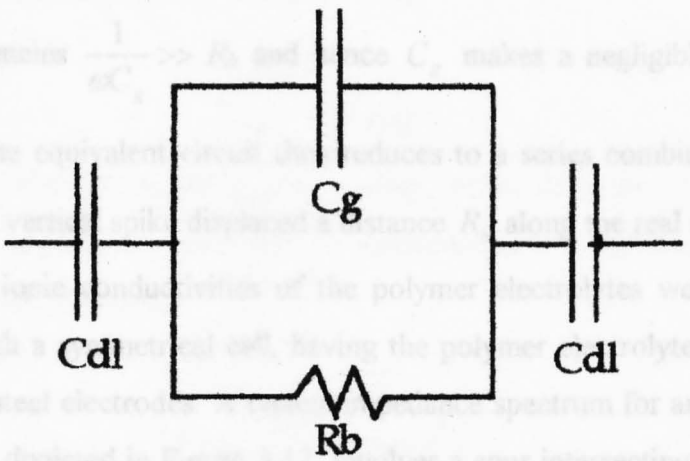

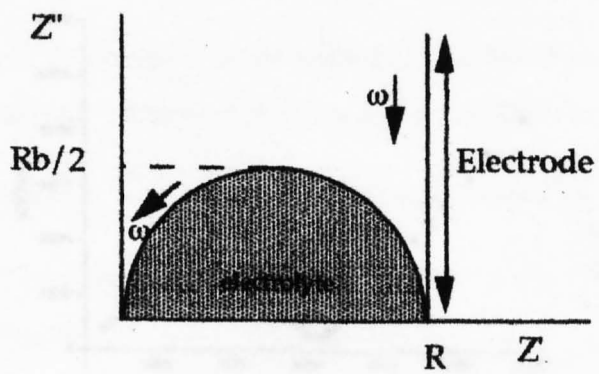

Figure 3.11 Equivalent circuit and related complex impedance plot.

The total impedance of the equivalent circuit is given below:

$$Z_T = \mathrm{R_b}\left[\frac{1}{1+(\omega R_b C_g)^2}\right] - j\left(R_b\left[\frac{\omega R_b C_g}{1+(\omega R_b C_g)^2}\right] + \frac{1}{\omega C_{dl}}\right)$$

From the equation it can be seen that the terms contain ω and hence they are frequency dependent. Therefore at high frequencies the equivalent circuit reduces to a parallel $R_b C_{dl}$ combination which gives rise to the semicircle in the complex impedance plane.

At low frequencies $\frac{1}{\omega C_g} >> R_b$ and hence C_g makes a negligible contribution to the impedance. The equivalent circuit thus reduces to a series combination of R_b and C_{dl} appearing as a vertical spike displaced a distance R_b along the real axis.

In reality the ionic conductivities of the polymer electrolytes were evaluated by a. c. impedance with a symmetrical cell, having the polymer electrolyte sandwiched between two stainless steel electrodes. A typical impedance spectrum for an ENR-based polymer electrolyte, as depicted in Figure 3.12, involves a spur intersecting the real axis (i.e., the Z' axis). It shows a flattened semi-circle and a non-vertical spike.

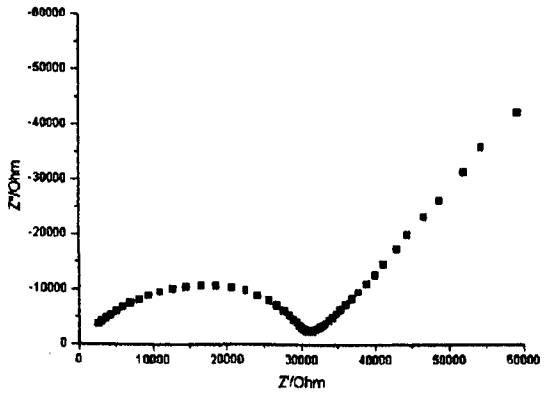

Figure 3.12 Impedance plot of (ENR) $_{11}LiCF_3SO_3$

In order to take into account for the flattening of the semi-circle and the tilting of the spike require the use of constant phase elements (Bottelberghs 1978).

3.3.1.1.4 Constant Phase Elements

Constant phase elements are best thought of as having characteristics intermediate between the capacitor and a resistor, i.e. a leaky capacitor (Latham and Linford 1987). The full mathematical representation of these would be beyond the scope of this thesis. This recognises that the components of the overall impedance may not be purely resistive or capacitative and CPE is defined by:

$$Z_{CPE} = \mathrm{k}(j\omega)^{-p}$$

where ω is the angular frequency, p has values, which lie in the range 0< p <1 and k is a constant. The expression above can be mathematically manipulated using de Moivre's theorem (Linford 1990) as:

$$Z_{CPE} = \frac{k}{\omega^{p}}\left(\cos\left[\frac{p\pi}{2}\right] - j\sin\left[\frac{p\pi}{2}\right]\right)$$

Thus, when $p = 0$, Z_{CPE} behaves as a resistance with a value R=k, whereas when $p = 1$, it behaves as a capacitance with a value $C = \frac{1}{k}$. The CPE is generally used to replace the capacitive elements in the equivalent circuit. For a simple circuit consisting of a resistor and constant phase element in series, the impedance plot is represented by a line, tilting at an angle $\frac{p\pi}{2}$ to the Z' axis and contacting this axis when Z' = R, as shown in Figure 3.13 (a). In the case of a resistor and a CPE in parallel, a depressed semicircle is produced as shown in Figure 3.13 (b).

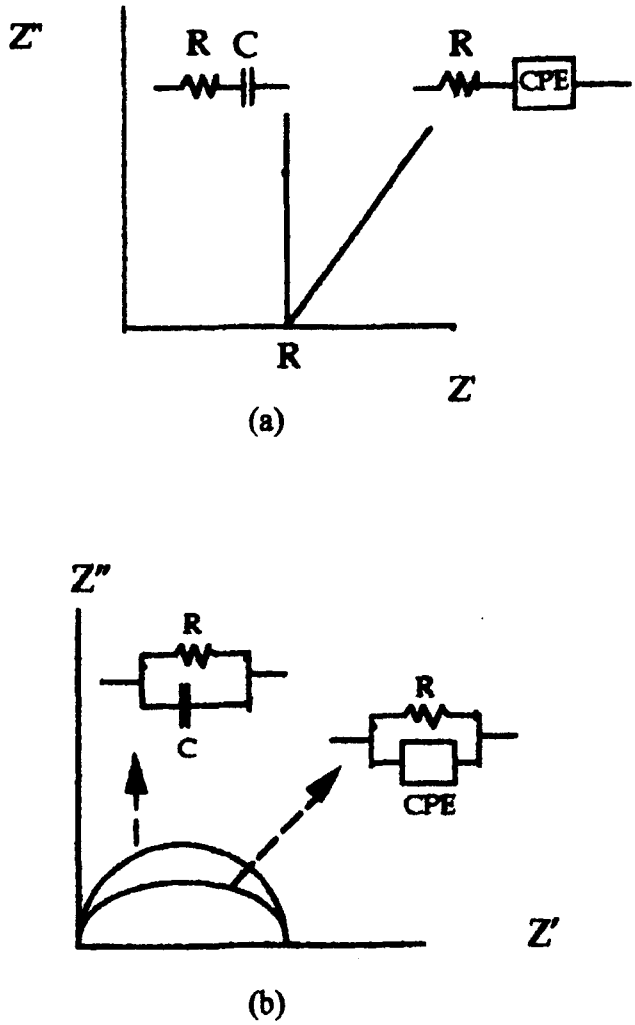

Figure 3.13. Impedance representation of the combination of a resistor and constant phase element (a) in series and (b) in parallel. From Linford (1990).

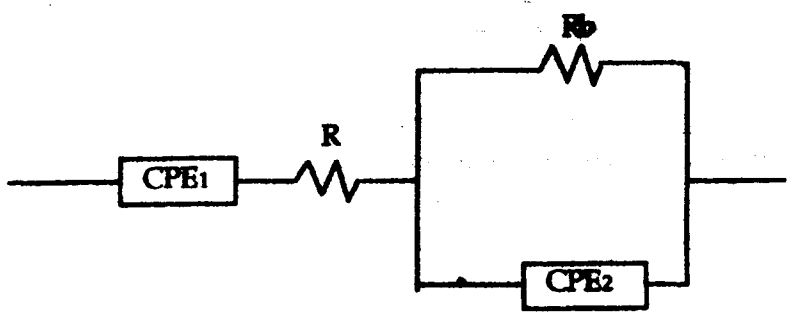

Figure 3.14

The impedance of circuit in Figure 3.14 can be expressed as

$$|Z| = R_s + \frac{k_2 C_2}{\omega^{P_2}} - j\frac{k_2 S_2}{\omega^{P_2}} + \left[\frac{1}{R_p} + \frac{\omega^{P_1}}{k_1 C_1 - jk_1 S_1}\right]^{-1}$$

3.3.1.2 Conductivity cell for liquid electrolyte

The range of ten samples were prepared and labelled as series S1-S10 for mixed plasticizers (EC/PC) and doped-EC/PC. The compositions of PC/EC mixtures in the ratios of 100/0, 75/25, 50/50, 25/75, and 0/100 respectively. The doped and undoped of mixtures of ethylene carbonate (EC) and propylene carbonate (PC) were contained in a square Teflon conductivity cell constructed in the laboratory and this was used to measure the conductivity. The cell employed stainless steel electrodes with a fixed distance of 1mm between them. The ionic conductivities of the liquid electrolytes were measured on equilibrated temperature 45^0C. A schematic diagram of the conductivity cell is given in Figure 3.6.

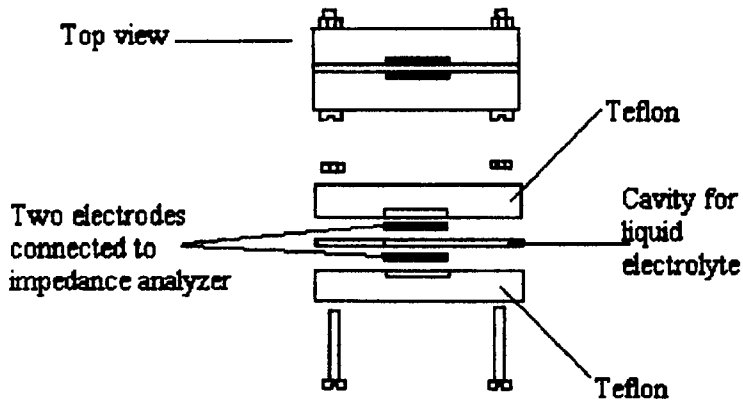

Figure 3.6: Schematic diagram of conductivity cell for liquid electrolytes

3.3.2 Mechanical properties

Stress-strain measurements were performed to determine the mechanical properties of the gel electrolytes. For the stress-strain measurements, tensile strength, modulus, and elongation at break were measured using an Instron machine (Model 4302, series ix).
The standard test method conducted on the samples followed procedures in accordance with British Standard 903 Part A2 (BS 903,1995). The details of sample preparation and stress-strain plots interpretations are described as follows:

Standard test pieces of dumb-bell shaped are preferable for determination of tensile strength. The test pieces are stretched in a tensile-testing machine at a constant rate of transverse of the driven grip. Readings of force and elongation are taken as required during the uninterrupted stretching of the test piece and finally when it breaks.

3.3.2.1 Preparation of test pieces

Dumb-bell test pieces were cut from the prepared cast films having the dimension outline given in Figure 3.7. The die cutter for preparation of dumb-bells has the dimensions given in Figure 3.8.

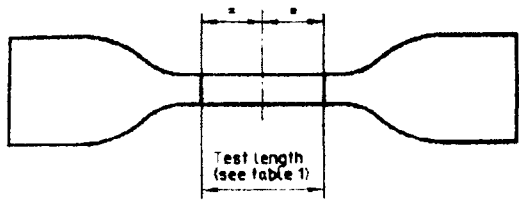

Figure 3.7: The dumb-bell shape of tensile test piece.

Source : Taken from BS* 903: Part * A2: (1995).

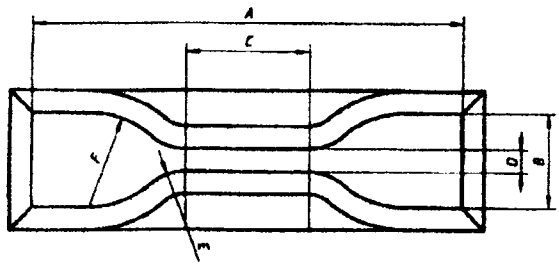

Figure 3.8: The schematic diagram of the dumb-bell die cutter

Source : From BS* 903: Part * A2: (1995)

A minimum of three duplicate test pieces were cut and marked with two reference parts to define the test length. The thickness at the centre and each end of the test length were determined with the thickness gauge. The median value of the three measurements was used in calculating the area of the cross-section. The width of the test piece was taken as the distance between the cutting edges of the die in the narrow part.

3.3.2.2 Definitions of stress-strain plots

The maximum tensile stress, TS, was recorded in extending the test piece to breaking point [see Figure 3.9]. The elastic modulus is a measure of resistance to deformation obtained from the slope of the stress/strain curve. The elongation, *E*, is the extension, expressed as a percentage of the test length, produced in the test piece by a tensile stress.

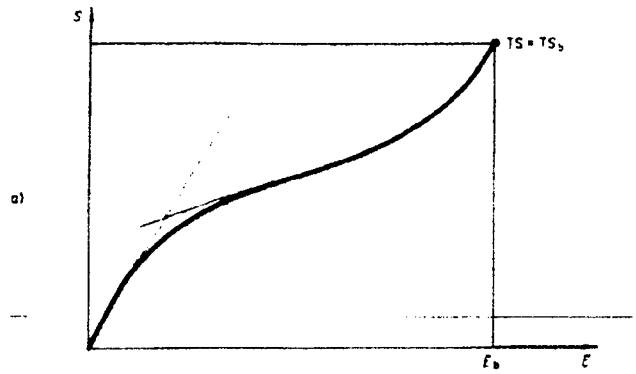

Figure 3.9 - Schematic of the tensile stress-strain plot
Source : From BS* 903: Part * A2: (1995).

3.3.3 Differential Scanning Calorimetry (DSC)

Differential Scanning Calorimetry (Perkin-Elmer DSC-4) (Fig. 3.10) was employed for thermal characterisation of the polymer gel electrolyte systems over temperature range of –80 to + 30^{0}C in a liquid nitrogen atmosphere. Samples were rapidly cool to – 80 and heated to 30^{0}C at a scan rate 10^{0}C min^{-1}. This allows observation of any salt precipitation phenomena and determination of transition glass temperature.

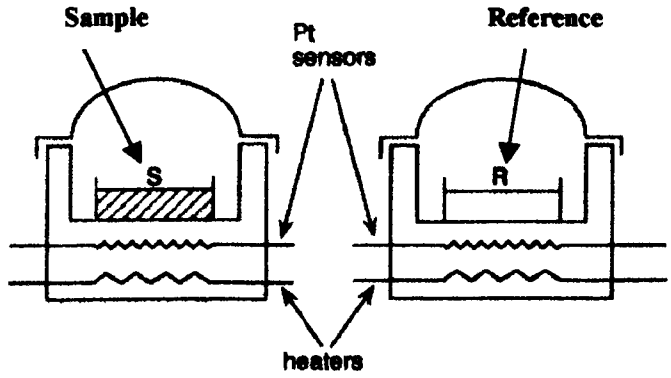

Figure 3.10. Schematic diagram representation of a typical DSC sample cell.
Source: Adapted from Fried (1995).

The DSC-4 Differential Scanning Calorimeter is a conducive and easy to use instrument for the measurement and characterization of the thermal properties of the materials. The System- 4 Microcomputer Controller is used to programme the DSC-4 from an initial temperature to the final temperature. The compartment for the two platinum alloy 'cups' function as the sample holders on the DSC-4. These cups are mounted in a solid aluminium block, which contain a heater and a sensor (see Figure 3.12). As the DSC-4 programs (up or down) in temperature transitions such as melting, boiling, dehydration or crystallization may occur in the material, resulting in an endothermic or exorthermic reaction. The amount of power needed to maintain the sample holder at the same temperature as the reference holder during the transition is recorded as a peak on the recorder or Data Station. The values are obtained directly in millicalories per second,

and this value is at all times equivalent to the rate of energy absorption or evolution of the sample.

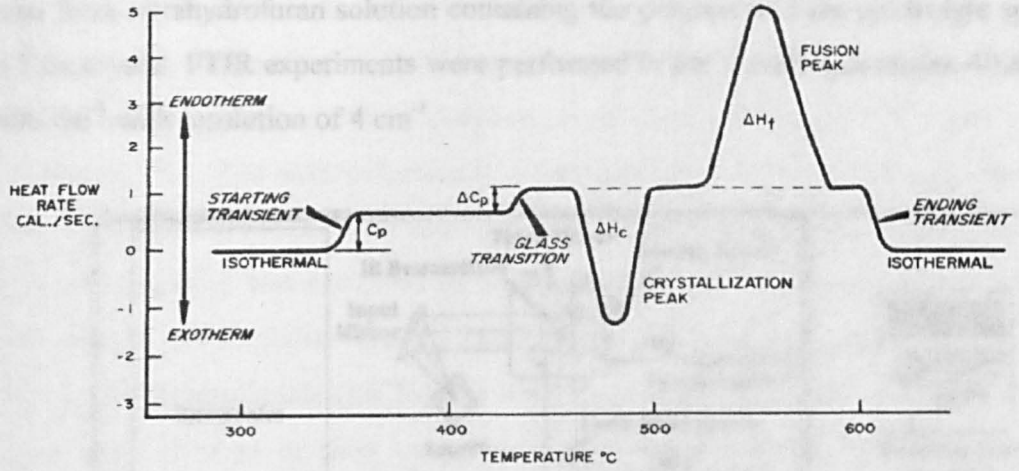

Figure 3.11 Profile of thermal analysis data. Source: From Perkin Elmer Instruction manual DSC 4 (1983).

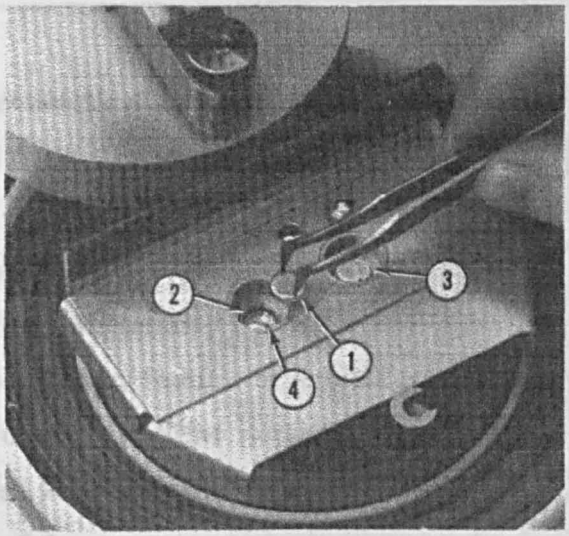

Figure 3.12 Photograph of the DSC 4 sample holder. Source: From Perkin Elmer Instruction manual DSC 4 (1983).

3.3.4 FTIR spectroscopy

The FTIR instrument model Nicolet 5.5 (Figure 3.13) was utilised to collect IR spectra of the investigated polymer electrolyte systems for this work. Films of electrolytes were cast from tetrahydrofuran solution containing the polymer and the electrolyte species on a KBr crystal. FTIR experiments were performed in the wavelength ranges 4000 cm^{-1} to 400 cm^{-1} with resolution of 4 cm^{-1}.

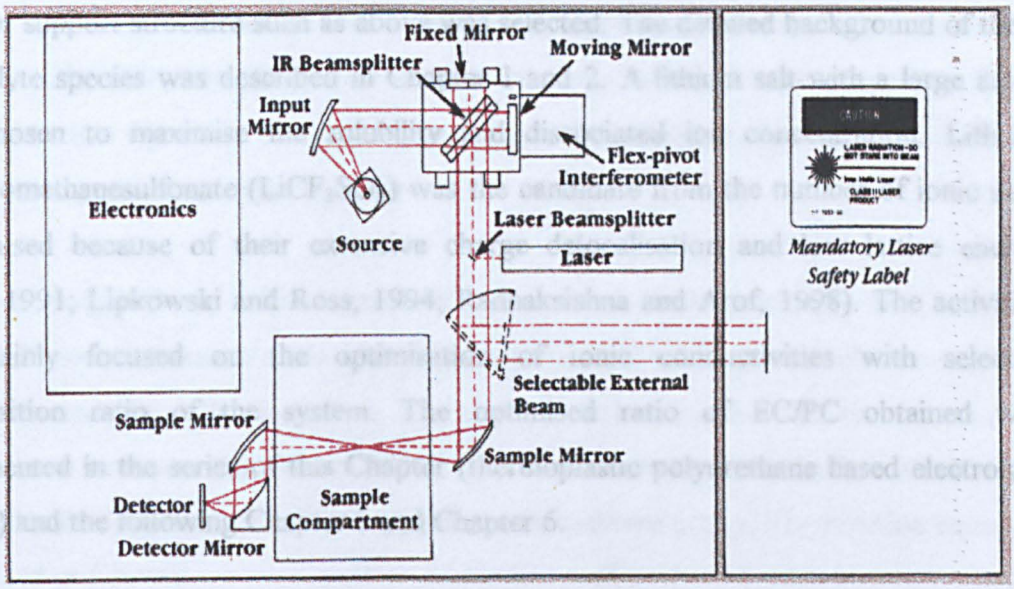

Figure 3.13 Schematic diagram of FTIR Michelson Interferometer.
Source: From Nicolet catalogue model FDXC/5SXC, (1992).

3.3.5 SEM studies

Scanning Electron Microscopy (SEM) is one of the useful techniques being used to examine the morphology features of polymeric materials. The SEM LEICA S430 model was used to obtain the SEM images for the series of blended film samples. The principle is well known to give a simulated visual image of a surface with extreme magnification of the structures to be investigated. The film samples were bonded to a small aluminium stub and sputtered with gold about 10.0 μm thickness.

Chapter 4 Polymer Electrolyte Based on Thermoplastic Polyurethane (TPU)

4.1 Introduction

The right choice of components that are compatible with each other in the electrolyte material, will contribute to the successful formation of polymer electrolyte system. In the early part of this Chapter in section 4.1 will be also described preliminary studies of salt-doped and undoped mixed solvents of ethylene carbonate (EC) and propylene carbonate (PC). The electrochemically active species or material to be absorbed by the polymer support structure such as above was selected. The detailed background of these electrolyte species was described in Chapter 1 and 2. A lithium salt with a large anion was chosen to maximise the solubility and dissociated ion concentration. Lithium trifluoromethanesulfonate ($LiCF_3SO_3$) was the candidate from the number of ionic salts being used because of their extensive charge delocalisation and low lattice energy (Gray, 1991; Lipkowski and Ross, 1994; Radhaksishna and Arof, 1998). The activities are mainly focused on the optimisation of ionic conductivities with selected composition ratio of the system. The optimised ratio of EC/PC obtained was implemented in the series of this Chapter (thermoplastic polyurethane based electrolyte system) and the following Chapter 5 and Chapter 6.

The most preferred polymer host to solvate lithium cation is highly amorphous polymer containing coordinating site with much lower tendency to crystallization as well as low glass transition temperature. In order to achieve the above criterion much effort has been done to obtain copolymer support structure to facilitate the transport of ions in highly amorphous phase environment couple with increase local segmental motion for high ionic conductivity at ambient temperature. Several types of copolymers such as PVDF/HFP copolymer, ethylene oxide-epichlorohydrin copolymers, exothy-propoxypolyether co-polymer and linear phosphate random copolymer were employed to produce high ionic conductivity polymer electrolyte systems (Sung, Wang and Wan, 1998; Gazotti, Spinace, Girotto and De Paoli, 2000; and Kim, Oh and Choi, 1999).

In parallel to the above described approach the thermoplastic polyester/urethane segmented block copolymer material was utilised for this work. The polymeric material under trade name abbreviated as Desmopan385 was supplied as a gift sample by the ALBIS Company, U.K.

The integral part of this chapter described investigation on non-plasticised and plasticised polyurethane based solvent cast films containing lithium triflate salt. The former one involved addition of lithium triflate salt of different concentration into the polymer system. The latter one was incorporating different percentage of mixed EC/PC into the TPU/$LiCF_3SO_3$. The effect of mixture compositions on the properties of the TPU electrolyte films was determined. Impedance spectroscopy, thermal analysis, FTIR studies were performed on the samples.

The term 'polyurethane' refers to materials that contain urethane group (~NHCOO~) in the backbone of macromolecule. For such materials the initial macromolecule tends to be a polyester or polyether; it is the crosslinks that involve the formation of a polyurethane structure (Nicholson, 1991). The reaction involved in the formation of the polyurethane is the reaction of an isocyanate with hydroxy-group. The reaction equation is depicted as follows:

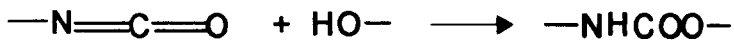

The prepolymers most frequently used for the preparation of polyurethanes are either polyester or polyethers. In this section of the experimental work polyurethane polyester elastomer has been employed as a polymer matrix for the preparation of plasticised polymer electrolytes. This thermoplastic material consists of block copolymer of hard and soft segments with urethane linkages on a polymer chain backbone. The structural formula is given below:

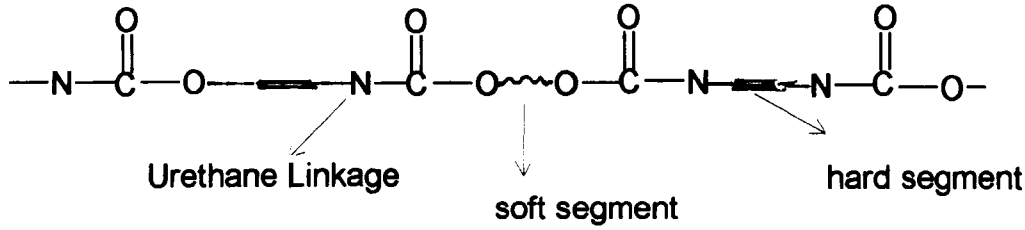

The alternate molecular chain segments of this polymer matrix give the physical advantage of both elastomeric and thermoplastic behaviour in respect to temperature.

Furthermore, characterisation of the physical properties of non-plasticised and plasticised polymer electrolyte systems was conducted at ambient temperature. From a practical viewpoint, it is preferred that polymer electrolyte systems attain high ionic conduction and are easy to handle. The experiments are mainly focused on the optimisation of ionic conductivities and thermal properties of the polymer electrolyte systems. The physical features of the thermoplastic polyurethane and modified natural rubber (Chapter 5 and 6) are that they are both amorphous and have similar transition glass temperatures that are below ambient temperature.

4.1.1 Liquid Electrolyte system

The choice of solvents is initially based on the conductivity of their salt solutions. There are several organic solvents such as THF, EC, PC or their mixtures that can dissolve lithium salt and being used as electrolytes. They have been proven to be among the most efficient in terms of battery cyclability (Aurbach, Gofer, Ben-Zion, and Aped, 1992). In response to the above consideration partly related to this thesis topic, preliminary studies on pure and salt-containing liquid solvent were conducted. The ionic conductivity measurements and thermal analysis were performed on various ratios EC/PC and EC/PC/ $LiCF_3SO_3$ system. Data have been collected and presented in Table 4.1.

Table 4.1 Properties of EC/PC and EC/PC/$LiCF_3SO_3$ systems.

Sample no.	EC	PC	$LiCF_3SO_3$	Conductivity/S cm^{-1}
S1	100			$4.51X10^{-6}$
S2	75	25		$6.13X10^{-6}$
S3	50	50		$7.7X10^{-6}$
S4	25	75		$5.86X10^{-6}$
S5		100		$4.73X10^{-6}$
S6	100		7	$1.47X10^{-3}$
S7	75	25	7	$1.67X10^{-3}$
S8	50	50	7	$1.92X10^{-3}$
S9	25	75	7	$1.39X10^{-3}$
S10	-	100	7	$1.25X10^{-3}$

(S1-S5), (S6-S10), refer to EC/PC and EC/PC/$LiCF_3SO_3$ respectively

EC/PC (ratio: w/w)

$LiCF_3SO_3$ (w/v %)

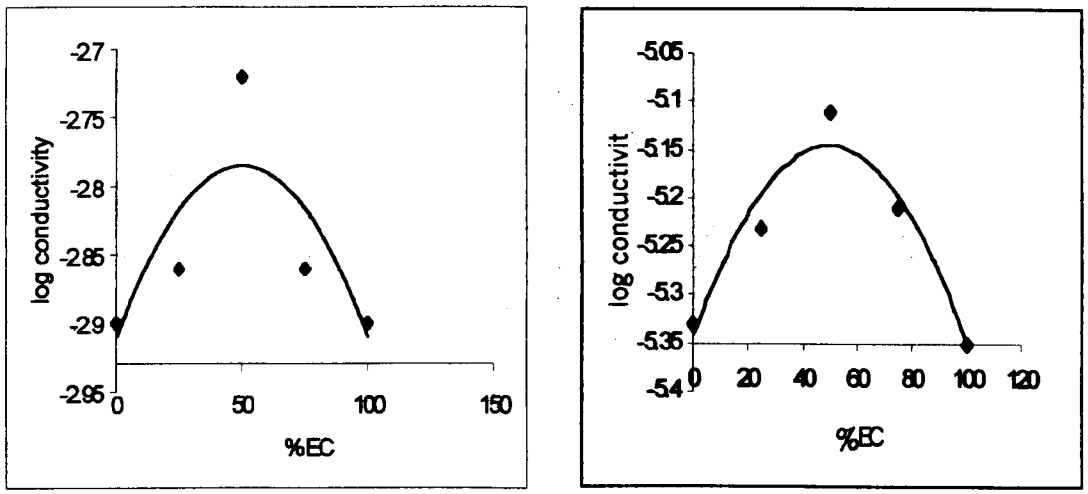

(a) (b)

Figure 4.1 EC concentration dependence of conductivity plots for (a) EC/PC/$LiCF_3SO_3$ (b) EC/PC system.

The ionic conductivities of salt-doped mixed EC/PC (Figure 4.1 a) show higher values than undoped one by almost two folds order in magnitude. The ionic conductivities of salt-doped EC/PC systems are 10^{-3} S cm^{-1} where as unsalted EC/PC (Figure 4.1 b) in the range 10^{-6} S cm^{-1}. The values obtained for salt-doped EC/PC mixtures appeared to be consistent with other investigations (Li and Balbuena, 1999). The highest ionic conductivity among the EC/PC ratios is 50/50. A number of studies have also been reported dealing with lithium-cation solvent interactions in mixed solvent ethylene carbonate (EC) and propylene carbonate (PC). This experimental work was carried out to select an appropriate ratio of EC/PC that yields maximum ionic conductivity.

The optimised ratio of EC/PC mixture was then implemented in the series of polymer gel electrolyte systems using polyurethane and modified natural rubber host-polymers. Some data of DSC traces on EC/PC and EC/PC/$LiCF_3SO_3$ systems are summarised in Table 4.1. DSC data for mixed plasticiser EC/PC and EC/PC/$LiCF_3SO_3$ systems show that transition glass temperature,T_g, is below ambient temperature. It was observed that the PC rich-electrolyte exhibits the lowest T_g (see S9 and S10) but only with present of salt (compare with S4 and S5). The data suggest that interaction of PC with $LiCF_3SO_3$ (solute-solvent) has resulted distribution of free ions, ion-pairs and aggregates, affecting the T_g value.

4.2 TPU polymer electrolyte systems

4.2.1 Ionic conductivity measurements

All the thermoplastic polyurethane (TPU)-$LiCF_3SO_3$ polymer electrolyte systems were prepared by the solution casting technique. The films showed a transparent rubbery appearance. Table 4.2 summarizes results of ionic conductivity and DSC measurements for the systems.

Table 4.2: Summary data of conductivities for PU/$LiCF_3SO_3$ system

Sample No.	PU (w/v)	$LiCF_3SO_3$ (w/w)	Conductivity (S cm^{-1})
1.	4	-	9×10^{-9}
2.	4	15	8.3×10^{-7}
3.	4	20	5.87×10^{-6}
4.	4	30	1.23×10^{-5}
5.	4	40	1.06×10^{-5}
6.	4	50	5.72×10^{-5}
7.	4	60	4.95×10^{-5}
8.	4	70	2.82×10^{-5}
9.	4	100	2.74×10^{-5}

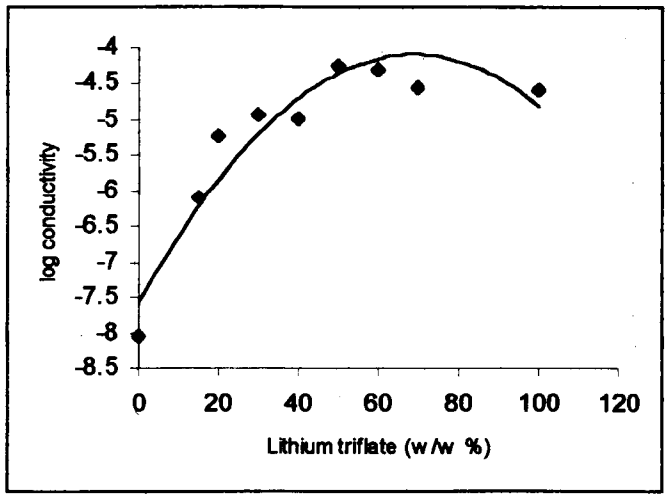

Figure 4.2 Conductivity isotherms plotted versus salt concentration for $LiCF_3SO_3$ in TPU

Figure 4.2 illustrates the trend of ionic conductivity, σ, for the TPU-$LiCF_3SO_3$ system against different salt concentration. It can be seen that the ionic conductivity increases with increase in salt concentration over the maximum concentration between 50 to 60 w/w %. This finding is in agreement with other studies of TPU/LiClO systems by Ferry *et al*, (1995). They have reported ionic conductivity value of ~ $1x10^{-9}$ S cm^{-1} at room temperature whereas TPU investigated for this work obtained ionic conductivity value 10^{-5} S cm^{-1}.

However, in this experimental work it was found that film sample containing 50 w/w per cent salt showed the highest ionic conductivity value of 5.72 x 10^{-5} S cm^{-1} (see Figure 4.2) at room temperature. The TPU copolymer has shown capability to solvate excessive salt with radical increase of ionic conductivity at ambient temperature. Although high salt concentration in host polymer would impede ion transport resulting in significant decrease of conductivity but for this work quite the opposite effect. This could be explained by alternate soft and hard segmented phases contained in TPU series salt systems. The high molecular weight of TPU with unknown structural features of hard and soft-segmented unit at present investigation can solvate a greater amount of salt. Other investigators (Fuller, Breda and Carlin, 1997) have also reported rubbery gel ionic liquid and poly (vinylidene fluoride)-hexafluoropropylene [PVdF (HFP)] system containing salt concentration more than 100 w/w percent of the PVdF present.

4.2.2 Differential Scanning Calorimetry

DSC was utilized to examine the effect of $LiCF_3SO_3$ on the phase transition of soft and hard segmented morphology of TPU understudied. The results presented in Table 4.3, have shown an increase in the T_g values in the system as a function of salt concentration.

Table 4.3: Summary of thermal data for TPU/$LiCF_3SO_3$ system

SampleNo.	PU (w/v)	$LiCF_3SO_3$ (w/w)	T_g / ^{0}C
1.	4	-	-43
2.	4	15	-39
3.	4	20	-33
4.	4	30	-36
5.	4	40	-31
6.	4	50	-24
7.	4	60	-22
8.	4	70	-22
9.	4	100	-21

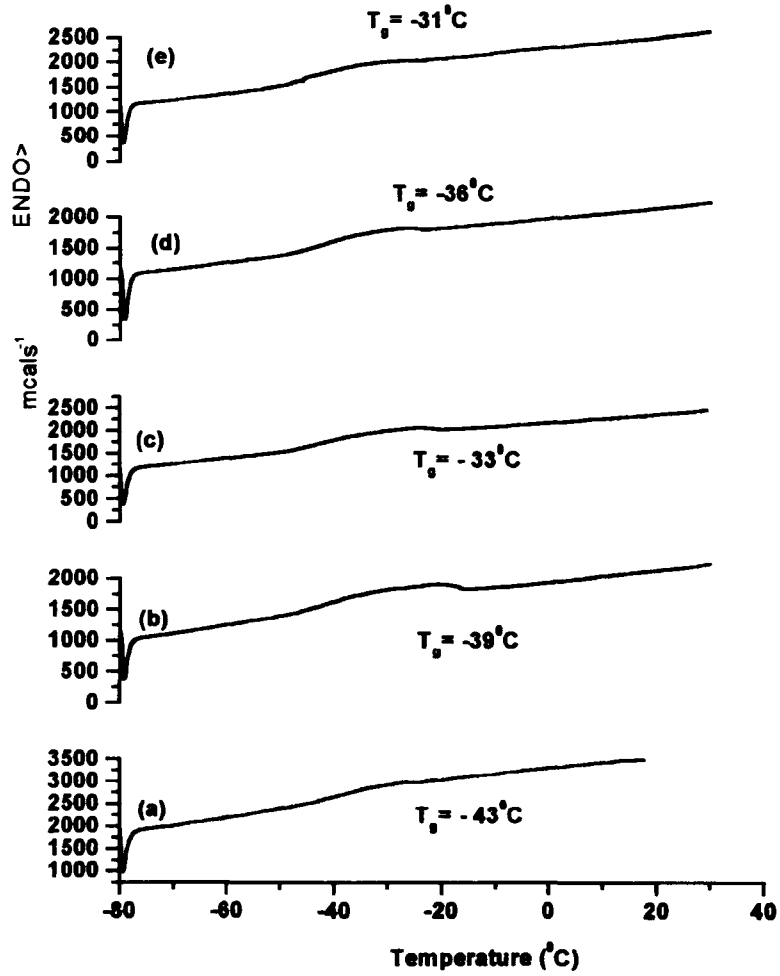

Figure 4.3 DSC traces of TPU doped with $LiCF_3SO_3$ concentration of (a) 0%; (b) 15%; (c) 20%; (d) 30%; (e) 40%. (Refer to Appendix II)

DSC traces of the TPU electrolyte system containing different concentration of $LiCF_3SO_3$ are shown in Figure 4.3 and Figure 4.4. The effect of $LiCF_3SO_3$ added into the system has increased the ionic conductivity as well as glass transition temperature, T_g

The trend shows that the ionic conductivity reached maximum value at 50 w/w salt concentration and T_g is tending towards a plateau. From the result might suggests that interaction has occurred between the TPU segregated phases and lithium salt.

The repeat unit of TPU chemical structure has not known at present time of investigation. The finding shows that TPU polymer matrix be able to uptake high concentration of lithium salt, which is contrary to polyether based system electrolyte. All DSC traces of the film samples display a single glass transition temperature and first order transition is not apparent. The glass transition temperature,T_g, value of pure TPU obtained at - 43^0 C has increased dramatically to -22^0 C upon addition of 60 wt.% lithium salt. Ferry and co-workers (1996) also reported increase in the T_g values as a function of salt concentration. The T_g of pure TPU is – 44^0C has increased to –12^0C upon addition of 2.0 mmol lithium perchlorate, $LiClO_4$, for one gram of TPU. TPU examined in the investigation was Estane 5714, B. F. Goodrich Company whereas for this work using TPU labelled with Desmopan 385 was supplied by ALBIS Company, U.K.

This finding is also consistent with other polymer electrolyte system reported by Gazotti and co workers (2000). They have investigated polymer electrolyte based on ethylene oxide-epichlorohydrin copolymers. The T_g values of the copolymers increased linearly with $LiClO_4$ concentration.

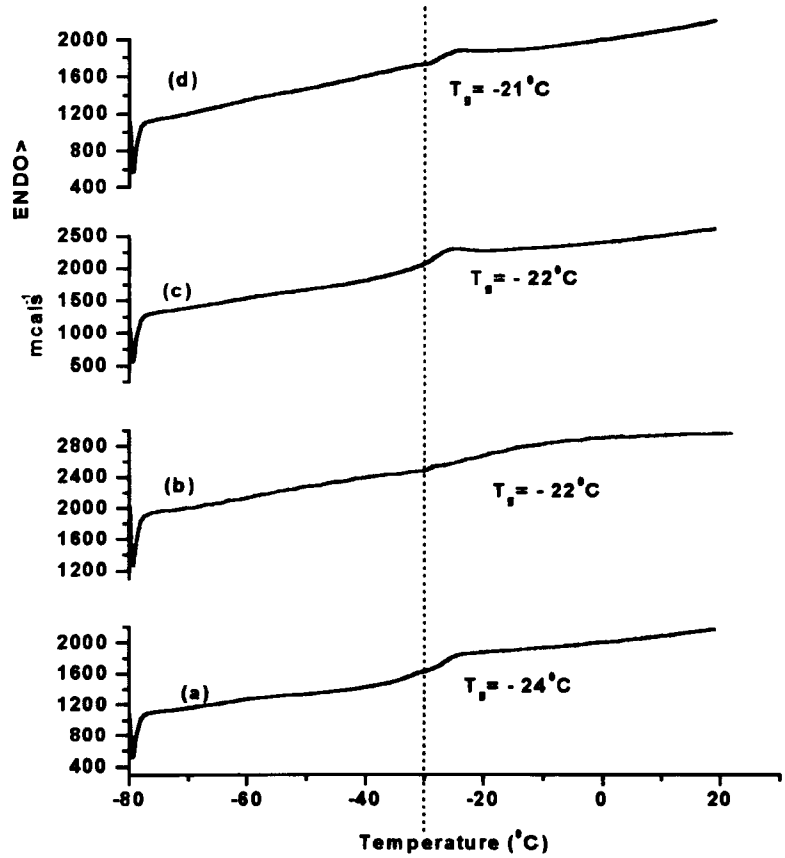

Figure 4.4 DSC traces of TPU doped with $LiCF_3SO_3$ concentration of (a) 50%; (b) 60%; (c) 70%; and (d) 100% respectively.

The relationship between ionic conductivity and T_g values of TPU/ $LiCF_3SO_3$ against salt concentration is shown in Figure 4.5. The trend shows that addition of salt has increased transition glass temperature and ionic conductivity until at 60 wt.% of concentration. The ionic conductivity reduced and stabilized upon further addition of salt greater than 60 wt. %.

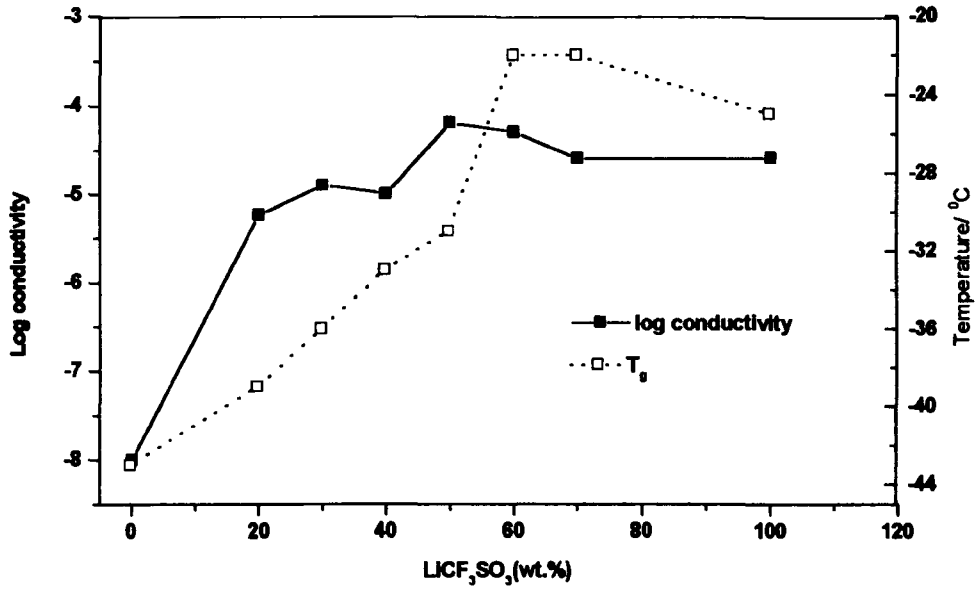

Figure 4.5 Influence of lithium salt on the ionic conductivity and T_g of TPU/ $LiCF_3SO_3$ polymer electrolyte systems.

4.2.3 Infrared Spectroscopy

Fourier transform infrared spectroscopy (FTIR) is one of the significant tools for monitoring the interaction of Li^+ cation and anion within the polymer electrolyte system environment. In the context of plasticised and doped TPU polymer electrolyte material, the lithium ion might, in principle, choose to coordinate with the anion, plasticiser, or the segregated phase TPU polymer chain. Each of these coordination types represented by the spectral band intensities of different strength depends on different amount of the various species present in the electrolyte system. Certain bands resulting from specific vibrations of each of the potentially coordinating species have been observed to split or shift to different frequencies on cation coordination.

The IR spectra of pure TPU and its $LiCF_3SO_3$ complexes of different concentration are shown in Figure 4.6. The samples were scanned in the absorption mode 4000-500 cm^{-1} at a resolution 4 cm^{-1}.

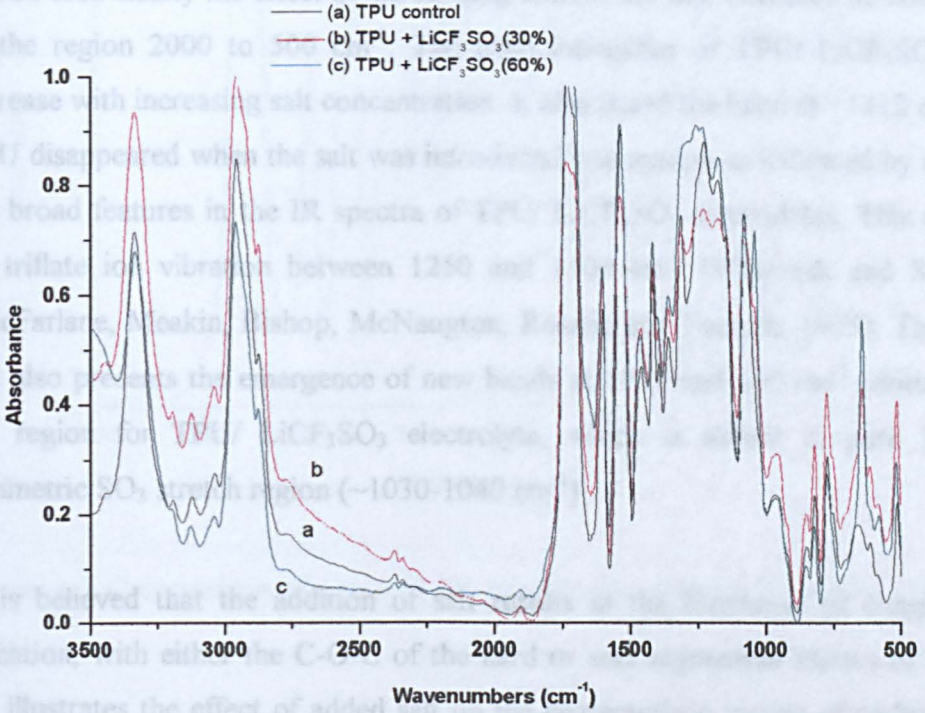

Figure 4.6 IR spectra of solvent cast film for TPU/ $LiCF_3SO_3$ electrolytes. (a) pure TPU (b) TPU /$LiCF_3SO_3$(30 wt %) (c) TPU/$LiCF_3SO_3$ (60wt %).

The IR spectra of the TPU/ $LiCF_3SO_3$ electrolytes show almost resemblance to the spectra of pure TPU itself, as illustrated in Figure 4.6. In the present investigation, there are not many differences observed among the samples in the hydrogen-bonded N-H stretching mode vibration in the region 3600 to 3100 cm^{-1} (Coleman, Skrovanek, Howe and Painter, 1986). It is seen a faint increased in the band intensities. However, it can be seen clearly the effect of introducing lithium salt and increased its concentration in the region 2000 to 500 cm^{-1}. The band intensities of TPU/ $LiCF_3SO_3$ complexes increase with increasing salt concentration. It also noted the band at ~1312 cm^{-1} for pure TPU disappeared when the salt was introduced into system as indicated by dotted line to the broad features in the IR spectra of TPU/ $LiCF_3SO_3$ electrolytes. This might caused by triflate ion vibration between 1250 and 1300 cm^{-1} (Wiezorek and Steven, 1997; MacFarlane, Meakin, Bishop, McNaugton, Rosalie and Forsyth, 1995). The addition of salt also presents the emergence of new bands at 1039 and 650 cm^{-1} (dotted line) from the region for TPU/ $LiCF_3SO_3$ electrolyte, which is absent in pure TPU. In the symmetric SO_3 stretch region (~1030-1040 cm^{-1})

It is believed that the addition of salt results in the formation of complex between Li^+cation, with either the C-O-C of the hard or soft-segmented phases of TPU. Figure 4.7 illustrates the effect of added salt on the characteristic modes of carbonyl region at 1732 cm^{-1} band increases with increasing salt concentration. This is related to the works but using different approach on TPU-$LiClO_4$ (Ferry, Jacobsson, Heumen and Steven, 1996) and TPU/ $LiCF_3SO_3$ (Heuman and Stevens, 1995).

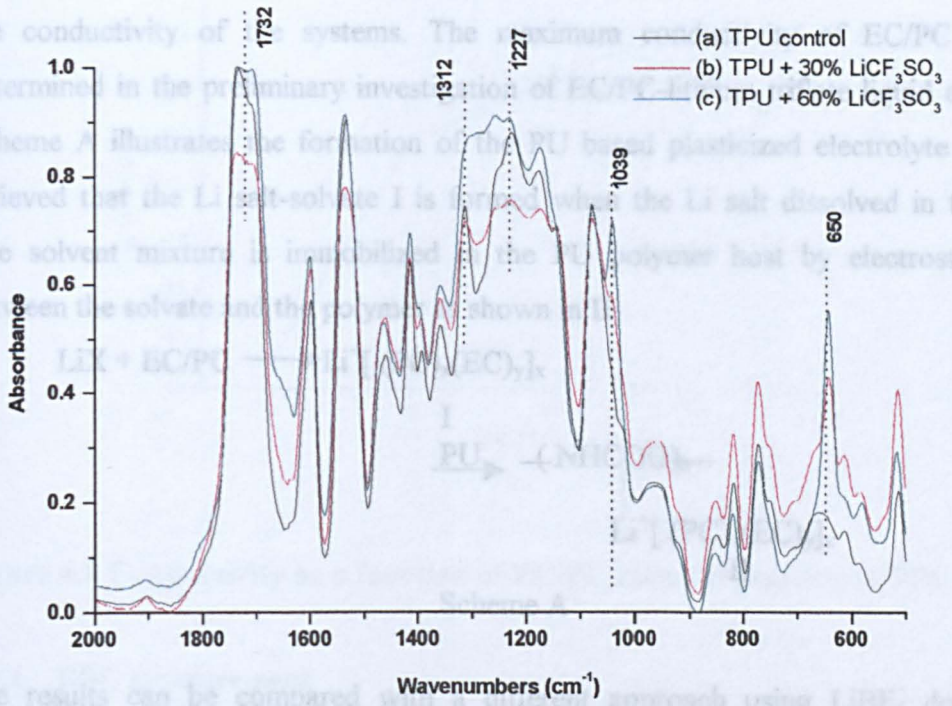

Figure 4.7 Comparison of the mid-IR spectra for with and without $LiCF_3SO_3$ salt TPU

4.3 Plasticized Thermoplastic Polyurethane based electrolytes

By definition of gel electrolyte system consists of a polymer mixed with a lithium salt and a plasticiser. The plasticiser, being an organic solvent capable to dissolve the salt, maintains a liquid-like state within the material. Concurrently, the polymer gives the gel mechanical strength approaching that of a solid. This section will describe using this technique for preparing plasticised polymer electrolyte employing polyester-polyurethane copolymer. Increased ionic conductivities have been observed at ambient temperature in plasticised or gel polymer electrolytes compared with previous solid polymer electrolyte systems. The incorporation of plasticising solvents has almost doubled the ionic conductivity. Figure.4.8 illustrates the plots of conductivity for plasticised TPUs systems as a function of EC/PC ratios.

The optimum ionic conductivity value of 8.0×10^{-3} S $cm^{-1}$was obtained at ambient temperature. It indicates that the mixtures of plasticiser at 50/50 ratios have influenced the conductivity of the systems. The maximum conductivity of EC/PC ratio was determined in the preliminary investigation of EC/PC-lithium triflate liquid electrolytes. Scheme A illustrates the formation of the PU based plasticized electrolyte films. It is believed that the Li salt-solvate I is formed when the Li salt dissolved in the EC/PC. The solvent mixture is immobilized in the PU polymer host by electrostatic forces between the solvate and the polymer as shown in II

$$LiX + EC/PC \longrightarrow \underset{I}{Li^{+}[(PC)_x(EC)_y]_x}$$

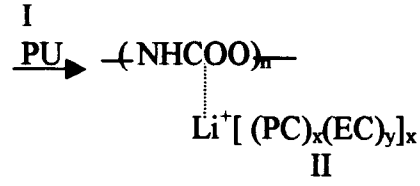

Scheme A

The results can be compared with a different approach using $LiBF_4$ doped TPUs plasticised with propylene carbonate (PC) (Venugopal *et al*, 1996). Also Venugopal *et al* has patented his work using TPU (Texin 285) based plasticised polymer electrolytes. It was revealed that ionic conductivity of the film was approximately $1.4\text{x}10^{-4}$ Scm^{-1}.

Table 4.4 Compositions of TPU based electrolytes with and without plasticisers.

Composition	Conductivity (S cm^{-1})	T_g/°C
TPU	9×10^{-9}	-42
PU (5%)/ $LiCF_3SO_3$ (60 %)	6×10^{-6}	-22
PU/ EC (20 %) / PC (20 %) / $LiCF_3SO_3$ (60 %)	1×10^{-3}	-66
PU/ EC (30 %) / PC (30 %) / $LiCF_3SO_3$ (60 %)	2×10^{-3}	-72
PU/ EC (40 %) / PC (40 %) / $LiCF_3SO_3$ (60 %)	5×10^{-3}	-81
PU/ EC (50 %) / PC (50 %) / $LiCF_3SO_3$ (60%)	8×10^{-3}	-68
PU/ EC (70 %) / PC (70 %) / $LiCF_3SO_3$ (60 %)	2×10^{-3}	-79

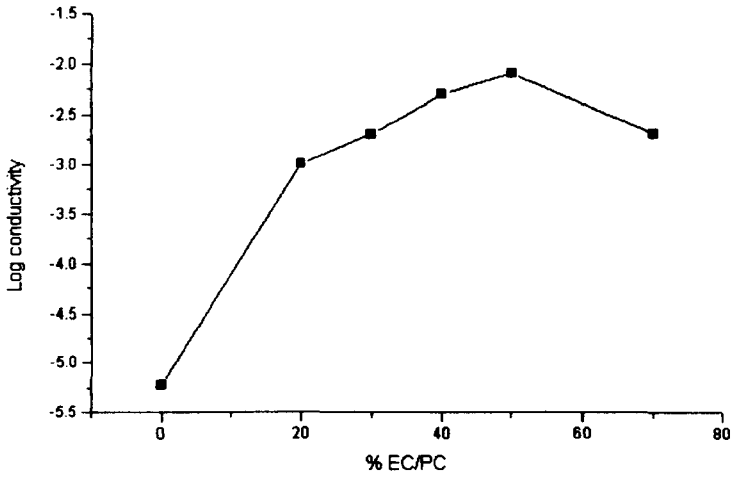

Figure 4.8 Conductivity as a function of EC/PC ratio for plasticised TPU system.

4.3.1 DSC measurement

DSC was utilised to examine the effect of lithium triflate doped TPU containing EC/PC on the morphologically based thermal transition. Table.4.4 shows the variation of transition glass temperatures of the TPU polymer electrolyte system as a function of EC/PC ratio composition.

Basically, the copolymer TPU consists of segregated soft and hard phase segments alternately in the main backbone. Figure 4.9 shows the DSC traces of the phase segregated morphology of the plasticised TPU/ $LiCF_3SO_3$ electrolytes compared with TPU/$LiCF_3SO_3$ (blue line) film sample. The transition glass temperature of the plasticised TPU polymer electrolytes has very much been reduced by the addition of EC/PC mixtures. From Table 4.4 shows that the TPU system containing EC/PC ratio 40/40 displayed the lowest Tg at -81^{0}C, where as the T_g of pure TPU is - 42^{0}C. It is assumed that the plasticising solvents might interact effectively with the soft or hard phase segment of the TPU, which reduced the T_g value dramatically.

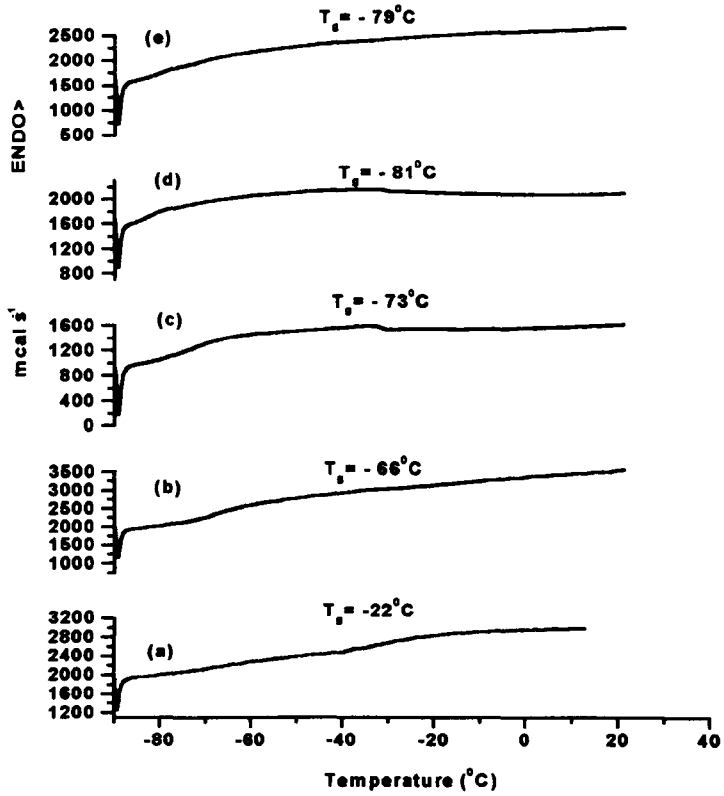

Figure 4.9 DSC traces of plasticised TPU electrolytes containing of EC/PC (a) control (b) 40 wt.% (c) 60 wt.% (d) 80 wt.% (e) 100 wt.%.

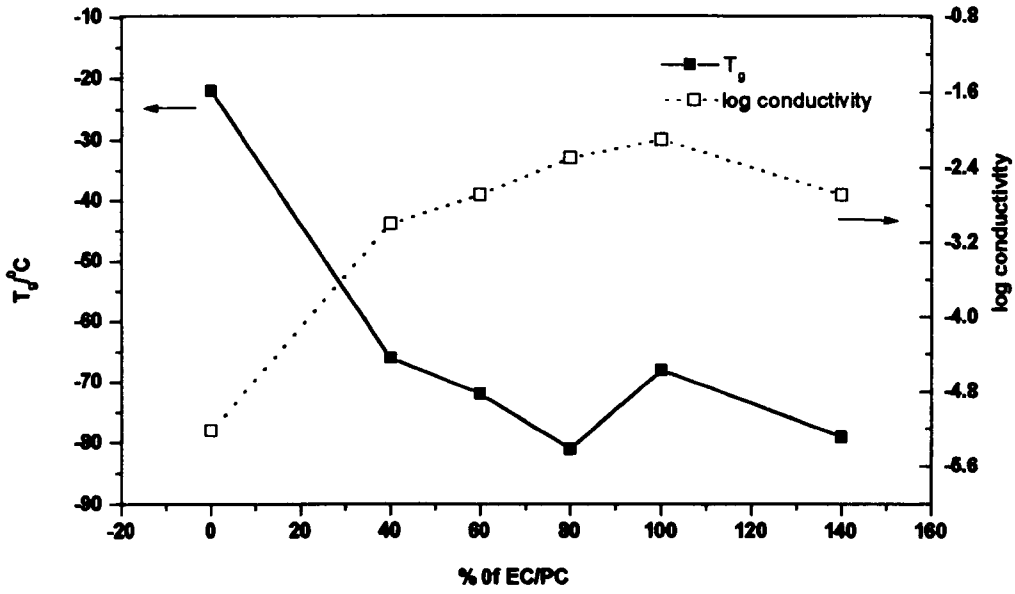

Figure 4.10 Influence of percentage of EC/PC on the ionic conductivity at room temperature and T_g.

4.3.1.1 Correlation between ionic conductivity, T_g, and plasticiser EC/PC

Figure 4.10 indicates the trend variation of ionic conductivity and glass transition temperature with total percentage of EC/PC at ambient temperature. As mentioned in the literature, studied by many researchers (Reddy, Sreekanth, and Rao, 1999; Andrieu, Vivedo and Fringant, 1995; Walker and Salomon, 1993) the effect of addition of plasticiser to modulate ionic conductivity and markedly reduces, T_g, of the polymer. The dramatic reduction of T_g in TPU/ $LiCF_3SO_3$/EC/PC electrolyte sample occurred at the change of total percentage EC/PC from 0 to 40 % follow up with an increment of ionic conductivity. This is in agreement with the role of plasticiser in the early part of this chapter in section 4.1 to improve the brittleness of the polymer and ease of transient crosslink for the non-plasticised TPU/ $LiCF_3SO_3$ system. The details of some of the electrolytes are presented in Table 4.5 along with the present data.

Table 4.5 Effect of the addition of plasticiser to polymer electrolytes.

Polymer Electrolyte	Remarks	Reference
macromonomer $LiClO_4$+PC	Adding PC as plasticiser to the macromonomer + $LiClO_4$ complex yielded an ionic conductivity of $3x10^{-3}$ S cm^{-1}, which is two orders of magnitude higher than that found for trifunctional macromonomer + $LiClO_4$ electrolyte.	(Kono, Hayashi and Watanabe 1999)
PEO+$LiCF_3SO_3$ EC/PC	By adding EC/PC as plasticiser to the $LiCF_3SO_3$ polymer electrolyte complex the ionic conductivity was increased two orders of magnitude when compared with PEO+$LiCF_3SO_3$ electrolyte	(Bandara, Dissanayake and Meliander, 1998)
TPU+ $LiCF_3SO_3$+EC/PC	By adding EC/PC as plasticiser to the TPU+ $LiCF_3SO_3$ polymer electrolyte, the ionic conductivity was increased 3 orders of msgnitude when compared with TPU+ $LiCF_3SO_3$ electrolyte system.	This work

4.3.2 Mechanical properties

4.3.2.1Tensile measurement

Stress-strain measurements were performed to characterise the mechanical properties of the TPU polymer electrolytes. The stress-strain, tensile strength, and elongation at break measurements were determined by using an Instron machine series X1. Table 4.6 shows the tensile properties of some polyurethane-based electrolytes. The elastic modulus falls with increasing plasticiser content, but remains sufficient for the materials to be characterized as soft elastomer (see Fig. 4.11). The figures indicate that at 20 weight percent of EC/PC content has a minimum strain value at 1100 % elongation.

Table 4.6 Summary of tensile test of polyurethane based electrolytes

Composition	Tensile stress (MPa)	Elongation at Break (%)	Modulus (MPa)
TPU	61	751	14
TPU $LiCF_3SO_3$ (60%)/	24	1005	4
TPU /$LiCF_3SO_3$ (60%) /EC+PC (40%)	9	1114	2.0
TPU /$LiCF_3SO_3$ (60%) /EC+PC (60%)	10	1364	1.1
TPU /$LiCF_3SO_3$ (60%) /EC+PC (80%)	8	1498	0.6
TPU /$LiCF_3SO_3$ (60%) /EC+PC (100%)	6	1299	0.8
TPU /$LiCF_3SO_3$ (60%) /EC+PC (120%)	5	1289	1.5

Figure 4.11 shows the change in tensile strength as a function of EC/PC for the plasticised TPU systems. The tensile strength decreased with increasing plasticiser content. It was observed that the plasticiser has weakened the polymer chain. The tensile stress showed a minimum value at 70 percent EC/PC. Fig 4.11 shows the steep increase of elongation as the percentage of EC/PC increases. This trend is attributed to the breakdown of the polymer gel network, which is non-recoverable. It also suggests that the plasticiser has diluted the crosslinking effect of the salt content in the system.

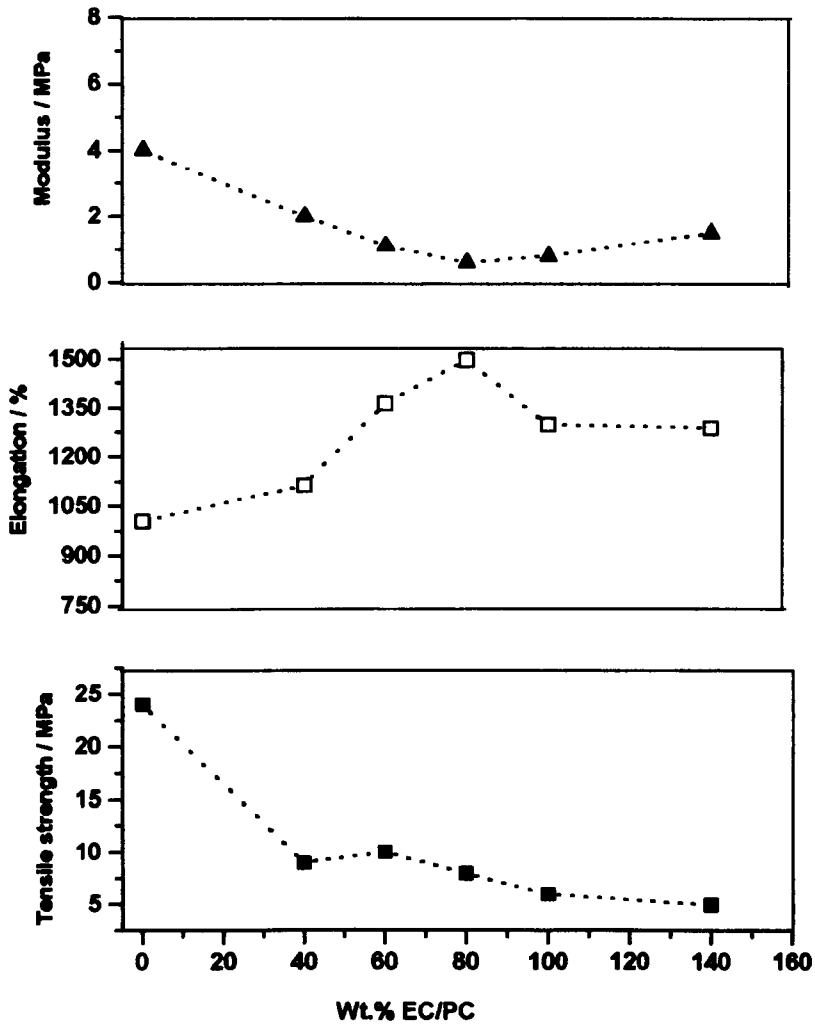

Figure 4.11 Effect of plasticiser on tensile strength, elongation and elastic modulus of TPU

There is little published data on the mechanical properties of gel electrolytes. It was reviewed from article that for PVDF-HFP gel electrolytes, a polymer host with >60- wt % plasticiser exhibited no gel property but formed a liquid electrolyte (Tarascon, Gozdz, Schmutz, Shokoohi, and Warren, 1996). However another research group (Jiang, Carroll and Abraham, 1997) claimed that PVDF-HFP gel electrolyte containing 80-wt.% liquid electrolyte had 1.4MPa tensile strength and 170% elongation at break, while keeping ionic conductivity of 1mS cm^{-1}. Ballard *et al* (1990) have studied that a plasticised polymer electrolyte had 13MPa tensile strength but contained only 30-wt.%

plasticiser. Other material using PAN-based gel electrolytes, Tatsuma *et al* (1997) indicate that the film showed good mechanical properties even when the liquid electrolyte content was higher than 90%, but the numerical value for the mechanical strength was not clear.

4.3.3 Infrared Spectroscopy

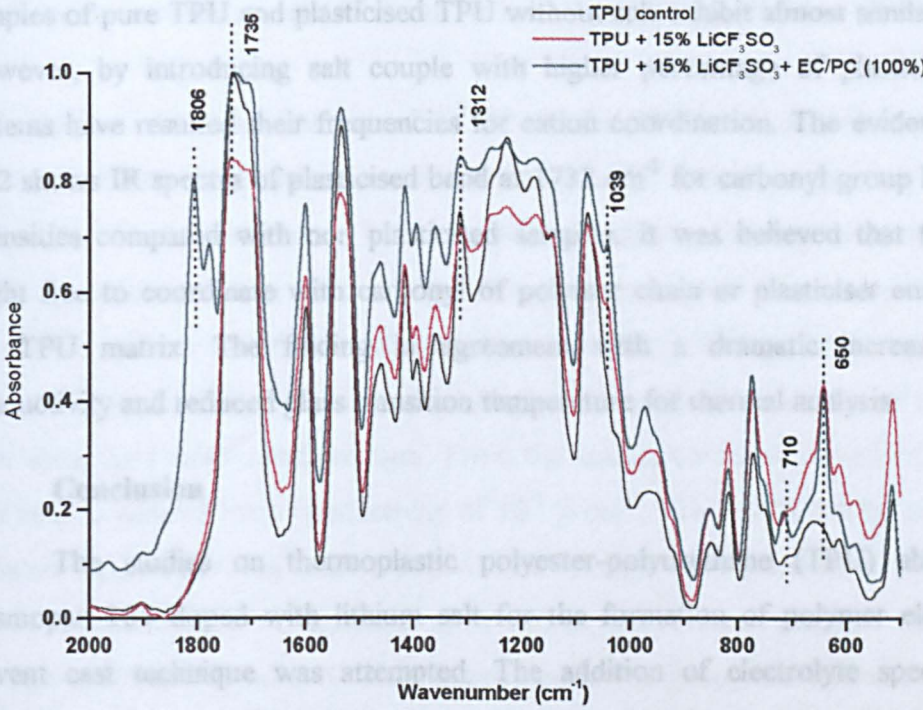

Figure 4.12 IR spectra of plasticised thermoplastic polyurethane based electrolytes

Figure 4.12 shows a stacked IR plot of TPU/ $LiCF_3SO_3$ and the plasticised electrolytes in the region 2000 to 500 cm^{-1}. It can be seen that there are several new peaks emerging from the region for the TPU/ $LiCF_3SO_3$ and plasticised TPU/ $LiCF_3SO_3$ electrolytes compared to pure TPU respectively.

The emerging peak occurred at 640, 740 and 1039 for both electrolytes but additional peaks appeared at 740, 995 and 1806 for the plasticised one. The results indicate that the samples of pure TPU and plasticised TPU without salt exhibit almost similar IR spectra. However, by introducing salt couple with higher percentage of plasticiser into the systems have resulted their frequencies for cation coordination. The evidence in Figure 4.12 shows IR spectra of plasticised band at 1732 cm^{-1} for carbonyl group has increased intensities compared with non plasticised samples. It was believed that the Li cation might free to coordinate with carbonyl of polymer chain or plasticiser encapsulated in the TPU matrix. The finding in agreement with a dramatic increased of ionic conductivity and reduced glass transition temperature for thermal analysis.

4.4 Conclusion

The studies on thermoplastic polyester-polyurethane (TPU) abbreviated as Desmopan 385 doped with lithium salt for the formation of polymer electrolytes by solvent cast technique was attempted. The addition of electrolyte species into the polymer systems has produced significant effect on their physical properties. Prior to the successful polymer electrolyte films, the selection of electrolyte components has been optimised for the entire experimental series. Thus, lithium triflruomethanesulfonate was solely utilised as charge carrier for this work whereas plasticiser of EC/PC mixed solvent as additive introduced to the understudied systems. By systematic increment the percentage amount of lithium salt component has increased the glass transition temperature values determined by DSC. It was found that the glass transition temperature of pure TPU at -43^0 C has increased to -25^0C when it was added to maximum 100 w/w per cent salt concentration.

The ionic conductivity was measured by AC impedance technique for different level of ionic salt containing polymer electrolyte systems. As the ionic conductivity trend behaviour is increased and then decline to plateau after reaching maximum, T_g can be seen to increase. The results of ionic conductivity measurements indicate that the systems investigated for TPU doped with lithium triflate attained optimum conductivity 10^{-5} Scm^{-1} at ambient temperature. Ionic conductivity value of TPU studied was compared with other commercial Estane TPU /$LiClO_4$ electrolye system, which produced ionic conductivity 10^{-9} S cm^{-1} at room temperature (Ferry *et al*, 1996).

The addition of a plasticiser (mixed EC/PC) to the TPU/$LiCF_3SO_3$ electrolyte modifies the conductivity and physical properties significantly. The plasticiser has the effect of reduction in cohesive forces between polymer chains and increases the segmental mobility, which promote conductivity. The plasticiser itself assists the dissociation of electrolyte species within the polymer electrolyte. The findings have shown a marked increase in conductivity but there was a slight increase in the tackiness of the film along with some loss mechanical strength. From the results obtained, optimised composition was able to achieve ionic conductivity of 10^{-3} S cm^{-1}. The results can be compared with different approach using $LiBF_4$ doped TPU (Texin 285) plasticised with propylene carbonate patented by Venugopal *et al* (1996). It was revealed that ionic conductivity of the film containing 80 w/w % of the liquid electrolyte (propylene carbonate/ $LiBF_4$) was approximately 1.4×10^{-3} S cm^{-1}.

Thermal data have shown that immobilising of plasticiser into the polymer system reduced the Tg values. The reduction in T_g has caused an increase in segmental motion of polymer chain; which modulate ionic conductivity. The T_g value for plasticised TPU obtained is - 79^0C compared to pure TPU - 43^0C. The great changes observed on the T_g values indicate that interaction between polymer and lithium salt has taken place both for non-plasticised and plasticised system. DSC and FTIR studies suggest that Li cation might be complexed with TPU. In this work was also found that with increasing concentration of plasticiser has affected the mechanical properties. Tensile strength of the materials decrease, while the elongation increased.

Chapter 5: Polymer Electrolyte based on Modified Natural Rubber

5.1 Introduction

This chapter discusses a novel modified natural rubber as an alternative to conventional PEO to act as polymer host for lithium ion conducting polymer electrolyte system. A series of rubbery films containing lithium triflate salt with and without plasticisers were produced and their physical properties were characterised. The beginning of this Chapter will describe briefly the background of the modified natural rubber and an insight view of its synthesis. The feature of its chemical structure and soft-elastomeric phases at room temperature are significant criteria for its choice as a polymer electrolyte.

Elastomers (or rubbers) are polymers, which are substantially amorphous in nature and consist of long flexible, mobile, entangled molecular chains. They are always used at temperatures higher than their glass transition temperature (T_g) and are generally characterised by a low modulus. Elastomers are, under normal circumstances, always used in crosslinked state. Some elastomers are capable of crystallising in the uncompounded state and have high physical property values.

Modified natural rubber elastomers have been investigated as matrices of ionic conductors for use in lithium batteries. Diversification of the traditional uses of natural rubber (NR) can be achieved by changing the properties of the base polymer through chemical modification. There appears to be no data in the literature for the use of polar modified natural rubber based polymer electrolytes in lithium battery applications. To date this material has not been explored as a potential candidate for polymer electrolytes in electrochemical device applications. Modified natural rubber has desirable properties suitable for making polymer electrolytes. These include low glass transition temperature, T_g, soft elastomer characteristics at room temperature and good elasticity.

Suitable elasticity can result in flat, thin and flexible paper-like batteries and electrochromic displays. It also gives excellent contact between the electrolytic layer and electrode. In other words, if an elastomer can act as polymeric 'solvent', a higher conductivity is expected compared with crystalline polymers.

Two suitably modified natural rubbers have been considered in this study and are briefly described as follows. They are poly(methyl methacrylate) grafted natural rubber (denoted Heveaplus MG-NR) and epoxidised natural rubbers (denoted ENR).

5.2 Poly (Methyl Methacrylate)-Grafted Natural Rubber (MG-49)

MG 49 is a graft copolymer containing 49 % by weight polymethyl methacrylate (PMMA) grafted onto polyisoprene. The composition consists of 80% graft copolymer, 10% polymethyl methacrylate and 10% polyisoprene. The graft copolymer contains about one or two PMMA chains grafted onto each polyisoprene (rubber) molecule. It was reported from research (Allen, Ayrey, and Moore, 1959; Subramanium, 1988; Ceresa, 1973) indicates that two mechanisms of grafting can occur:

(1) By abstraction of allylic hydrogen atoms to give a polyisoprene radical which initiates methyl methacrylate polymerisation (see **reaction 5.1**) to give structure **1** as below;

(2) By addition of initiator radical (R) to the double bond to give a polyisoprene radical, which initiates methyl methacrylate polymerisation (see **reaction 5.2**) to give structure **II** as below;

The **structure II** product is likely to predominate (Figure 5.1).

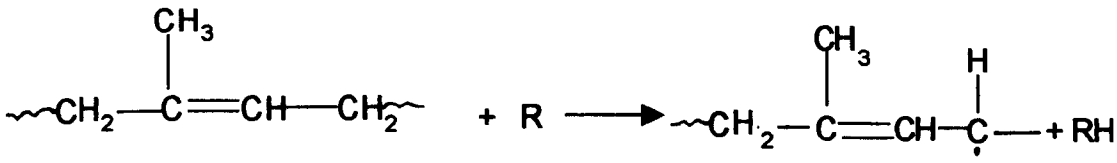

Reaction 5.1

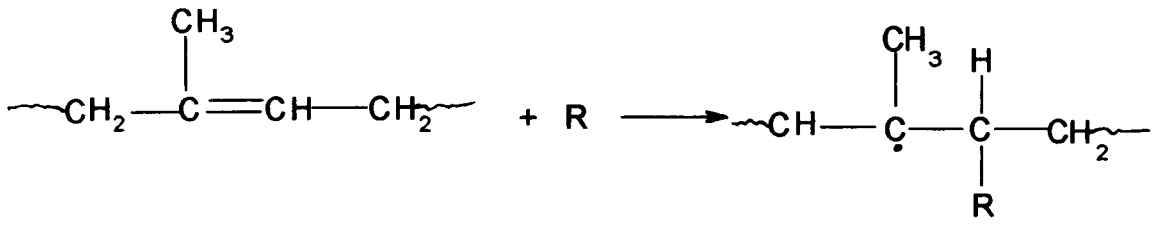

Reaction 5.2

R = C_6H_5 and C_6H_5COO

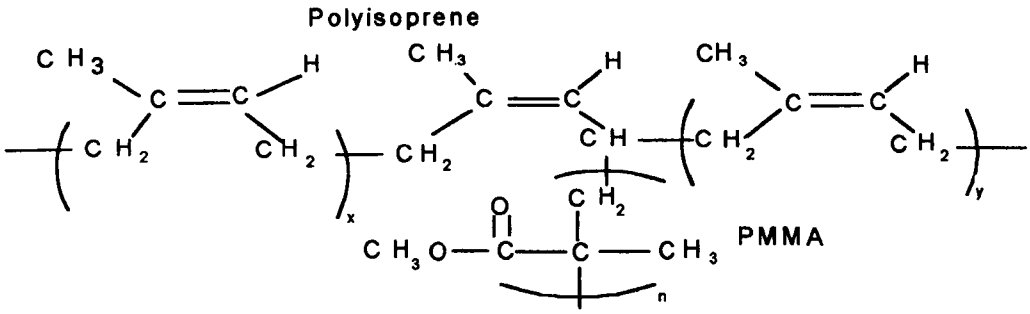

Structure I

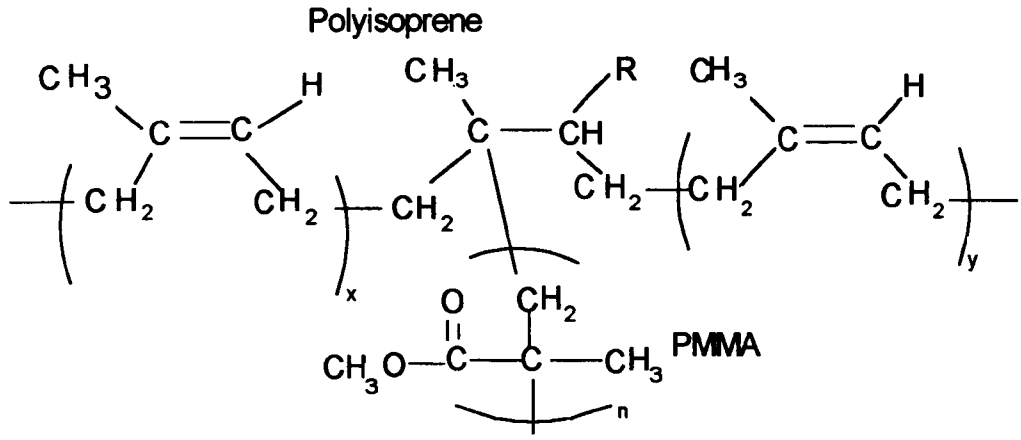

Structure I I

Figure 5.1 The chemical structure of polymethylmethacrylate grafted natural rubber (abbreviated MG-49)

5.3 Epoxidised Natural Rubber (ENR)

Epoxidation represents a particularly attractive and convenient method for transforming natural rubber to a new polymer with certain outstanding properties. Epoxidised natural rubber (ENR) contains both epoxide and unsaturated sites along the rubber main chain (Gan and Burfield, 1989). Epoxidation reactions are stereo-specific and thus ENR is a cis 1,4-polyisoprene with epoxide groups randomly situated along the polymer backbone. A variety of reaction conditions have been published and the products variously described as ranging from hard thermoplastic to soft rubbery polymers. Under carefully controlled conditions, NR latex can be epoxidised to over 75 mol% without the formation of ring-opened structures. Both preformed peroxyacetic acid (Gelling and Smith, 1979; Gelling, 1985; British Patent,1982) from hydrogen peroxide and formic acid can be employed (**reaction 5.3**). The latter is the preferred route for commercial production, as only hydrogen peroxide is consumed.

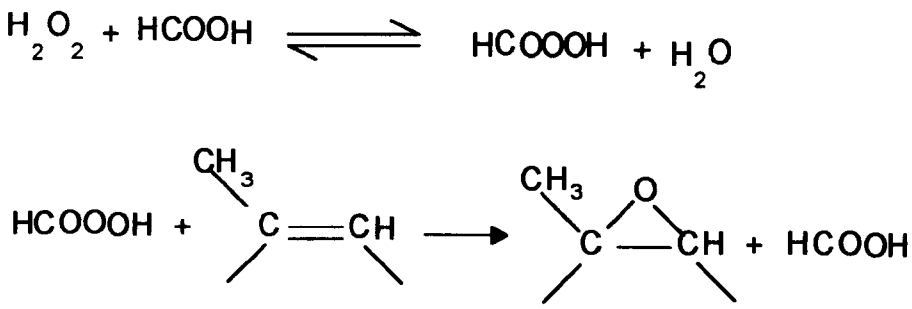

Reaction 5.3

The *in-situ* epoxidation of NR employing hydrogen peroxide and formic acid.

Epoxidation reactions are stereo-specific (Gelling, Tinker and Abdul Rahman, 1991) and thus ENR is a cis 1,4-polyisoprene with epoxide groups randomly situated along the polymer backbone. Figure 5.2 shows that the natural rubber unit cell of ENR50, has four isoprene repeat units, which can accept two epoxide groups whereas ENR25 posses one epoxy group in the polymer chain. Thus, there is no regular repeat unit, but random distribution of unreacted double bonds and epoxy groups in the ratios 2:2 and 3:1, respectively. As such the average molar masses for four isoprene units (epoxidised or unreacted) are 304 and 288 for ENR50 and ENR25, respectively. The presence of oxygen atom in the epoxy groups of modified natural rubber may facilitate lithium ion conducting properties when it is doped with lithium salt. The chemical features of ENR almost resemble PEO, which is known to solvate varieties of alkali metal salts. The ionic conduction and thermal behaviour of ENR based electrolyte systems were studied via experimental work in the following section. In addition further work on ENR blend with PEO was conducted and described in Chapter 6.

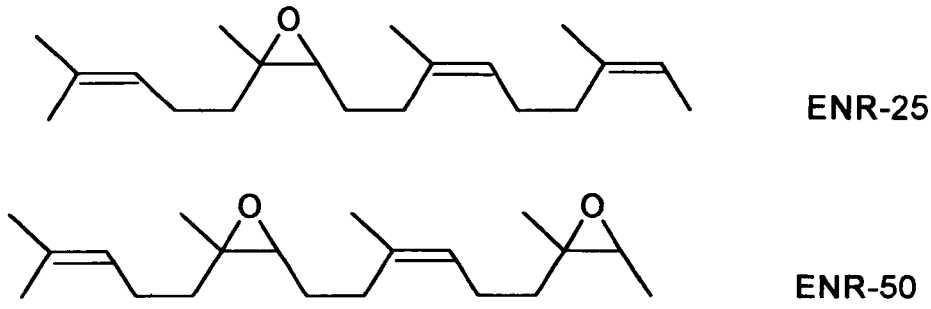

Figure 5.2 Chemical structure of 25% and 50%epoxidised natural rubbers

5.4 Polymer Electrolyte Based on Modified Natural Rubbers

Polymer films have been produced from three types of modified natural rubbers by casting from solvent-based viscous solutions. They are namely masticated 25% epoxidised natural rubber (ENR-25), masticated 50% epoxidised natural rubber (ENR-50) and, 49 % methyl methacrylate grafted natural rubber (MG-49). Tables 5.1,5.2 and 5.3 summarise results for different sample compositions. The electrolyte films made from modified natural rubbers, which are opaque, self-supporting and exhibit a good degree of flexibility were investigated. Summary data of DSC and conductivity measurements of various epoxidised and methyl methacrylate grafted polymer electrolytes are tabulated in the following tables:

Table 5.1 Properties of ENR-25 systems with salts

	Composition		Electrical properties	Thermal behavior
Sample	ENR/ SALT	O/Li	Conductivity (S cm^{-1})	T_g (^{0}C)
E25/S1s	100/2	27/1	$6.9x10^{-6}$	-27
E25/S2s	100/5	11/1	$1.6x\ 10^{-5}$	-40
E25/S3s	100/10	5/1	$1.8x\ 10^{-5}$	-32
E25/S4s	100/15	4/1	$1.4x\ 10^{-5}$	-30
E25/S5s	100/20	3/1	$6.2x\ 10^{-5}$	-37
E25/S6s	100/60	1/1	$1.8x\ 10^{-4}$	-25
E25/C	100/0		$2.1x10^{-7}$	-41

Table 5.2 Properties of ENR-50 systems with salts

	Composition		Electrical properties	Thermal behavior
Sample	ENR/ SALT	O/Li	Conductivity (S cm^{-1})	T_g (^{0}C)
E50/1	100/2	51/1	$5.0x10^{-6}$	-22
E50/2	100/5	20/1	$2.0x10^{-5}$	-22
E50/3	100/10	10/1	$1.6x10^{-5}$	-17
E50/4	100/15	7/1	$1.9x10^{-5}$	-17
E50/5	100/20	5/1	$2.3x10^{-5}$	-13
E5O/6	100/60	2/1	$1.0x10^{-4}$	-19
E50/C	100/0		$3.1x10^{-6}$	-21

Table 5.3 Properties of MG-49 systems with salts

	Composition	Electrical properties	Thermal behavior
Sample	MG-49/SALT	Conductivity (S cm^{-1})	T_g (^{0}C)
MG-49/S1	100/2	$4.0x10^{-6}$	-62
MG-49/S2	100/5	$4.1x10^{-6}$	-67
MG-49/S3	100/10	$5.9x10^{-6}$	-62
MG-49/S4	100/15	$6.1x10^{-6}$	-63
MG-49/S5	100/20	$3.7x10^{-5}$	-59
MG-49/S6	100/60	$2.5x10^{-5}$	-63
MG-49/C	100/0	$2.8x10^{-6}$	-61

Initially, lithium contents in ENR-25 and ENR-50 based electrolyte systems are expressed in term of O/Li ratio. On the other hand for MG-49 based electrolyte systems, the contents of lithium are based on weight percent.

5.4.1 Ionic conductivity measurements

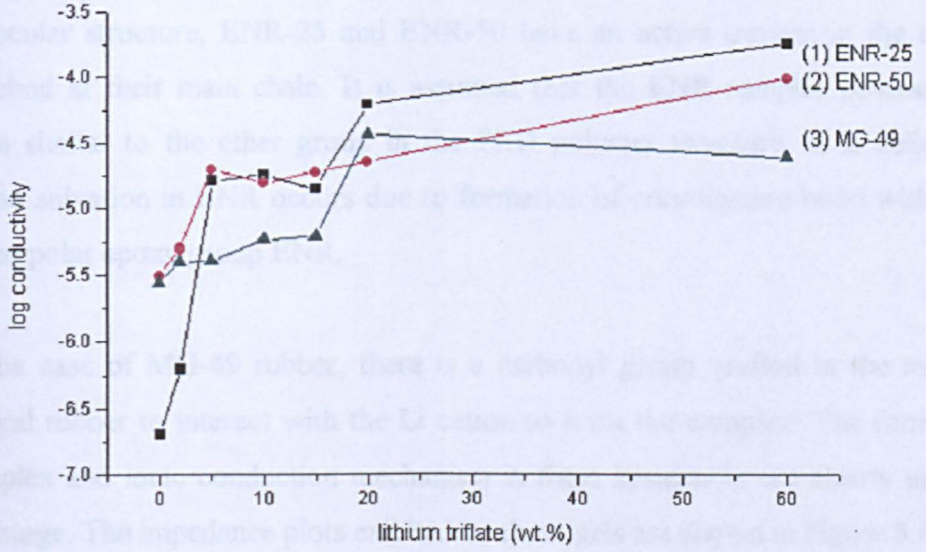

Figure 5.3 Conductivity as a function of salt concentration for modified natural rubber based systems

The variation of the ionic conductivity, log σ, of the modified natural rubber based gels prepared is shown in Figure 5.3. It indicates that at a fixed polymer concentration the conductivity of the gel is increased as the salt concentration is elevated. The ionic conductivities achieved are in the range of 10^{-6} to 10^{-4}S cm^{-1}.

The ionic conductivity reaches $6.2x10^{-5}$S cm^{-1} at room temperature when the salt content is 20 wt.% and reaches $1.8x10^{-4}$ S cm^{-1} at 60% salt content. It was observed that further increase in salt concentration, results in an abrupt increase in conductivity values but leading to $LiCF_3SO_3$ phase separation. The reason for the particular conductivity behaviour of highly concentrated ENR-25- $LiCF_3SO_3$ electrolytes are not fully understood at this present time. The ENR-25- $LiCF_3SO_3$ system containing 20 wt. % of salt corresponds to mole ratio O/Li ~ 3/1.

Among the three types of modified natural rubbers, ENR-25 shows the highest conductivity at room temperature. Overall the conductivities of doped modified natural rubber based electrolytes have shown higher conductivity than conventional polyethylene oxide (PEO) based electrolyte at ambient temperature. In terms of polymer molecular structure, ENR-25 and ENR-50 have an active oxygen in the epoxy group attached at their main chain. It is assumed that the ENR samples possess an oxygen atom similar to the ether group in the PEO polymer structure. It is believed that Li cation solvation in ENR occurs due to formation of coordination bond with the oxygen of the polar epoxy group ENR.

In the case of MG-49 rubber, there is a carbonyl group grafted in the main chain of natural rubber to interact with the Li cation to form the complex. The formation of the complex and ionic conduction mechanism in these systems is not clearly understood at this stage. The impedance plots exibited by these gels are shown in Figure 5.4.

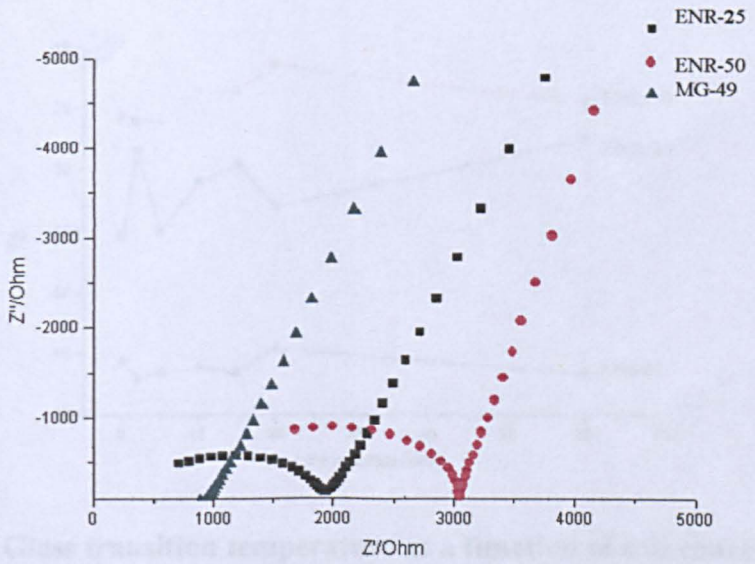

Figure 5.4 Impedance plots of salt-doped modified natural rubber based gel electrolytes (Frequency range: 10 Hz - 65 kHz)

5.4.2 Differential Scannning Calorimeter (DSC)

The presence of more than one phase in the polymer electrolyte system complicates analysis of the transport property data. For this reason, it is desirable to investigate the thermal properties prior to study. Basically, modified natural rubbers are typically amorphous at room temperature and above; salt solubility limits are calculated in analogous polyethylene oxide (PEO) systems.

For this work, the phase behaviour of polymer-$LiCF_3SO_3$, polymer- $LiCF_3SO_3$-EC/PC with O/Li ratios ranging between 57/1 and 5/1 was investigated using differential scanning calorimetry (DSC). Films made from modified natural rubbers- $LiCF_3SO_3$ solutions appeared homogenous and fully amorphous (clear to the eye) at room temperature, and no melting transitions were observed between –80 and $+30^0$C. The ENR-25, ENR-50 and MG-49 types of modified natural rubbers doped with lithium triflate in this study exhibited a single Tg in the DSC experiments. This indicates that no microphase separation occurs in this system.

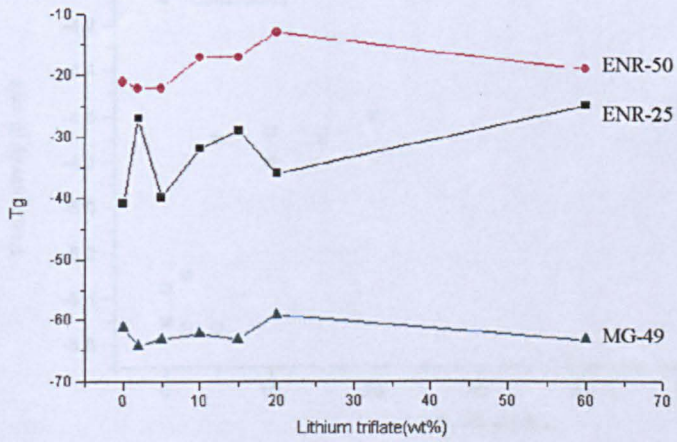

Figure 5.5 Glass transition temperature as a function of salt concentration for modified natural rubber based systems.

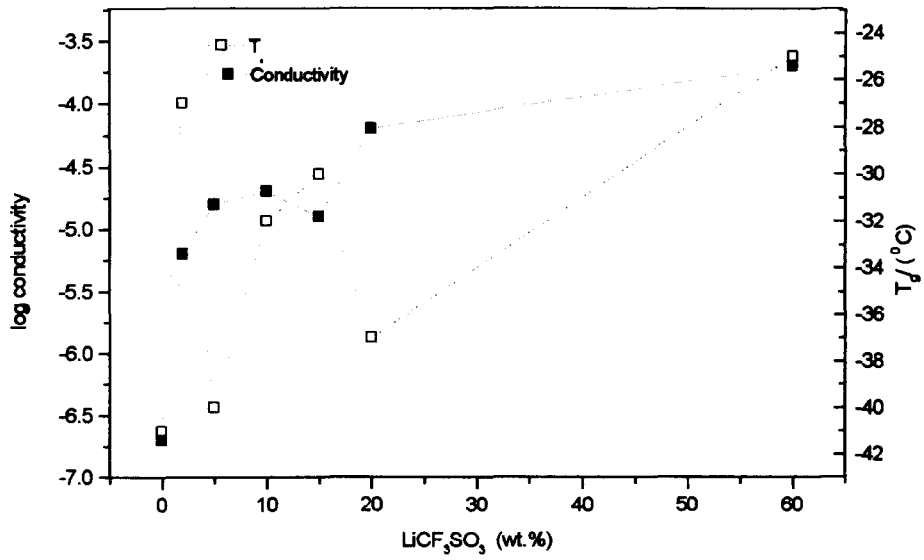

Figure 5.6 Variation of T_g and ionic conductivity for ENR25 /$LiCF_3SO_3$ with the salt concentration.

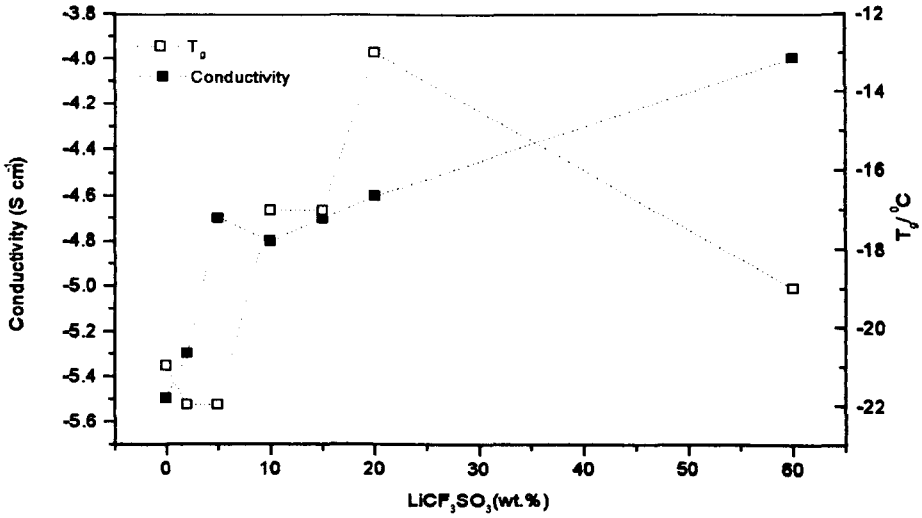

Figure 5.7 Variation of T_g and ionic conductivity for ENR50 /$LiCF_3SO_3$ with the salt concentration.

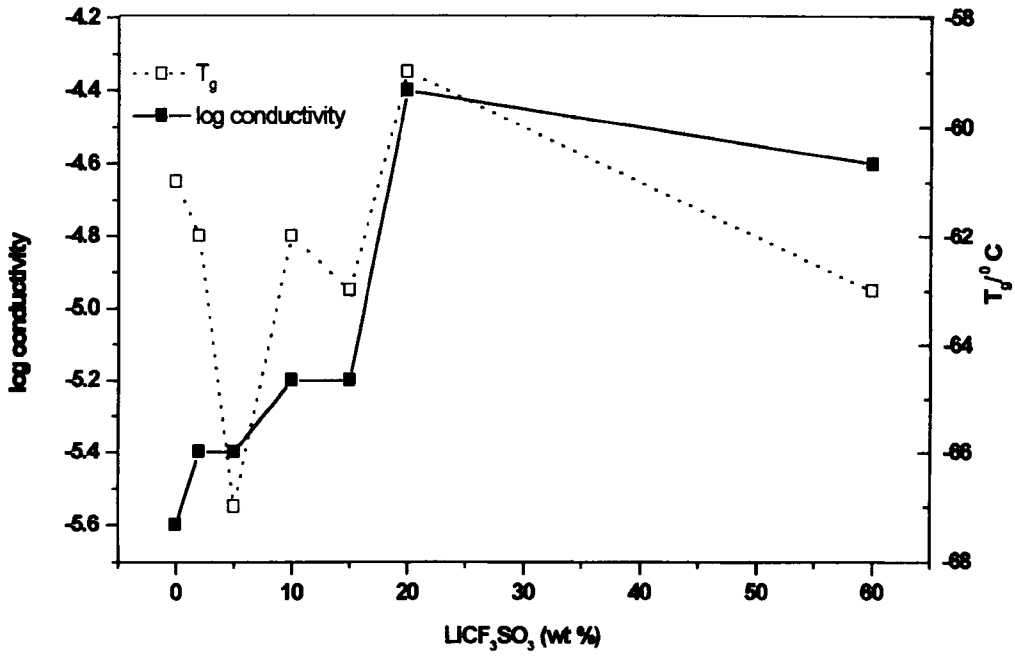

Figure 5.8 Variation of T_g and ionic conductivity for MG-49 /$LiCF_3SO_3$ with the salt concentration.

Figure 5.6, 5.7 and 5.8 show the variation of glass transition temperature and ionic conductivity with the salt concentration for ENR25/$LiCF_3SO_3$, ENR50 /$LiCF_3SO_3$ and MG-49/$LiCF_3SO_3$ electrolytes at ambient temperature. The trend of these systems indicates that the increased T_g provides lower conductivity, which is unusual for this case. The radical increase of T_g in ENR25/ $LiCF_3SO_3$ occurred at the change of salt concentration from 15 wt percent to 20 wt. Per cent, accompanying a reduction of ionic conductivity. It is believed that, the incorporated salt dissociates to produce mobile ions via solvation of epoxy group in the polymer backbone.

The ions remain coordinated to the polar polymer, which could be acting as virtual transient crosslinks to increase T_g values. The excessive addition of salt to the system increases its viscosity, however the conductivity has increased steadily despite the presence of ion pairs or aggregated ions.

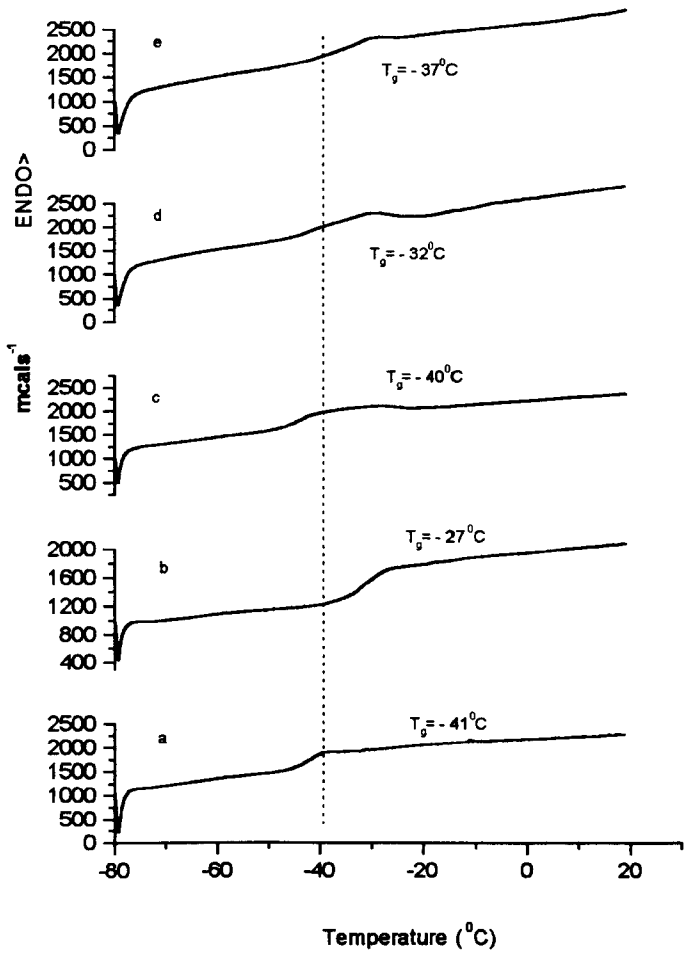

Figure 5.9 DSC traces of ENR25 doped with $LiCF_3SO_3$ (a) pure ENR-25 (b) 2% (c) 5% (d) 10% (e) 20%

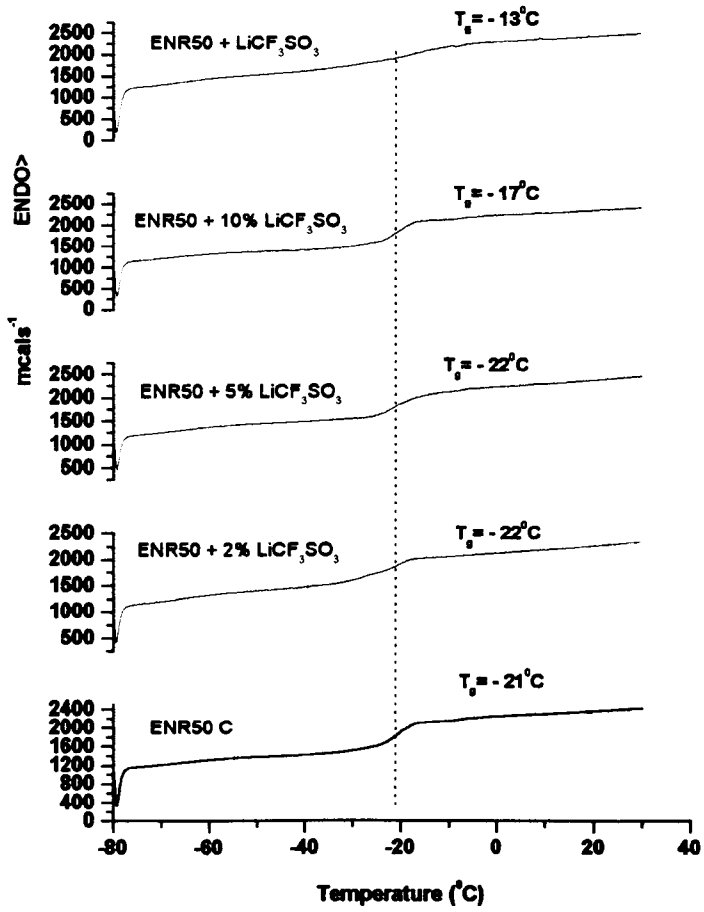

Figure 5.10 DSC traces of ENR50/ $LiCF_3SO_3$ (a) pure ENR-50 (b) 2% (c) 5% (d) 10% (e) 20%

Figures 5.9, 5.10 and 5.11 show the trends of glass transition temperature of the modified natural rubber based systems as a function of the salt concentration. The traces show an increase of glass transition temperature, T_g, for the three types of modified natural rubber based polymer electrolyte systems. The concentration of salt added to the polymer at O/Li ratio ranged from 27/1 to 1/1.for the ENR-25 series (see Table. 5.1). The Tg of control ENR-25, is -41^0C and that of (ENR-25)$_3$($LiCF_3$ SO_3) is -37^0C. Thus, the effect of added salt has increased the T_g value. T_g is found, in general, to increase with increasing salt concentration.

This indicates that a complex has formed between the rubber polymer and the lithium salt. The ionic mobility is closely related to the relaxation modes of the polymer host. This can be observed through the increase in Tg of polymeric systems as salt concentration is increased. The statement is agreed with the above finding.

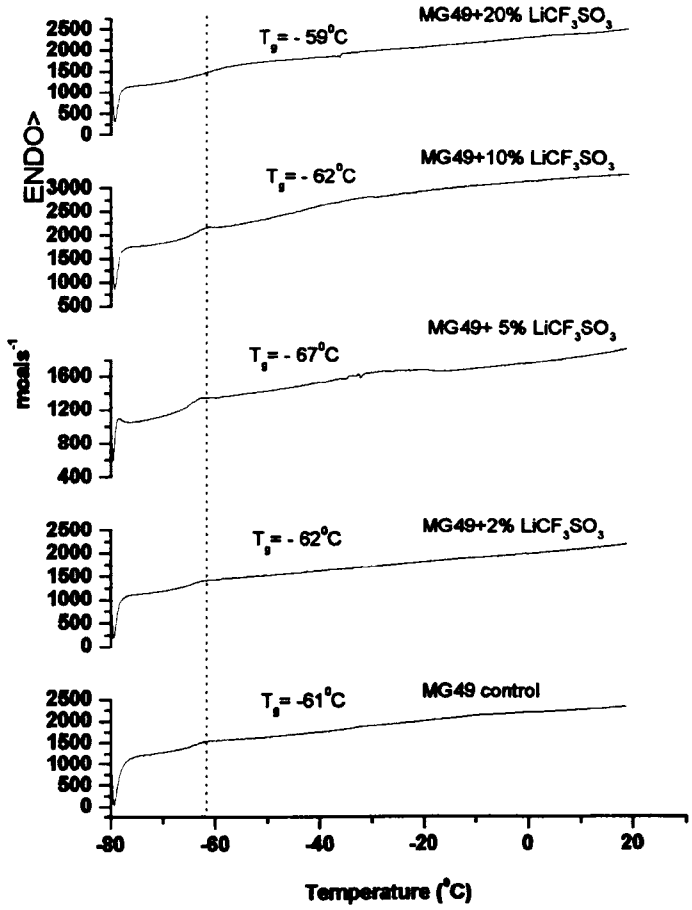

Figure 5.11 DSC traces of MG49/$LiCF_3SO_3$ electrolytes

Figure 5.11 shows the DSC traces of MG 49 based polymer electrolytes prepared from solvent cast. The glass transition temperatures of the samples calculated from DSC traces are from -59^0C to -67^0C. The Tg values are lower in comparison with epoxidised natural rubber based polymer electrolytes studied in the preceding section. The addition of lithium triflate into the MG rubber polymer system has a little increased on the glass transition temperature. In the case of epoxidised based electrolyte system has caused slightly higher increased glass transition temperature upon addition of lithium triflate salt. This finding almost in agreement with other polymer electrolyte systems reported from literature such as PEO based system (Bandara, Dissanayake and Mellander, 1998). It reported that T_g is about 20^0C higher than that of uncomplexed PEO. Wieczorek and Steven (1997) have reported that the initial value for the undoped EO-PO copolymer is -67^0C has increased to -56^0C after addition of $LiCF_3SO_3$.

5.4.3 Infrared

Infrared absorption spectroscopy has been very useful in the study of polymer electrolytes because it provides indication of cation-anion contact in both crystalline and amorphous salt complexes over a wide concentration range. Variation in vibrational frequency can provide information about the influence of the environment on the molecular ions. In this chapter, infrared vibrational- studies on plasticised and non-plasticised epoxidized natural rubber doped with lithium salt electrolytes are presented in the range of 4000 to 500 cm^{-1}. However, the results are focused on the mid-range vibration frequencies from 1600 to 500 cm^{-1}. It is expected to occur for the characteristics of lithium cation to complex with oxygen atom of epoxy group natural rubber polymer in the vibrational frequencies, 1034.6 cm^{-1}, 1065.7 cm^{-1} and 1096 cm^{-1}observed in Raman spectrum (Nakamoto1997). Other frequencies associated with linear structure of ^{6}Li ^{6}LiO and bending O^{6}LiO at 1028.5 cm^{-1} and 730 cm^{-1}. The IR spectra of pure ENR25 and polymer electrolytes based on modified natural rubber containing lithium triflate salt ($LiCF_3SO_3$) are shown in Figure 5.12.

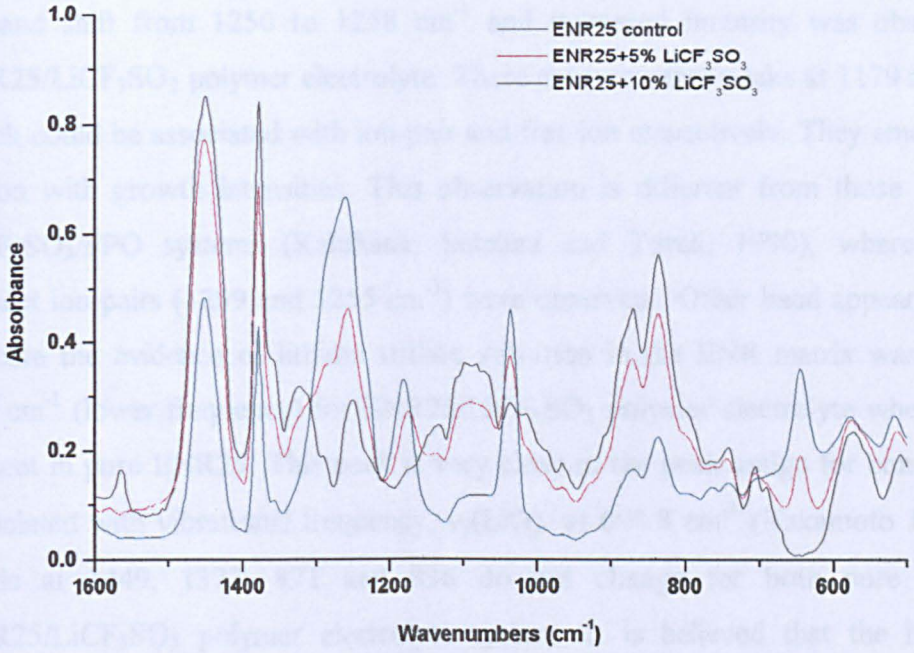

Figure 5.12 Comparison of the IR spectra of the pure ENR-25 and ENR-25/$LiCF_3SO_3$ electrolytes.

ENR25 polymer is a polar polymer induced by the epoxy group situated randomly at the natural rubber main chain by chemical modification. It is assumed that mobile anions/cations from the lithium triflate are responsible for the ionic conduction, and the polymer (ENR25) acts as substrate that solvate lithium salt into the polymer framework. It is possible that the polymer chains of ENR interacts with the dissociated ions or with associated ion pairs in the polymer framework, because the ENR polymer is highly polar material. In order to investigate the interaction of lithium salt with ENR polymer and the changes of its environment within the system FTIR was utilized. Figure 5.12 shows the comparison IR spectra of pure ENR25 and $LiCF_3SO_3$ in the frequency range 1600 to 600 cm^{-1}. If the Li^+ ions of $LiCF_3SO_3$ were coordinated with epoxide groups situated in the natural rubber mainchain, there must be changes in the vibrational modes, which involve the epoxide oxygens. It was cited in the literature that a peak at 1250 cm^{-1} assigned to epoxy whole ring stretching (Decker et al 1995).

A band shift from 1250 to 1258 cm^{-1} and increased intensity was observed in the ENR25/$LiCF_3SO_3$ polymer electrolyte. There are two other peaks at 1179 and1032 cm^{-1} which could be associated with ion-pair and free ion respectively. They emerge from the region with growth intensities. This observation is different from those observed for $LiCF_3SO_3$/PPO systems (Kakihana, Schantz and Torell, 1990), where bands with contact ion-pairs (1299 and 1255 cm^{-1}) were observed. Other band appear which might indicate the evidence of lithium triflate solvation in the ENR matrix was observed at 640 cm^{-1} (lower frequency) for ENR25/$LiCF_3SO_3$ polymer electrolyte whereas no peak present in pure ENR25. This peak is very close to the peak assign for compound $^7LiO_2$ associated with vibrational frequency, ν_s(LiO) at 698.8 cm^{-1} (Nakamoto 1997). Other bands at 1449, 1377, 871 and 836 do not change for both pure ENR25 and ENR25/$LiCF_3SO_3$ polymer electrolyte system. It is believed that the interaction of lithium salt with oxygen of the epoxy group of ENR-25 might occur, which produces a series of different IR active bands as its environment changes.

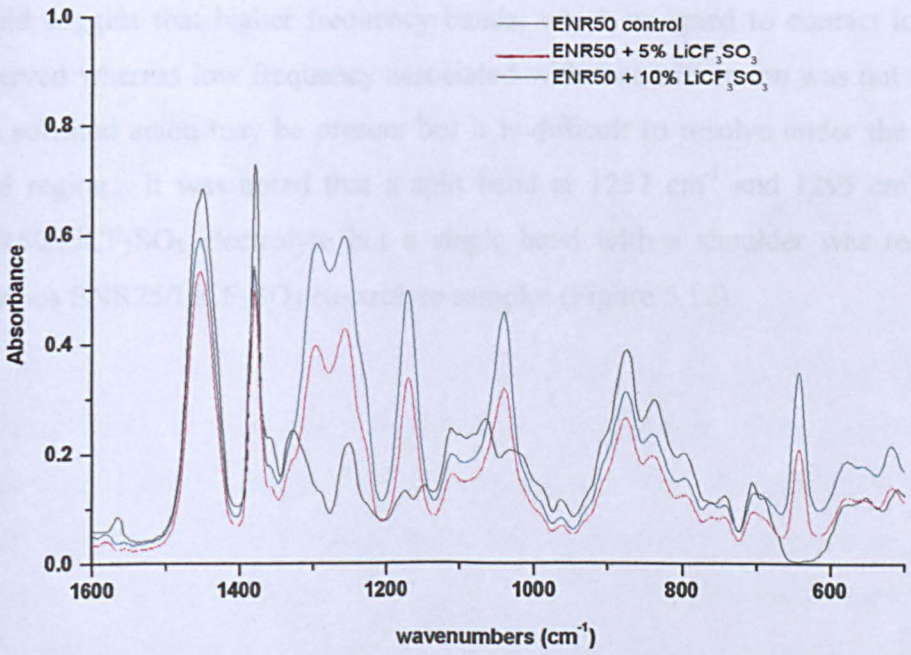

Figure 5.13 Comparison of IR spectra of pure ENR50 and ENR50/$LiCF_3SO_3$ electrolyte.

Figure 5.13 shows a stack plot of pure ENR50 and ENR50/$LiCF_3SO_3$ polymer electrolytes in the region 1600-600 cm^{-1}. The changes in the IR spectra of undoped ENR50 occurred with emergence of new peaks upon addition of lithium salt into the polymer matrix. These peaks were observed at 1040 and 642 cm^{-1}. These peaks appear almost similar position with those collected for ENR25/$LiCF_3SO_3$ in Figure 5.12. The peak at 1040 cm^{-1} most likely assign to monodentate ion pairs (MacFarlane *et al* 1995). The absorption bands collected at 1295, 1257, 1170 and 1040 cm^{-1} could attribute to the existence of monodentate ion pairs and free triflate ions. These data are different compared to those described for triflate vibrational frequencies (Huang, Frech and Wheeler, 1994) and $LiCF_3SO_3$/PPO systems (Kakihana, Schantz and Torell, 1990). It was reported that the bands with contact ion pairs at 1299, 1258, and 1043 cm^{-1} and free triflate ion at 1272 cm^{-1}.

Other peak at 642 cm^{-1} was observed in the IR spectra of $LiCF_3SO_3$/ENR50 system as lithium triflate salt was introduced into the polymer matrix. From this information it would suggest that higher frequency bands, which assigned to contact ion pairs, were observed whereas low frequency associated with free triflate ion was not apparent. The free solvated anion may be present but it is difficult to resolve under the broad C-O-C band region. It was noted that a split band at 1257 cm^{-1} and 1295 cm^{-1} appeared in ENR50/$LiCF_3SO_3$ electrolyte but a single band with a shoulder was recorded in the previous ENR25/$LiCF_3SO_3$ electrolyte samples (Figure 5.12).

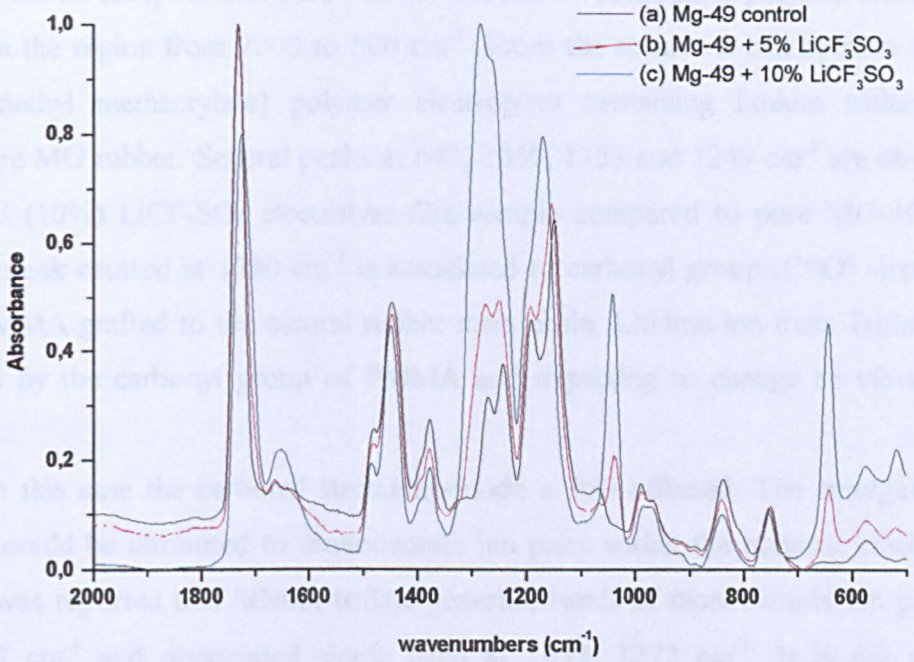

Figure 5.14 Comparison of IR spectra for (a) pure MG-49;(b) MG-49/5% $LiCF_3SO_3$; (c) MG-49/ 10 % $LiCF_3SO_3$.

Polymethyl methacrylate grafted natural rubber (MG-49) as polymer host and incorporated with lithium triflate to produce lithium ion conducting electrolyte films has been attempted. Many types of polymer electrolyte system have been investigated using PEO based materials but no work reported using polymethyl methacrylate grafted natural rubber. FTIR spectroscopy has been carried out at ambient temperature to monitor the effect of lithium triflate salt on the phase morphology of the poly(methyl methacrylate) grafted natural rubber. In lithium ion conducting polymer electrolytes the lithium ion, in principle might coordinate with anion or the polymer chain. Certain bands resulting from specific vibrations of each of the potentially coordinating species have been observed to split or shift to different frequencies on cation coordination (Bakker, Lindgren and Hermansson 1996).

Figure 5.14 shows IR spectra of pure MG-49 and MG-49/$LiCF_3SO_3$ polymer electrolyte cast films in the region from 2000 to 500 cm^{-1}. From the spectra it can be seen clearly that poly(methyl methacrylate) polymer electrolytes containing lithium triflate salt differ to pure MG rubber. Several peaks at 642, 1040, 1153 and 1249 cm^{-1} are observed for MG-49/ (10%) $LiCF_3SO_3$ electrolyte film sample compared to pure MG-49 film. The strong peak centred at 1730 cm^{-1} is associated to carbonyl group (C=O) stretching mode of PMMA grafted to the natural rubber main chain. Lithium ion from Triflate can be solvated by the carbonyl group of PMMA and expecting to change its vibrational mode.

However in this case the carbonyl stretching-mode is less affected. The emergence of new peaks could be attributed to monodentate ion pairs within the polymer electrolyte system. It was reported that lithium triflate generate bands of monodentate ion pairs at 1043, 1257 cm^{-1} and dissociated single band at 1033, 1272 cm^{-1}. It is not clearly understood at the present stage that the ion-pairs seem to exist in the polymer electrolyte. This fact suggests that ion aggregates may reduce the mobility of the polymer chain and impeding ionic conductivity.

5.5 Plasticised modified natural rubber systems

For the past few years many research groups in various research institutions have focused on polymer gel electrolytes to obtain high ionic conductivity at room temperature. Thus, various polymer electrolyte systems such as employing network of polymers from difunctional macromonomers (Kono, Hayashi and Watanabe, 1999), acrylonitrile-methyl methacrylate-styrene terpolymer (Kim, Oh and Choi, 1999) and polyethylene diacrylate (PEGDA) (Hikmet and Peeters, 1999). In addition, the systems using synthetic rubber blended with other polymer have been explored (Matsumoto, Rutt and Nishi, 1995; Ju *et al* 1998).

Matsumoto and co-workers have proposed a new concept based on dual-phase polymer electrolyte (DPE) using poly(acrylonitrile-co-butadiene)(NBR)/poly(styrene-co-butadiene)(SBR) polymer hosts. The systems described that a highly polar polymer impregnated with a lithium salt solution form ionic continuous pathways and non-polar

polymer produces good mechanical strength. Then, Ju and co-workers extended the Matsumoto's concept to a novel dual-phase system prepared from poly(epichlorohydrin-*co*-Oxirane) (ECO), nitrile butadiene rubber (NBR), and lithium perchlorate ($LiClO_4$) in propylene carbonate (PC). In this system, the ECO was selected as a highly polar matrix. In parallel to the above work, a novel approach using modified natural rubber was investigated for this thesis. So far, no other modified natural rubber has been used for polymer electrolyte system.

The masticated rubbers and electrolyte components, such as lithium salt solution in the mixtures of ethylene carbonate and propylene carbonate (PC) mixed very well in the THF solvent overnight and formed viscous homogenous solutions. The viscous homogeneous solutions were cast onto glass ring with Teflon substrate underneath. The resultant cast films were slightly sticky and difficult to peel off from the substrate. The films bonded strongly to the Teflon substrate. However, they were stripped off when cooled to liquid nitrogen temperature. The films were immediately transferred into the vacuum oven for further removal of solvent and moisture. From the DSC traces it was found that the morphology of the film is not affected by the treatment of liquid nitrogen.

The ionic conductivity and thermal analysis results as a function of salt concentration are given in Tables 5.4, 5.5, and 5.6 respectively. The details of thermal history of these films will be discussed in the later part of this section. The strong adhesive property is significant for efficient contact with the electrodes in the cell systems. This is one of the promising features discovered in this work.

Table 5.4 Properties of ENR-25 systems with plasticisers

	Composition		Electrical properties	Thermal behavior
Sample	ENR/ SALT/EC+PC	O/Li	Conductivity (S cm^{-1})	T_g(^{0}C)
E25/1p	100/5/25	11/1	$3.7x\ 10^{-5}$	-41
E25/2p	100/5/50	11/1	$5.1x\ 10^{-5}$	-42
E25/3p	100/5/100	11/1	$1.8x\ 10^{-4}$	-42
E25/4p	100/5/200	11/1	$2.9x10^{-4}$	-43
E25/5c	100/5	11/1	$1.6x10^{-5}$	-40

Table 5.5 Properties of ENR-50 systems with plasticizers

	Composition		Electrical properties	Thermal behavior
Sample	ENR/ SALT/EC+PC	O/Li	Conductivity (S cm^{-1})	T_g(^{0}C)
E50/1p	100/5/25	20/1	$3.3x10^{-5}$	-37
E50/2p	100/5/50	20/1	$3.5x10^{-5}$	-37
E50/3p	100/5/100	20/1	$4.0x10^{-5}$	-31
E50/4p	100/5/200	20/1	$1.3x10^{-4}$	-35
E50/5c	100/5/0	20/1	$2.0x10^{-5}$	-21

Table 5.6 Properties of MG-49 systems with plasticizers

	Composition	Electrical properties	Thermal behavior
Sample	MG-49/SALT/EC+PC	Conductivity (S cm^{-1})	T_g (^{0}C)
MG-49/P1	100/5/25	$6.0x10^{-5}$	-68
MG-49/P2	100/5/50	$1.8x10^{-4}$	-67
MG-49/P3	100/5/100	$3.2x10^{-4}$	-68
MG-49/P4	100/5/200	$4.3x10^{-4}$	-64
MG-49/5c	100/5	$4.1x10^{-6}$	-59

5.5.1 Conductivity measurement

Tables 5.4, 5.5 and 5.6 show the results of the modified natural rubber based films containing 5 percent lithium triflate salt with various weight percent ratios of EC/PC. The average ionic conductivity value of the system was 10^{-5} S cm^{-1} at ambient temperature when plasticiser content is 50 wt. % and reaches10^{-4} S cm^{-1} at 100 wt. %.

Figure 5.15 shows the trend of conductivity behaviour of the system is plotted as a function of weight percent of EC/PC. It was observed that the modified natural rubber based film has the ability to uptake a high loading of polar low molecular weight organic solvent. The polymer electrolyte films with ionic conductivities in the order 10^{-4} S cm^{-1} still retain their rubbery characteristic in spite of the presence of much absorbed electrolyte solution. The typical impedance plots for the modified natural rubber based electrolyte films are presented in Figure 5.16. The resistance was measured from the high frequency intercept on the real axis.

The conductivity of the polymer electrolyte was calculated from the measured resistance and the known area and thickness of the polymer film. Similar procedures were followed for all other experiments, as shown before in Table 5.1, 5.2, and 5.3.

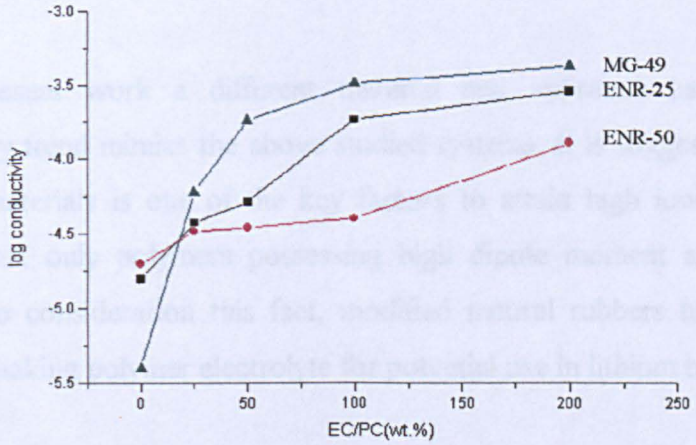

Figure 5.15 Conductivity as a function of EC/PC for modified natural rubber based systems

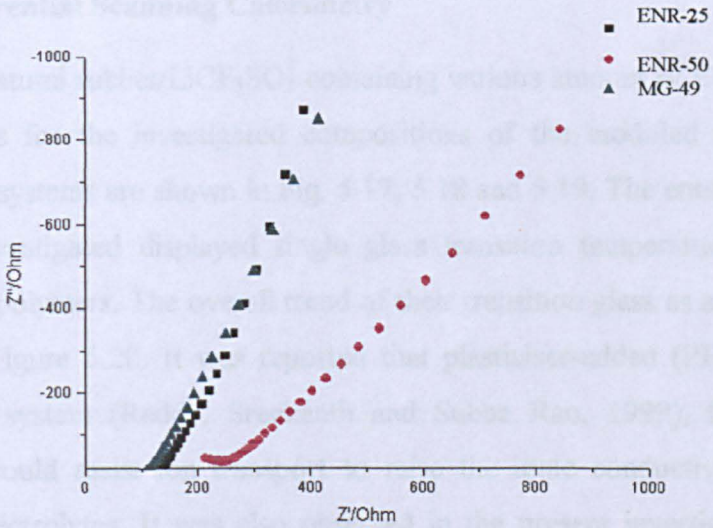

Figure 5.16 Impedance plots of plasticised modified natural rubber based gel electrolytes.

Ionic conductivities of gel electrolytes consisting of different polymer hosts but using the same liquid electrolytes have been reported (Bohnke *et al* 1993; Matsuda *et al* 1993). The polymer hosts function as containers of the liquid electrolytes. Elastomeric-based material using synthetic rubber has also been studied by Matsumoto (1996). It was reported that ionic conductivity of 10^{-3} S cm^{-1} was obtained by swelling this polymer with plasticiser.

In this present work a different material and approach has been used but the conductivity trend mimics the above studied systems. It is suggested that the polarity of the both materials is one of the key factors to attain high ionic conductivity. It was reported that only polymers possessing high dipole moment are suitable candidates. Taking into consideration this fact, modified natural rubbers have fulfilled the above criteria in making polymer electrolyte for potential use in lithium batteries.

Many of the recent works on gel electrolytes have also been reported employing polar matrices such as diacrylates, acrylonitrile-methyl methacrylate-styrene terpolymer, and so forth (Kono, Hayashi and Watanabe, 1999; Nashiura *et al* 1998).

5.5.2 Differential Scanning Calorimetry

Modified natural rubber/$LiCF_3SO_3$ containing various amount of EC/PC were produced. DSC traces for the investigated compositions of the modified natural rubber based electrolyte systems are shown in Fig. 5.17, 5.18 and 5.19. The entire polymer electrolyte systems investigated displayed single glass transition temperatures, typical of highly plasticised polymers. The overall trend of their transition glass as a function of EC/PC is shown in Figure 5.20. It was reported that plasticiser-added (PEO +$NaYF_4$) polymer electrolyte system (Reddy, Sreekanth and Subba Rao, 1999), the increase of chain flexibility could assist ion transport to raise the ionic conductivity of the plasticised polymer electrolytes. It was also observed in the present investigation that plasticised modified natural rubber based electrolyte systems with lower T_g values showed higher conductivity compare with salt-doped system.

In the plasticised ENR-25 series the gel systems were prepared at fixed value O/Li = 11/1, with incorporation of various EC/PC ratios has reduced its Tg value to -43^{0}C. For the ENR-50 series the plasticised films have been prepared at O/Li ratio (20/1). In the case of pure ENR-50 the T_g value is -21^{0}C. The addition of 5 wt.% (O/Li = 20/1) lithium triflate salt into ENR50 has not change its Tg value (see Table 5.2). However increasing the salt content to 20 wt.% (O/Li = 5/1) has increased the T_g value to -13^{0}C. In contrast to this, by adding 200 wt.% EC/PC to $(ENR\text{-}50)_{20}(LiCF_3SO_3)$ complex has registered T_g value - 35^{0}C. The plasticising effect of the solvents has reduced the Tg value dramatically.

However, in the case of MG-49 series, the gel systems show lower Tg values (see Table 5.6) compared to epoxidised natural rubber based. The glass transition temperature of MG-49 control recorded by DSC is -62^{0}C whereas ENR50 control – 21^{0}C. Addition of EC/PC (100 wt.%) into MG-49 containing lithium triflate salt (5 wt.%) has slightly lowered its T_g value to – 68^{0}C. The above findings are in agreement with other polymer electrolyte systems investigated by several research groups. The effective addition of PC to a PAN matrix has reduced its T_g value (Tsutsumi, Matsuo, Onimura, and Oishi, 1998).

The initial T_g of pure PAN is 97^{0}C (Branchup and Immergut, 1975), and that of $(PAN)_{20}$ $(LiClO_4)$(PC) was – 54^{0}C. The effect of plasticiser on the physical /chemical properties of the radiation-polymerised polyether formed by cross-linking a mixture of acrylate oligomer and dissolved salt has been investigated (Huq, Koksbang, Tonder and Farrington, 1992). The plasticisers used were propylene carbonate, ethylene carbonate and a mixture of ethylene carbonate and propylene carbonate. The T_g of the complex is – 65^{0}C. When 25 wt % PC is added the T_g shift to lower value to about – 75^{0}C.

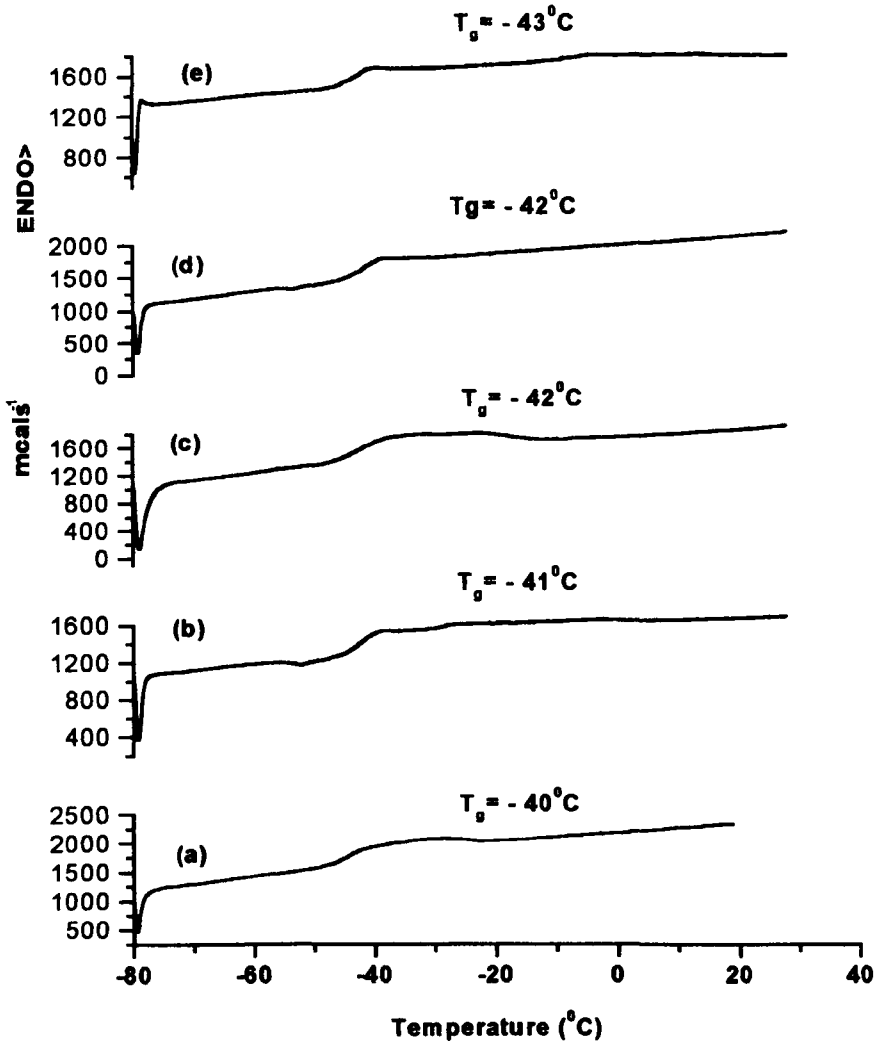

Figure 5.17 DSC traces of ENR25 electrolyte system (a) unplasticised (b) 25 wt % EC/PC (c) 50 wt % EC/PC (d) 100 wt % EC/PC (e) 200 wt % EC/PC.

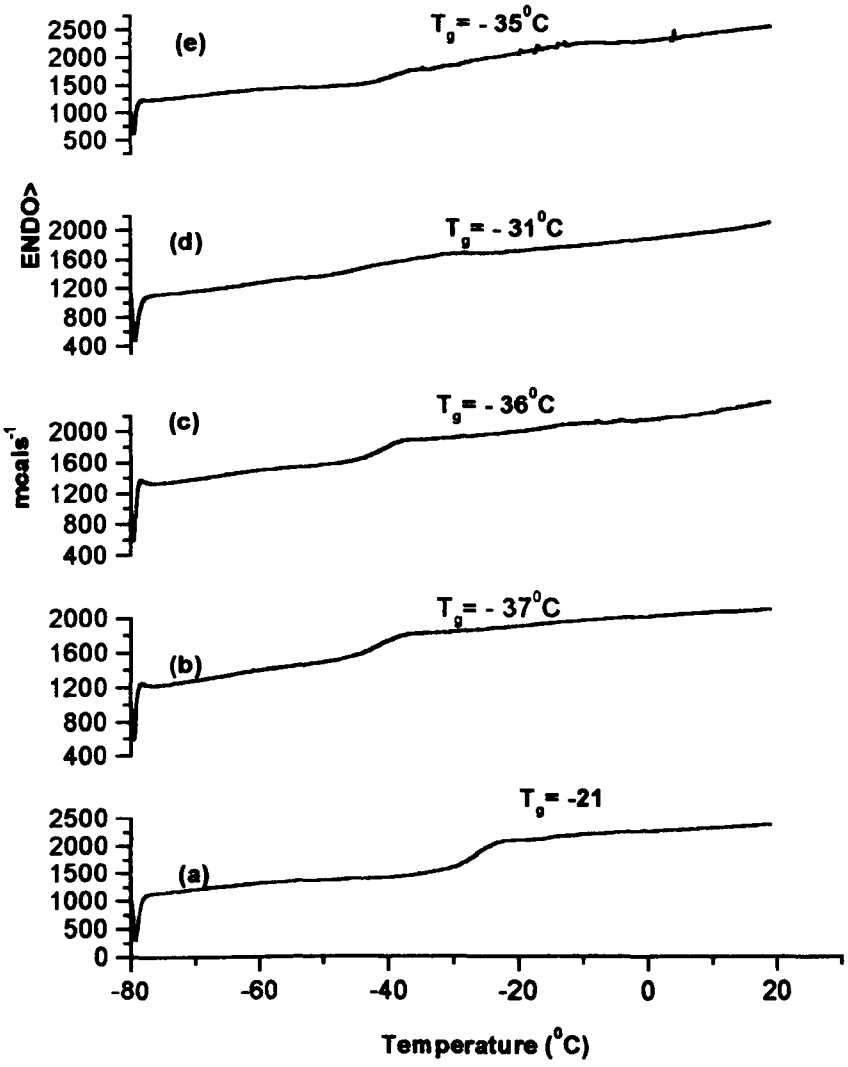

Figure 5.18. DSC traces of ENR50 electrolyte system (a) unplasticised (b) 25 wt % EC/PC (c) 50 wt % (d) 100 wt % (d) 200 wt %.

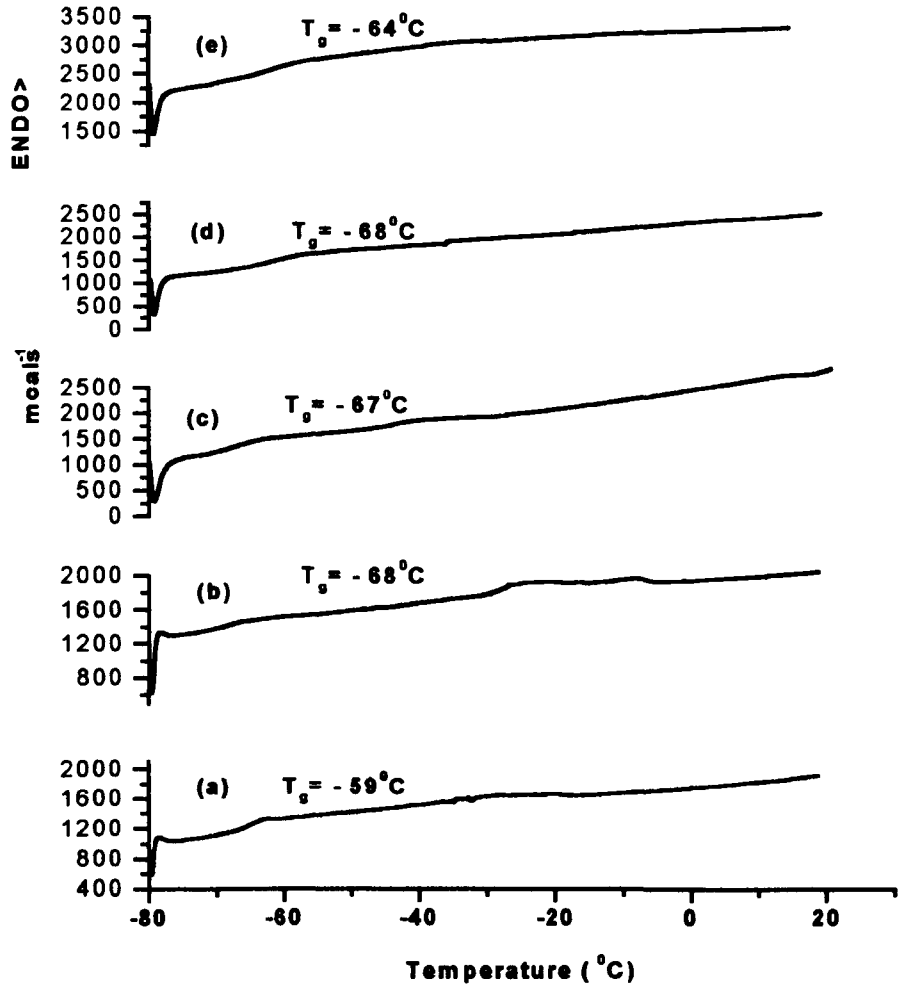

Figure 5.19 DSC traces of MG-49 electrolyte system (a) unplasticised (b) 25 wt.% EC/PC (c) 50 wt.% EC/PC (d) 100 wt. % EC/PC (e) 200 wt. % EC/PC .

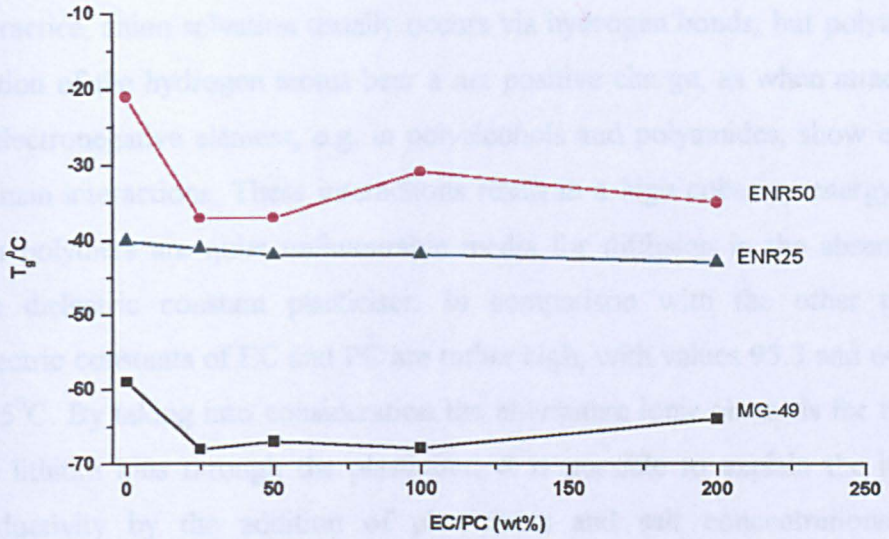

Figure 5.20. Glass transition temperature as a function of EC/PC for plasticised modified natural rubber systems

5.5.2.1 Correlation between T_g and conductivitiy

Basically, plasticised polymer electrolytes are represented as compromising of three components, namely polymer, plasticiser and the lithium salt. In the case of plasticised polymer electrolyte system, a modest amount of solvent is added to the host polymer in order to reduce T_g of the system and hence the mobility at a given temperature. By a systematic investigation of the changes in the properties of the plasticised films, incorporated by variation of electrolyte species and their relative amount, the interaction between the components and their ionic transport within the system can be determined. The effect of the plasticisers on the polymer mobility and the conductivity also depends on the nature of the plasticiser including viscosity, dielectric constant, polymer-plasticiser interaction,and ion-plasticiser coordination. The effect of the plasticisers on the conformation and mobility of the host polymer depends on the plasticiser structure and the molecular weight, which influence the degree of mixing and the polymer-polymer interactions. Ethylene carbonate (EC) is solid at room temperature with a molecular weight of 88.05g whereas propylene carbonate is a viscous liquid with a molecular weight of 102.09g.

In practice, anion solvation usually occurs via hydrogen bonds, but polymers in which a fraction of the hydrogen atoms bear a net positive charge, as when attached directly to an electronegative element, e.g. in polyalcohols and polyamides, show extensive chain-to chain interactions. These interactions result in a high cohesive energy, and therefore such polymers are quiet unfavourable media for diffusion in the absence of a protic, high dielectric constant plasticiser. In comparison with the other plasticisers, the dielectric constants of EC and PC are rather high, with values 95.3 and 64.4 respectively at 25^0C. By taking into consideration the alternative ionic channels for the migration of free lithium ions through the plasticiser, it is possible to explain the improvement of conductivity by the addition of plasticisers and salt concentrations (Gray, 1987; Cameron, Ingram and Sarmouk, 1990). Lithium ions may prefer to conduct through these new channels because the medium is less viscous, thus enhancing the mobility of the ions.

On the other hand, the plasticiser can interrupt polymer-polymer interactions by occupying the inter-and intra-chain free volume. The plasticiser structure can influence the polymer plasticiser interactions by increasing inter- and intra-chain separation and hence the free volume of the system. The decrease in polymer-polymer interactions and the increase in polymer-plasticiser interaction in turn influence the glass transition temperature behaviour (Forsyth, Meakin, Mac Farlane and Hill, 1995).

The lowering of Tg values was revealed as a result of incorporating plasticisers or solvents into the modified natural rubber matrices. It is believed that the compatibility of the rubber and the solvent determines the increase uptake of electrolyte species in the composition. Figure 5.21, 5.22 and 5.23 indicate that the lower of T_g values provides the higher conductivity in the system. The reduction of T_g in modified natural rubber based electrolyte systems occurred at the change of EC/PC concentration from 0 to 25 wt per cent accompanying an increment of conductivity.

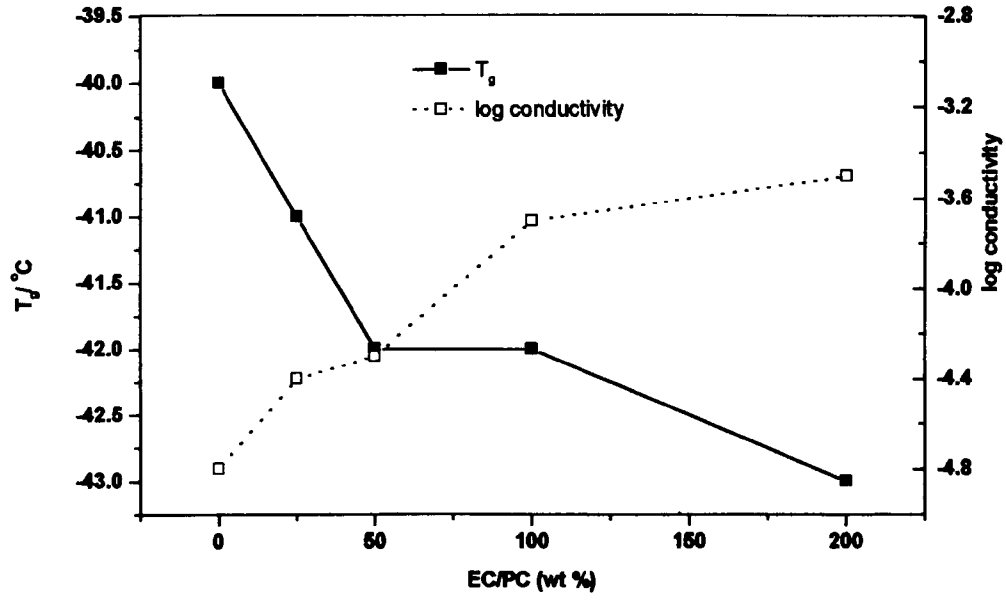

Figure 5.21 Variation of T_g and conductivity as a function of EC/PC concentration for ENR25 system.

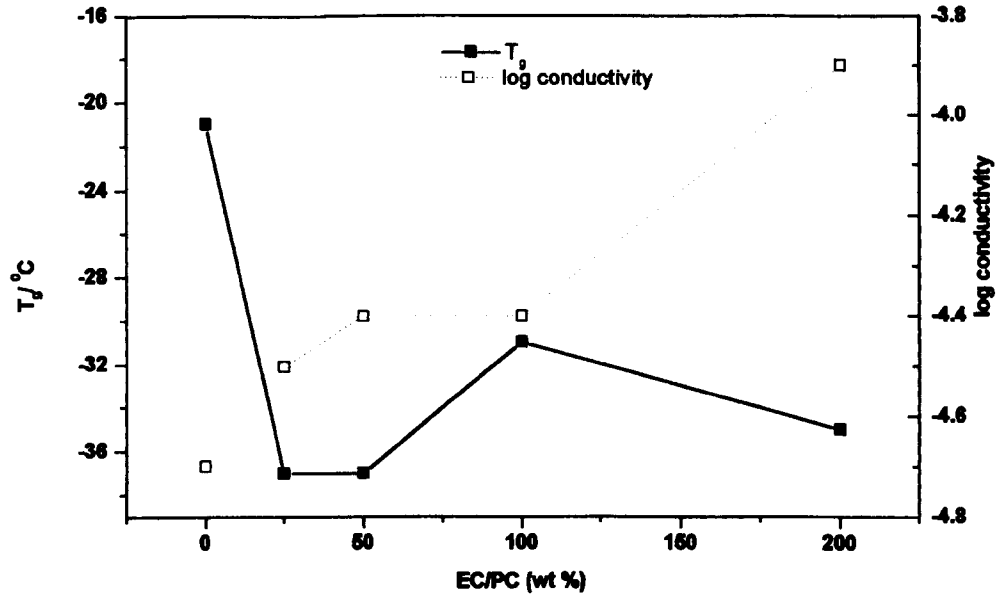

Figure 5.22 Variation of T_g and conductivity as a function of EC/PC concentration for ENR25 system.

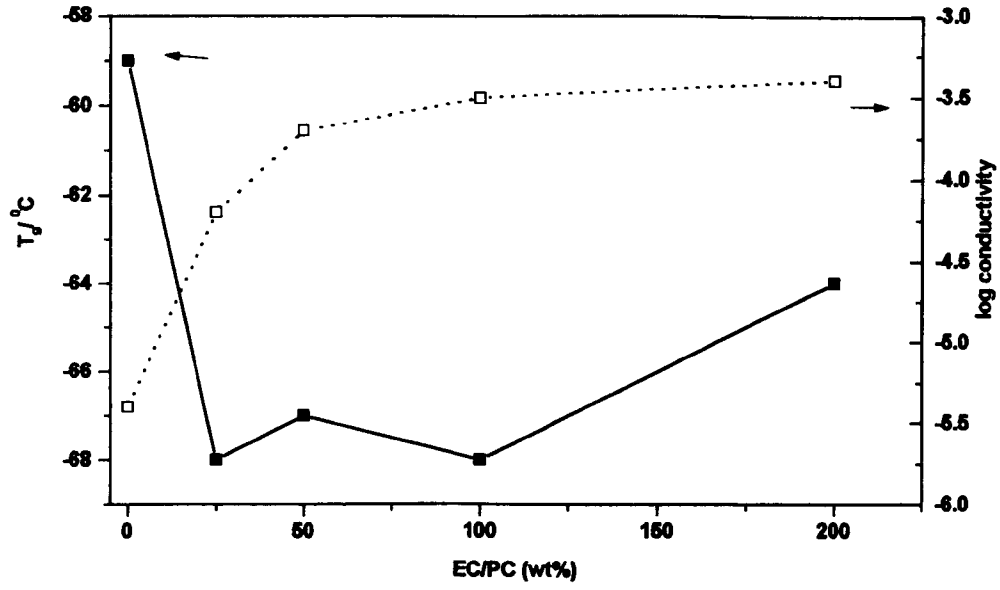

Figure 5.23 Variation of T_g and conductivity as a function of EC/PC concentration for MG-49 system.

5.5.3 Infrared Spectroscopy

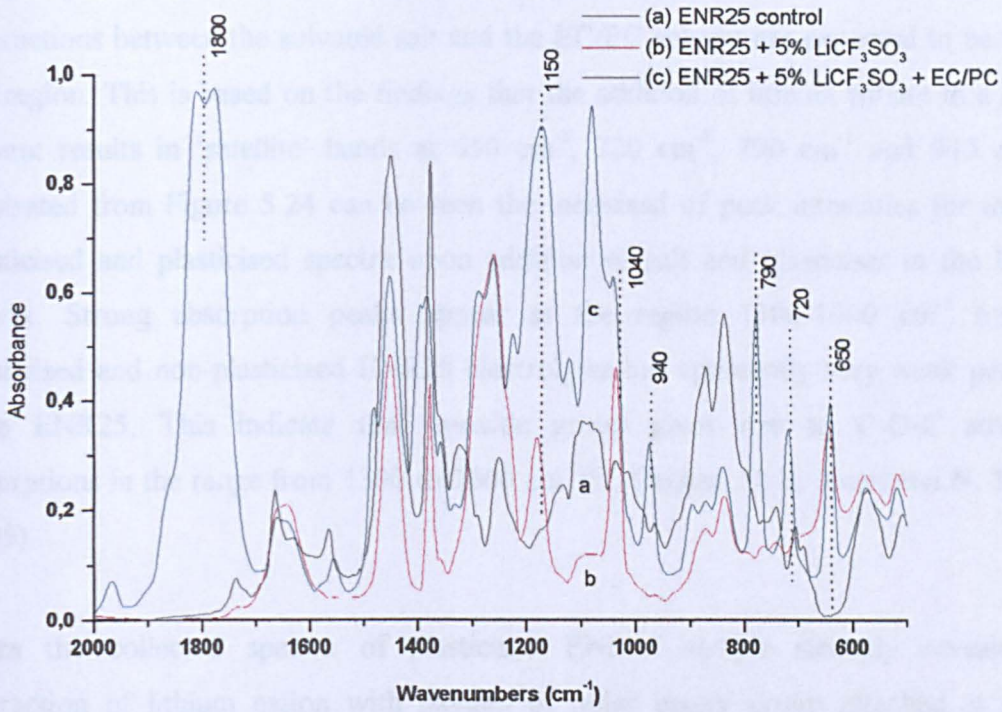

Figure 5.24 Comparison of IR spectra for ENR25 based electrolyte. (a):ENR25 control (b): ENR25/$LiCF_3SO_3$ (c) ENR25/$LiCF_3SO_3$/EC/PC

The room temperature mid-infrared spectra of ENR25/$LiCF_3SO_3$, pure ENR25 and ENR25/$LiCF_3SO_3$/EC/PC are shown in Figure 5.24a, Fig. 5.24b and Fig. 5.24c respectively. The IR bands and their assignments are listed in Table 5.7. A comparison shows that the IR spectra of non-plasticised and plasticised ENR25 systems are different to that of pure ENR25. Several peaks at 650, 790, 720, 940 and 1800 cm^{-1} were observed in the spectrum of plasticised ENR25/$LiCF_3SO_3$ (Fig. 5.24c) whereas unnoticeable peaks apparent in pure ENR 25 (Fig. 5.24b). The spectra region are normalised for comparison. The emergences of new peaks are observed by addition of electrolyte species into the polymer matrix of ENR25. The peaks might come from coordination of Li^+ with EC/PC- polar ENR25 polymer interaction.

The situation is somewhat different in the system ENR25/$LiCF_3SO_3$/EC/PC (Figure 5.24). Special attention has been paid to spectral region between 600-1000 cm^{-1}. Interactions between the solvated salt and the EC/PC solvent are expected to be seen in the region. This is based on the findings that the addition of lithium triflate in a EC/PC solvent results in 'satellite' bands at 650 cm^{-1}, 720 cm^{-1}, 790 cm^{-1} and 940 cm^{-1}. is illustrated from Figure 5.24 can be seen the increased of peak intensities for the non-plasticised and plasticised spectra upon addition of salt and plasticiser in the ENR25 matrix. Strong absorption peaks appear at the region 1300-1000 cm^{-1} for both plasticised and non-plasticized ENR25 electrolytes but apparently very weak peaks for pure ENR25. This indicate that epoxide group gives rise to C-O-C stretching absorptions in the range from 1300 to 1000 cm^{-1}(C. Decker, H. L. Xuan and N. T. Viet, 1995).

From the collected spectra of plasticised ENR25 sample strongly revealed the interaction of lithium cation with oxygen of polar epoxy group attached at natural rubber main chain. Addition of lithium triflate has increased the peak intensity compared to pure ENR25. This has resulted in strong growth of peaks at 1258 and 1036 cm^{-1} for ENR25/$LiCF_3SO_3$/EC/PC and ENR25/$LiCF_3SO_3$ electrolyte samples (Figure 5.24a and 5.24c). All the peaks are normalised for comparison within the region. The peak at 650 cm^{-1} frequently observed for non plasticised and plasticised modified rubber electrolytes from all the spectra collected. This is almost in agreement with the peak observed for PEO-$NaCF_3SO_3$ system (Papke *et al* 1981). The absorption peak observed at 1800 cm^{-1}, is assigned to carbonyl from plasticiser added ENR25/$LiCF_3SO_3$ sample

Table 5.7 IR bands / cm^{-1} of ENR25, ENR25/$LiCF_3SO_3$ and ENR25/$LiCF_3SO_3$/EC/PC

ENR-25	ENR25/$LiCF_3SO_3$	ENR25/$LiCF_3SO_3$/EC/PC	Assignment [a,b,c,d,e,f]
3500	3500	3500	OH stretching
2950	2950	2950	CH, CH_2, CH_3 Stretching
		1800	Carbonyl
1450	1451	1451	CH_2 asymm. bending
1377	1377	1377	CH_3 deformation
1250	1258	1258	[d]Epoxy: whole ring stretching
	1178	1150	[f]CC stretching, [f]COC asymm.
1097			
1037	1036	1036	$\nu(SO_3)$[a]
		940	ν(COC)[b]
871			[d]Epoxy: half ring stretching
837	836	836	
		790	
		720	OLiO
	650	650	[b,c]Li-O,[7]LiO_2

a- MacFarlane, Meakin, Bishop, McNaughton, Rosalie and Forsyth, (1995)
b- Papke, Ratner and Shriver, (1981)
c- Nakamoto (1997)
d- Decker, Xuan and Viet (1995)
e- Munichandraiah, Sivasankar, Scanlon and Marsh (1997)
f- Hashmi, Kumar, Maurya and Chandra (1990)

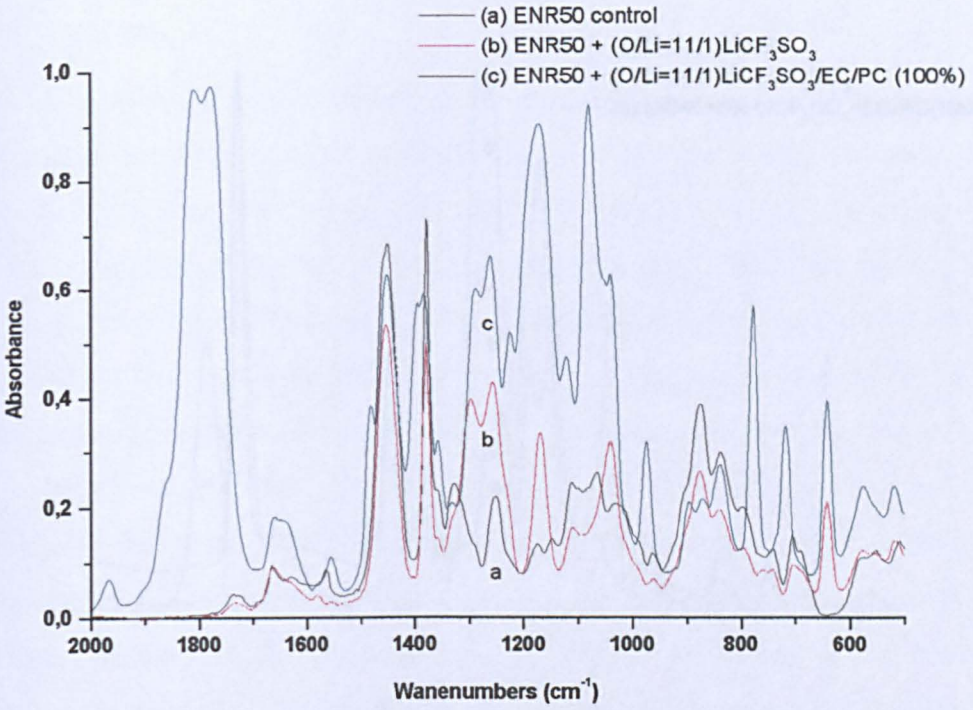

Figure 5.25 Comparison of IR spectra for ENR50 based electrolyte. (a): pure ENR50; (b): ENR50/$LiCF_3SO_3$ (c) ENR50/$LiCF_3SO_3$/EC/PC

Figure 5.25 shows that the spectra of non-plasticised and plasticised ENR50/$LiCF_3SO_3$ polymer electrolytes are almost similar but not identical to plasticised ENR25 based systems. ENR50/$LiCF_3SO_3$/EC/PC presents a number of new peaks in the 600-1000 cm^{-1} region but no peaks appear for pure ENR50. The assignments of the peaks are given in Table 5.7. The satellite peaks at 650 cm^{-1}, 720 cm^{-1} and 790 cm^{-1} appear to favour for Li interaction with ENR50 containing EC/PC. Similarly, the strong peak centred at at1800 cm^{-1} indicates the present of carbonyl (C=0) from EC/PC environment in the plasticised electrolyte sample. The carbonyl region frequency value at 1800 cm^{-1} is caused by the highly electronegative oxygen atoms in the ethylene carbonate strengthens the C=O bond through an enhanced inductive effect and shifts the frequency to higher values than normal carbonyl.

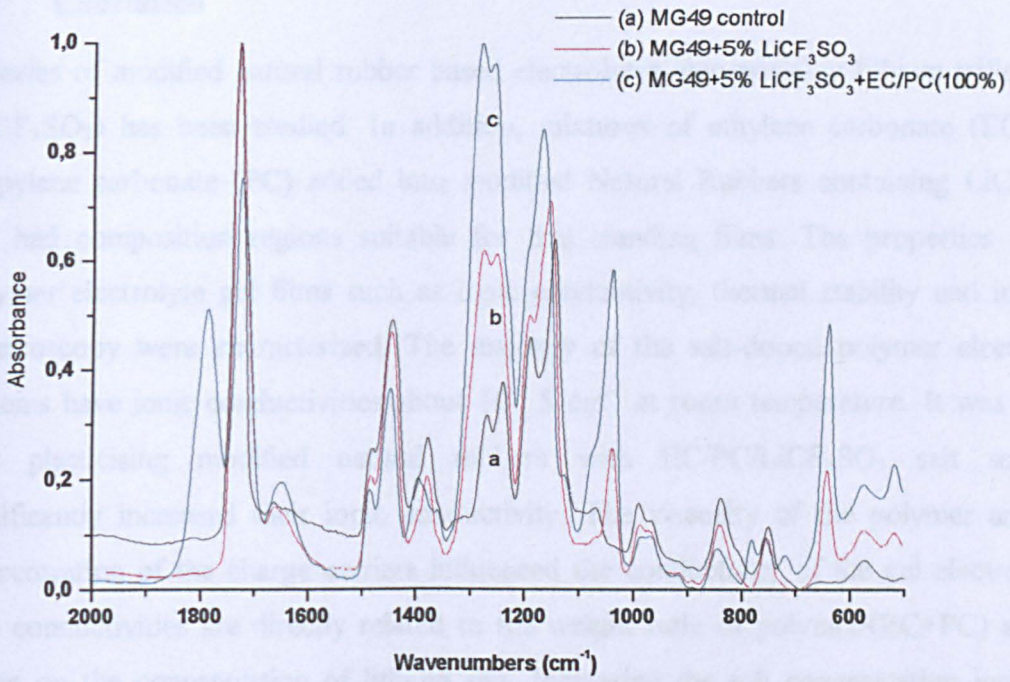

Figure 5.26 Comparison of IR spectra for MG-49 based electrolyte. (a): pure MG-49; (b): MG49/$LiCF_3SO_3$ (c) MG-49/$LiCF_3SO_3$/EC/PC

The infrared spectra observed in Figure 5.26 shows that they are normalised for peak intensity comparison. It illustrates that plasticised MG49/$LiCF_3SO_3$ has new peaks appearing at 650 cm^{-1}, 720 cm^{-1} and 790 cm^{-1} and 1040 cm^{-1} regions. This information indicates that similar trends are observed when lithium salt introduced into the systems when compared to the previous peaks assigned for both plasticised ENR25 and 50 based polymer electrolytes in the frequency range of 600-1000 cm^{-1}. Some of the peak intensities of plasticised MG49/$LiCF_3SO_3$ polymer electrolyte increased upon addition of EC/PC compared to pure MG-49 rubber Figure 5.26(b) and added salt MG-49 Figure 5.26(c). Preliminary conclusions indicate that there is preferred lithium cation coordination to the polar stretching of the ester carbonyl group (C=O) in the polymethyl methacrylate grafted repeat unit. This argument is supported by the fact that carbonyl region is affected by the introduction of lithium salt in both the Raman and the infrared

data suggests coordination between the carbonyl oxygen and the Li^+ cation (Ferry *et al* 1995).

5.6 Conclusion

A series of modified natural rubber based electrolytes incorporating lithium triflate salt ($LiCF_3SO_3$) has been studied. In addition, mixtures of ethylene carbonate (EC) and propylene carbonate (PC) added into modified Natural Rubbers containing $LiCF_3SO_3$ salt had composition regions suitable for free standing films. The properties of the polymer electrolyte gel films such as ionic conductivity, thermal stability and infrared spectroscopy were characterised. The majority of the salt-doped polymer electrolyte systems have ionic conductivities about 10^{-5} S cm^{-1} at room temperature. It was found that plasticising modified natural rubbers with EC/PC/$LiCF_3SO_3$ salt solution significantly increased their ionic conductivity. The viscosity of the polymer and the concentration of the charge carriers influenced the conductivity of the gel electrolytes. The conductivities are directly related to the weight ratio of polymer/(EC+PC) and its effect on the concentration of lithium salt. Increasing the salt concentration increases ionic conductivity.

Addition of 100 wt percent of EC/PC (1:1) into the salt-doped polymer system has considerably increased an average ionic conductivity by almost two orders of magnitude. The ionic conductivities obtained were in the range of 10^{-4} to10^{-3} S cm^{-1} at room temperature. From the experimental work it was observed that the increase in the ionic conductivity of the complex both plasticised and non-plasticised cannot simply explained by the increased concentration of the salt content or the amount of the plasticiser added. However, it is clear that a reasonable conductivity enhancemant can be achieved by the choosing the correct amount of suitable plasticiser, if it is compatible with the host polymer. This approach of using EC/PC, which is polar proved to be soluble in highly polar nature of epoxidised natural rubber (Decker et al 1995). The plasticiser might diffuse out in the long-term storage. According to Sheldon *et al* (1989), the preparation methods utilising a heating stage to promote drying tend to minimize the benefits obtained from plasticization. Maximum plasticizer retention

results from preparation regimes in which heating is avoided. These authors have also concluded that there is evidence of plasticiser loss during long- term storage.

The DSC traces of the salt-doped polymer electrolytes displayed a single and increasing trend of transition glass (T_g) temperatures when an increasing amount of salt concentration was introduced into the polymer matrix. However the incorporation of EC/PC into the system has resulted in a marked reduction in their Tg values. The presence of a highly flexible amorphous phase in DSC measurements seems to be responsible for the increase in conductivity. DSC and FTIR investigations show that Li^+ cation can be complexed by both non- plasticised and plasticised modified natural rubbers.

Chapter 6. Polymer Electrolytes based on ENR/PEO blend

6.1 Introduction

This chapter mainly describes the outcome of investigations carried out on physical properties of ENR/PEO blends based polymer electrolyte systems. The observation and evaluation studies solely focused on using characterisation techniques such as DSC, SEM, FTIR, and ac Impedance Spectroscopy performed on the prepared films. However, preliminary to this chapter some related work, which is vital in respect to the series of experimental task largely contributing to the thesis, was discussed.

The drawback of PEO-based polymer electrolytes systems due to highly crystalline phases has prevented their use for practical application at room temperature. However, despite the setbacks or limitations repeatedly mentioned in many papers published (Sun, Sohn, Yamamoto, Takeda and Imanishi, 1999; Reiche, Steurich, Sandner, Lobitz and Fleischer, 1995; Berthier, Gorecki, Minier, Armand, Chabago and Rigaud, 1983) PEO still has attracted the highest attention as the best highly viscous polymeric matrix. In the recent investigation reported by Scrosati and co-workers (2000) that incorporation of nano-sized ceramic into PEO has produced promising composite polymer electrolyte system. The study has indicated that the increased ionic conductivity by the addition of ceramic filler due to disorder rearrangement of crystalline phases with the absence of liquid solvent. It was suggested that the ceramic additive acts as a solid plasticiser.

Several blend based polymer electrolyte systems using PEO blend with other polymers as polymer hosts have been investigated. The polymers employed in the blends such as polymethylmethacrylate (PMMA), APMMA, PAAM (Wieczorek,1995), PPO (Acosta and Morales, 1996), PVDF (Jacob, Prabaharan, Radhakrishna, 1997), polyacrylonitrile (PAN) (Munichandraiah, Sivasankar, Scanlon and Marsh, 1997) and PVA (Mishra and Rao,1998). These studies have shown that the common characteristic of these polymers is a high transition glass temperature, T_g.

In the studies have shown that it provides the structural stability at molecular level, the ultimate physical properties and the effect on the crystallisation degree of PEO. These polymers should have some common requisites to partner with PEO. Firstly, compatibility between the polymers, and the salt; secondly interaction with cations not too strong to avoid ion trapping; thirdly both polymers are polar. The main goal of these studies is to obtain systems with promising physical properties and with a much higher conductivity than crystalline phases of pristine PEO-complex. Following the principles of the work described above, reported in the literature, this chapter describes an investigation of modified natural rubber blended with PEO to act as polymer host. Epoxidised natural rubber containing 25 per cent epoxidation level (abbreviated as ENR-25) and epoxidised natural rubber of 50-% epoxidation level were used to blend with PEO. The physical characteristics of the materials were described in Table 3.1(Chapter 3, p. 31). The structural features of these materials are depicted below.

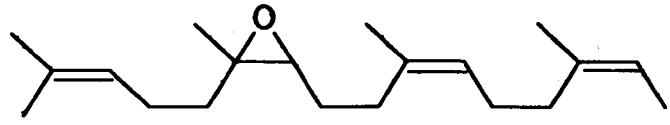

ENR-25

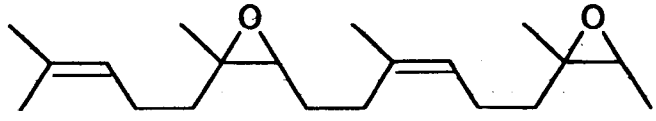

ENR-50

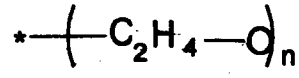

Poly(ethylene oxide)

The series of experimental work in the following was categorised into three main groups namely, undoped ENR (25/50)/PEO polymeric blends, ENR (25/50)/PEO-salt systems, and plasticised ENR (25/50)/PEO-salt systems.

6.2 Undoped ENR/PEO polymeric blends

The initial finding of pure ENR based electrolyte in the preceding work prompted a further investigation of the miscibility of PEO with ENR as a host for Li ion conducting polymer electrolyte. Initially, it is important to obtain the compositions and optical clarity of ENR/PEO polymeric blends. A comparison of the clarity, degree of crystallinity and DSC data of ENR/PEO blends are shown in Table 6.1 and 6.2. The relevant characteristics of pure polymers for both PEO and ENR are also included in the table. Then, the addition of PEO into ENR matrix was effectively studied as a function of PEO concentration. As described in the experimental section, the blends were prepared in the usual manner by the solvent casting technique. There are eight different compositions which were chosen expressed, in weight per cent (w/o) of ENR and PEO, such as 98:2, 95:5, 90:10, 75:25, 25:75, 10:90, 5:95, and 2:98. The ENR was considered as principle host into which the blending character of PEO (molecular weight 600,000) was determined by means of Differential Scanning Calorimeter (DSC) and Scanning Electron Microscopy (SEM) studies.

6.2.1 Differential Scanning Calorimeter (DSC)

The blend samples with thickness range 0.043 cm were prepared by solvent casting and kept under dry condition in the desiccator prior to run for thermal analysis using liquid Nitrogen low temperature PERKIN-ELMER DSC4 equipment. The samples were scanned in the temperature range – 80^0C to + 20^0C. The details background of this equipment was explain in the experimental part Chapter 3.

Table 6.1 Thermal transition temperature and appearance of undoped PEO/ENR-25 blend samples

Sample	% of PEO	X_{cPEO} (%)	Transition temperature/ ^0C		Appearance
			T_g	T_m	
ENR25	0	-	-43	-	Transparent, film
B/1	2	1	-41	61	Translucent, film
B/2	5	3	-41	65	Translucent, film
B/3	10	5	-45	58	Translucent, film
B/4	25	16	-39	61	Translucent, film
B/5	75	50	- 41, -58	67	Translucent, film
B/6	90	53	- 43	68	Hazy, film
B/7	95	56	-	69	Hazy, film
B/8	98	63	-	69	Hazy, film
PEO	100	70	-60	69	Hazy, film

Table 6.2 Thermal transition temperature and appearance of undoped PEO/ENR-50 blend samples.

Sample	% of PEO	X_{cPEO} (%)	Transition temperature/ ^0C		Appearance
			T_g	T_m	
ENR50	0	-	-23		Transparent, film
B/1	2	1	-24	60	Translucent, film
B/2	5	3	-23	62	Translucent, film
B/3	10	5	-20	65	Translucent, film
B/4	25	9	-21	63	Translucent, film
B/5	75	49	-21	66	Hazy, film
B/6	90	57	-	67	Hazy, film
B/7	95	59	- 25	68	Hazy, film
B/8	98	63	-	68	Hazy, film
PEO	100	70	-60	69	Hazy, film

As can be seen from Table 6.1 and Table 6.2, the film samples were partially clear at low concentration of PEO whereas hazy films prevail when higher concentration of PEO was added into the ENR mixture. The thermal behaviour of the blended films of amorphous elastomeric ENR-25/50 with PEO was examined. DSC was utilised to determine the effect of adding PEO into ENR mixture on the morpholologically based thermal transitions of the blends.

DSC traces obtained for the blends with 2, 5, 10, 25, 75, weight per cent of PEO are shown in Fig. 6.1 and 6.2. DSC data for all the blends are presented in Table 6.1 and 6.2. The polyethylene oxide (PEO) used in this investigation was purchased from ALDRICH. It is white powder form and highly crystalline. The degree of crystallinity obtained from DSC, X_c is approximately 70%. The glass transition temperature, T_g, which is sometimes difficult to obtain due to high crystallinity, is about to -60^0C.

Table 6.1 and Table 6.2, show that at higher PEO concentration, substantially a little decrease in the degree of crystallinity of PEO component but dramatically lower at very low concentration. The onset temperature of the melting peak, T_m, shifts to slightly lower temperatures in comparison to that for the pure PEO sample. The trend indicates that the present of non-crystallisable component in the blend has depressed the melting point of PEO in the blend when compared with pure PEO. The ENR rubber component, which is chemically modified natural rubber could act as internal plasticiser to reduce the melting point of PEO.

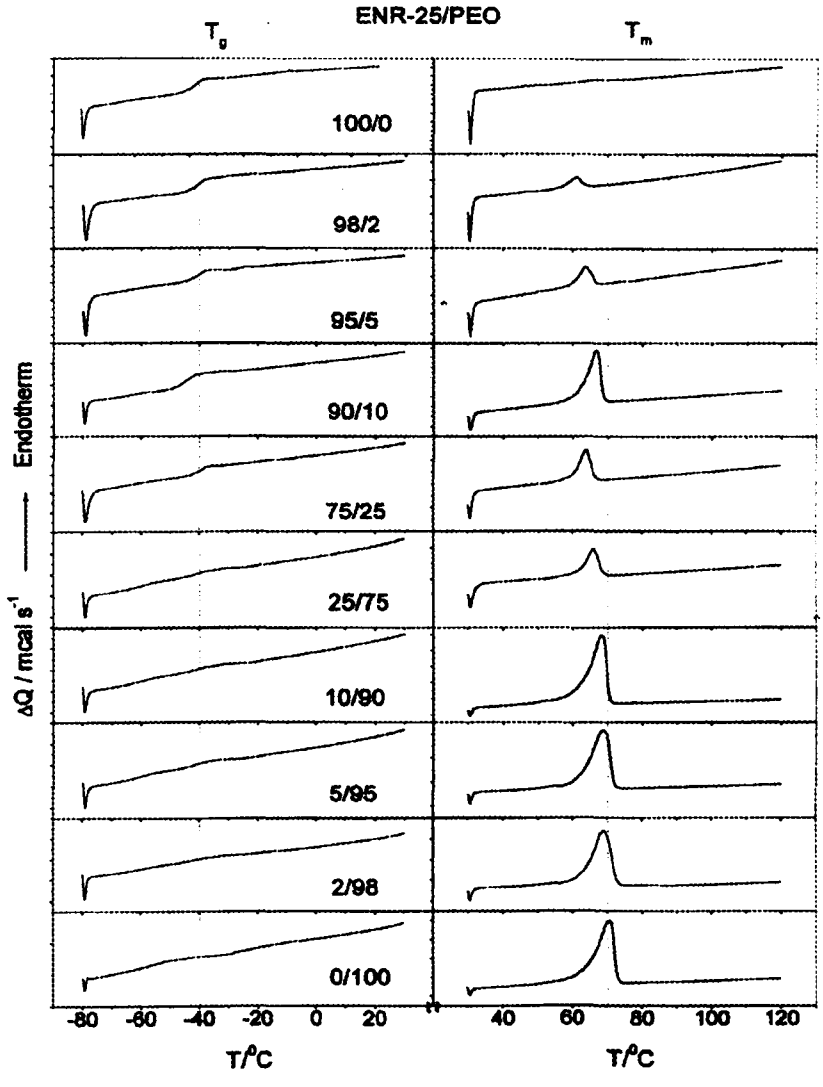

Fig. 6.1 DSC traces of ENR-25/PEO blends (samples containing 0-100% w/o PEO)

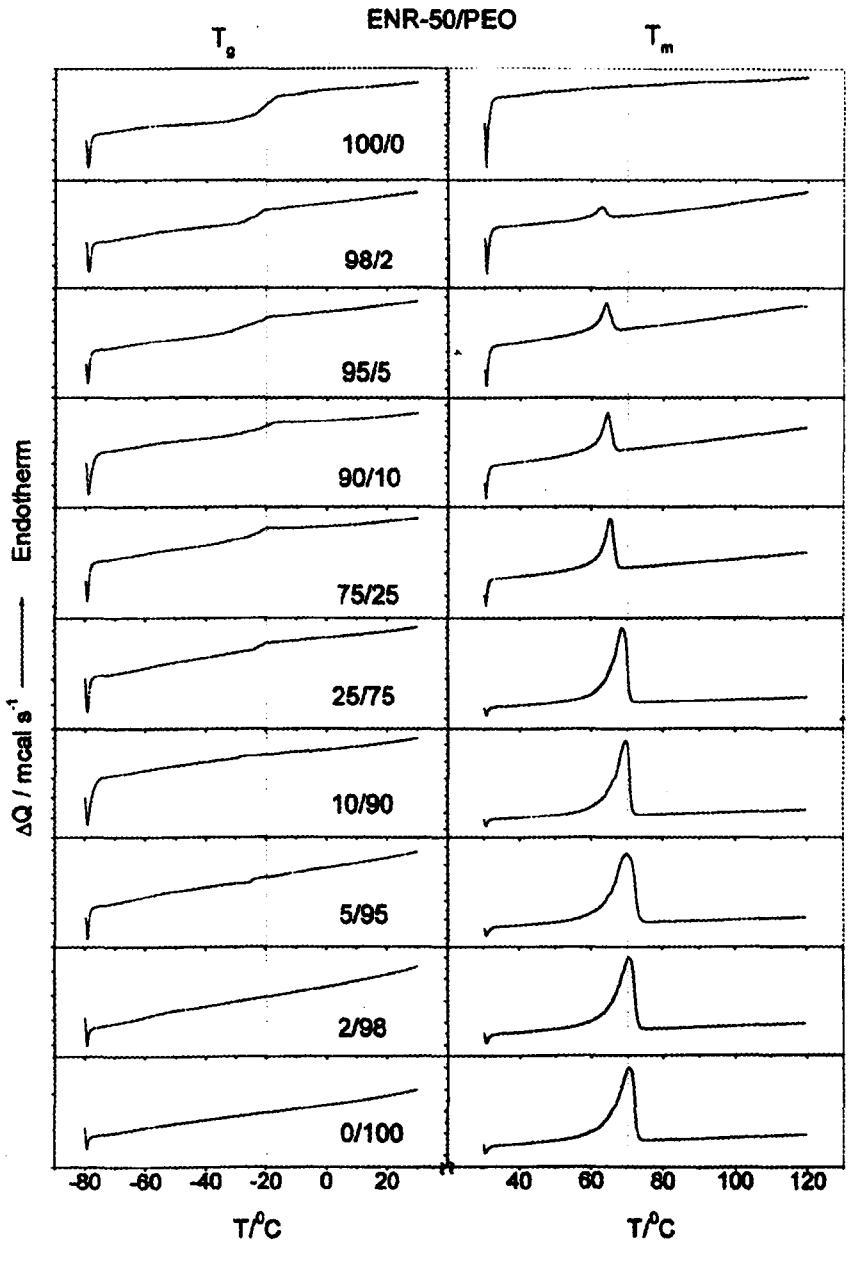

Fig. 6.2 DSC traces of ENR-50/PEO blends (samples containing 0-100% w/o PEO)

DSC data for ENR-25/PEO and ENR-50/PEO blended film compositions display only a single transition glass temperature (a step curve) in the lower range temperature, but the 75/25 ratio for ENR-25/PEO composition two transition glass temperatures are apparent. For the latter one the first T_g value is considerably higher at -58^0 C, which is closer to the pristine PEO whereas the second T_g value is at -21^0 C very close to pure ENR-50. It shows that T_g values of ENR very little affected with increasing PEO concentration. The two transition glass temperatures at -41^0 C and -21^0 C obtained in the lower range temperature correspond to amorphous phases of ENR-25 and ENR-50, which predominate in the blend compositions. However, T_g, of PEO not detectable in the DSC traces of the blends but its melting temperatures prevail in the upper range temperature for all blend compositions. It is expected that the blend of two polymers might consist each component of ENR and PEO or new material being produced. From the thermal event the blend compositions indicate that it might consist of two-phase systems.

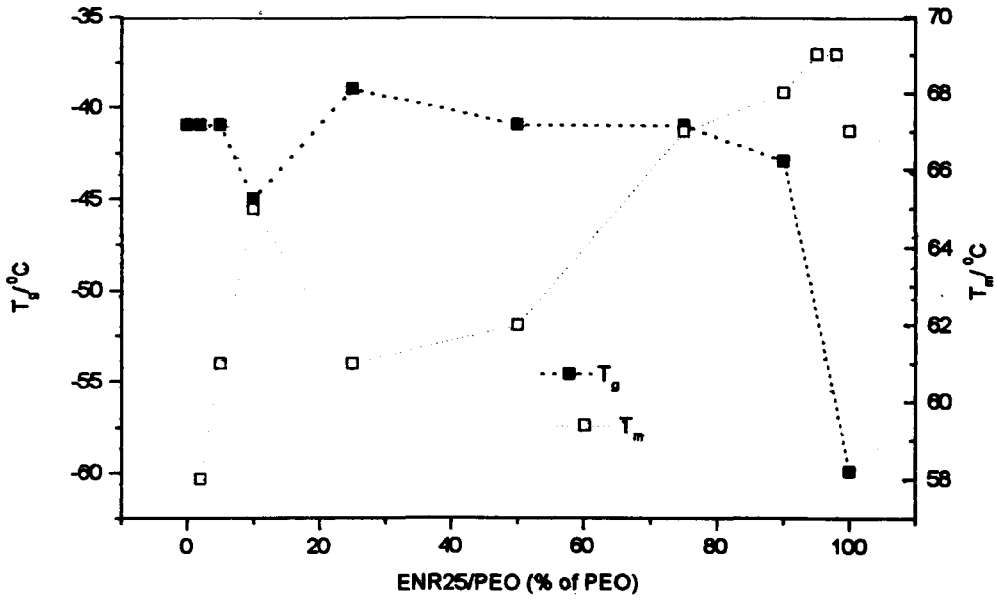

Figure 6.3. The trend of transition glass temperature, T_g, and melt temperature, T_m, of ENR25/PEO blends as a function of PEO concentration.

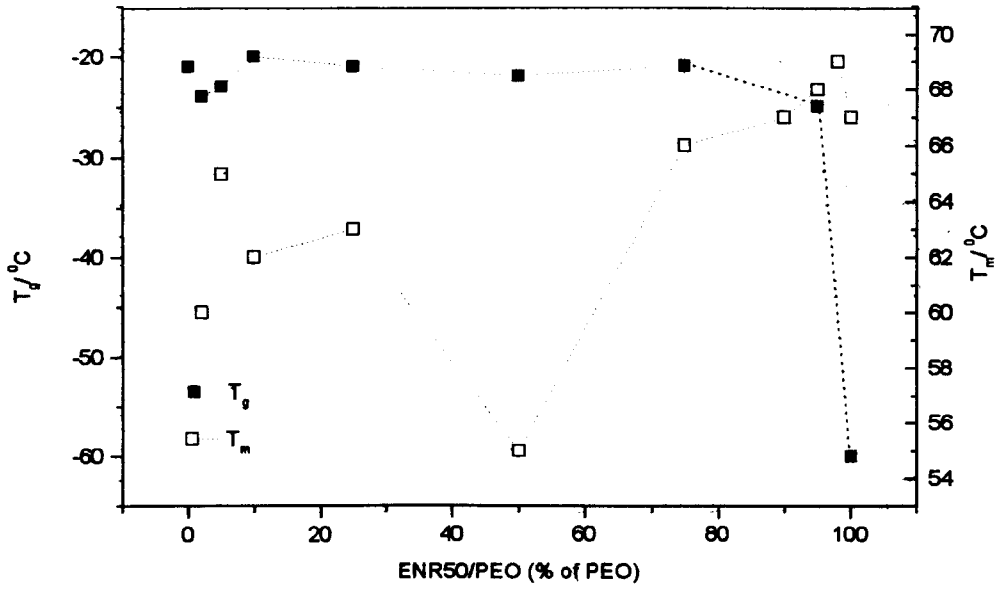

Figure 6.4. The trend of T_g, and T_m, of ENR50/PEO blends as a function of PEO concentration .

For compatible polymer blends, the glass-transition temperature (T_g) is expected to be intermediate between that of the two components. The expected transition glass temperature is not apparent. In the case of present investigation for undoped ENR25/PEO and ENR50/PEO blends, T_g for the PEO component is not observable (by DSC) because PEO is semicrystalline. However, from Figure 6.3 and Figure 6.4 show that the trend of the graphs for both types of blends display a melting temperature, T_m, depression that depends on the volume percentage of PEO additives. Unless the additive is compatible with the polymer and acts as a plasticiser, it will not depress its melting temperature (H. Wang, H. Huang, and S.L. Wunder, 2000) . Therefore, the melting point depression of the crystalline portion of the blend can be used as a criterion for compatibility. It is believed from this finding that ENR-25 or ENR50 can also act as internal plasticizer is compatible with PEO, as indicated by a lowering of the melt temperature T_m of the crystallite in the blend.

6.2.2 Scanning Electron Microscopy (SEM)

The structure of polymer blend consists of amorphous phase, a crystalline phase and at least one of a range of mixed phases formed between ENR and PEO. This has resulted differences in morphology between composition ratios of the ENR/PEO blends polymeric components in the formation of the films. Scanning electron micrographs of the undoped ENR/PEO blends possibly indicate the two phases of polymers might have a micro phase separated, a single phase or partially single-phase systems.

Figure 6.5 to 6.8 compare the morphology of the films prepared using solvent casting technique with those formed employing undoped ENR-25/PEO blends and undoped ENR50/PEO blends. The polymeric-blended films containing low concentration of PEO with 2/98, 5/95, 10/90 and 25/75 ENR-25/PEO and ENR50/PEO compositions were homogenous as shown in Fig. 6.7 and Fig. 6.8. There appear to be small spherulites of PEO crystal grains aggregated in between the amorphous phase of the blend. In comparison to the films with PEO-rich phase (Fig. 6.5 and 6.6), the films with 98/2, 95/5, 90/10 and 75/25 PEO/ENR-25 and PEO/ENR50 compositions were somewhat heterogeneous showing spherulite structure randomly distributed in within the phases of the blend. This corresponds well to the fact that these films were all translucent. In the case of the PEO-rich blended films, all the films were heterogeneous and had a two-phase structure with the PEO domain dispersed in the ENR-25 matrix. In the fact, the phase separation led to opaque or hazy films for these blends.

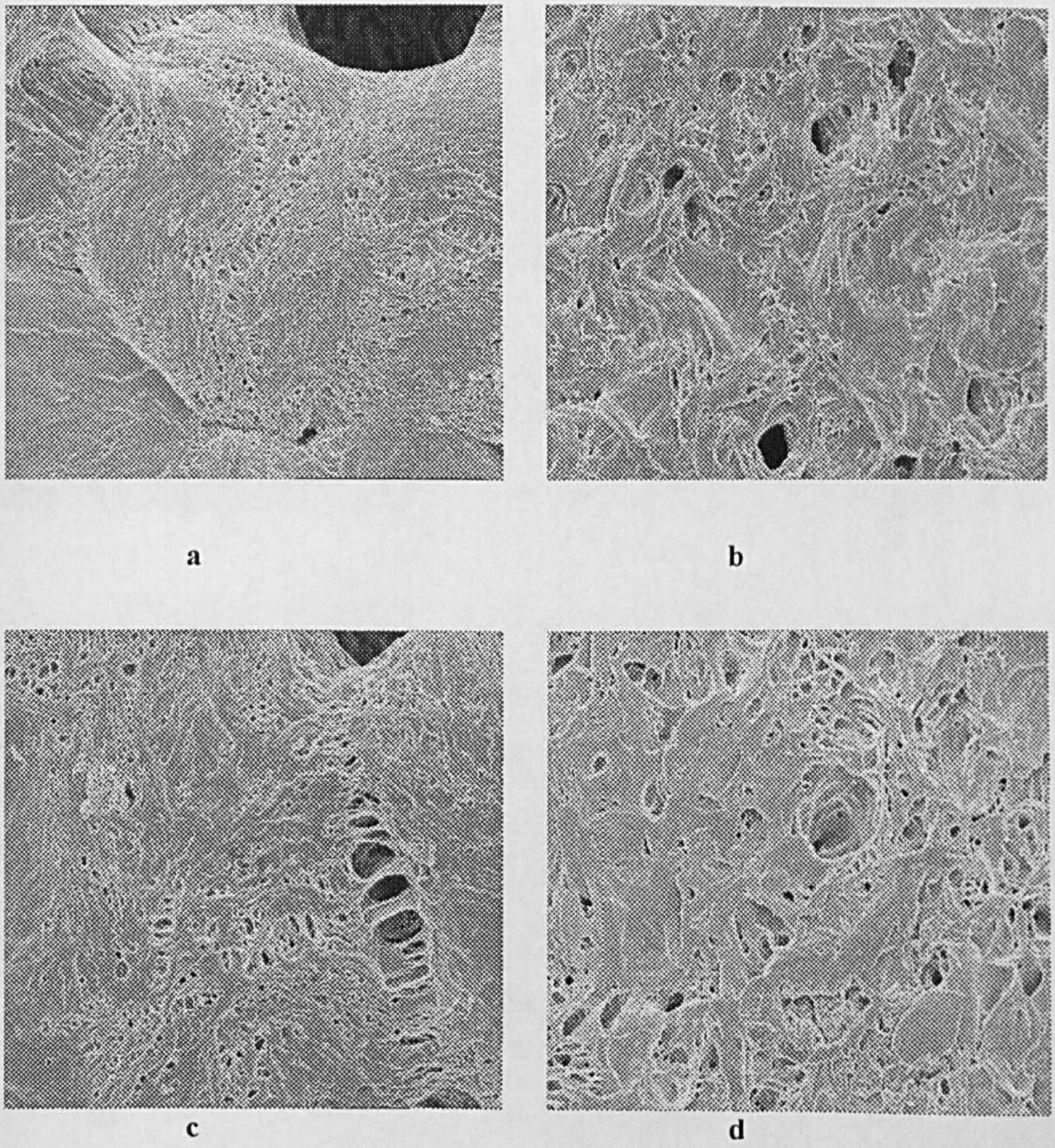

Figure 6.5. SEM images of undoped PEO/ENR-25 blend films containing high concentration PEO content. The SEM photo (4000X) for (a) 98 % PEO (b) 95 % PEO (c) 90 % PEO (d) 75 % PEO.

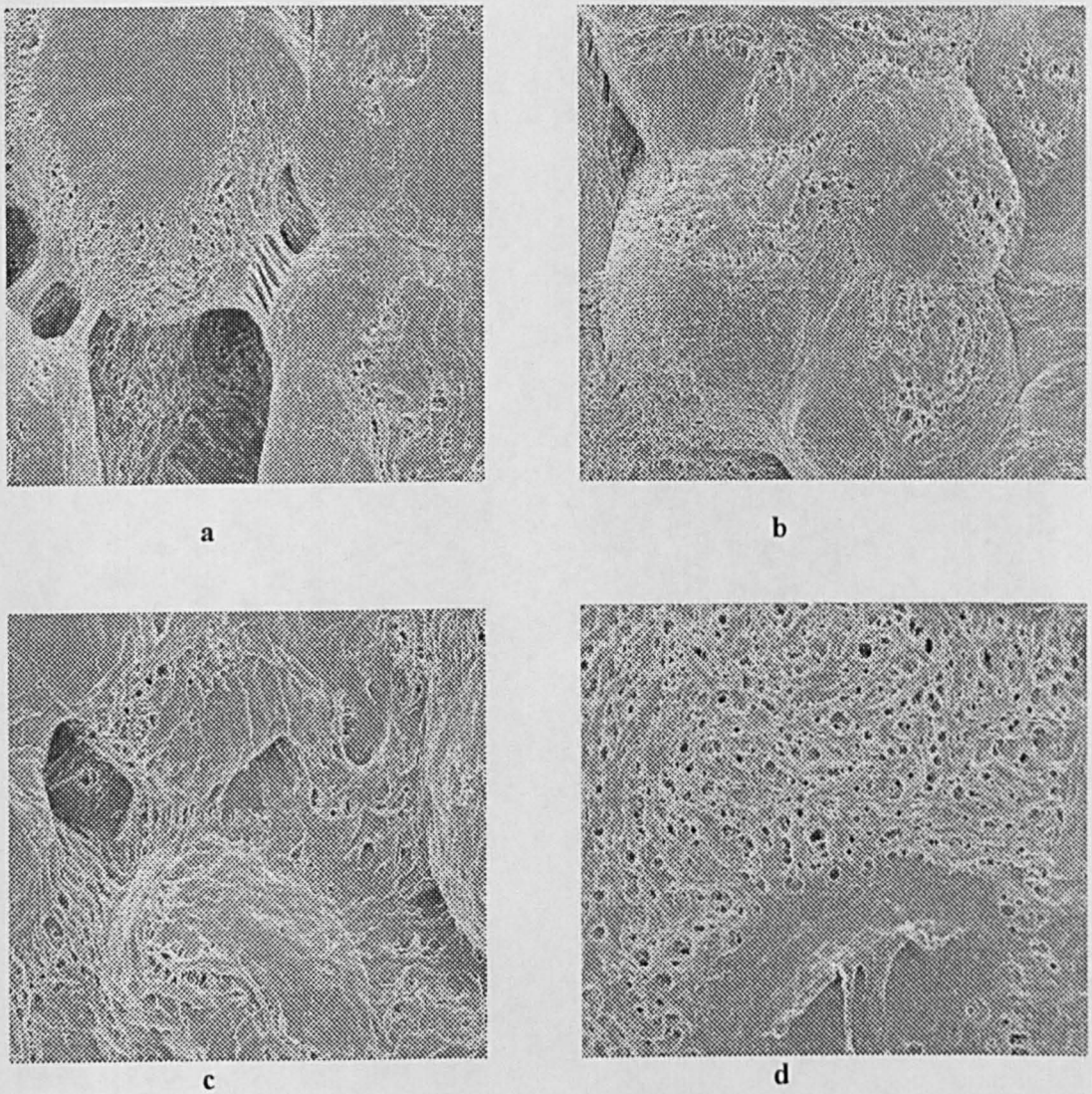

Figure 6.6. SEM images of undoped PEO/ENR-50 blend films containing high concentration PEO content. The SEM photo (4000X) for (a) 98 % PEO (b) 95 % PEO (c) 90 % PEO (d) 75 % PEO.

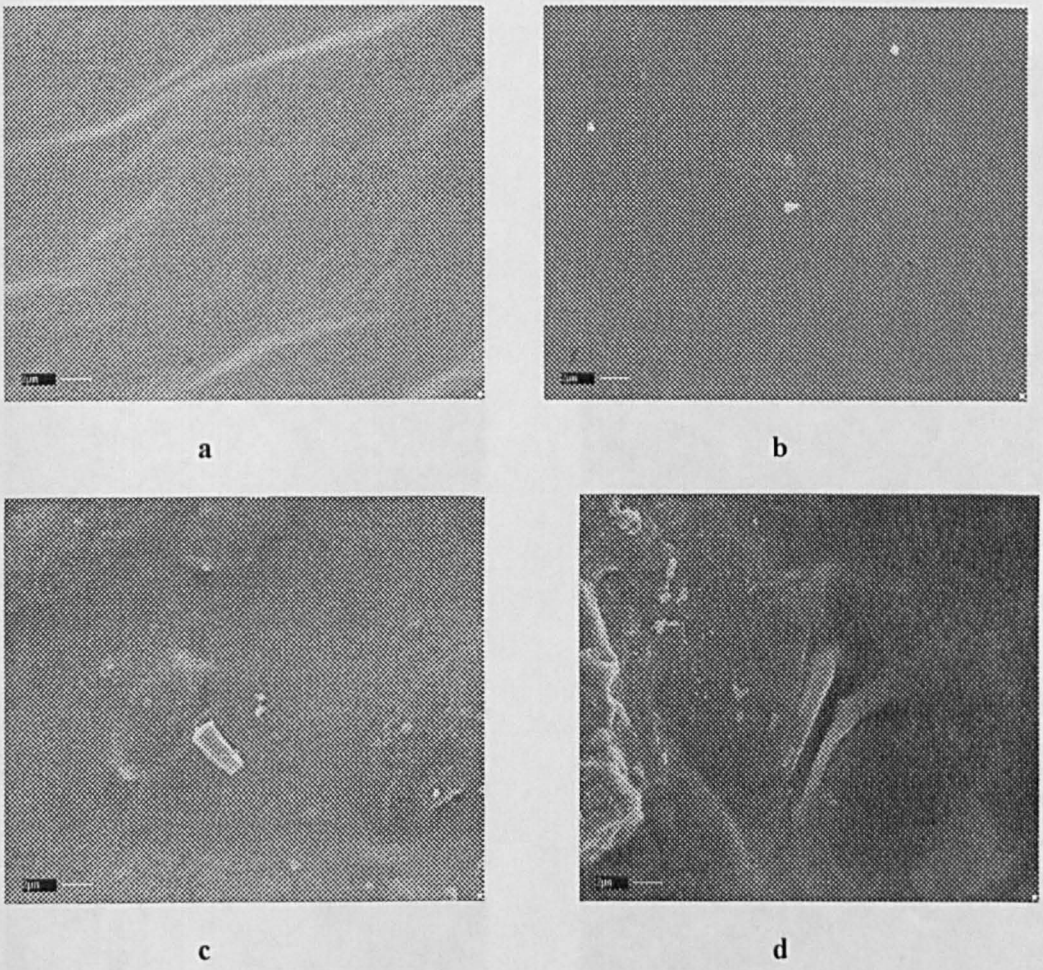

Figure 6.7. SEM images of undoped ENR25/PEO blend films containing low concentration PEO content. The bar scale shown is 2μm (a) 2% PEO; (b) 5% PEO; (c) 10% PEO; (d) 25% PEO.

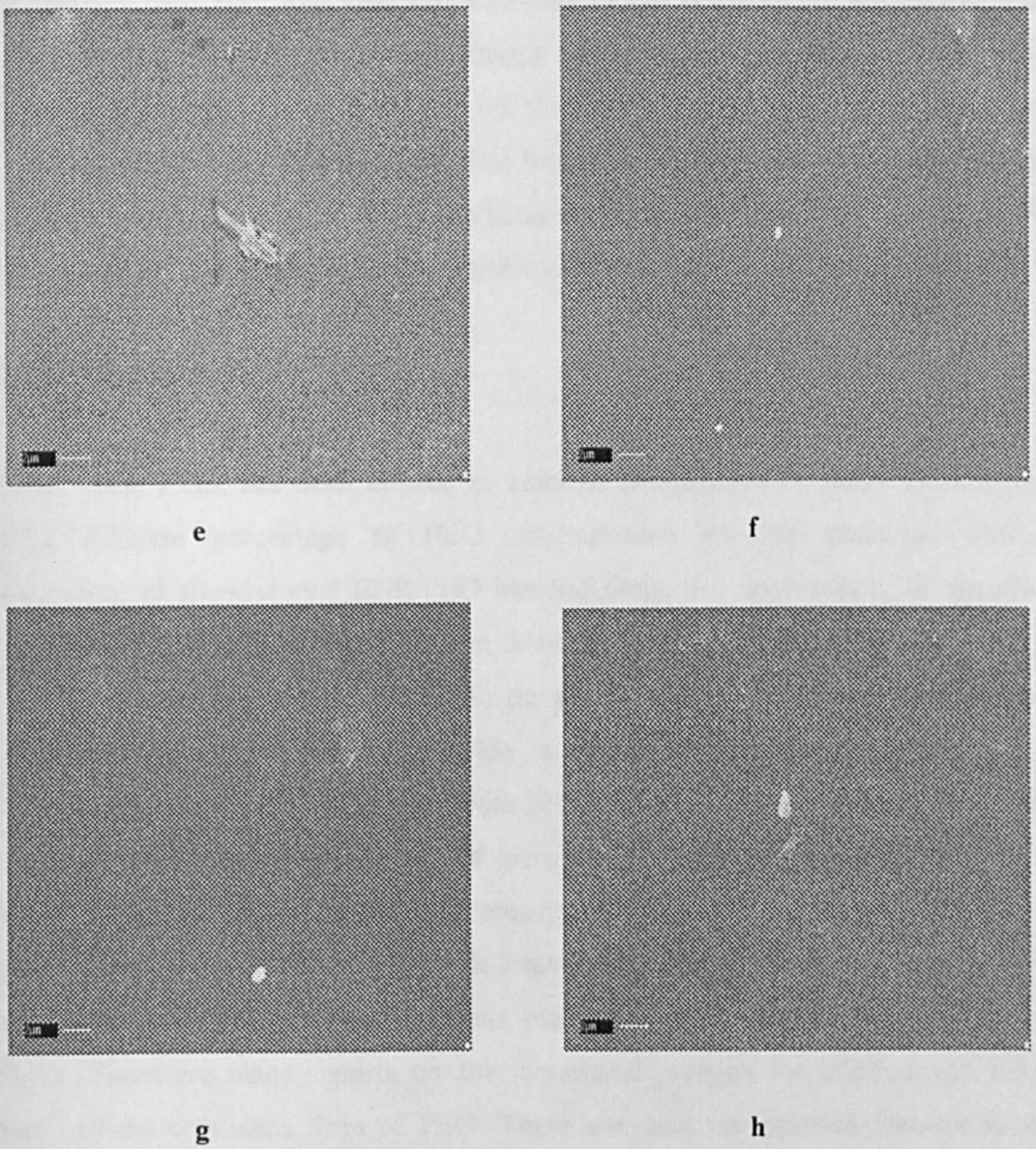

Figure 6.8. SEM images of ENR50/PEO blend undoped films containing low concentration PEO content. The bar scale shown is 2μm (e) 2% PEO; (f) 5% PEO; (g) 10% PEO (h) 25% PEO

The blended films with low PEO concentration in the ratios 2/98, 5/95, 10/90, 25/75 ENR-50/PEO and ENR25/PEO compositions were homogeneous whereas in the higher PEO concentration in the ratios 98/2, 95/5, 90/10, 75/25 PEO/ENR-50 and PEO/ENR-25 compositions were heterogeneous. The former one exhibits smooth surface without showing any crystal grains of PEO. The latter shows a two-phase system with the PEO predominate in the ENR-50 or ENR-25 polymer host.

6.2.3 FTIR Spectroscopy

In this work, FTIR has been utilized at ambient temperature to study the effects of adding different percentage of PEO concentration on the structural chemical environment of the undoped ENR/PEO blended films. For comparison, IR spectra of pure ENR and PEO were also obtained from experiment and literature. Some of the articles have been reviewed in relation to the vibrational spectra of pure PEO and their complexes. The cited articles provide a suitable foundation to analyze the microstructures of PEO when blended with ENR rubber. It is important and informative to examine the vibrational spectra of pure PEO, ENR before characterizing the ENR/PEO blends. The focus of the IR absorption of the systems under study is in the region 1500 –500 cm^{-1} .In the crystalline state of PEO for chain conformation involves the mode of internal rotation such as trans and gauche about the O-CH_2, CH_2-CH_2, and CH_2-O. There are many reports on the vibrational analysis for infrared and Raman spectra of the crystalline form of PEO. There are quiet complicated features such as considerable coupling

All spectra of PEO/ENR25 blended films containing high PEO content are presented in Figure 6.9. They were labelled as weight percent ratios 98/2, 95/5, 90/10 and 75/25 respectively. For the purpose of comparison, the spectral data of neat PEO and ENR are also obtained (Figure 6.10 and 6.11). The spectra of the blends are collected in the frequency range of 1500 to 500 cm^{-1}. Figure 6.9 shows the ir spectra of the PEO/ENR25 blends are almost similar as the progress of ENR25 polymer is added into the blend.

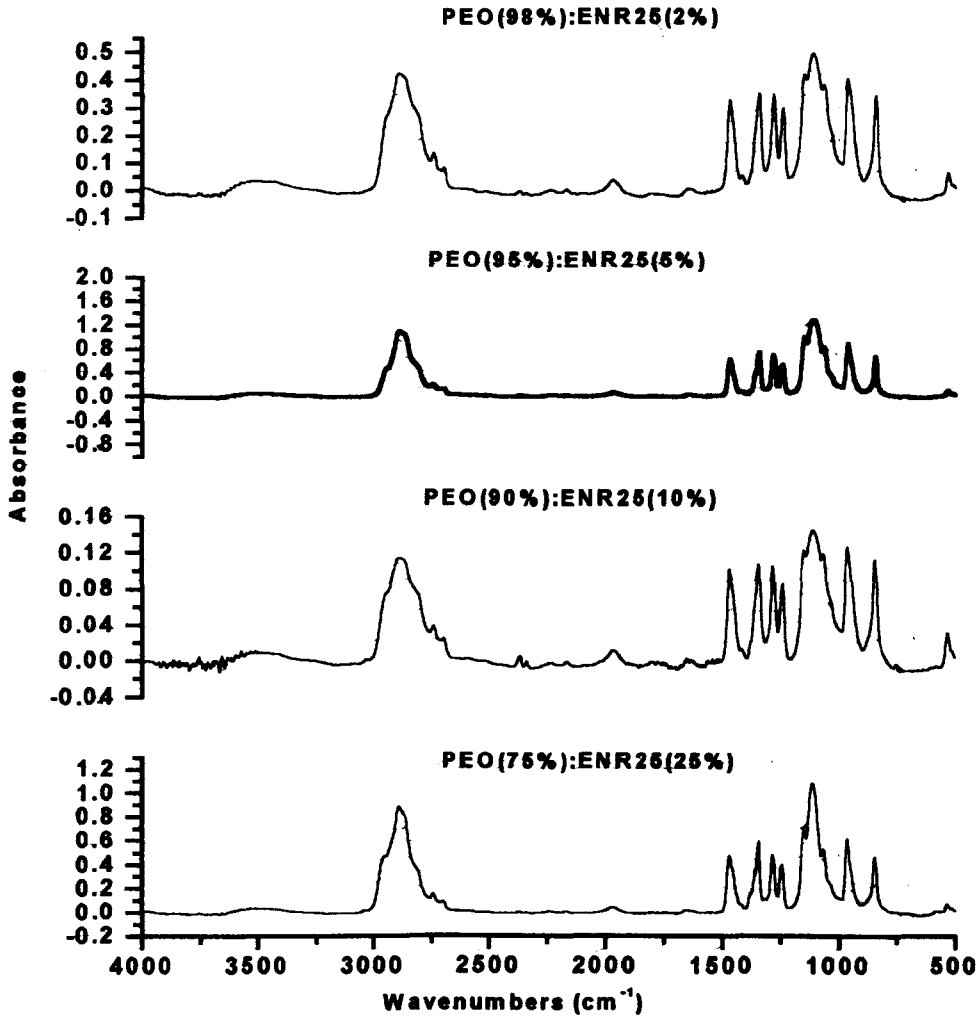

Figure 6.9 IR spectra of undoped PEO/ENR-25 blends containing high PEO concentration.

In accordance to ir spectroscopic data in Figure 6.9 the component of PEO is slightly affected upon addition of ENR25 until a maximum of 25 wt.%. This has been shown in Figure 6.10 the comparison of 75/25 PEO/ENR25and 95/5 PEO/ENR25 blends. In order to see the effect of ENR25 presence in the PEO/ENR25 blend the crystallization peaks of PEO are focused in the 1500-800 cm^{-1} regions.

In the vibrational spectra studies of crystalline PEO the peaks are sensitive to chain conformation changes. It is expected that the changing PEO chain conformation due to the presence of ENR rubber in this studies. The spectroscopic techniques have the high selectivity that can yield details of chain microstructure in the blends. Figure 6.11 indicates that the peak intensities have little changes when ENR component was introduced from 5 wt% to 25 wt.% into the blends.

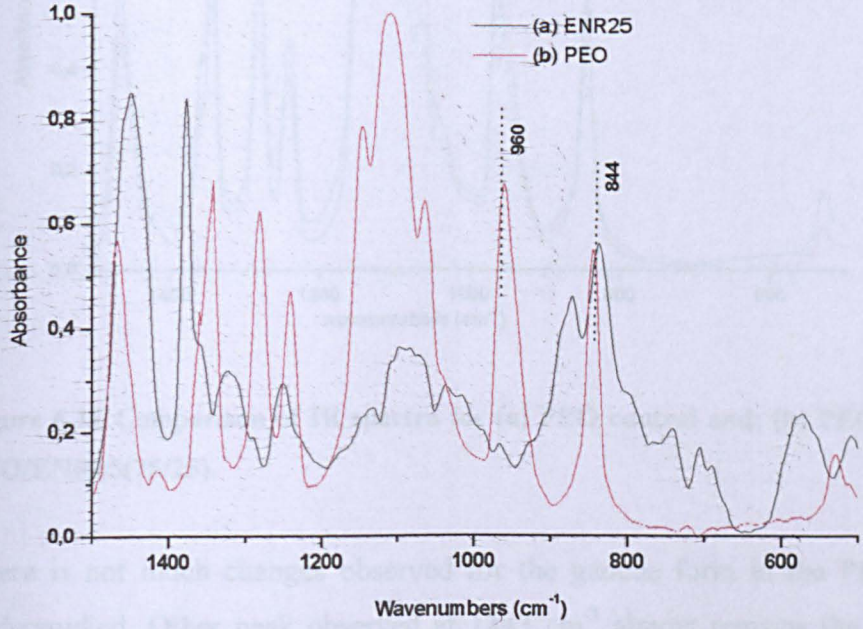

Figure 6.10 IR spectra of (a) ENR25 (b) PEO; resolution 4 cm^{-1}; cast from THF solution at room temperature.

Davidson, (1955) has used the selection rules and vibrational assignments for the gauche and trans forms of ethylene dichloride (Brown and Sheppard, 1952) to model the O-$[CH]_2$-O portion of the PEO chain. For a gauche configuration two strong bands at about 880 and 944cm^{-1} are expected. Figure 6.10 is shown the spectra of neat PEO and ENR 25 in the mid-frequency range collected for this work. It indicates that two strong bands at 844 and 960 cm^{-1} almost very close to a gauche configuration.

In the vibrational studies on the undoped PEO/ENR blends and their complexes with lithium triflate, all of the bands may be assigned to a gauche configuration for the O-$[CH]_2$-O group.

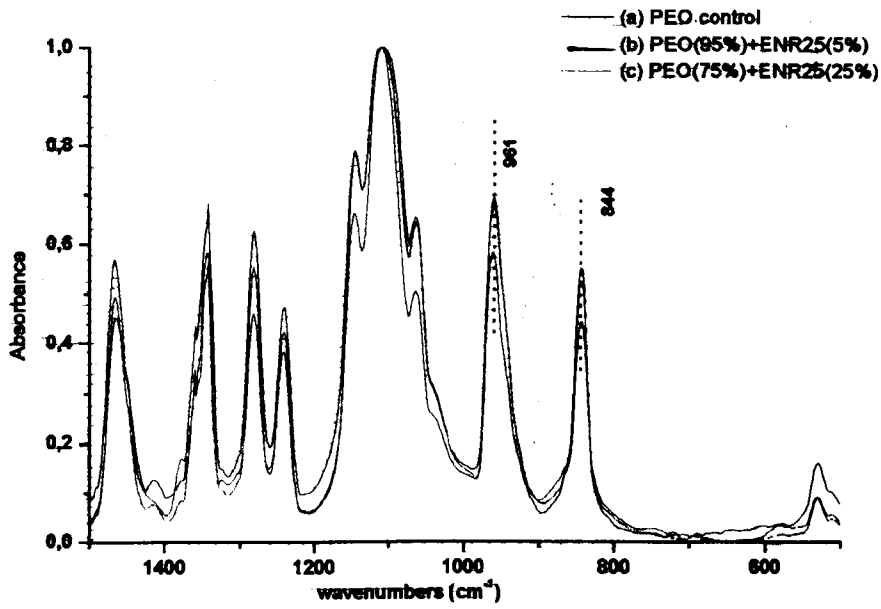

Figure 6.11 Comparison of IR spectra for (a) PEO control and; (b) PEO/ENR25 (95/5) (c) PEO/ENR25(75/25).

There is not much changes observed for the gauche form in the PEO/ENR25 blends understudied. Other peak observed at 1343 cm^{-1} almost remains the same position for blends containing high PEO concentration. For these undoped blends of PEO/ENR25 has found that the gauche state is favoured for PEO. Ir spectra of PEO/ENR25blends containing low PEO content in Figure 6.12 have a strong peak in the1000-1200 cm^{-1} region. As can be seen in Figure 6.13 for sample containing PEO concentration of 25 wt.% the ir peak favour to PEO component, even though ENR25 dominant component in the blend. It suggests that phase separation might take place; i.e., there are two amorphous regions; one at PEO-rich and the other ENR-rich; indicating rather complicated morphology, which is composition dependent, exists in the blend system.

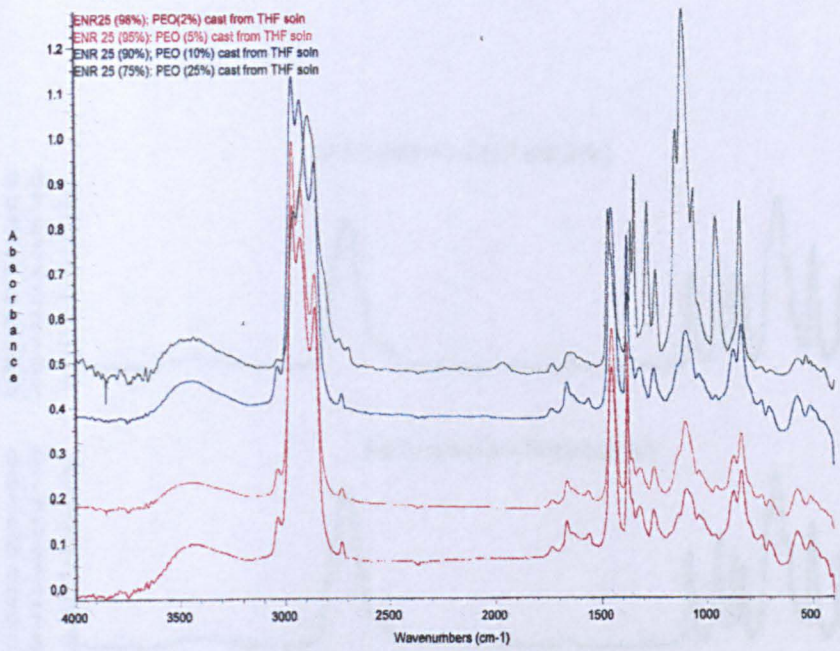

Figure. 6.12 IR spectra of undoped ENR25/PEO blends containing low PEO concentraion content.

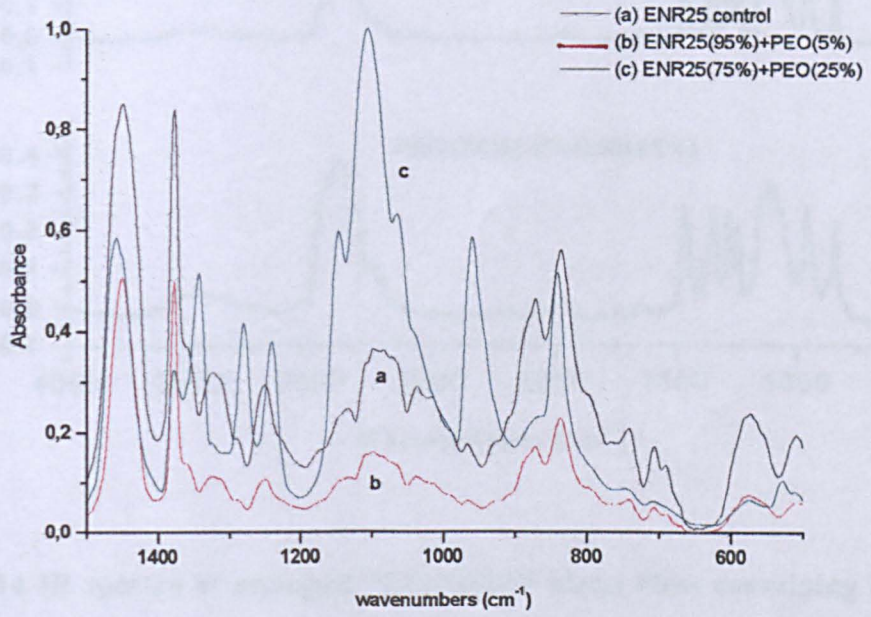

Figure 6.13 Comparison of IR spectra of (a) ENR25 and PEO/ENR25 blends containing low PEO content (b) 5wt.%; (c) 25 wt.%.

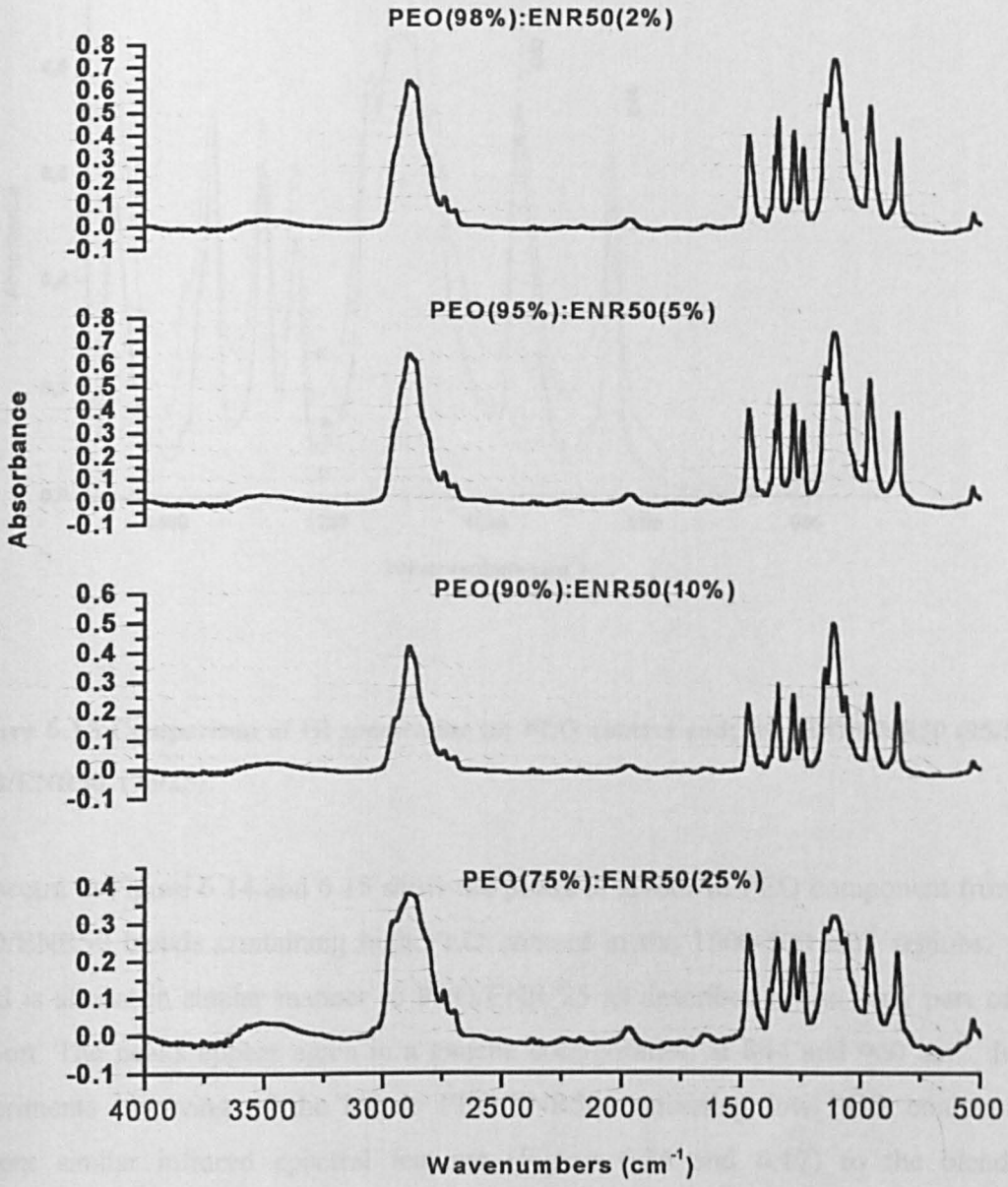

Figure 6.14 IR spectra of undoped PEO/ENR50 blend films containing high PEO content.

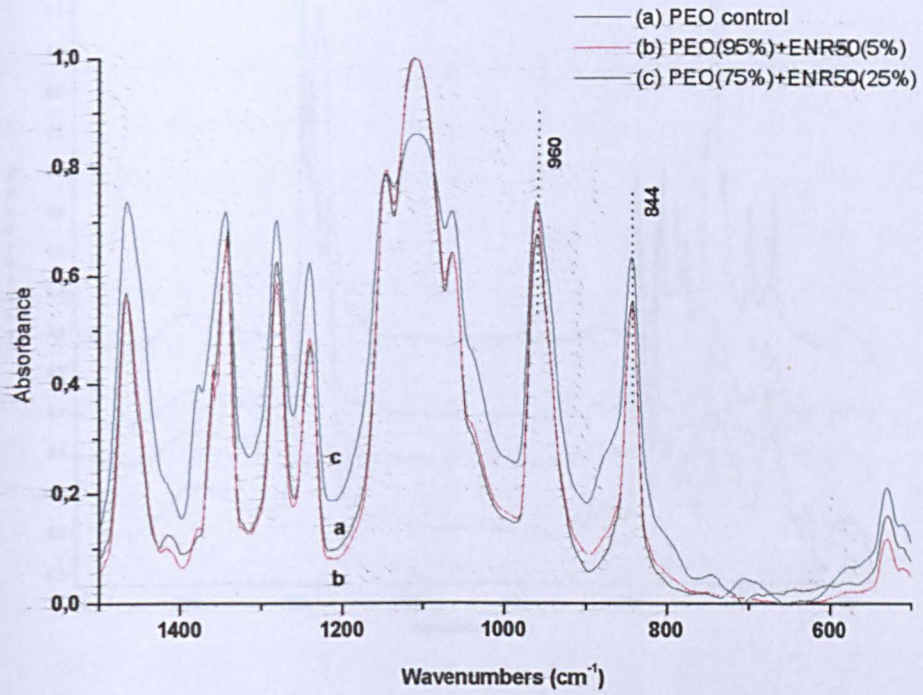

Figure 6.15 Comparison of IR spectra for (a) PEO control and; (b) PEO/ENR50 (95/5) (c) PEO/ENR50 (75/25).

Ir spectra in Figure 6.14 and 6.15 show the peaks in favour to PEO component from the PEO/ENR50 blends containing high PEO content in the 1500-500 cm^{-1} regions. The trend is almost in similar manner to PEO/ENR 25 as described in the early part of this section. The peaks appear again in a gauche configuration at 844 and 960 cm^{-1}. In the experiments involving of the blends PEO/ENR50 containing low PEO content also present similar infrared spectral features (Figure 6.16 and 6.17) to the blends of PEO/ENR25. Preliminary conclusions indicate that the PEO/ENR blends containing for low and high PEO content is hard to predict their specific influence of each components. At present stage a limited information regarding either the interaction between the two components or the effect of conformational distribution of PEO cause by ENR rubber reported in the literature.

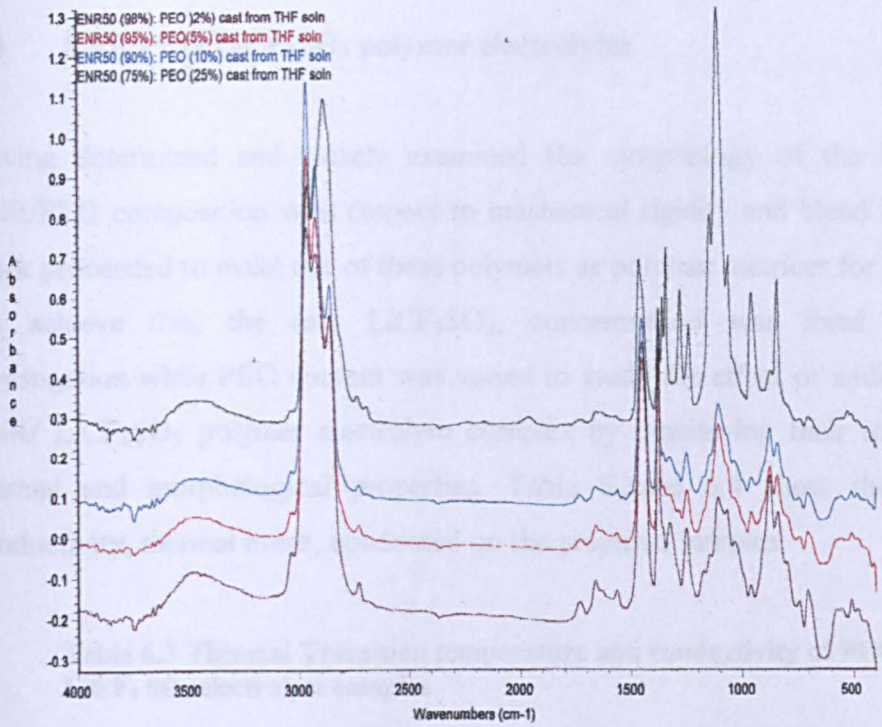

Figure 6.16 IR spectra of undoped ENR 50/PEO blend cast films containing low concentration PEO content.

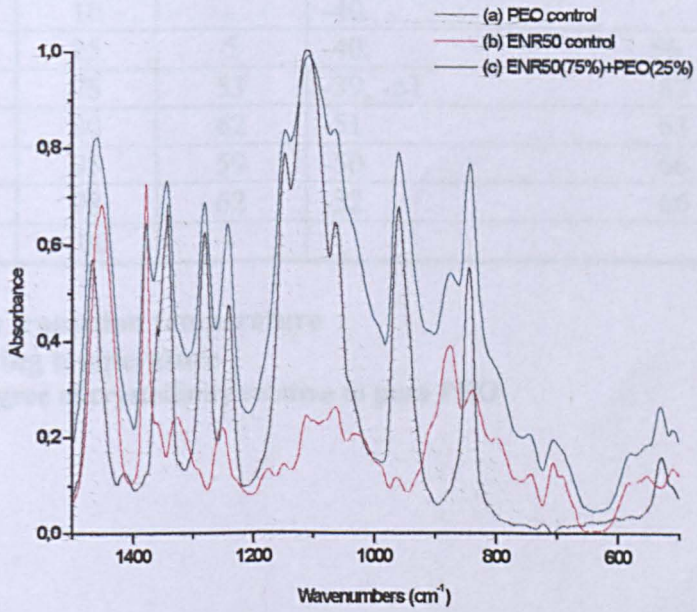

Figure 6.17 Comparison of IR spectra of (a) PEO; (b) ENR50; (c) ENR50/PEO (75/25).

6.3 ENR/PEO/$LiCF_3SO_3$ polymer electrolytes

Having determined and closely examined the morphology of the blended films of ENR/PEO composition with respect to mechanical rigidity and blend homogeneity, the work proceeded to make use of these polymers as polymer matrices for lithium ion.

To achieve this, the salt, $LiCF_3SO_3$, concentration was fixed throughout this investigation while PEO content was varied to study the effect of addition of PEO into ENR/ $LiCF_3SO_3$ polymer electrolyte complex by monitoring their ionic conductivity, thermal and morphological properties. Table 6.3and 6.4 show the data for ionic conductivity, thermal event, conducted on the prepared samples.

Table 6.3 Thermal Transition temperature and conductivity of PEO/ENR-25/ $LiCF_3SO_3$ electrolyte samples

Sample	% of PEO	X_{cPEO} (%)	Transition temperature/ ^0C		Conductivity (S cm^{-1})
			T_g	T_m	
ENR25/S	0	-	-43	-	$1.6x10^{-5}$
B/1S	2	-	-39	-	7.8×10^{-6}
B/2S	5	-	-40	-	5.4×10^{-6}
B/3S	10	-	-40	-	4.2×10^{-6}
B/4S	25	5	-40	56	2.9×10^{-6}
B/5S	75	53	-39, -51	63	1.2×10^{-5}
B/6S	90	62	-51	63	5.7×10^{-6}
B/7S	95	59	-50	66	5.4×10^{-6}
B/8S	98	62	-52	66	3.1×10^{-6}
PEO/S	100	-			10^{-8} - 10^{-7}

T_g – glass transition temperature
T_m- melting temperature
X_{cPEO}- degree of crystallinity relative to pure PEO

Table 6.4 Thermal tansition temperature and conductivity of PEO/ENR50/ $LiCF_3SO_3$ polymer electrolyte samples

Sample	% of PEO	X_{cPEO} (%)	Transition temperature/ ^0C		Conductivity (S cm^{-1})
			T_g	T_m	
ENR50S	0	-	-22		$2.0x10^{-5}$
B/1S	2	-	-20	-	1.3×10^{-6}
B/2S	5	-	-20	-	1.1×10^{-6}
B/3S	10	-	-21	-	3.2×10^{-6}
B/4S	25	9	-19	56	2.7×10^{-6}
B/5S	75	61	-52	66	4.7×10^{-6}
B/6S	90	64	-52, -28	65	6.0×10^{-6}
B/7s	95	68	-51	67	2.7×10^{-6}
B/8S	98	69	-52	66	2.9×10^{-6}
PEO/S	100	70	-60		10^{-8} - 10^{-7}

6.3.1 Complex ac-impedance studies

Impedance data are presented in the form of imaginary, Z'' (capacitive) against real , Z' (resistive), impedances. The typical impedance plots (Z' vs. Z'') for the blended-films of ENR-50/PEO compositions are shown in Figure 6.18

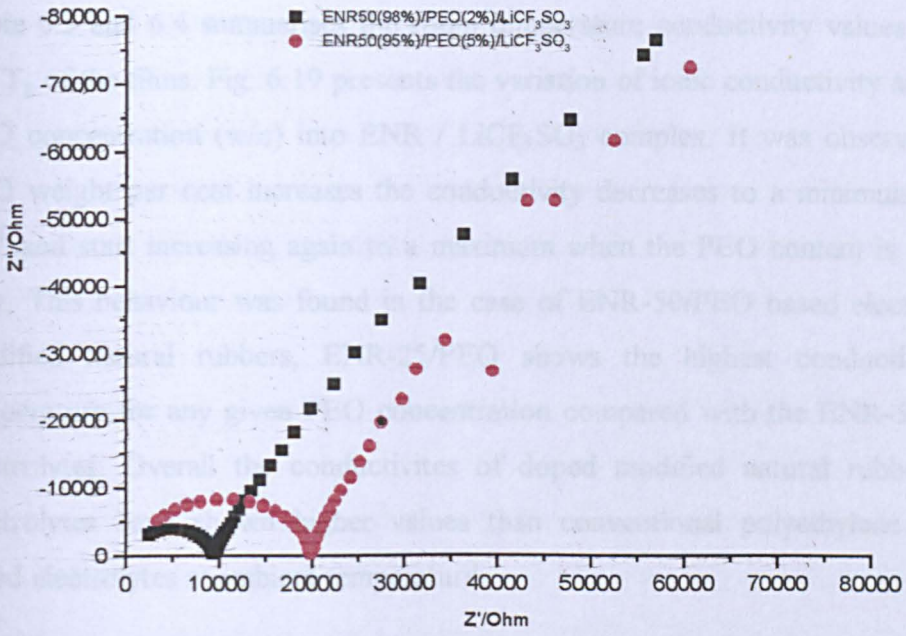

Figure 6.18 Impedance plot of ENR50/PEO blend doped with $LiCF_3SO_3$

The impedance response on the film samples was collected by means of conductivity cell whose details described in Chapter 3 (Experimental part). The electrodes of the cell were made of stainless steel as blocking electrode .In the complex impedance representation measure at room temperature as shown in Figure 6.18, the low frequency response appears as slanting spikes and it is a characteristic of a blocking double-layer capacitance (C_{dl}), whose magnitude may be estimated from any position on the spike using the equation $Z'' = 1/2\pi f$ where f is the frequency and C is capacitance associated with the frequency f. For a blocking electrode as in this study, the semicircle at the high frequency region usually represents the bulk electrolyte impedance.

The impedance response of ENR50/PEO (98/2)/$LiCF_3SO_3$ shows a typical impedance behaviour such as a semicircle segment followed by a spike. The high frequency semicircle indicates the bulk response of the film samples. The disappearance of the semicircular part in the complex impedance plots of other compositions is due to ion conduction taking place. Thus from the complex impedance plot, the bulk impedance value was taken and used to calculate the bulk ionic conductivity .

Table 6.3 and 6.4 summarises the room temperature conductivity values together with the T_g of the films. Fig. 6.19 presents the variation of ionic conductivity as a function of PEO concentration (w/o) into ENR / $LiCF_3SO_3$ complex. It was observed that as the PEO weight per cent increases the conductivity decreases to a minimum 3.2 x 10^{-6} S cm^{-1} and start increasing again to a maximum when the PEO content is 75 weight per cent. This behaviour was found in the case of ENR-50/PEO based electrolyte. Of the modified natural rubbers, ENR-25/PEO shows the highest conductivity at room temperature for any given PEO concentration compared with the ENR-50 blend-based electrolytes. Overall the conductivites of doped modified natural rubber/PEO based electrolytes have shown higher values than conventional polyethylene oxide (PEO) based electrolytes at ambient temperature.

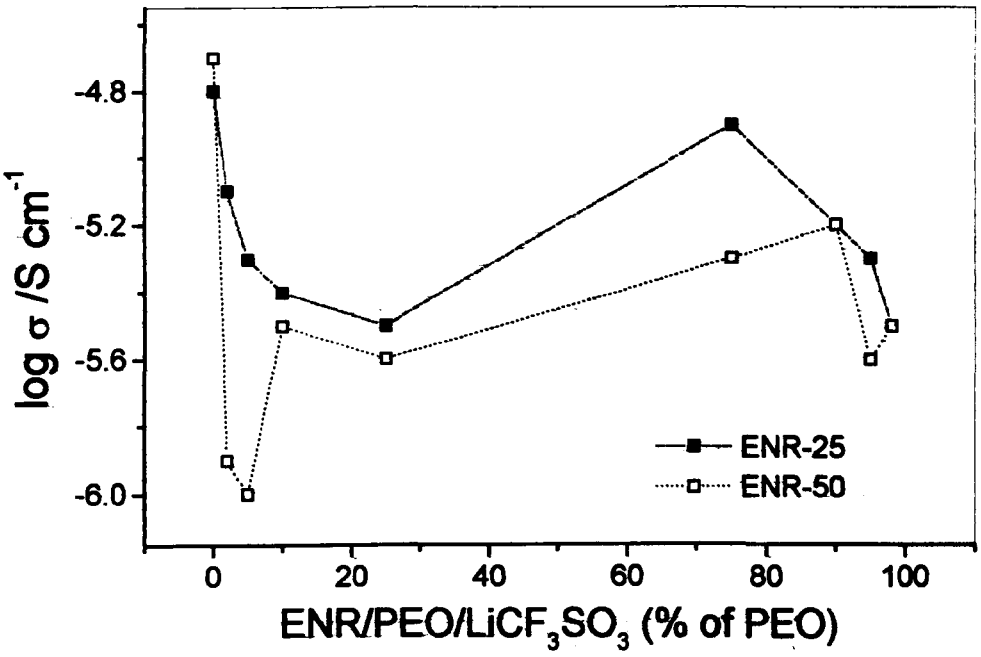

Figure 6.19 Variation of ionic conductivity for ENR/PEO/ $LiCF_3SO_3$ electrolytes as a function of PEO concentration.

In term of the polymer molecular structure, ENR-25 and ENR-50 have an active oxygen in the epoxy group attached to their main chain. It is assumed that the ENR oxygen atom takes a role similar to the ether group in the PEO polymer structure. The Li^+ on solvation in the ENR occurs due to formation of co-ordination bond with oxygen of the polar epoxy group ENR. The blend of PEO into the ENR mixture has little effect on ionic conductivity but render its film handling process after casting.

6.3.2 Differential Scanning Calorimetry

The presence of more than one phase in the polymer electrolyte system complicates analysis of the transport property data. For this reason, it is desirable to investigate the thermal properties prior to study. Polymer electrolyte systems carried out in this study consisting of blended polymer network and inorganic salt differ from conventional electrolyte systems. The blended samples might contain more amorphous features and increase polarity of the polymer host, which create better environment for ionic conduction. In the case of conventional electrolyte system like PEO is relatively has a low volume fraction of amorphous phase of the PEO-complex below the melting point of the crystalline PEO phase (Berthier, Gorecki, Minier, Armand, Chabago and Rigaud, 1983). Addition of salt into the blended system may cause changes in glass transition temperatures as well as improve its ionic conductivity.

The effect of PEO concentration on the thermal property of the electrolyte systems has resulted in some unusual observations. The exact nature thermal phase transition of ENR/PEO blend as polymer host is still not known at this stage. For this work the thermal phase behaviour of ENR/PEO/ $LiCF_3SO_3$ electrolytes were investigated using differential scanning calorimetry. Films made from modified natural rubbers/PEO/ $LiCF_3SO_3$ solutions appeared visually homogeneous at room temperature. . The ENR-25/PEO and ENR-50/PEO types of modified natural rubbers doped with lithium trifluoromethane sulfonate in this study exhibited a single T_g in the DSC experiments. The glass transition, T_g , and melting temperature, T_m of the electrolytes based on ENR/PEO/ $LiCF_3SO_3$ are shown in Figure 6.20 and 6.21.

This indicates that there is no microphase separation occurs in this system. The transition glass temperature, T_g is found, in general to increase with increasing salt concentration. This indicates that a complex has formed between the rubber polymer and the lithium salt. The ionic mobility is closely related to the relaxation modes of the polymer host (Gray, 1991). This can be observed through the increase in Tg of polymeric systems as salt concentration is increased.

The relationaship of glass transition temperature with the cause of the decrease in segmental motion is usually interpreted as being the effects of an increase in intramolecular and intermolecular cooordinations between coordinating sites on the same or different polymer chains caused by the ions acting as transient cosslinks(Le Nest, Gandini and Cheradame, 1988). The ionic conductivity is reduced as the result of the stiffening of the polymer matrix. The availability of vacant coordinating sites is also greatly reduced by the increased of salt concentration. In addition, strong ion-ion interactions in system of low permittivity such as polyether are probable and therefore ion migration is likely to involve the cooperative motion of several ions. This has also been explained in preceding Chapter 2, section 2.3.

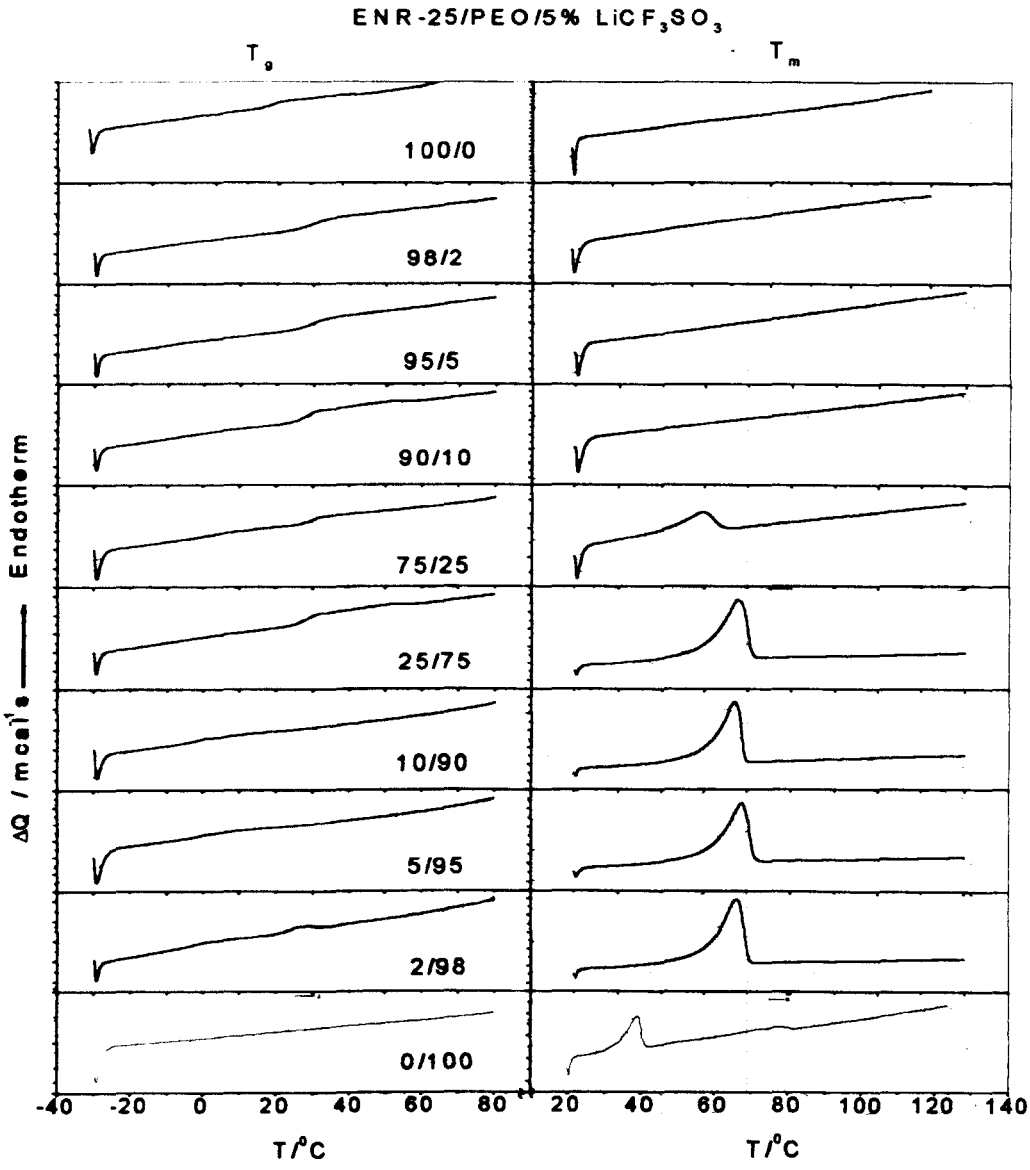

Figure 6.20 DSC traces of ENR25/PEO/$LiCF_3SO_3$ electrolytes

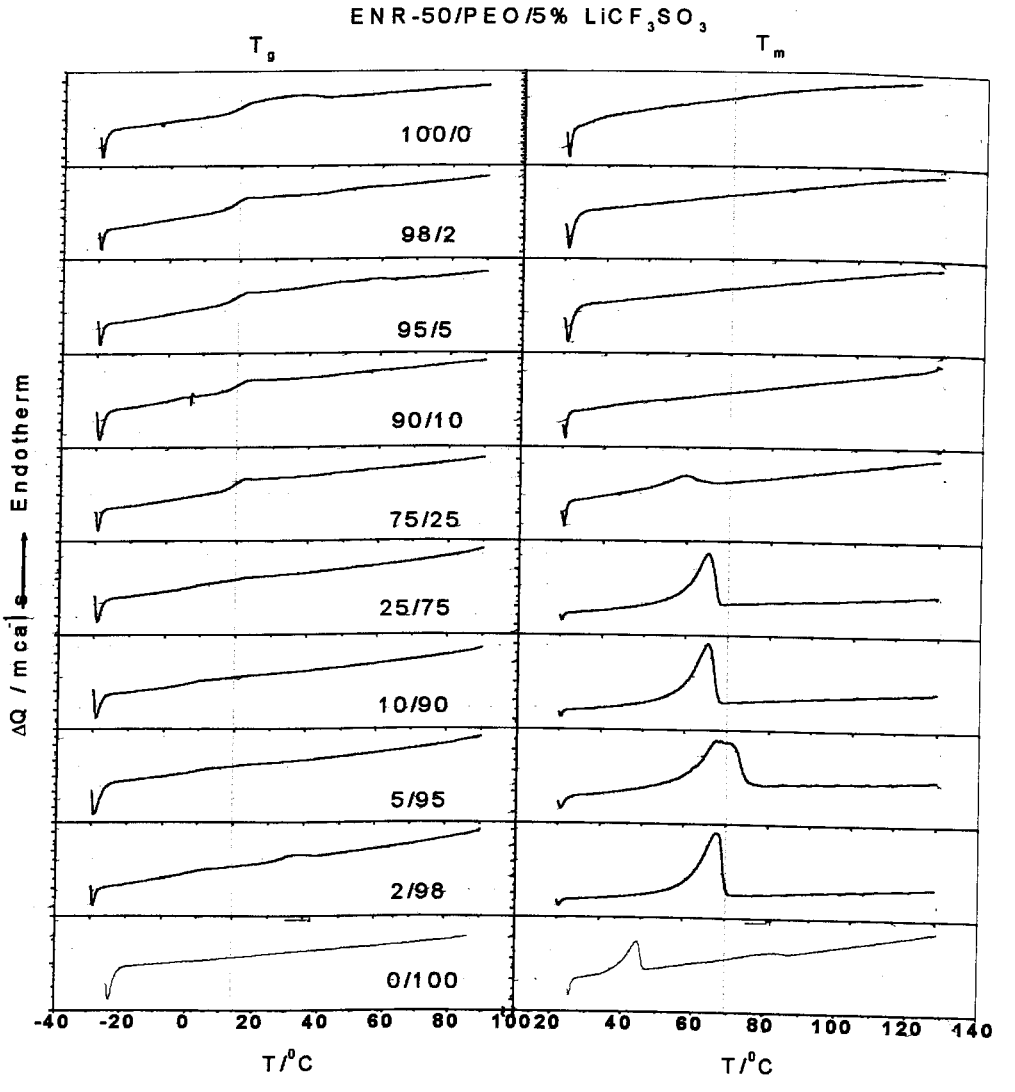

Figure 6.21 DSC traces of ENR50/PEO/$LiCF_3SO_3$ electrolytes

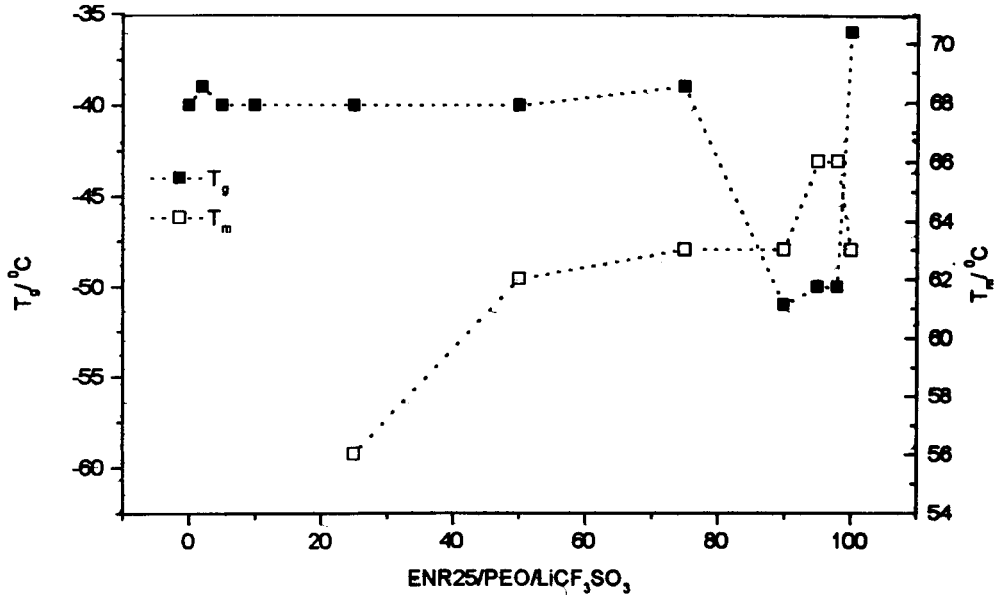

Figure 6.22 The trend of T_g and T_m of ENR25/PEO/$LiCF_3SO_3$ as a function of PEO concentration.

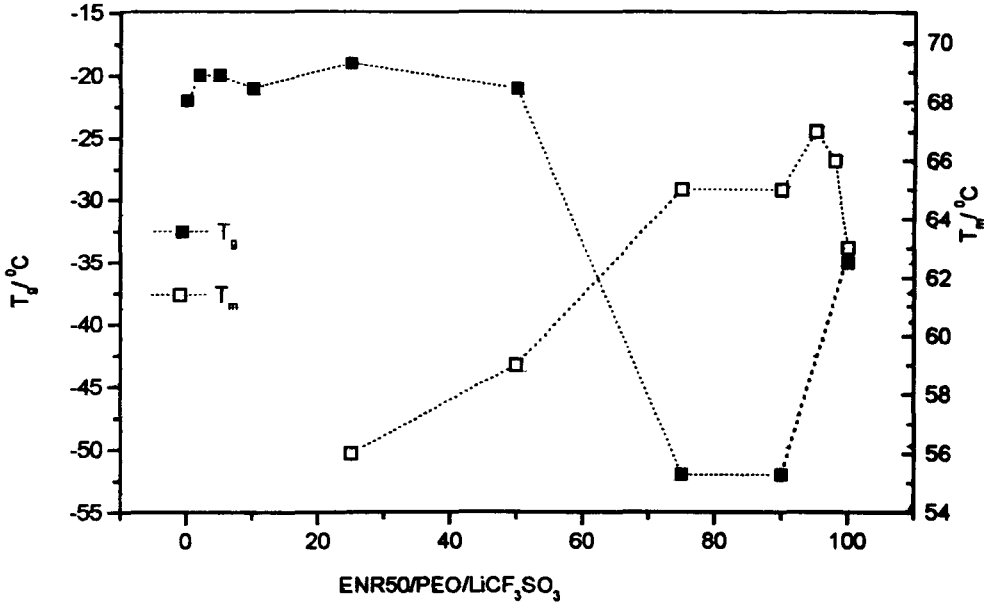

Figure 6.23 The trend of T_g and T_m of ENR50/PEO/$LiCF_3SO_3$ as a function of PEO concentration.

DSC studies show evidence of the amorphous and semicrystalline character of ENR/PEO/ $LiCF_3SO_3$ electrolytes (see Table 6.3 and 6.4). The degree of crystallinity calculated from DSC (Table 6.3 and 6.4) is significantly reduced from that for PEO based electrolytes. The blended films with 92/2, 95/5, 90/10 ENR25/PEO compositions containing lithium triflate salt revealed no melting peak temperature. This was also observed in similar manner with ENR-50/PEO/ $LiCF_3SO_3$ blended film electrolytes.

6.3.3 SEM Observation

SEM micrographs of ENR-25/PEO/ $LiCF_3SO_3$ and of ENR-50/PEO/ $LiCF_3SO_3$ films are shown in Figure 6.24 and Figure 6.24. It can be seen that there is no crystalline grain present in the plasticized blended films of 98/2, 95/5, 90/10 and 75/25 ENR/PEO compositions and inferred that the electrolytes are homogeneous.

In contrary to the higher concentration of PEO with 98, 95, 90 and 75 weight per cent dispersed in the ENR-salt matrix indicated a phase-separated microstructure. It is assumed that the salt has been found to play a vital role in miscibilizing the two polar polymers by interacting with the oxygen of the polyether and epoxy group of epoxidized natural rubber (ENR). It was known at this stage whether a thermodynamic single phase was formed or the blends had a micro-phase separated morphology. It is revealed from the SEM studies that the salt serves as an emulsifier to the multiphase morphology by improving the dispersion of PEO in the ENR matrix and prevents the coalescence of the phases. The effect of the salt is similar to that of a block copolymer, which is known to reside at the interface (Fayt, R. Herome and Teyssie, 1986) between the polymer phases and reduce interfacial tension (Anastasiadis, Gancarz and Stevens, 1989).

The role of the salt as compatibiliser to the multiphase morphology can also be seen clearly by comparing the results of ENR/PEO/ $LiCF_3SO_3$ system. At low PEO concentration in the blended films with 98/2, 95/5, 90/10, and 75/25 ENR/PEO compositions, where lithium salt was fixed at 5% concentration, results in smooth and homogeneous films. Increasing the PEO concentration in the blends with 25/75, 10/90, 5/95 and 2/98 ENR/PEO compositions has caused in coalescence of the two phases. The resulting films were cloudy or opaque. The addition of higher PEO concentration in the blend has produced highly crystalline electrolyte as indicated by the domain spherulite in the matrix phases. It seems likely that the highly polar epoxy group of ENR may also interact with etheric units of PEO in heterogeneous systems.

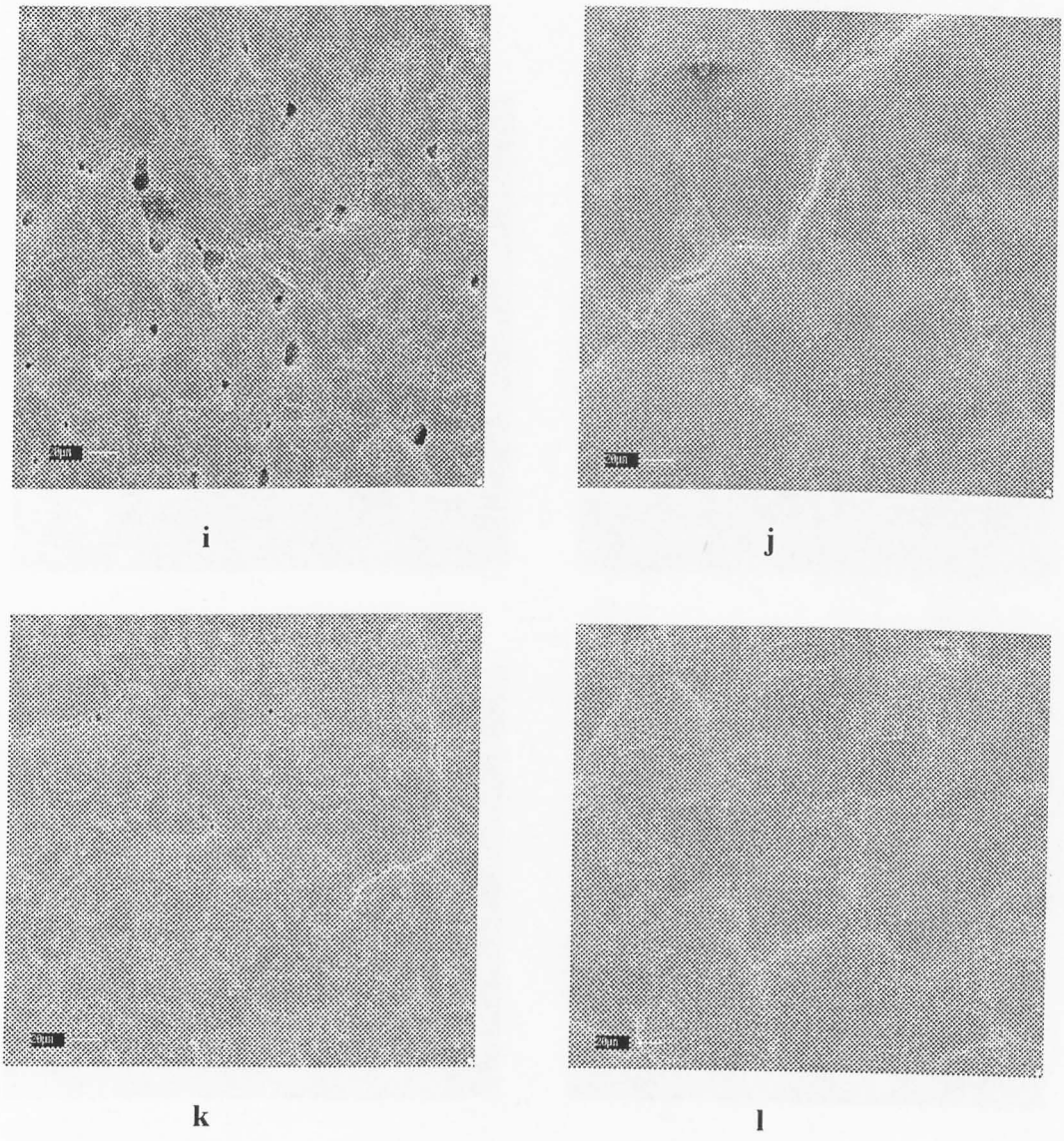

Figure 6.24.SEM images of PEO/ENR25/$LiCF_3SO_3$ polymer electrolyte films prepared by solvent casting. The bar scale shown is 20μm (i) 98% PEO; (j) 95% PEO; (k) 90% PEO; (l) 75% PEO

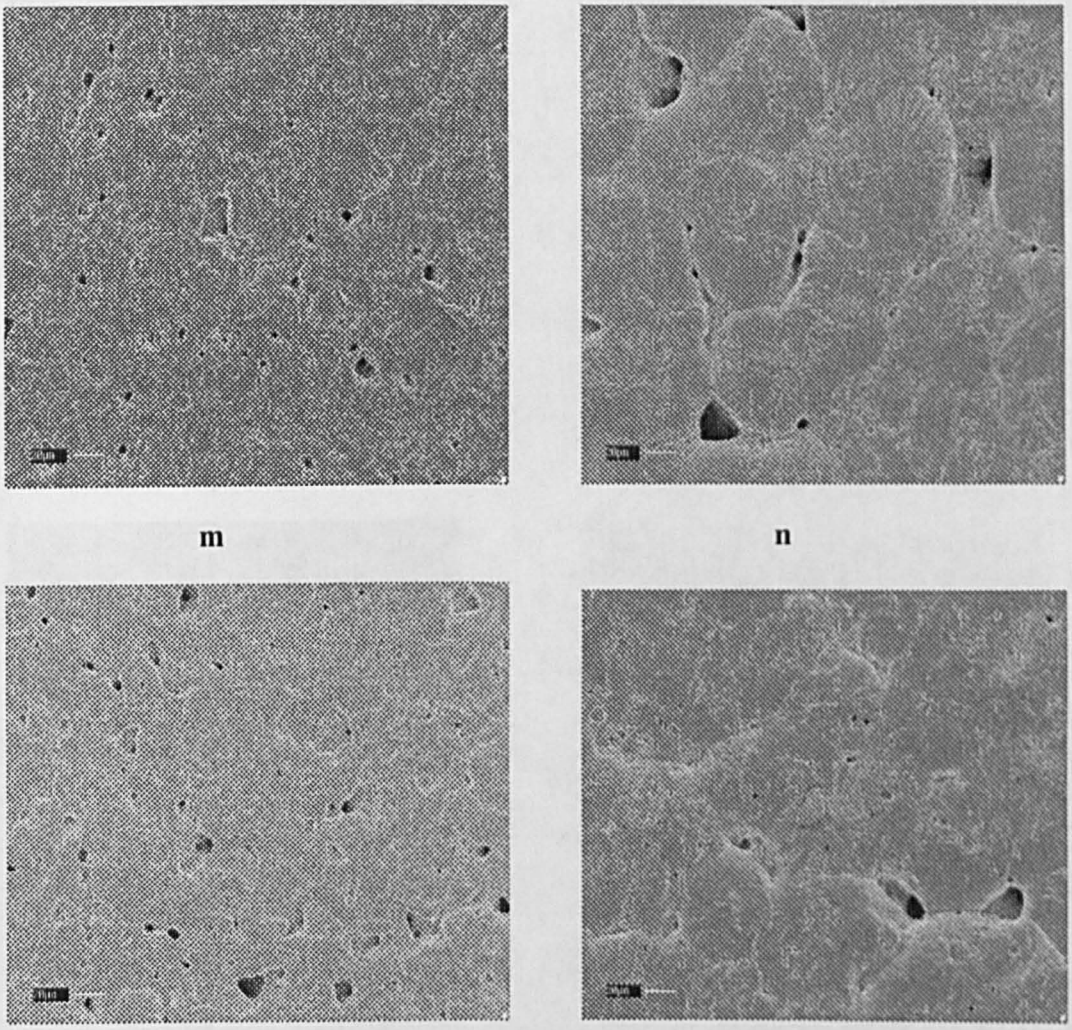

Figure 6.25.SEM images of PEO/ENR50/$LiCF_3SO_3$ polymer electrolyte films prepared by solvent casting. The bar scale shown is 20μm (m) 98 % PEO; (n) 95% PEO; (o) 90% PEO (p) 75% PEO.

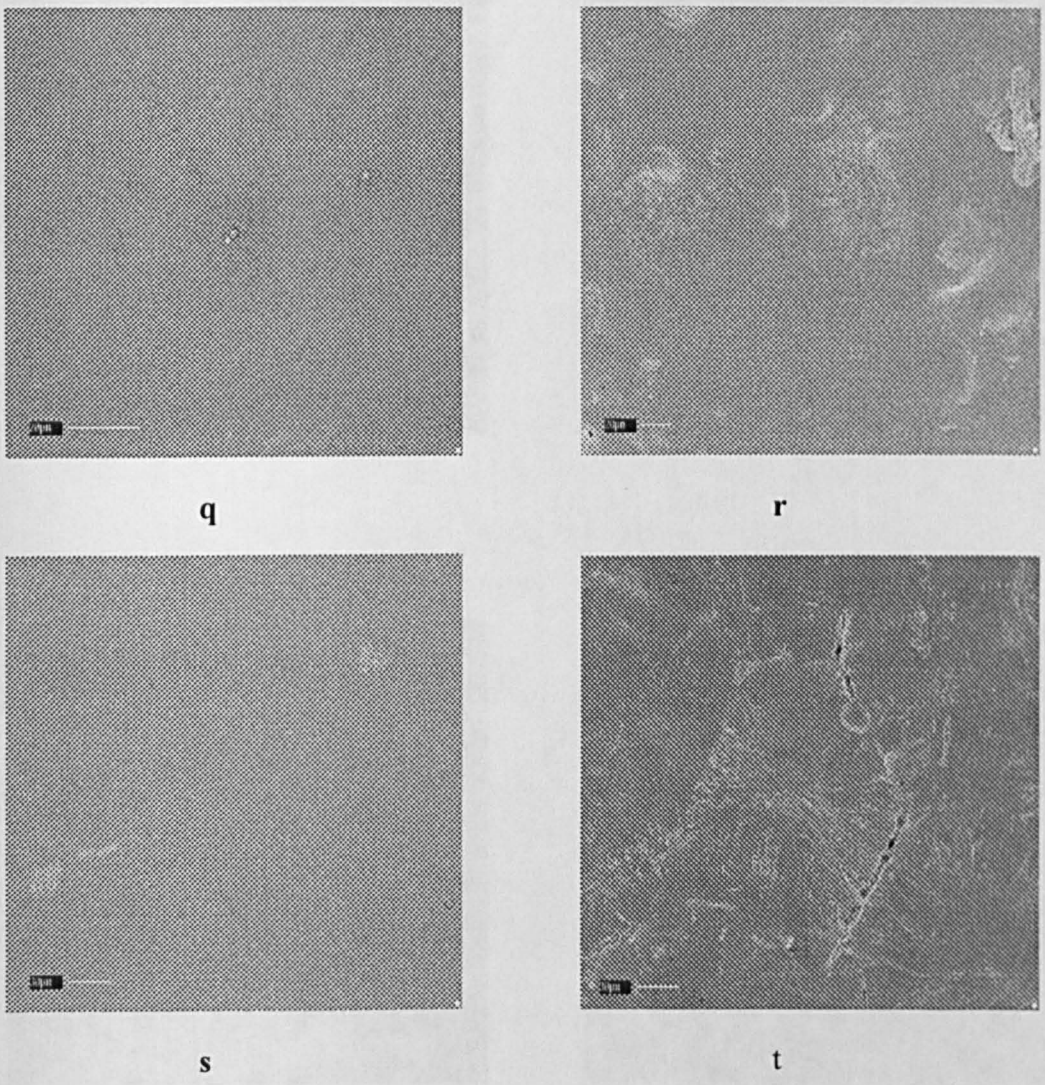

Figure 6.26.SEM images of ENR25/PEO/$LiCF_3SO_3$ polymer electrolyte films prepared by solvent casting. The bar scale shown is 20 μm (q) 2% PEO; (r) 5% PEO; (s) 10 % PEO; (t) 25% PEO

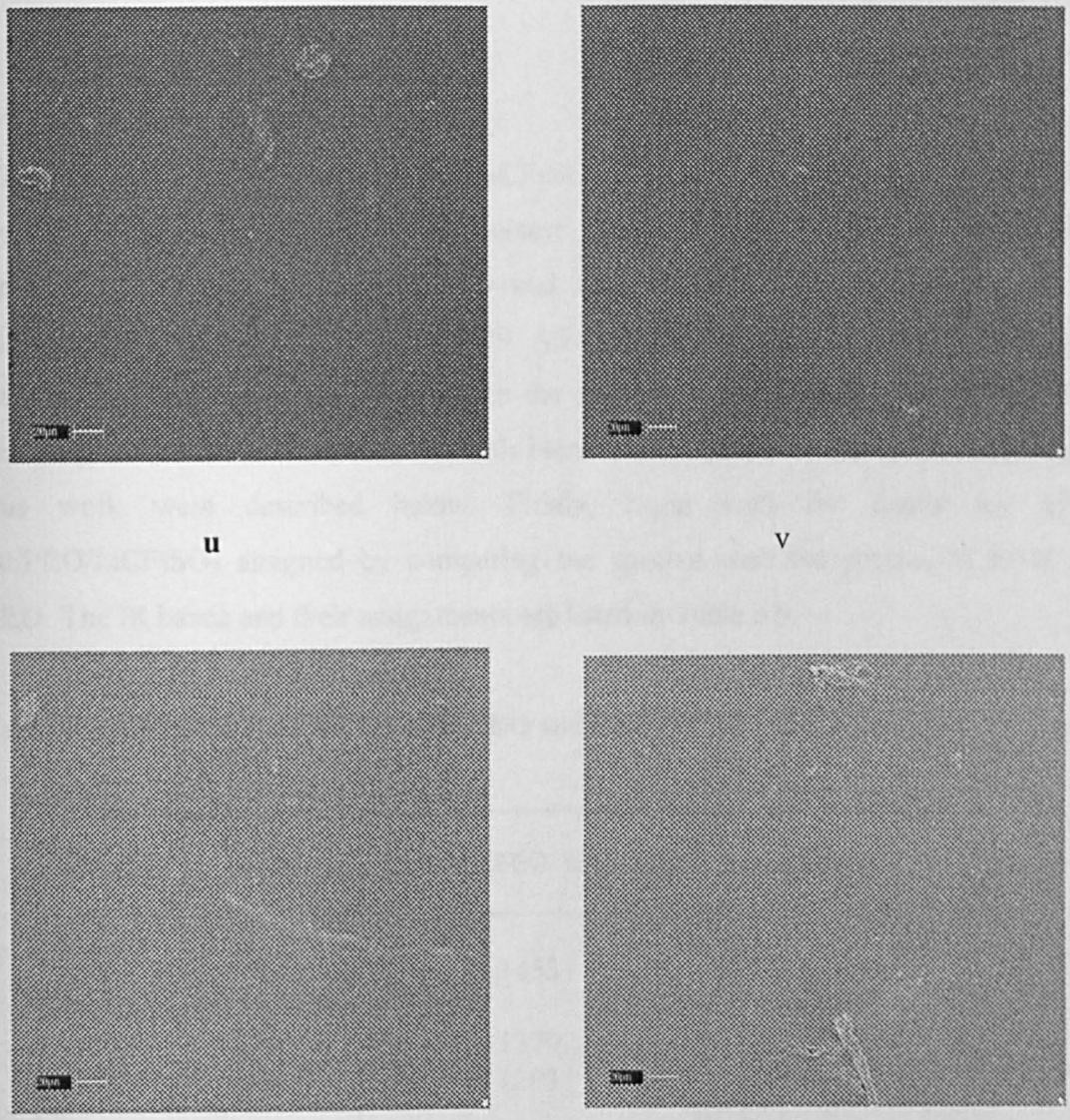

u v

w x

Figure 6.27.SEM images of ENR50/PEO/$LiCF_3SO_3$ polymer electrolyte films prepared by solvent casting. The bar scale shown is 20μm (u) 2% PEO; (v) 5% PEO; (w) 10% PEO; (x) 25% PEO

6.3.4 Infrared spectroscopy

The incorporation of lithium triflate ($LiCF_3SO_3$) salt in ENR/PEO blend was observed by IR spectral studies at ambient tempearture. The FTIR spectra of a solvent cast films produced from both of ENR-25/PEO and ENR-50/PEO blends containing salt are illustrated in Figure 6.28 and Figure 6.29. All of the ENR-25/PEO/$LiCF_3SO_3$ complexes have almost similar (but not identical) to the spectra for ENR-50/PEO/$LiCF_3SO_3$ blend electrolytes. Thus the IR spectra of both blend based system electrolytes conducted in this work were described below. Firstly, begin with the bands for ENR-50/PEO/$LiCF_3SO_3$ assigned by comparing the spectra with the spectra of ENR and PEO. The IR bands and their assignments are listed in Table 6.5. .

Table 6.5. Mid-IR spectra for ENR-50, PEO and ENR-5/PEO $LiCF_3SO_3$ blends (500-1500 cm^{-1})

ENR-50	PEO	ENR-50/PEO/ $LiCF_3SO_3$	Assignment
1451	1467	1453	CH_2 asymm. bending
1378	1359	1379	
1327	1343	1293	CH_3
	1240		
1251		1257	Epoxy
1111	1146		
1064			
1032	1064		
	960	1168	ν(COC)
875			
837	844	1109	
780		1041	LiX
		876	Epoxy: half ring stretching
		839	
		643	δ(SO_3)

In the doped blended films with 2/98, 5/95, 10/90, and 25/75 ENR-25/PEO compositions, the following new features appear after complexation: The following i.r. regions have been obtained and examined: (1) 3000 to 2800 cm^{-1} containing CH_2, CH_3, CH stretching mode; (2) 1450 to 1350 cm^{-1} CH, CH asymm, bending; (3) 1250 cm^{-1} epoxy: whole ring stretching; (4) 1150 to 1050 cm^{-1} CC stretching, C-O-C asymm. stretching; (5) 850 cm^{-1}, assymm. rocking and 950 cm^{-1}, symm rocking; (6) 650 cm^{-1} is assigned to S-O stretching.

The appearance of new peaks other than those of the component materials undoped PEO/ENR indicates the complexation of the system. The emergence of new peaks might prove the result of complex system between the salt and the ENR/PEO blend was formed. Though not all new peaks could be identified a few assigned peaks are discussed below.

The peaks in the region of 3000 to 2800 cm^{-1} are associated with the group such as CH_2, CH_3, CH stretching mode in the ENR backbone. Fom IR spectra of ENR50/PEO/$LiCF_3SO_3$ electrolytes with ratios 98/2, 95/5, 90/10, 75/25 ENR/PEO compositions revealed that ENR component is prominent. The ENR rubber component has almost suppress PEO crystalline phase as indicated from IR spectra (Figure 6.26). As the result the peaks observed at 1146 and 1063 cm^{-1} from PEO have reduced the intensities. It is believed that Lithium cation interact with the epoxy group randomly distribute along the rubber main chain. The peaks at 1168,1109, 876, 839 and 643 cm^{-1} collected from the spectra of ENR-50/PEO/ $LiCF_3SO_3$ electrolyte are compared to the vibrational frequencies of ^6Li ^6LiO and O^6Li O (1028 and 730 cm^{-1}) cited from literature (Nakamoto, 1997). In contrary to the IR spectra of PEO/ENR50/ $LiCF_3SO_3$ polymer electrolytes containing high PEO content it shows clear peaks of a gauche configuration at 843 and 960 cm^{-1}. The peaks indicate a crystalline state of PEO predominate in the blended polymer electrolytes. The addition of lithium triflate has increased the glass transition temperature for the formation of virtual crosslink. The multiphase polymer electrolyte system in this regime is very hard to predict the IR spectra. However the intensity of the satellite band (Figure 6.28 and 6.29) becomes strong as concentration of PEO in the blended electrolyte is progressed.

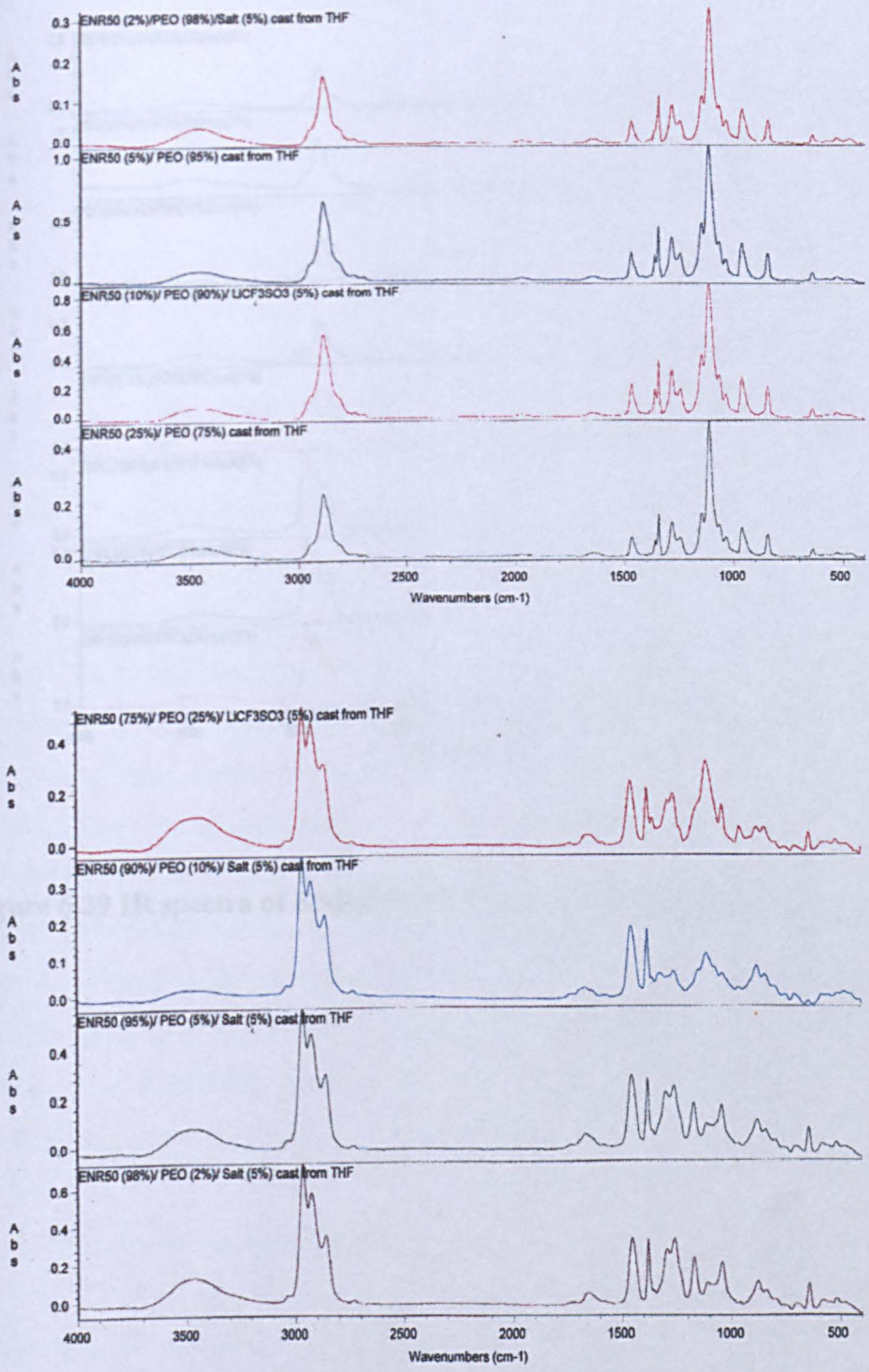

Figure 6.28 IR spectra of ENR50/PEO/$LiCF_3SO_3$ films with solvent cast.

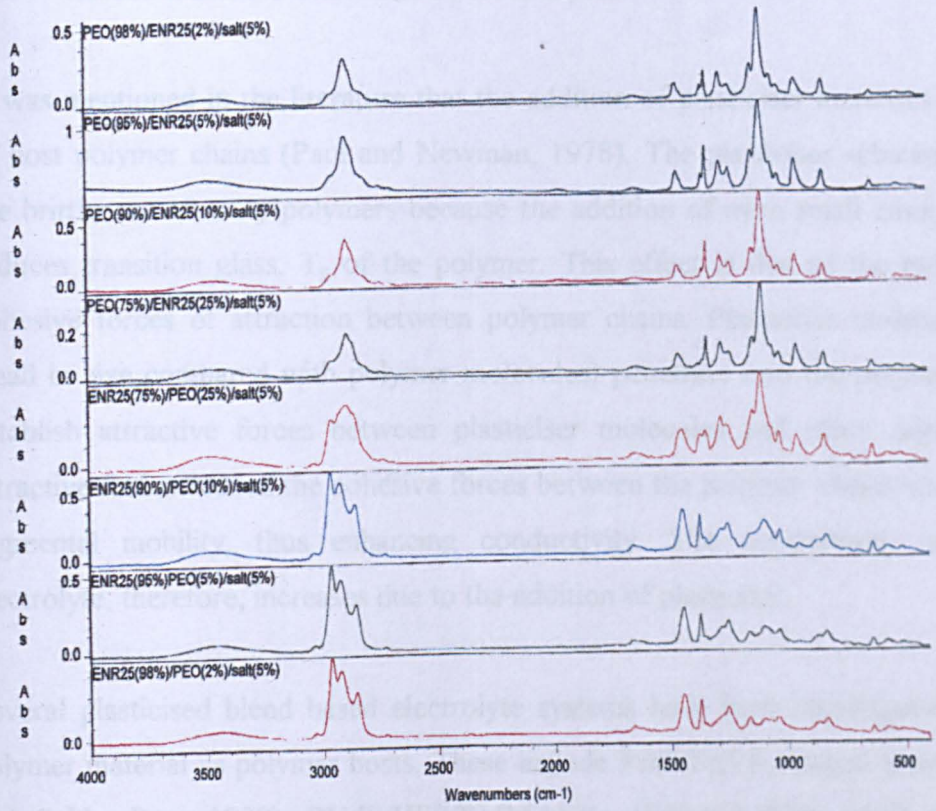

Figure 6.29 IR spectra of ENR25/PEO/$LiCF_3SO_3$ films with solvent cast

6.4. ENR/PEO/EC/PC/$LiCF_3SO_3$ electrolytes

It was mentioned in the literature that the addition of plasticiser increases the flexibility of host polymer chains (Paul and Newman, 1978). The plasticiser substantially reduces the brittleness of many polymers because the addition of even small amounts markedly reduces transition glass, T_g of the polymer. This effect is due to the reduction in the cohesive forces of attraction between polymer chains. Plasticiser molecules relatively small in size compared with polymer molecules) penetrate into the polymer matrix and establish attractive forces between plasticiser molecules and chain segments. These attractive forces reduce the cohesive forces between the polymer chains and increase the segmental mobility, thus enhancing conductivity. The conductivity of a polymer electrolyte, therefore, increases due to the addition of plasticiser.

Several plasticised blend based electrolyte systems have been investigated using blend polymer material as polymer hosts. These include PEO/$NaYF_4$ (Jaipal Reddy, Sreekanth and Subba Rao, 1999), PVdF-HFP/PMMAVAc (Oh and Kim, 1999), PVC/PMMA (Rhoo, Kim, Park, and Hwang, 1997), PPG/PMMA (Mani, and Steven, 1993), PEO/PVdF (Jacob, Prabaharan and Radhakrishna, 1997), PEO/PVC (Mishra and Rao, 1997) and PEO/PAN (Munichandran, Sivasankar, Scanlon and Marsh, 1997). In addition to the list of these blended based electrolytes was explored ENR/PEO blend of various ratios as polymer hosts to produce plasticised blend based polymer electrolyte system. The ENR/PEO blend regimes provide a novel system to investigate their physical properties behaviour and its ionic conductivity.

6.4.1 Conductivity measurement

Resistances of the films were measured using impedance plots, and one of them is shown in Fig. 6.30 From the impedance plot, the bulk resistance was obtained and ionic conductivity was calculated. The conductivity values of the plasticized ENR-25/PEO and ENR-50/PEO systems containing lithium triflate are shown in Table 6.6

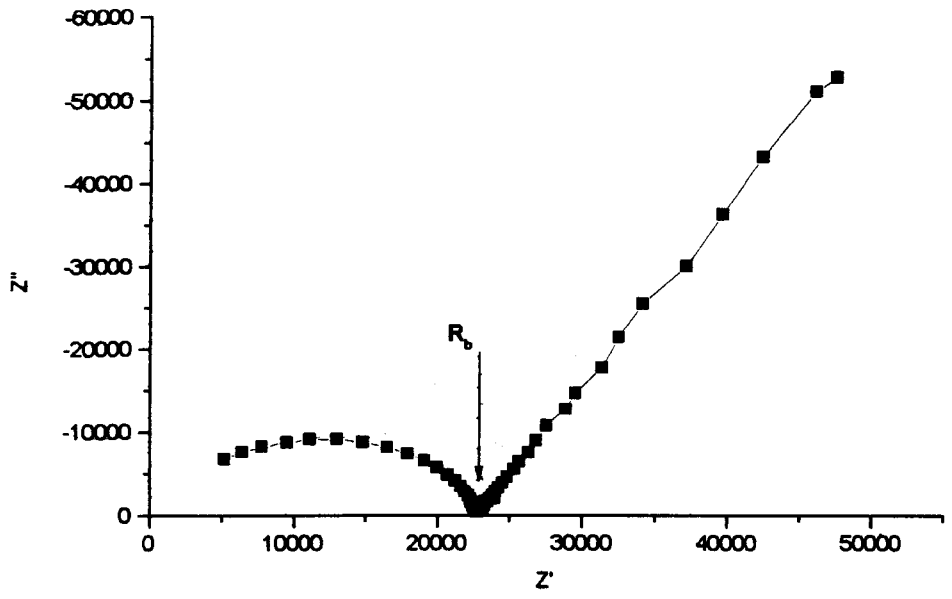

Figure 6.30 Impedance plot of ENR50/PEO/$LiCF_3SO_3$ polymer electrolyte.

From Figure 6.31 the graph shows that by adding PEO progressively in the blend the trend of ionic conductivity decreases then slightly increase to maximum and subsequent decrease. For all PEO concentrations in the blend compositions present lower ionic conductivity than non-blend plasticized ENR-25/50 containing the same salt content. The lower conductivity values of the samples are caused by the higher degree of crystallinity, as confirm by DSC curves in Figure 6.32 and 6.33 was found that at low per cent PEO content the blend electrolyte in amorphous state but crystalline state predominate at higher per cent. The ionic conductivity is assumed to occur by Lewis acid-base interaction between the Li^+ ions and the oxygen atom in the ether bonds. Both repeating units of the polymer posses oxygen atom, however, it seem that the ENR is highly amorphous but not PEO. Thus, the ionic conduction is more preferential in amorphous phase than crystalline phases. Due to this it is believed that the Li interact strongly with oxygen atom in the epoxy group of ENR in similar manner to ether group of PEO. However, to support this hypothesis there is no experimental evidences for ionic transport mechanism in multiphase electrolyte system at this stage.

Table 6.6 Ionic conductivity of ENR25/PEO/EC/PC polymer electrolyte samples

Sample	% of PEO	ENR25/p Conductivity ($S\ cm^{-1}$)	ENR50/PEO/EC/PC Conductivity ($S\ cm^{-1}$)
	0	1.8×10^{-4}	4.0×10^{-5}
	2	6.9×10^{-5}	5.2×10^{-5}
	5	6.0×10^{-5}	9.7×10^{-5}
	10	4.3×10^{-5}	7.1×10^{-5}
	25	3.0×10^{-5}	2.5×10^{-5}
	75	3.4×10^{-5}	6.9×10^{-5}
	90	8.6×10^{-5}	1.3×10^{-5}
	95	5.9×10^{-5}	7.9×10^{-5}
	98	3.6×10^{-5}	2.5×10^{-5}
	100	$10^{-4} - 10^{-5}$	$10^{-4} - 10^{-5}$

It was observed that the modified natural rubber/PEO based films have the ability to uptake a high loading of polar low molecular weight organic solvent. The polymer electrolyte films with ionic conductivities in the order of 10^{-4} S cm^{-1} still retain their rubbery characteristic in spite of the presence large amount of absorbed electrolyte solution and the crystalline PEO. These finding were compared with the work (Morihiko, 1996) on elastomeric-based materials using synthetic rubber as the polymer host. It was reported that an ionic conductivity of the order of 10^{-3} S cm^{-1} was obtained by swelling a polymer electrolyte system with electrolyte solvent. Recently, (Ju, Xu, and Yang, 1998) also reported the conductivity of nitrilic rubber with the copolymer of ethylene oxide and epichlorohidrin swollen by a solution of lithium perchlorate ($LiClO_4$) in propylene carbonate. For the blend containing 40% (w/w) of solution, conductivity 10^{-3} S cm^{-1} at room temperature. In this present work a different material and approach has been used but the conductivity trend mimics the above systems. It is suggested that the polarity of the both materials is one of the key factors to attain high ionic conductivity. It was reported that only polymers possessing high dipole moments are suitable candidates (Wieczorek, 1995).

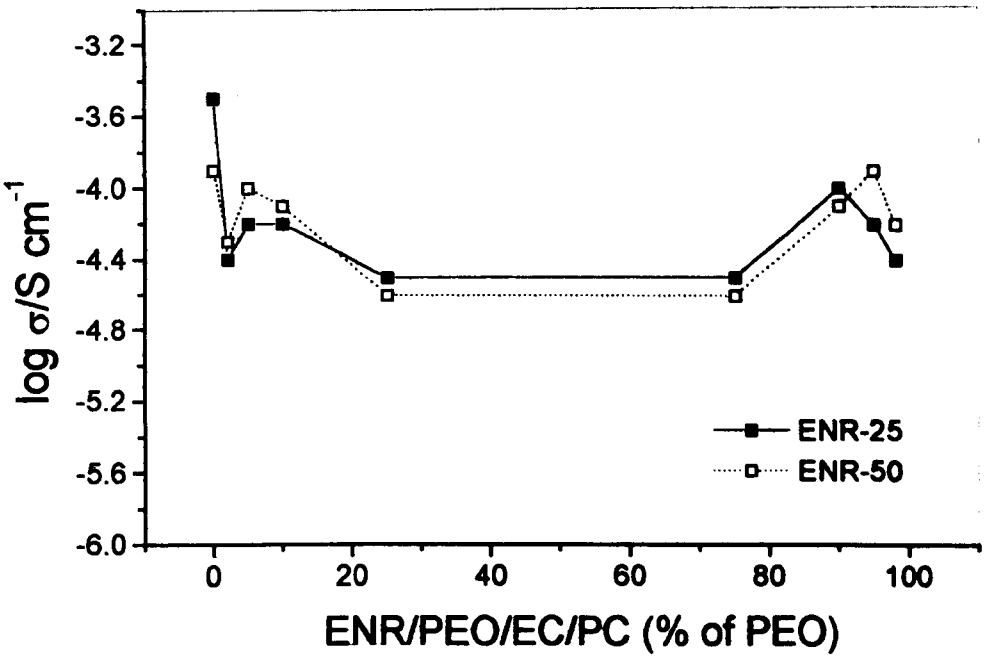

Figure 6.31.Conductivity as a function of PEO concentration for ENR/PEO/EC/PC/$LiCF_3SO_3$ electrolytes at room temperature.

6.4.2 Differential Scanning calorimeter (DSC)

The ENR/PEO/EC/PC$LiCF_3SO_3$ polymer electrolyte is considered multiphase system, which consists of blend polymer network and a solution of inorganic salt in low molecular weight polar solvents. This polymer electrolyte system can be explained by the existence of non-crystallizable component of ENR, semicrystalline of PEO and a crystal mixture of the plasticizer and salt. The phase structure of this plasticized ENR/PEO blend is not exactly known at present time. From the experimental observations indicate that, ENR component introduced in the blend system might act as internal plasticizer reducing the crystallinity of PEO chain, and hence increasing the concentration of the highly conducting amorphous phase. As shown in Figure 6.32 and 6.33, the melting peak and transition glass temperature of the plasticized electrolyte films are scanned at temperature range – 80^0 C to + 250^0 C respectively in the DSC thermogram.

The ionic conductivity of polymer electrolytes is strongly affected by their thermal behaviour. Thus, the knowledge of their thermal transitions, like transition glass temperature, T_g, and melting temperature, T_m, (Figure 6.34 and 6.35) is particularly informative. Figure 6.33 and 6.33 shows the DSC curves for the pure ENR, pure PEO and their plasticized blended films with different PEO concentration in weight per cent. It was observed that the three samples namely, ENR-25, PEO and plasticized PEO/ENR/$LiCF_3SO_3$ present T_g, at -43^0 C, -60^0 C, and -43^0 C respectively. From the DSC data shows that with addition of plasticicer, EC/PC, there is no melting peak, T_m observed for the blend, containing low percentage of PEO (2 to 25 w/o). In the case of plasticised blended film ENR/PEO composition with high percentage PEO content (75 to 98 w/o) present T_m, and T_g. For this material T_m, is close to that observe for pure PEO, suggesting that crystalline phase is rich in the blend. The T_g obtained is intermediate value between the T_g's of pure PEO and ENR-25 (T_g - PEO = -60^0 C, T_g – ENR-25= -43^0 C). This indicates that plasticized blended ENR/PEO/ $LiCF_3SO_3$ present a crystalline phase composed by PEO and amorphous phase composed by a miscible mixture between PEO and ENR-25. The blend showed high conductive sample although presents a crystalline domain.

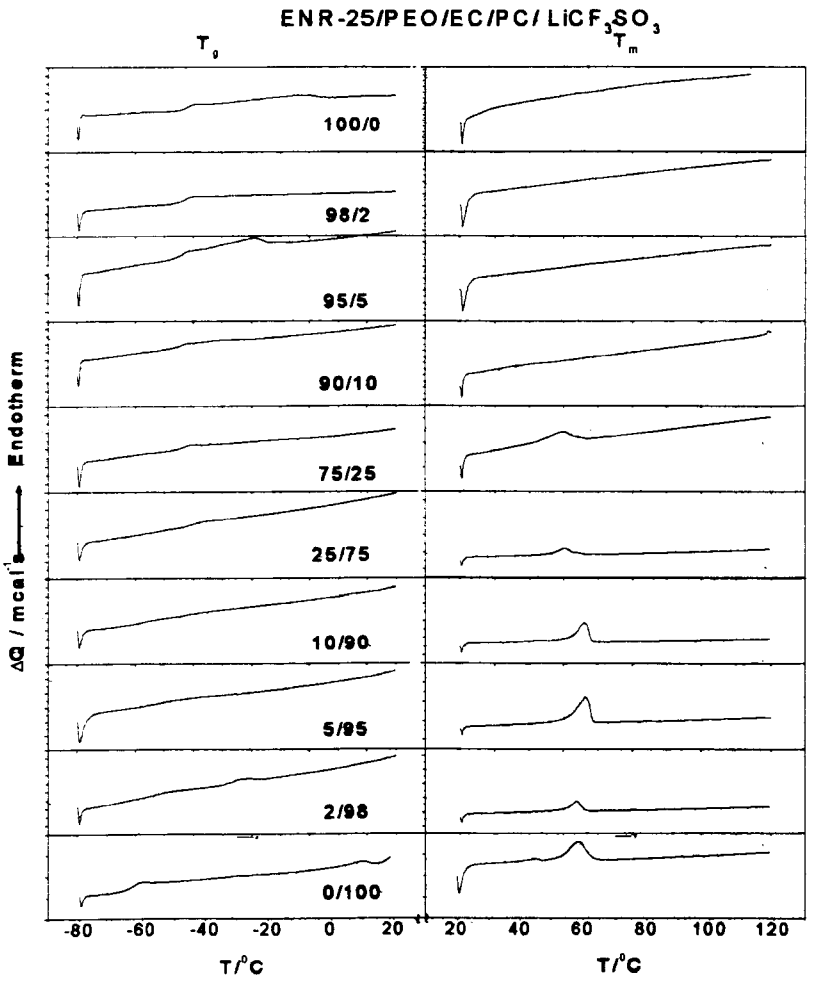

Figure 6.32 DSC traces of ENR25/PEO/EC/PC/ $LiCF_3SO_3$ electrolytes

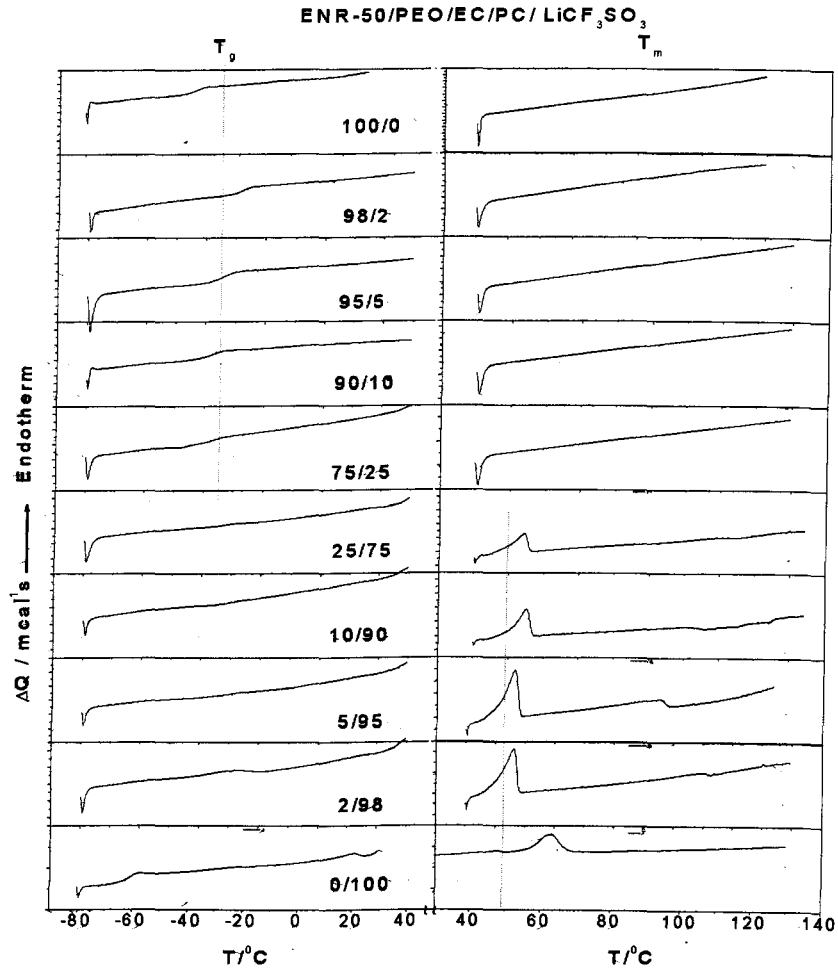

Figure 6.33 DSC traces of ENR50/PEO/EC/PC/ $LiCF_3SO_3$ electrolytes

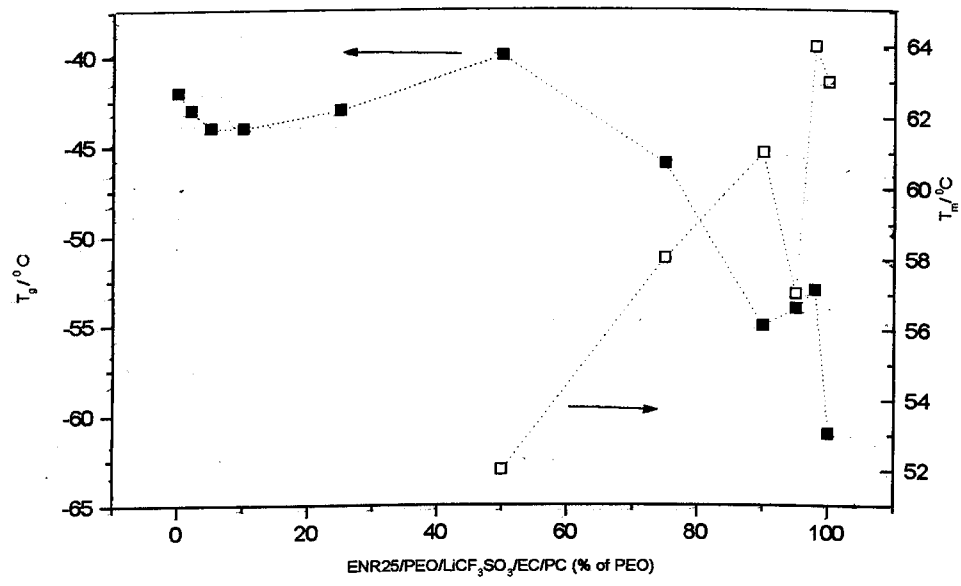

Figure 6.34 Variation of T_g and T_m of the ENR25/PEO/EC/PC/$LiCF_3SO_3$ electrolyte as a function of PEO concentration in the ENR mixture.

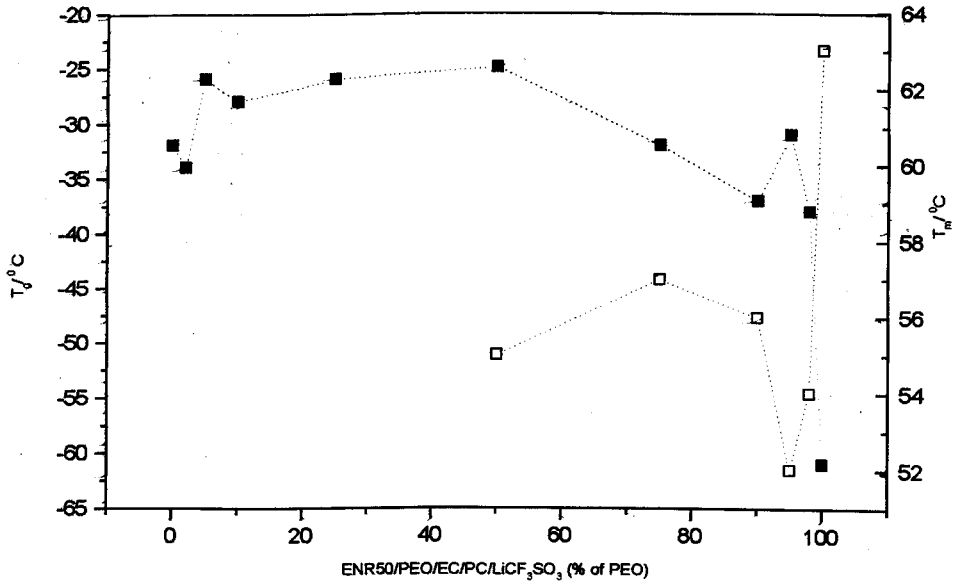

Figure 6.35 Variation of T_g and T_m of the ENR25/PEO/EC/PC/$LiCF_3SO_3$ electrolyte as a function of PEO concentration in the ENR mixture

6.4.3 Scanning Electron microscopy studies

Scanning electron microscopy (SEM) was performed for the plasticized ENR/PEO blended films of various per cent PEO additives to determine the homogeneity of the polymer electrolytes. From the SEM micrographs in Figure 6.36 show that the phase behaviour of plasticized blended films containing low and higher percentage of PEO regimes. The plasticized blended electrolyte samples with 98/2, 95/5, 90/10 and 75/25 ENR/PEO ratios indicate smooth amorphous phases structure whereas the blends with higher percentage PEO regimes revealed low crystalline phases. The SEM results in agreement with DSC traces. DSC traces obtained for the ENR/PEO blended films with low per cent PEO show only single Tg and no first order transition. For blended samples with higher PEO regimes show single Tgs and first order transitions are apparent.

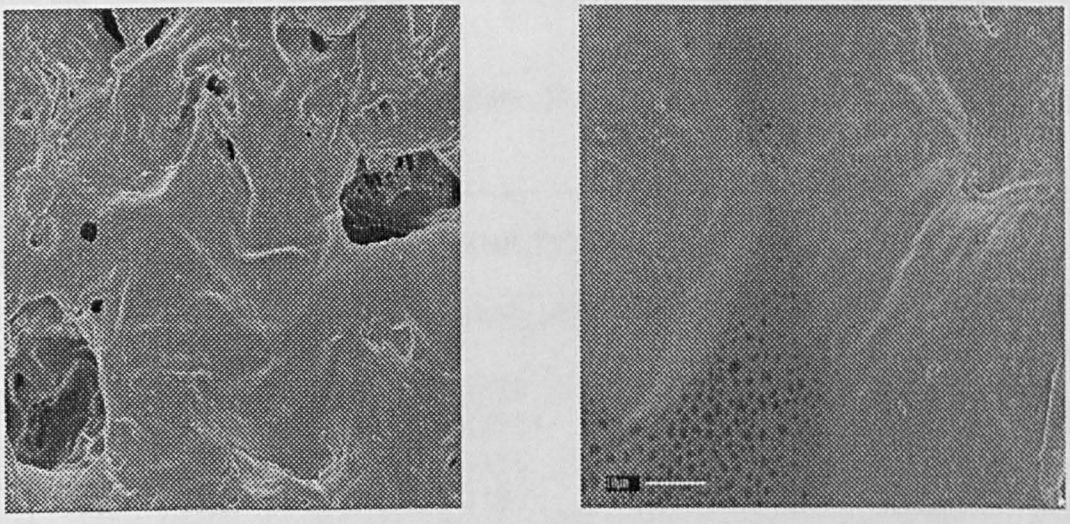

(a) (b)

Figure 6.36 SEM images of (a) ENR50 (25%)/PEO (75%)/$LiCF_3SO_3$/EC:PC and (b) ENR50 (75%)/PEO (25%)/$LiCF_3SO_3$/EC:PC solvent casting films

6.5.Infrared spectroscopy.

All IR spectra were obtained and recorded on computer interfaced Nicolet FTIR system 5.5 instrument in the frequency range 4000 to 500 cm^{-1} with resolution of 4 cm^{-1}.

Figure 6.37 and 6.3.8 show the spectra of the plasticized ENR 25 and 50 blended films with different PEO concentrations. From the spectra indicate that the emergence of new peaks not present in PEO are seen. This has proven the complexations of the systems were formed. All of the plasticized blended samples with low per cent of PEO (98/2, 95/5, 90/10 and 75/25 ENR25/PEO ratios) have almost similar (not identical) IR spectra but they are different compared to high PEO content (98, 95, 90, and 75 weight per cent) regime samples. The differences occur in the following frequency region: (1) Special attention has been paid to FTIR spectra in the mid range frequency region at 1500 cm^{-1} to 800 cm^{-1}. The assignment of the functional group of chemical are given in Table 6.8

Table 6.7. Mid-IR spectra forpure ENR-25, pure PEO and undoped ENR-25/PEO blends (500-1500 cm^{-1})

ENR-25	E/NR-25PEO/EC/PC	ENR-25/PEO/EC/PC/$LiCF_3SO_3$	Assignment
		1659,1638	
1495	1451	1452	CH, CH_2, CH_3
1377	1377	1382	
	1356	1355	CH_2 asym.
1323	1321	1283	bending
1250	1247	1258,1225	Monodentate
		1225	ionpairs
		1168	
	1108	1076	$CF_3SO_3^{-1}$
1097	1039	1037	ν(COC)
1037			LiX
	959	971	C-O-O
871	872		ν(COC)
837	840	840	CH_2
		777	epoxy
		714	EC
		641	ν(SO_3)

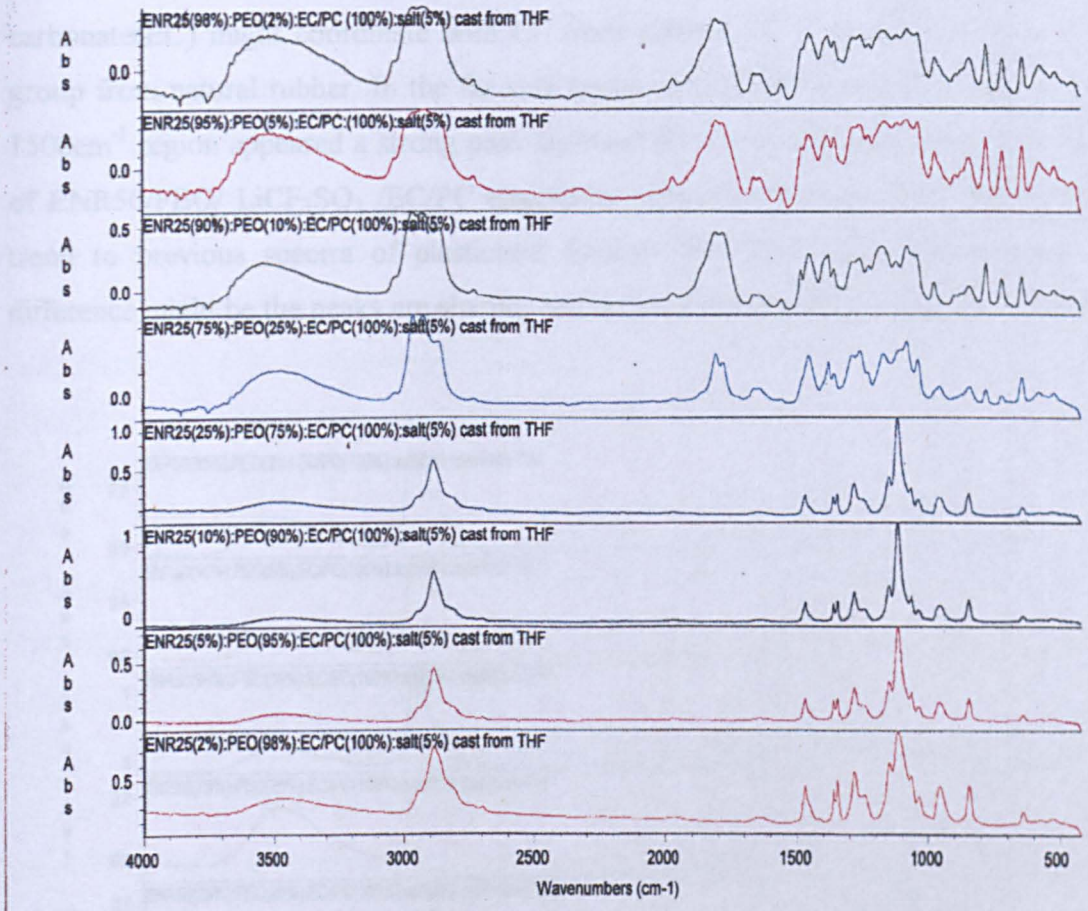

Figure 6.37 IR spectra of ENR25/PEO/ EC/PC /$LiCF_3SO_3$ electrolytes

Ir spectra in Figure 6.38 shows different trend of spectral features for the blend of ENR25/PEO/EC/PC/$LiCF_3SO_3$ electrolytes when the PEO content in the blend progresses from low to high concentration. In the high PEO concentration indicates that a clear gauche configuration (843 and 960 cm^{-1}) at 98 wt.% PEO and satellite band (1100 cm^{-1}). The crystalline state of PEO slowly diminish as ENR content approach 75 wt.%. The presence of plasticiser in the blend has caused the the spectra for the system very complex and contains many bands. The three bands found for the plasticised blend

containing low PEO content are 777, 714 and 641cm^{-1}. It is indication of ethylene carbonate(EC) might coordinate with Li^+ from triflate salt or together with the epoxy group from natural rubber. In the far side higher end frequencies (~1850 cm^{-1}) beyond 1500cm^{-1} region appeared a strong peak carbonyl (C=O) for EC plasticiser. The spectra of ENR50/PEO/ $LiCF_3SO_3$ /EC/PC electrolyte presented in Figure 6.38 almost similar trend to previous spectra of plasticised ENR25/ PEO/$LiCF_3SO_3$ blend system. The difference might be the peaks are sharper and isolated split band appeared at 1800 cm^{-1}.

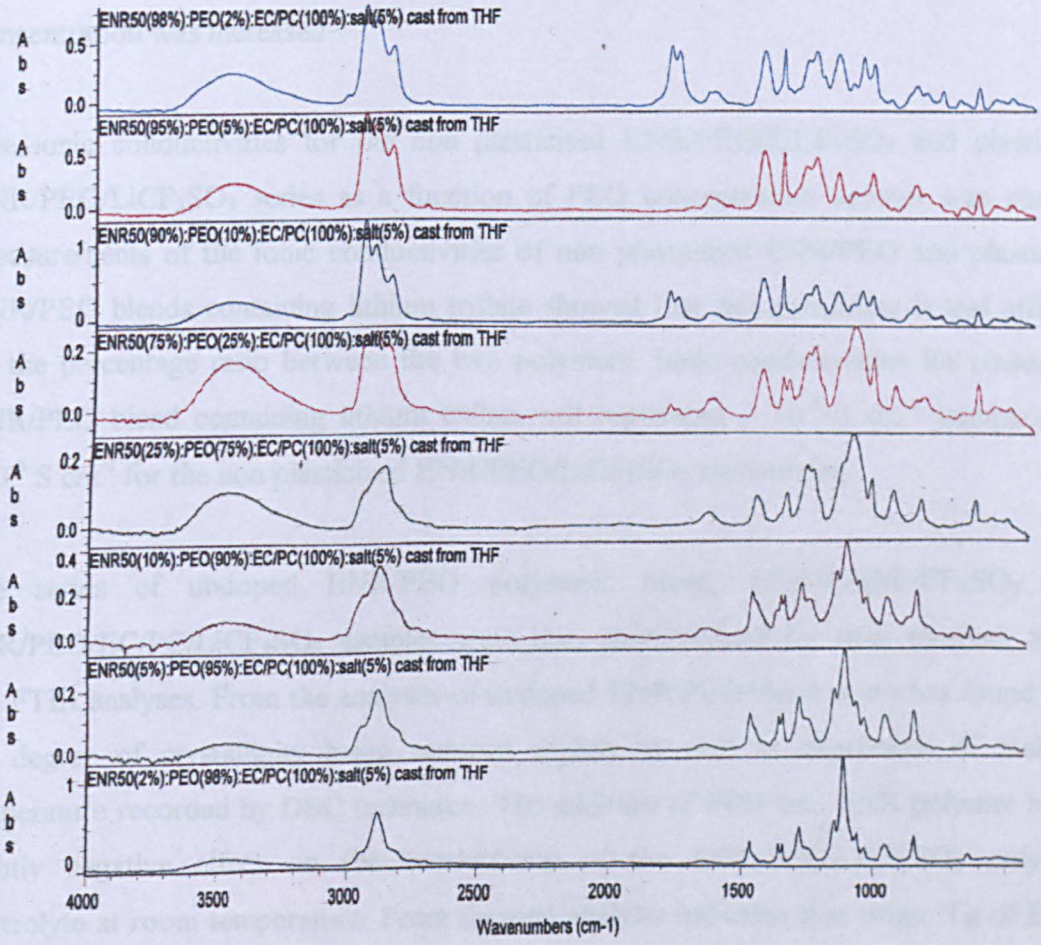

Figure 6.38 IR spectra of plasticized ENR50/PEO/ $LiCF_3SO_3$ blend electrolytes

6.6. Conclusion

The three types of undoped ENR/PEO polymeric blend, ENR/PEO/$LiCF_3SO_3$ and ENR/PEO/EC/PC/$LiCF_3SO_3$ blend of dual-phase polymer electrolyte systems were designed for comparison to the previous work using single phase polymer host polymer electrolyte system of polyurethane, ENR and poly (methyl methacrylate) grafted natural rubber. The blended polymer electrolyte films were successfully prepared using solvent cast technique. Visual observation indicated that the undoped blends with low PEO concentration content was translucent whereas the blended films turn hazy as PEO concentration was increased.

The ionic conductivities for the non plasticised ENR/PEO/$LiCF_3SO_3$ and plasticised ENR/PEO/$LiCF_3SO_3$ series as a function of PEO concentration content was studied. Measurements of the ionic conductivities of non plasticized ENR/PEO and plasticized ENR/PEO blends containing lithium triflate showed that this parameter is less affected by the percentage ratio between the two polymers. Ionic conductivities for plasticized ENR/PEO blend containing lithium triflate salt registered ~ 10^{-5} S cm^{-1} compared to ~10^{-6} S cm^{-1} for the non plasticized ENR/PEO/$LiCF_3SO_3$ electrolytes.

The series of undoped ENR/PEO polymeric blend, ENR/PEO/$LiCF_3SO_3$ and ENR/PEO/EC/PC/$LiCF_3SO_3$ samples were also characterized for their thermal, SEM and FTIR analyses. From the analyses of undoped ENR/PEO blend series has found that the degree of crystallinity being reduced slightly as well as depression of melting temperature recorded by DSC technique. The addition of PEO into ENR polymer has a slightly negative effect on the conductivity of the ENR/PEO/$LiCF_3SO_3$ polymer electrolyte at room temperature. From thermal analysis indicates that single Tg of ENR was detected for composition containing PEO concentration ≤ 75% suggest that the ENR polymer predominate in the blend. In the blend ENR/PEO/$LiCF_3SO_3$ series containing PEO high concentration content the T_g values close to PEO was apparent.

In the experimental works involving blends containing high PEO content, even though both the degree of crystallinity and crystallization rates are reduced, the melting temperature is relatively constant as a function of composition. The two T_g's are hard to observe for blends containing higher PEO content because of the higher degree of crystallinity. It is possible that the crystallization process occurs together with phase separation for blends containing low concentrations of PEO. Concerning the thermal properties, different behaviours are observed by adding $LiCF_3SO_3$ to the blends. The blends containing low PEO content become amorphous (single T_g's) by adding about 5 wt % of $LiCF_3SO_3$ (O/Li = 11). Whereas for the blends containing high PEO content present Tg's and T_m respectively.

Chapter 7. Concluding remarks and future work

7.1 Conclusion

With regard to the chapters discussed in this thesis topic the following final conclusion may be drawn.

1. The electrolytes using polymer hosts thermoplastic polyurethane (TPU), modified natural rubbers and modified natural rubber/PEO blends containing $LICF_3SO_3$ salt had various compositions suitable for isolating free standing films. In addition to this similar manner have been obtained for the plasticised regimes. The series of solvent cast films of thermoplastic polyurethane (TPU) and modified natural rubber/lithium triflate salt electrolytes as well as plasticised of these electrolytes with EC/PC has increased ionic conductivities from 10^{-6} to 10^{-5} S cm^{-1} at ambient temperature. In the series of non plasticised modified natural rubber/PEO blend containing lithium triflate salt electrolytes exhibit ionic conductivity 10^{-6} S cm^{-1} whereas addition of EC/PC plasticiser to the system increased ionic conductivities to 10^{-4} S cm^{-1} at ambient temperature.

2. The majority of the salt-doped polymer electrolyte systems have ionic conductivities 10^{-5} S cm^{-1} at ambient temperature, which is higher than pristine PEO/salt complex. Addition of 100-wt % of EC/PC into the $LICF_3SO_3$ salt-doped polymer system has considerably increased an average ionic conductivity by almost two folds in magnitude.

3. The DSC traces of the salt-added polymer electrolytes displayed a single and increasing trend of transition glass temperature (T_g) when increasing amount of salt concentration was introduced into polymer matrix. However the immobilization of EC/PC into the system has resulted a marked reduction in their T_g values. Comparison between thermal behaviour and ionic conductivity of polyurethane, epoxidised and poly (methyl methacrylate) grafted natural rubbers with blend polymers showed that the single polymers present better performance for using as polymeric electrolyte. The performance of the blend is affected by crystallisation and phase segregation.

4. Other factor to be considered for practical application is the excellent contact properties of the polymer electrolyte film to electrode substrate. From the experimental task conducted for preparation of film was found that modified natural rubber based electrolytes had excellent contact to PTFE substrate.

5. For practical considerations, the mechanical rigidity of the polymer electrolyte films and its retention of liquid electrolyte solution have shown promising in the presence of polar modified natural rubber.

6. In summary, from spectroscopic data in conjunction with thermal analysis show that the degree of crystallisation, melting temperature and microstructure of PEO in PEO/ENR blends has been perturbed by the presence of ENR. In addition the present data showed rather complicated blend morphology, which is composition dependent, arising from phase separation. FTIR data showed that a decreasing PEO crystalline intensity with increasing ENR content. Spectroscopic data of the three types of polymers used in the experimental works present similar peaks at lower frequency has tendency to coordinate with lithium salt despite the presence of monodentate ion-pairs.

7.2 Future work

This thesis has uncovered a novel polymer host modified natural rubber as alternative to PEO to materialize plasticised and non-plasticised polymer electrolyte films. The excellent finding of plasticised modified natural rubbers based on epoxidised natural rubber and methyl methacrylate grafted regimes prompted to further explore two main aspects of work in the future. They are the practical aspect mechanical properties and application in the lithium cell systems. At present stage has found that for ENR and MG49- salt complexes the addition of plasticiser to polymer electrolytes can increase the conductivity substantially. For practical implementation of such materials, knowledge of their mechanical properties, such as tensile strength and elastic modulus and the effects of plasticiser and salt on these mechanical properties, is desirable. As cited in the literature little work has been reported on this aspect of thus far.

The future work is proposed as follows ;

The experimental work will involve preparation of film samples using different technique than present one. Although solvent cast technique is simple to practice but the solvent has undesirable implication to health effect in the long term. An approach using internal mixing process such as Brabender can be used for epoxidised natural rubber based product. Brabender machine, which is normally use for thermoplastic and rubber material is conducive to prepare dry plastised polymer electrolyte film in the closed system. The operation using Brabender machine is computer controlled for small volume of plastic/rubber mixing tailored to formulation of sample. Additives such as plasticiser and composite filler could easily measure and held into the hopper of the Brabender machine. In addition to this is the advantage of monitoring the process of mixing from the computer interface to required temperature for the polymer in use.

The blending process of two different polymers is very useful using this machine to achieve the right composition of sample with the ingredient as being practiced for the current research work. The extension of present work using this method can improve the performance of the physical properties of the material by using latest technology parallel to plastic industry of present time. Preparing of test pieces for tensile sound simple but it needs proper attention to cut neat test pieces using standard cutter comply to standard method to produce reliable data with minimum error. The test samples need to be conditioning with controlled humidity similar to polymer electrolytes to avoid contact with moisture prior to testing operation. The profile of the entire process for polymer electrolyte could easily monitor using internal mixer such as the maximum temperature, which is required for its final application in the lithium battery system. The optimized compositions from the current's work using ENR25, 50 and blended ENR/PEO polymer hosts are selected. The plasticised composition with the target of ionic conductivity 10^{-4} S cm^{-1} using other type of plasticiser will be look into as alternative to EC/PC.

The second part of work involves the assembly of plasticised ENR polymer electrolyte in the lithium cell system. It has found that plasticised ENR electrolyte and methyl grafted natural rubber exhibit excellent contact to low adhesion substrate such as Teflon. The rubbery film and good adhesive properties provides an added advantage as separator and electrolyte medium in the cell system. Plasticised epoxidised natural rubber and methyl methacrylate grafted natural rubber based electrolyte are flexible which enable them to undertake expansion and contraction process in the lithium cell system during operation. The use of EC/PC as solvent in the polymer electrolyte system has caused passivative layer to form between the interfacial layer of electrode and polymer electrolyte.

The next series of work will investigate the use of polyethylene glycoldimethl ether as alternative to EC/PC to be added into modified natural rubber for the formation of polymer gel electrolytes. Glycol is familiar name to rubber industry as well as polymer technologist to improve processing of highly crystalline polymer. The concept of acting as lubricant in rubber processing is also apply to polymer electrolyte to further improve the polymer matrix environment for small lithium cation to move efficiently within the polymer host . However, characterization of polymer electrolyte is crucial to determine the final properties of the polymer electrolyte compatible to electrode component in the cell system. The compatibility of an electrolyte with the lithium electrode is essential to guarantee acceptable performance and lifetime in rechargeable lithium-polymer batteries. This is the aim of future work to investigate the interfacial behaviour of a lithium electrode in contact with the polymer electrolyte under prolonged exposure.

Possible approaches for improving the stability of the lithium electrode/gelionic membrane interface include:

(i) the selection of the most suitable solvent and/ or salt and / or polymer components.;

(ii) the addition of interfacial stabilizer, e.g., ceramic powders, and

(iii) the use of dry membranes, ie., plasticizer-free membrane.

A convenient method for testing the compatibility of a given electrolyte with lithium metal electrode is that of monitoring, by impedance spectroscopy. In order to demonstrate the usefulness of the modified natural rubber basedpolymer electrolyte in rechargeable lithium batteries, it is necessary to fabricate Li/ solid polymer/$Li_{i+x}Mn_2O_4$ cell using the polymer and $Li_{i+x}Mn_2O_4$ composite cathode.

Proposed assembly of the battery cell is described as follows;

The target voltage is 3V.

Preparation of anode material ; Composite carbon anode using graphite mix with polymer electrolyte.

Polymer electrolyte system using modified natural rubber added with plasticiser

The composite cathode contained the same polymer electolyte and electronic conductor along with $LiMnO_4$.

REFERENCES

Abbrent, S., Lindgren, J., Tegenfeldt, J., Furneaux, J. and Wendsjo, A. (1999) *Journal of The Electrochemical Society*, **146** (pt. 9), pp. 3145-3149.

Abraham, K. M. and Alamgir, M. (1990) *Journal of Electrochemical Society*, **137**, p. 1657.

Abraham, K. M. and Alamgir, M. (1993) *Journal of Power Sources*, **43/44**, pp. 195-208.

Abraham, K., Koch, V. R. and Blakely, T. J., (2000) *Journal of The Electrochemical Society*, **147** (pt. 4), pp. 1251-1256.

Allen, P. W., Ayrey, G., and Moore, C.G., (1959) in *The British Rubber Producers' Research Association*: Publication No. 321, **Vol. XXVI** (pt. 2), pp. 66-67.

Almdal, K. (1993) *Polymer Gels and Networks*, **1**, pp. 5-17.

Andrieu, X., Vivedo, T. and Fringant, C., (1995) *J. of Power Sources*, **54**, pp. 487.

Angell, C. A. (1983) *Solid State Ionics*, **9/10**, pp. 3-16

Appetecchi, G. B., Croce, F. and Scrosati B., (1997) *Journal of Power Sources*, **66**, pp. 77-82.

Armand, M. B., Chabagno, J. M., Duclot, M., (1979) in: P. Vashishta et al. (Eds.), Elsevier, New York, p. 131.

Armand, M. B., (1986) *Ann. Rev. Material Sc*, **16**, p. 245

Armand, M. B., (1990) *Advanced Materials*, **2** (pt. 6/7), pp. 279-286.

Armand, M. B., (1994) *Solid State Ionics*, **69**, pp. 309-319.

Aurbach, D., Gofer, Y., Ben-Zion, M. and Aped, C., (1992) *J. Electroanal. Chem.*, **339**, p. 451.

Bakker, A., Gejji, S., Lingren, J., Hermansson, K. and Probst, M. M., (1995) *Polymer*, **23**, pp. 4371.

Bakker, A., Lindgren, J. and Hermansson, K., (1996) *Polymer*, **10**, p. 1871.

Ballard, D.G.H., Cheshire, P., Mann, T. S. and Prezeworski, J. E., (1990) *Macromolecules*, **23**, p.1256.

Bandara, L. R. K., Dissanayake, M. A. K. L., and Mellander, B. E., (1998) *Electrochimica Acta*, **43** (pt.10-11), pp. 1447-1451.

Baril, D., Michot, C. and Armand, M.B., (1997) *Solid State Ionics*, **94**, 34-47.

Berson, A. and Lindgren, J., (1993) *Solid State Ionics*, **60**, p. 37.

Berthier, C., Gorecki, W., and Minier, M., Armand, M. B., Chabago, J. M. and Rigaud, P., (1983) *Solid State Ionics*, **11**, p. 91.

Best, A. S., Ferry, A., MacFarlane, D. R. and Forsyth, M., (1999) *Solid State Ionics*, **126**, pp. 269-276.

Bohnke, O., Frand, G., Rezrazi, M., Rousselot, C. and Truche, C., (1993) *Solid State Ionics*, **66**, pp. 105-112.

Bottelberghs, P. H., (1978), *Materials Science Series – Solid Electrolytes- General Principles, Characterization Material Appplications*, eds. Hagenmuller, P. and van Gool, W., Academic Press, New york, Chapter 10, pp. 145-172.

Branclup, J. and Immergut, E. H., (1975) *Polymer handbook*, Wiley, New York,

British Patent 2 113 692 (1982) A Method of Making Epoxidized *cis*-1,4 Polyisoprene Rubber.

Bruce, P. G. and Vincent, C. A., (1993) *J. Chem. Soc. Faraday Transactions*, **89**, p. 3187.

Bruce, P.G., (1995) *Solid State Electrochemistry*, Cambridge University Press, Cambridge, p. 23.

Bushkova, O. V., Zhukovsky, V. M., Lirova, B. I. and Kruglyashov, A. L., (1999) *Solid State Ionics*, **119**, pp. 217-222.

Cameron, G. G., Ingram, M. D. and Sarmouk, K., (1990) Eur. Polym. J., 26, p. 197.

Ceresa, R. J., (1973) *Block and Graft Copolymerisation*, Chap. 2, Wiley, London, **Vol. 1**, pp. 47-82.

Chintapalli, S. and Frech, R., (1996) *Solid State Ionics*, **86-88**, pp. 341-346.

Choe, H. S., Carroll, B. G., Pasquariello, D. M. and Abraham, K. M. (1997) *Chem. Mater.*, **9**, pp. 369-379.

Choi, Y., Kim, S. K. and Chang, K. H. (1997) *Journal of Applied Electrochemistry*, **27**, pp. 1118-1121.

Coleman, M. M., Skrovanek, D. J., Howe, S. E. and Painter, P. (1986) *Macromolecules*, **18**, p. 2149.

Cowie, J. M. G and Cree, S. H. (1989) *Ann. Rev. Phys. Chem.*, **40**, p. 85.

Croce, F., Appetecchi, G. B., Mustarelli, P., Quartarone, E., Tomasi, C. and Cazzanelli, E. (1998) *Electrochimica Acta*, **43** (pt. 10/11), pp. 1441-1446.

Croce, F., Brown, S. D., Greenbaum, S. G., Slane, S. M. and Solomon, M. (1993)

Decker, C., Xuan, H. L. and Thi Viet, T. N. (1995) *Journal of Polymer Science: Part A: Polymer Chemistry*, **33**, pp. 2759-2772.

Dell, R. (2000) *Chemistry in Britain*, **36**, 35.

Doeff, M. M., Georen, P., Qiao, J., Kerr, J. and De Jonghe, L. C. (1999) *Journal of Electrochemical Society*, **146** (pt. 6), pp. 2024-2028.

Ferry, A., Jacobsson, P., Heuman, J. D. and Stevens, J. R. (1996) *Polymer*, **37**, pp.737-744.

Forsyth, M., Meakin, P., MacFarland, D. R. and Hill, A. H. (1995) Electrochemical Acta, 40 (pt. 13/14), 40, p. 2349.

Fuller, J., Breda, A. C. and Carlin, R. T. (1997) *J. Electrochem. Soc.*, **144** (pt. 4), pp. L67-L69.

Gazotti, W.A., Spinace, M. A. S., Girotto, E. M. and De Paoli, M. A. (2000) *Solid State Ionics*, **130**, pp. 281-291.

Gelling, I. R. (1985) Modification of Natural Rubber Latex with Paracetic Acid. *Rubb. Chem. Tech.*, **58**, p. 86.

Gelling, I. R. and Smith, J. F. (1979) Controlled Viscosity by Natural Rubber Modification: *Proc. Int. Rubb. Conf. Venice*.

Gelling, I. R., Tinker, A. J. and Haidzir Abdul Rahman (1991) Solubility Parameters of Epoxidized Natural Rubbers, *J. Nat. Rubb. Res.*, 6 (pt. 1), p. 20.

Gozdz, A. S., Tarascon, J. M., Gebizlioglu, O. S., Schmutz, C. N., Warren, P. C. and Shokoohi, F. K. (1995) in Rechargeable Li and Li-ion Batteries, Eds. Megahed, S., Barnett, B. M. and Xie, L., *The Electrochemical Society*, Penington, NJ, **PV94-28**, p. 400.

Gray, F. M. (1987) in *Polymer Electrolyte Reviews*, Ed. MacCallum, J. R. and Vincent, C. A., **1**, p. 139.

Gray, F. M. (1991) *Solid Polymer Electrolytes*: Fundamental and Technological Applications, VCH, New York, p. 117.

Gray, F. M. (1991) *Solid Polymer Electrolytes*: Fundamental and Technological Applications, VCH, New York, p.2, 85.

Gray, F. M. (1997) *Polymer Electrolytes*, The Royal Society of Chemistry, p.1, 55.

Halpert, G. Frank, H. and Surampudi, S. (1999) *The Electrochemical Society Interface*, **8**, 25.

Hayamizu, K., Aihara, Y., Arai, S. and Price, W. S. (1998) Solid State Ionics, 107, pp. 1-12.

Heuman, J. D. and Stevens, J. R. (1995) *Macromolecules*, **28**, pp. 4268-4277.

Hikmet, R. A. M. and Peeters, M. P. J. (1999) *Solid State Ionics*, **126**, pp. 25-39.

Hikmet, R. A. M., Peeters, M. P. J., Lub, J and W. Nijssen (1999) *Journal of Electrochemical Society*, **146** (pt. 7), pp. 2397-2403.

http://www.lithiumpolymerbattery.com/perform.html

http://www.edtn.com/news/oct12/101298tnews2.html.

http://www.edtn.com/news/dec04/120498tnews2.html

http://www.batteryeng.com/whats_new.htm

http://www.polymerbattery.com/sss.html

http://www.grc.nasa.gov/WWW/RT1998/5000/5420hagedorn.html

Huang, W., Frech, R. and Wheeler, R. A. (1994) *J. Phys. Chem.*, **98**, p. 100.

Huq, R., Koksbang, R., Tonder, P. E. and Farrington, G. C. (1992) *Electrochimica Acta*, **37** (pt. 9), pp. 1681-1684.

Jacob, M. M. E., Prabaharan, S. R. S. and Radhakrishna, S. (1997) *Solid State Ionics*, **104**, pp. 267-276.

Jiang, Z., Carroll, B. and Abraham, K. M. (1997) *Electrochim. Acta*, **42**, p. 2667.

Ju, J. L., Gu, Q. C., Xu, H. S. and Yang, C. Z. (1998) *Journal of Applied Polymer Science*, **70**, pp. 353-357.

Kakihana, M., Schantz, S. and Torell, L. M. (1990) *Solid State Ionics*, **40/41**, p. 641.

Kim, D. W., Oh, B. K. and Choi, Y. M. (1999) *Solid State Ionics*, **123**, pp. 243-249.

Kim, S. H., Kim, J. Y., Kim, H. S. and Cho, H. N. (1999) *Solid State Ionics*, **116**, pp. 63-71.

Kohjiya, S., Kawabata, T., Maeda, K. and Yamashita, S. (1990) in *Second International Symposium On Polymer Electrolytes*, Ed. Scrosati, B., pp. 187-189.

Kono, M., Hayashi, E. and Watanabe, M. (1999) *Journal of Electrochemical Society*, **146** (pt. 5) pp. 1626-1632.

Latham, R. J. and Linford, R.G., (1987), Electrochemical Science and Technology of Polymers, ed. Linford, R.G., Elsevier Applied Science, London, pp. 17-21.

Lee, M. H., Kim, H. J., Kim, E., Rhee, S. B. and Moon, M. J. (1996) *Solid State Ionics*, **85**, pp. 91-98.

Lewandowski, A., Majchrzak, I. And Stepniak, I. (2000) *Solid State Ionics*, 132, pp. 101-106.

Li, T. and Balbuena, P. B. (1999) *Journal of Electrochemical Society*, **146** (pt. 10), pp. 3613-3622.

Li, X., and Hsu, S. L. (1984) *Journal of Polymer Science*, **22**, pp. 1331-1342.

Le Nest, J. F., Gandini, A. and Cheradame, H. (1988) *Br. Polymer. J.*, **20**, p. 253.

Linford, R. G. (ed) (1987,1990) *Electrochemical Science and Technology of Polymers*, Elsevier Applied Science, London, Vol. 1, pp. 47-51.

Lipkowski, J. and Ross, P. N. (1994) *Electrochemistry of Novel Materials*: Frontiers of Electrochemistry, VCH, New York, p. 77.

Liu, X. and Osaka, T. (1997) *J. Electrochem. Soc.*, **144** (pt. 9), pp. 3066-3071.

MacCallum, J. R. and Vincent, C. A. (1987) *Polymer Electrolyte Reviews*, **1/2**, Elsevier, London.

MacGlashan, G. S., Andeeev, Y. G., and Bruce, P. G. (1999) *Nature*, **398**, pp. 792.

Mandal, B. K., Walsh, C. J., Sooksimuang, T., and Behroozi, S. J. (2000) *Chem. Mat.* **12**, pp. 6-8.

Matsuda, Y., Morito, M. and Tsutsumi, H. (1993) *J. of Power Sources*, **43**, p. 439.

Matsumoto, M. (1996) *Polymer*, **37** (pt. 4), pp. 625-631.

Matsumoto, M., Rutt, J. S. and Nishi, S., (1995) *J. Electrochem. Soc.*, **142** (pt. 9), pp. 3052-3057.

Mishra, R. and Rao, K. J. (1998) *Solid State Ionics*, **106**, pp. 113-127.

Morales, E. and Acosta, J. L. (1998) *Solid State Ionics*, **111**, pp. 109-115.

Munichandraiah, N., Sivasankar, G., Scanlon, L. G. and Marsh, R. A. (1997) *Journal of Applied Polymer Science*, **65**, pp. 2191-2199.

Munshi, M. Z. A. (1995) *Handbook of Solid State Batteries and Capacitors*, World Scientific, pp. 393-403.

Murai and others (1997) *Japanese Patent* Application 97 106 023, p. 8

Nakamoto, K (1997) *Infrared and Raman Spectra of Inorganic and Organic and Coordination Compounds (Part A)* , Chicester Wiley, p. 156.

Nashiura, M., Kono, M., Namegaya, N., and Matsuda, Y., (1998) *Electrochemical and Solid-State Letters*, 1(pt. 6), pp. 246-248.

Nicholson, J. W., (1991) *The chemistry of Polymers*, Royal Society of Chemistry, pp. 19-20.

Osaka, T. (2000) *Chemistry in Britain*, **36** (pt. 3), p. 38.

Ostrovskii, D., Torell, L. M., Appectecchi, G. B. and Scrosati, B. (1998) *Solid State Ionics*, **106**, pp. 19-24.

Papke, B. L., Ratner, M. A. and Shriver, D. F. (1981) *J. Phys. Chem. Solids*, **42**, pp. 493-500.

Periasamy, P., Tatsumi, K., Shikano, M., Fujeida, T., Sakai, T., Saito, Y., Mizuhata, M., Kajinami, A. and Deki, S. (1999) *Solid State Ionics*, **126**, pp. 285-292.

Quartarone, E., Tomasi, C., Mustarelli, P., Appetecchi, G. B. and Croce, F. (1998) *Electrochimica Acta*, **43** (pt. 10-11), pp. 1435-1439.

Radhakrishna, S. and Arof, A. K. (1998) *Polymeric Materials*, Narosa Publishing House, London, p. 29.

Ratner, M. A. and Shriver, D. F. (1988) *Chem. Rev.*, **88**, p. 109.

Reddy, M. J., Sreekanth, T. and Subba Rao, U. V. (1999) *Solid State Ionics*, 126, p. 57.

Reddy, M. J., Sreekanth, T. and Subba Rao, U. V. (1999), *Solid State Ionics*, **126**, pp. 55-63.

Reiche, A. and Sten, T. (1995) *Electrochim. Acta.* **40**, p. 2153.

Rhoo, H. J., Kim, H. T., Park, J. K. and Hwang, T. S. (1997) *Electrochimica Acta*, **42** (pt. 10), pp. 1571-1579.

Sheldon, M. H., Glasse, M. D., Latham, R. J. and Linford, R. G., (1989) *Solid State Ionics*, 34, p.134.

Song, J. Y., Wang, Y. Y. and Wan, C. C. (2000) *Journal of Electrochemistry Society*, **147** (pt. 9), pp. 3219-3225.

Starkey, S. R. and Frech, R. (1997) *Electrochimica Acta*, **42** (pt.3), pp. 471-474.

Subramaniam, A. (1988) *Encyclopedia of Polymer Science and Engineering*. In: Mark, H. F., Bikales, N. M., Overberger, G. and Menges, G. eds. Graft copolymers of Natural Rubber (NR), 2nd ed., Wiley-Interscience, New York, pp. 762-786.

Such, K., Steven, J. R., Wieczorek, W., Siekierski, M. and Florjanczyk, Z. (1994) *Journal of Polymer Science: Part B: Polymer Physics*, **32**, pp. 2221-2233.

Scrosati, B., Croce, F. and Persi, L. (2000) *Journal of Electrochemical Society*, **147**, pp. 1718-1721.

Sun, H. Y., Sohn, H. J., Yamamoto, O., Takeda, Y., and Imanishi, N. (1999) *Journal of The Electrochemical Society*, **146**, (5), pp. 1672-1676.

Sung, H. Y., Wang, Y. Y. and Wan, C. C. (1998) *J. Electrochem. Soc.*, **145** (pt. 4), pp. 1207-1211.

Tamura, K. and Horiba, T. (1999) *Journal of Power Sources*, **81/82**, pp. 156-161.

Tarascon, J. M., Gozdz, A. S., Schmutz, C., Shokoohi, F. and Warren, P. C. (1996) *Solid State Ionics*, **86**, p. 49.

Tatsuma, T., Taguchi, M., Iwaku, M., Oyama, N. and Sotomura, T. (1997) in *Extended Abstract of 38th Battery Symposium in Japan*, p. 275.

Tsuchida, E., Ohno, H. and Tsunemi, K. (1983) *Electrochim. Acta*, **28**, pp. 59, 833.

Tsutsumi, H., Matsuo, A., Onimura, K. and Oishi, T. (1998) *Electrochemical and Solid-State*, 1 (pt. 6), pp. 244 to 241.

Venugopal, G., Reichert, V. R. and Zhang (1996) US Patent 5,549,987.

Vincent, C. A. (1989) *Prog. Solid State Chem.*, **88**, p. 109.

Vincent, C. A. and Sucrosati, B. (1997) *Modern Batteries*: An Introduction to Electrochemical Power Sources, John Wiley and Son, New York, p. 241.

Voice, A. M., Davies, G. R. and Ward, I. M. (1997) *Polymer Gels and Networks*, **5**, pp. 123-144.

Voice, A. M., Southall, J. P., Rogers, Mattews, K. H., Davies, G. R., McIntyre, J. E. and Ward, I. M. (1994) *Polymer*, **35** (pt. 16), pp. 3363-3372.

Walker, C. W. and Salomon, M. (1993) *J. Electrochem. Soc.*, **140**, p. 3409.

Wang, H., Huang, H. and Wunder, S. L. (2000) *Journal of The Electrochemical Society*, **147** (pt. 8), pp. 2853-2861.

Wieczorek, W., Such, K., Florjanczyk, Z. and Steven, J. R. (1995) *Electrochimica Acta*, **40** (pt. 13/14), pp. 2417-2420.

Wright, P. V. (1973), *Polymer*, **14**, p.589.

Yarovoy, Y. K., Wang, H. P. and Wunder, S. L. (1999) *Solid State Ionics*, **118**, pp. 301-310.

Appendix 1

Conference Papers / Publications

1) M D Glasse, R Idris, R J Latham, R G Linford and W S Schlindwein
An oral Abstract Papers of Modified Natural Rubber based polymer electrolyte presented at International Conference on Interfacial Phenomena in Batteries, Rome December 1999.

2) M D Glasse, R Idris, R J Latham, R G Linford and W S Schlindwein
Electrochem 2000 Symposium, Dublin.

3) Razali Idris, M.D.Glasse, R J Latham, R G Linford and W S Schlindwein
(2001) Journal of Power Sources, **94**, pp. 206-211.

4) M D Glasse, R Idris, R J Latham, R G Linford and W S Schlindwein
Polymer Electrolytes Symposium 2001, Noordwijkerhout, The Netherlands.

Appendix II

DSC traces

PU control

PU+15 (w/w %) $LiCF_3SO_3$

PU+20 (w/w %) $LiCF_3SO_3$

PU+30 (w/w %) $LiCF_3SO_3$

PU+40 (w/w %) $LiCF_3SO_3$

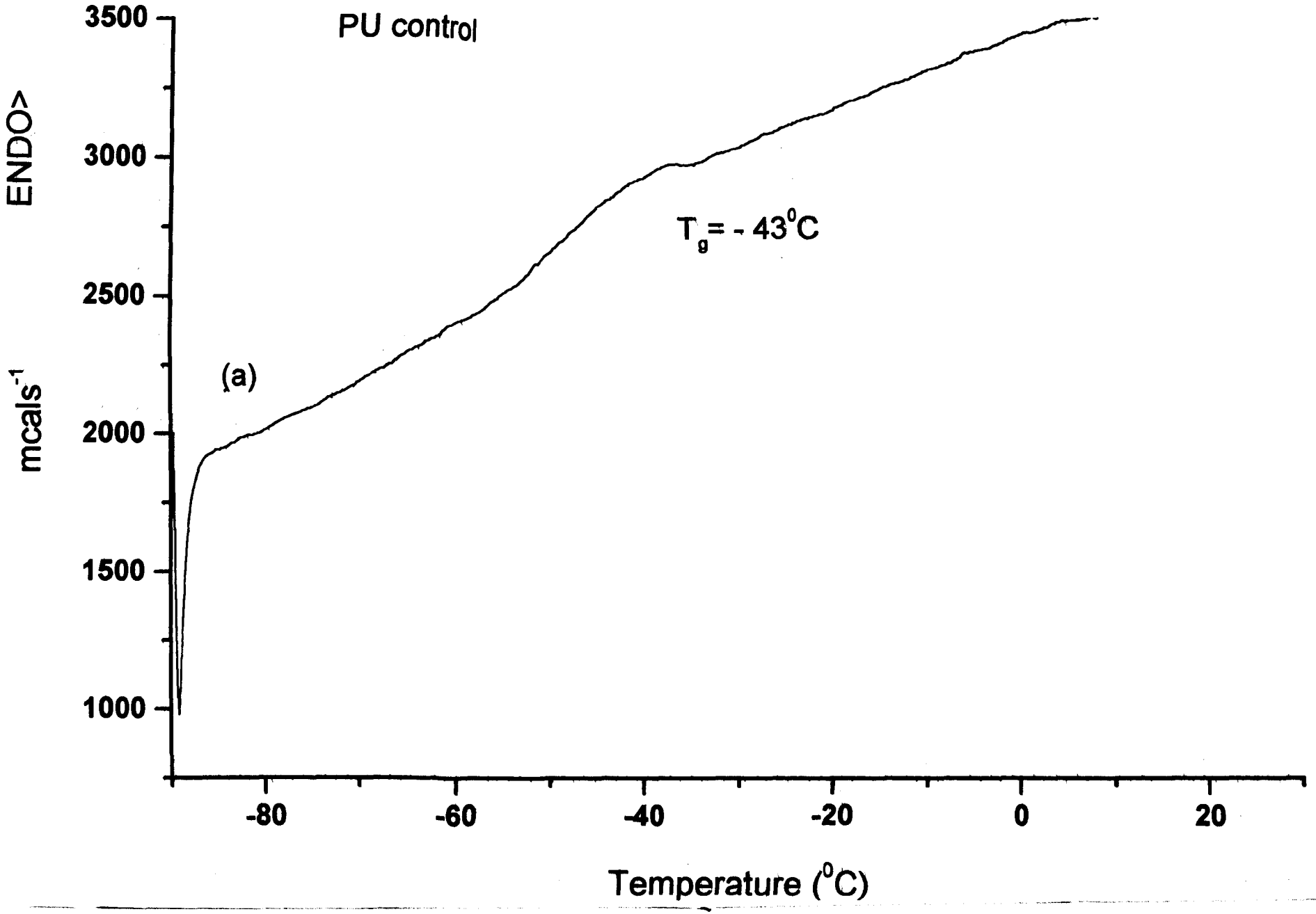
PU control
(a)
T_g= - 43^{0}C
ENDO>
mcals^{-1}
3500
3000
2500
2000
1500
1000
-80
-60
-40
-20
0
20
Temperature (^{0}C)

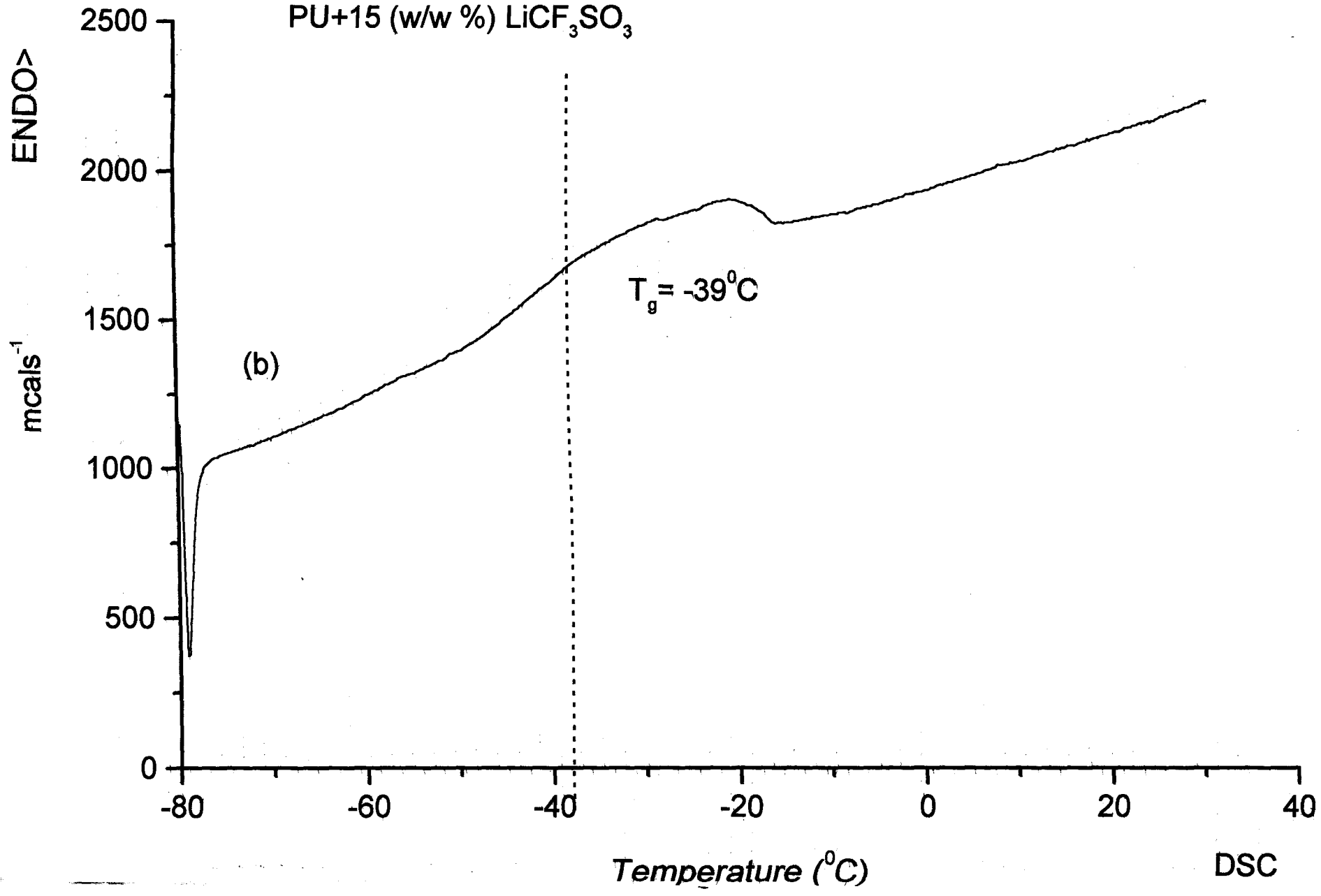
PU+15 (w/w %) LiCF3SO3
ENDO>
mcals-1
2500
2000
1500
1000
500
0
(b)
Tg= -39°C
-80
-60
-40
-20
0
20
40
Temperature (°C)
DSC

APPENDIX 11

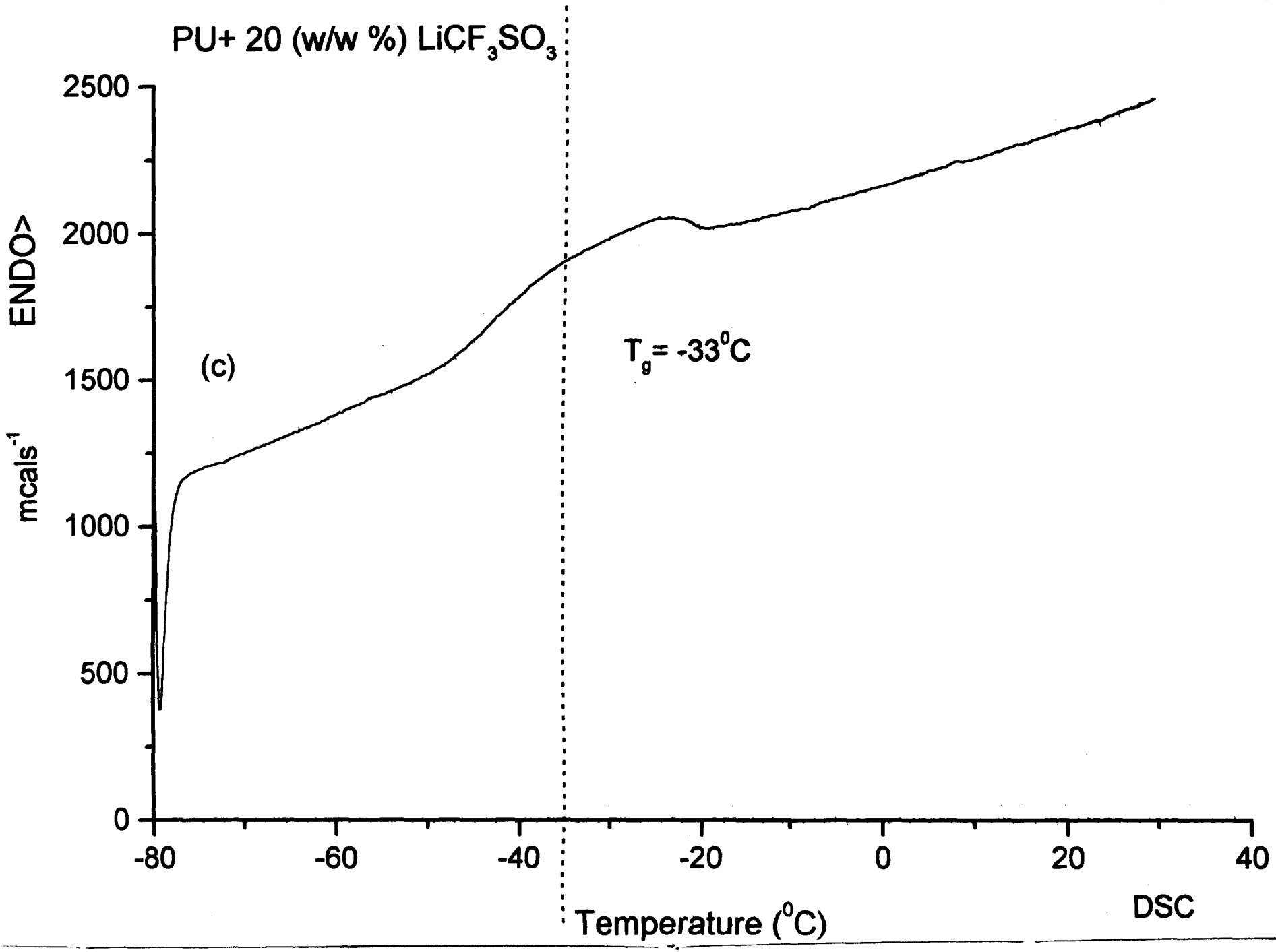
PU+ 20 (w/w %) LiCF3SO3
2500
2000
1500
1000
500
0
ENDO>
mcals-1
(c)
Tg= -33°C
-80
-60
-40
-20
0
20
40
Temperature (°C)
DSC

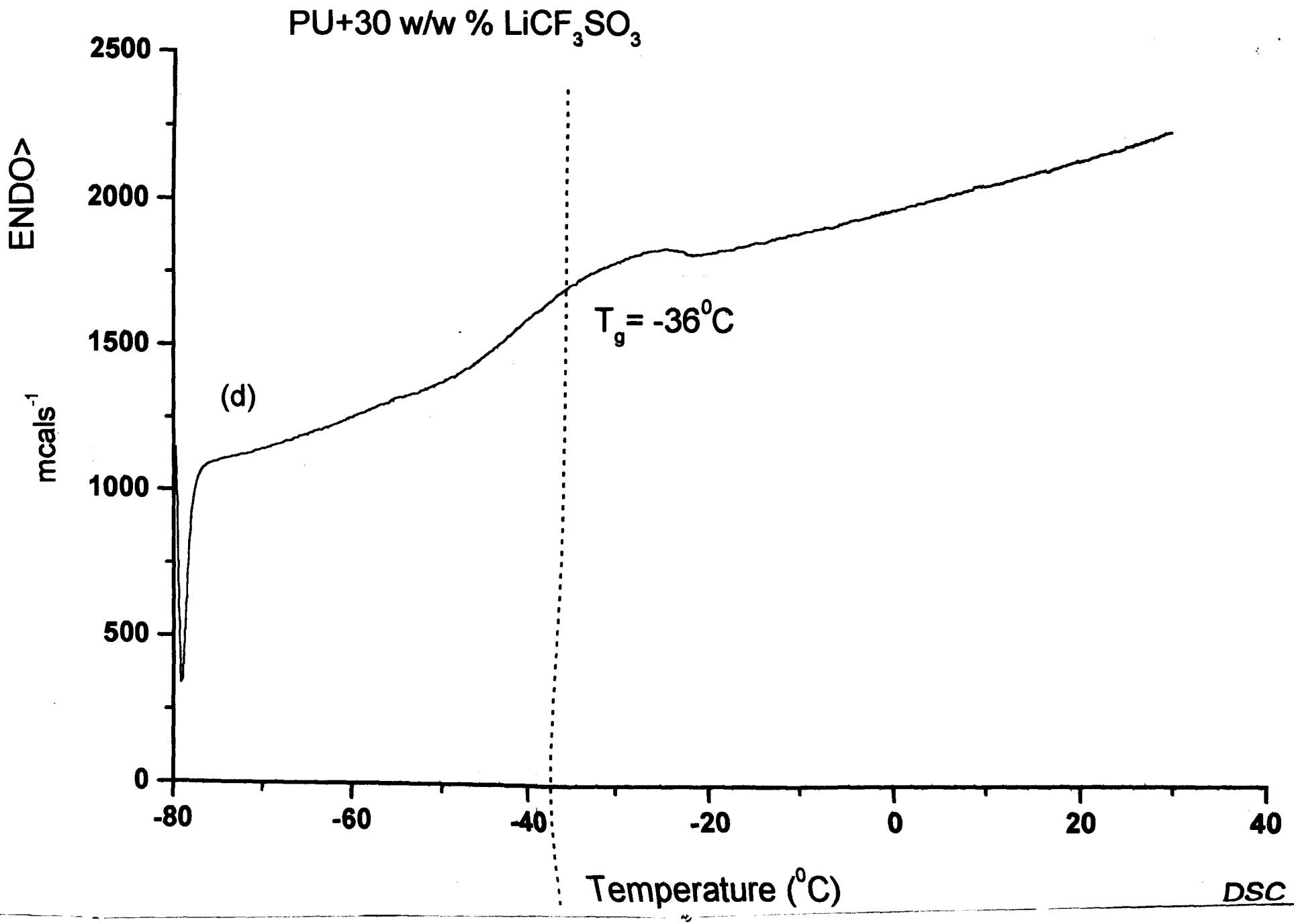
PU+30 w/w % LiCF3SO3
2500
2000
1500
1000
500
0
ENDO>
mcals-1
(d)
Tg= -36°C
-80
-60
-40
-20
0
20
40
Temperature (°C)
DSC

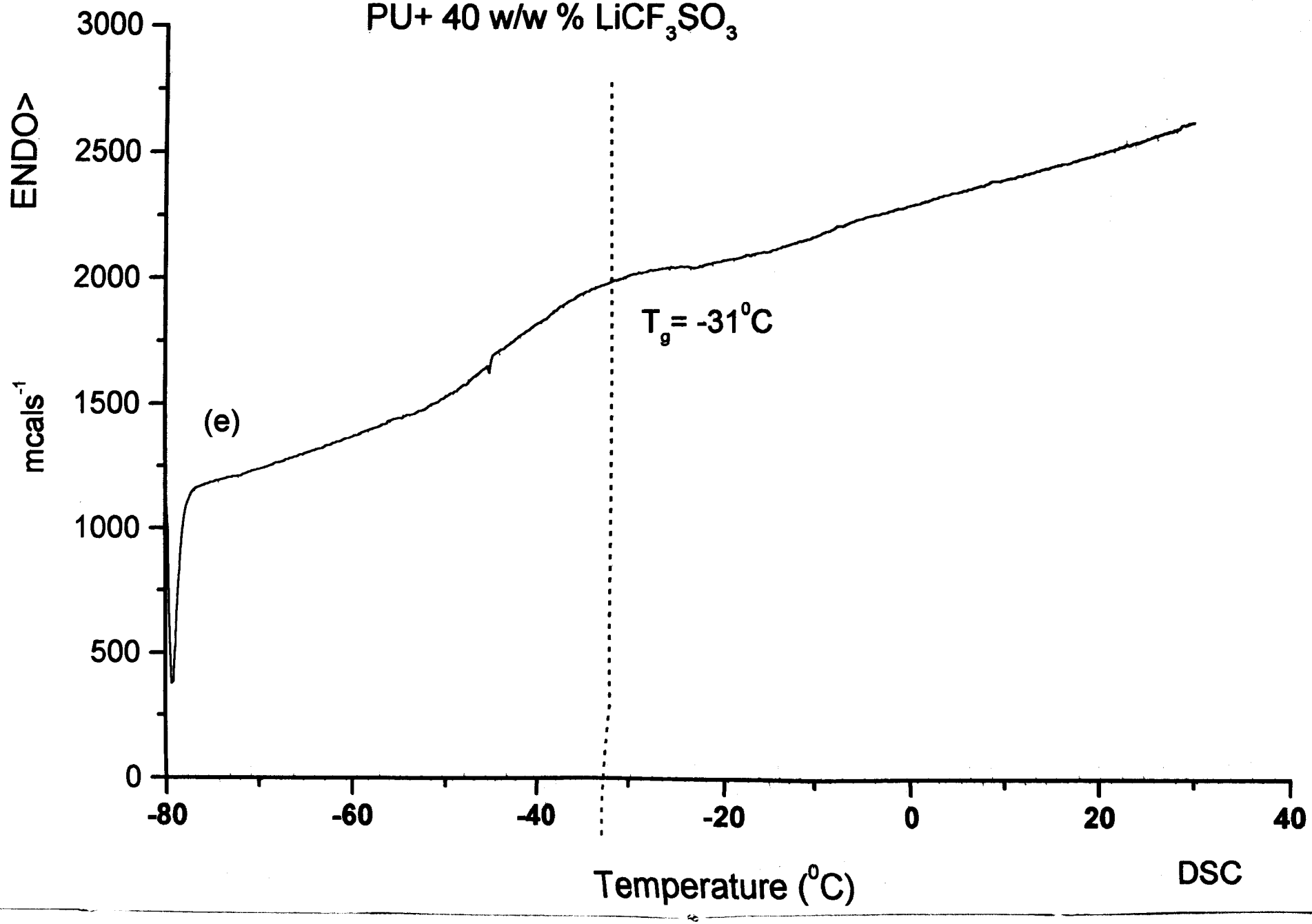
PU+ 40 w/w % LiCF3SO3
ENDO>
mcals-1
3000
2500
2000
1500
1000
500
0
(e)
Tg= -31°C
-80
-60
-40
-20
0
20
40
Temperature (°C)
DSC